AMIRA P544

Proterozoic sediment-hosted copper deposits

February 2003 report

Contents

** Powerpoint® presentation follows report.*

P544 Annual Report 2002 : Introduction

This volume is the penultimate major report prepared for ARC/AMIRA Project P544 'Proterozoic sediment-hosted copper deposits'. The final meeting and reports are scheduled for early July 2003. This annual report contains fourteen separate contributions from CODES and CSM researchers, many of which are based on the presentations made at sponsors' meetings held in Golden and Hobart on 1 November and 10 December 2002, respectively.

P544 has a number of important objectives that include:

1. To understand the processes responsible for transporting, concentrating and fixing Cu and other ore constituents during sedimentary basin evolution
2. To document the various stages and paragenesis of copper deposition and remobilisation during basin evolution
3. To develop a range of geological, geochemical and isotopic vectors that point toward ore, both on a district and a deposit scale
4. To determine what is different about the setting and geological evolution of the Zambian Copperbelt (ZCB), compared to Australian Proterozoic sedimentary basins, that may explain the difference in Cu (and Co) endowment in these areas
5. To apply research results from both Africa and Australia to produce better empirical exploration models for Proterozoic sediment-hosted Cu deposits

The reports presented here make some progress toward addressing several of these objectives.

Objective 3 is the focus of four reports presenting new geochemical and isotopic analyses for ZCB rocks. The reports discuss geochemical signatures of mineralisation and/or fluid-flow events. Analytical techniques and sampling strategy are described in the first report by **McGoldrick** (Report 1) and the geochemical character of the 'Ore Shale' is identified by **McGoldrick, Croaker and Broughton** (Report 2). They conclude that as well as Cu and Co, the element-association characterising argillite-hosted mineralisaton includes Ag, Bi, Au and possibly Mo and U. Several chalcophile elements (As, Sb, Ni, Pb, Tl and Zn) are present at levels at or below 'average shale' values. These observations are consistent with oxidised fluids being responsible for metal transport. In samples from the Konkola 'barren gap', of the ore association elements, only Co is present at levels seen in mineralised samples.

The third geochemical study briefly summarises preliminary observations from the Konkola North deposit (**Pollington and McGoldrick**, Report 3). Many of the Konkola North 'Ore Shale' samples show evidence of secondary oxidation effects with little S remaining in the rocks and ore associated metals being hosted in secondary Mn oxides and phosphate. None the less, the Cu-Bi-Mo-U association is preserved in the oxidised samples. The Konkola North 'Ore Shale' samples have some of the highest K_2O contents observed to date in our ZCB datasets.

In the last of the geochemical studies (Report 4), **Large, McGoldrick and Croaker**, present an assessment of geochemical and C/O isotope data from two drill cores in the Chambishi Basin that provide a continuous section through lower Mwashia and Roan rocks. Comparisons are made between 'shaley' rocks in these drill holes and 'Ore Shale' samples

from Nkana. The data show that immobile elements (Ti/Zr ratios) in siliciclastic units may assist with correlations, and the 'Ore Shale' at Nkana has a distinct Ti/Zr ratio of 22-26. There are systematic variations in K, Na and Al_2O_3 in siliciclastics that define a halo of K-feldspar enrichment in the hanging wall to the 'Ore Shale'. The 'Ore Shale' at Nkana and Konkola is enriched in K and depleted in Na compared to normal shales. Carbonates and carbonate-rich units have more variable Ti/Zr ratios than the siliciclastics, but their C/O isotopes may provide a vector to ore. Carbonates proximal to ore have isotopically light C and light O, compared with other carbonates. This coupled C-O isotope depletion is consistent with a moderate to high temperature fluid (150°-350°C), with $\delta^{18}O$ near zero (seawater?), interacting with organic carbon and sedimentary carbonate at the site of ore deposition.

The next four reports discuss work on Chambishi Basin deposits and the tectono-stratigraphic evolution of their host sequences. Work on drill-core from the Mwambashi deposit is presented in a major report (Report 5) by **Selley, Bull, Scott and Cooke**. They conclude that sedimentation of Lower Roan in the Chambishi Basin was controlled by WNW-trending half graben structures and subordinate NW- to NNW-trending transfer zones. At the onset of extension, the basin geometry was highly compartmentalised, resulting in lateral facies variation of predominantly arenaceous lithotypes and complex sediment dispersal patterns. Subaerial depositional environments typify this early phase of basin growth, however an upward transition to marine conditions is recorded within depocentre maxima. Transfer zones were the principal sites of locally derived, coarse-grained sediment input, which accumulated in restricted depocentres characterised by lateral pinch outs and limited accommodation development. Stratigraphy in the region of transfer zones is condensed and anomalously coarse-grained. The combination of 3-D pinch outs and quality reservoir strata in these regions made them optimal trap sites for migrating hydrocarbons. Upward transition to finer-grained, predominantly marine lithofacies is abrupt and records a fundamental change in basin configuration involving widespread sediment starvation. Depositional compartments became broader and more rapidly subsident, perhaps in response to a regional extensional pulse. Strata transgressed older basin compartments, providing a regional seal on an underlying system of semi-connected, permeable sandstone bodies. Cu mineralisation at Chibuluma West, Mwambashi B and parts of Chambishi occurs below the level of the Ore Shale. It is concentrated towards the top of clean, permeable arenaceous units, with indistinct geological footwalls, but sharp upper contacts with less permeable media. Host arenites occur within restricted depocentres and have pronounced feldspathic alteration. The architecture of host packages is consistent with that of a hydrocarbon reservoir. A strong spatial association of Cu-sulphides with radiogenic heavy mineral phases at Chibuluma West, may be considered indirect evidence of former hydrocarbons. In a speculative ore-genesis scenario, pathways and reservoirs utilised by migrating hydrocarbons, remained 'open' during subsequent passage of hydrothermal metal-bearing brines. Thus fluids directly responsible for mineralisation must have been introduced prior to complete consolidation of the clastic sediments (i.e., pre-peak metamorphism).

Three reports (6, 7 and 8) from Mawson **Croaker** describe aspects of his PhD studies at Nkana-Mindola deposit. The first of these is a short report summarising his activities during 2002. This is followed by a more comprehensive report on the stratigraphy and sedimentology of the deposit, based on his new underground mapping at Mindola North Shaft, Mindola Shaft, Central Shaft and SOB Shaft, and logging of new holes from the Mindola Deep Project and the Synclinorium Project areas. His third report compares the C/O isotope signatures of 25 samples from Nkana-Mindola 'Ore Shale' with regional samples from the Chambishi Basin described in Large et al. (this volume).

Report 9 by **Pollington and Bull** describes the sedimentology the Konkola North deposit, and will form part of Pollington's PhD thesis. Detailed logging of the ore horizon has been completed and a number of units have been identified. These include

the Kafufya, Ore Shale, Upper Ore Shale and Konkola Conglomerate which were formerly recognized units in the area, and Interbedded Siltstone and Sandstone, Arkosic Sandstone and Conglomerate, and Mixed Zone which are newly defined. The Kafufya is interpreted to be a subaerial debris flow with a proximal clastic sediment source. A rapid transgression is indicated by the onset of the subwave base Ore Shale sedimentation. The Interbedded Siltstone and Sandstone facies and the Arkosic Sandstone to Conglomerate facies together comprise an upward thickening and coarsening apron of clastic debris sourced from distal faults infilling accommodation space generated at the Ore Shale time. As the effect of these faults died off the Mixed Sequence was deposited as a combination of deltaic and shoreline sediments. The Upper Ore Shale could represent either another transgression event or the top of a fining upward sequence marking the end of the clastic influx. The Konkola Conglomerates are debris flows, which may indicate new growth faulting and relief.

The next report (**Scott,** Report 10) is a description of Anglo American's Ndola West prospect on the NE side of the Kafue Anticline. At Ndola West, all rocks intersected by the Anglo drill holes are interpreted to lie dominantly or entirely within the Lower Roan. The succession is divided into (i) Footwall, (ii) Ore and (iii) Hanging wall formations. The "Ore formation" represents an abrupt transgression-regression cycle that heralded a significant change in the character of Lower Roan sedimentation. Whole rock geochemical data (partial digestion) provided by Anglo American supports the interpretation that the Ore formation marks a transition from the deposition of relatively clean to argillaceous clastic sediments. There is also an apparent systematic change in mica composition from Footwall to Hanging wall. An apparent increase in MgO/Al_2O_3 and decrease in K_2O/Al_2O_3 ratio of mica may indicate the Hanging wall sediments were originally more dolomitic.

Textural relations described in this report, and the distribution of Cu at Mufulira and Ndola West suggest it was introduced prior to significant folding and tectonic and fabric development. The absence of an obvious fracture control on the ingress of the mineralising fluids indicates grain-scale permeability was relatively high at this stage, suggesting either that the sequence was not deeply buried at the onset of Lufilian deformation, or that reaction-enhanced permeability was important. SHRIMP dating by Dawson (Nov-Dec 2002 P544 meeting Powerpoints - available at AMIRA's website) indicates a Lufilian (560–510 Ma) age for arenite-hosted copper mineralisation at Mufulira, and a similar age for mineralisation at Ndola West is inferred.

Report 11 by David **Broughton** summarises work to date on his PhD project, and describes the stratigraphy and stratigraphic correlations of the Lower Katangan section in the Copper Belt based on his new logging. Two fences of regional drill holes are described that cover the western and eastern sides of the Copperbelt. The correlations are depicted on a series of Powerpoint slides accompanying this report.

The last Zambian contribution in this Annual Report is a Powerpoint presentation (Report 12) by Murray **Hitzman** which attempts to pull together much of our Zambian work to date. It summarises areas we now understand better as a result of P544 research, and highlights others areas that will be the focus of work planned between now and the final meeting.

The final two contributions (Reports 13 and 14) cover P544 research from Australian Neoproterozoic sequences in the Paterson Orogen and the Adelaide Fold Belt, respectively. Report 13 (**Scott**) is a preliminary review of the geological development and mineralisation in the Yeneena Basin, Paterson Orogen of Western Australia. This report synthesises the results of recent regional mapping in the Paterson Orogen by Geological Survey of Western Australia geologists, and the findings of recent PhD and Masters studies of mineral deposits in the region. The age, setting, structural evolution and mineral endowment of the Yeneena Basin all invite comparisons with the Zambian Copperbelt. Available evidence indicates major deposits in the Yeneena Supergroup (Telfer, Nifty and Maroochydore) formed during inversion of the Yeneena Basin succession during the Miles Orogeny. The age of this orogeny is broadly similar

to the Lufilian event in Africa, which may have heralded major copper mineralisation in Zambia. However, characteristics of the Nifty deposit, the largest stratabound Cu deposit in the Yeneena Basin, are distinctly different to the Copperbelt deposits, and suggest much closer affinities to Mt Isa-style copper ore bodies.

Report 14 by Wallace **Mackay** is part of his PhD research and describes the structure of the Curdimurka Subgroup in the Willouran Ranges, South Australia. Three folding events are recognised in this area, and minor Cu mineralisation at Dunn's Mine is thought to form during re-mobilization of low grade Cu from siltstone and shale into the fault zone on the limb of an F2 fold during D2 folding.

Acknowledgements: I would like to take the opportunity to thank the members of the P544 team, both at CODES and CSM for their outstanding efforts sometimes under considerable duress during 2002, Katie McGoldrick, Christine Cook and Phil Robinson produced the high quality geochemical and isotopic analyses performed at University of Tasmania, and June Pongratz has once again tamed the Corel Draw [and P544] beasts!

Peter McGoldrick
February 2003

Zambian Copperbelt geochemistry I: Introduction

Peter McGoldrick
Centre for Ore Deposit Research, University of Tasmania

Introduction

A major aim of AMIRA Project P544 is to carefully document geochemistry of the ores and host sequences to the Zambian Copperbelt (ZCB) deposits. As well as major and trace element geochemistry, C and O isotopes in carbonates, and sulfide and sulfate S isotopes form an important part of this work.

This type of information will be used to

(a) better characterise individual deposits, or groups of deposits, and to help deduce mechanisms responsible for metal transport and deposition
(b) determine if ZCB deposits have recognisable primary dispersion halos of ore associated or alteration-related elements
(c) help distinguish ore-related alteration from diagenetic and/or metamorphic effects unrelated to the mineralising process or processes
(d) determine if a recognisable chemo- or isotope stratigraphy exists in the Roan and overlying sequences that can assist in lithostratigraphic correlations

Sample Sets

To date several sample sets comprising around 500 samples have been analysed (Fig. 1). These include drill core sampled as part of the regional stratigraphic PhD work (Broughton, this volume) and the Konkola North and Nkana PhDs (Pollington and Bull; Pollington and McGoldrick; Croaker; this volume). In addition a small number of underground samples from Konkola and Mufulira have been analysed, and Zamanglo provided an assay data set from drilling at the Ndola West prospect (Scott, this volume).

Analytical Techniques

The samples discussed here have been prepared and analysed by different techniques in different laboratories. Most were analysed either, by XRF for major and trace elements at the University of Tasmania, or by alkali fusion/acid digestion followed by ICP finish at ACME Laboratories, Vancouver.

In addition, many of the samples analysed at University of Tasmania were sent to Bequeral, Sydney, for INAA analysis for low-level Au. In addition to Au another 28 elements are measured using RNAA and these include several REE).

Table 1 provides a list of elements measured by the different laboratories.

The Ndola West samples were also analysed at ACME Vancouver, but an aqua regia digestion was used that does not readily dissolve refractory minerals and more resistant silicates. Chalcophile elements can be reliably analysed by this technique, but many major and trace elements will report low. However, Scott (this volume) recognises consistent patterns in the Ndola West data and this suggests these analyses are internally consistent for most elements.

The XRF facility at the University of Tasmania provides excellent quality precise and accurate analyses. ACME Analytical Laboratories Ltd have ISO 9002 accreditation, and produce consistent and reliable results (Chris Oates, pers. comm.) A direct cross check of samples for both labs has not yet been

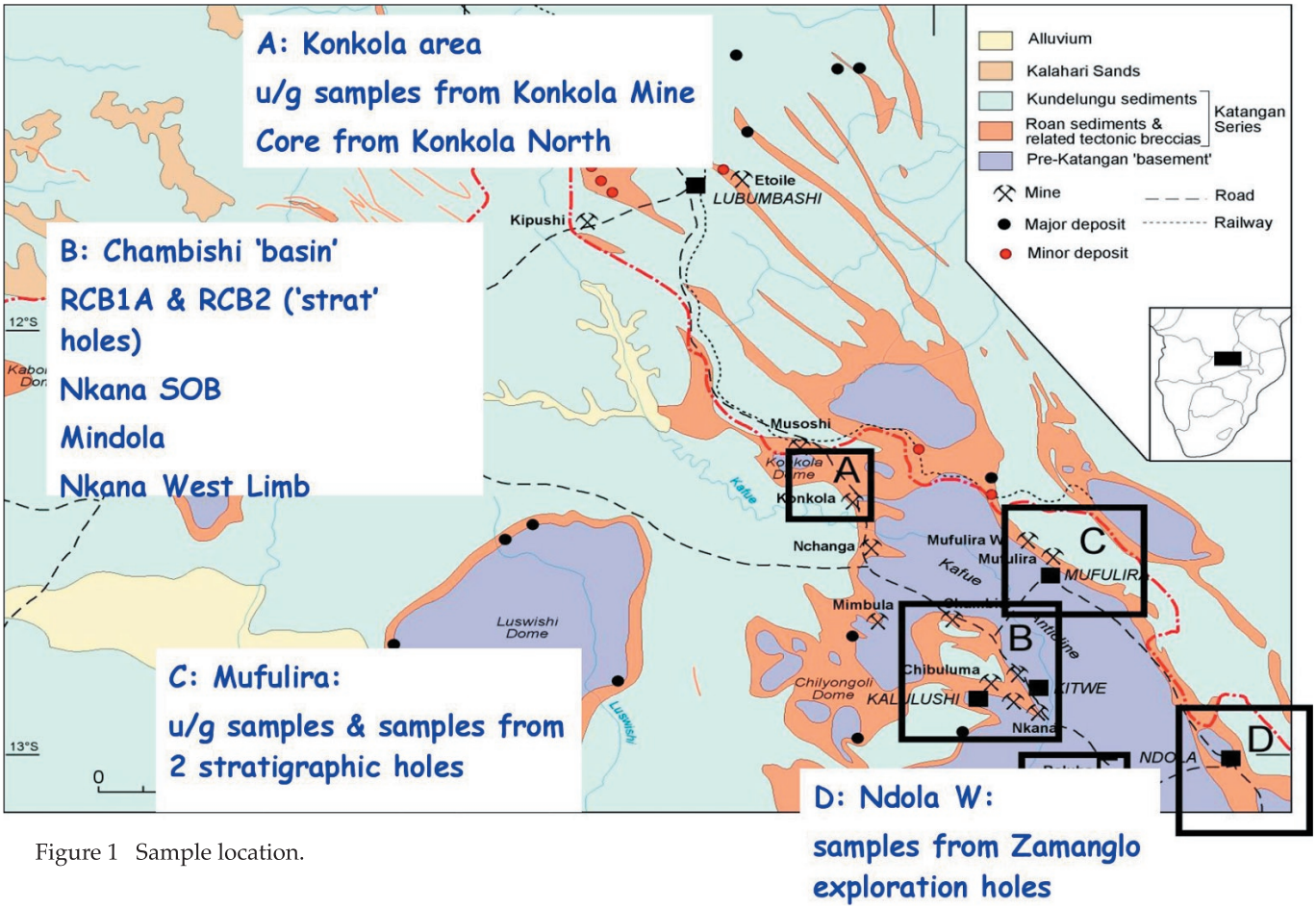

Figure 1 Sample location.

made for AMIRA P544, but this is planned as part of the 2003 analytical program (see below).

A small number of samples from Nkana, Konkola and Mufulira have been analysed for both inorganic and organic C, and these results are discussed in McGoldrick et al., this volume. The technique used is based on a difference method described by Krom and Berner (1983).

2001 Annual Report

The Zambian geochemical reults presented at the P544 sponsors' meetings in Golden and Hobart in late 2002 discussed a sub-set of the samples described above. Separate reports arising from those presentations are presented here. McGoldrick et al., discuss 'Ore Shale' samples from Nkana-Mindola and Konkola, Pollington et al. is a brief summary of the chemistry the 'Ore Shale' at Konkola North. Large et al., describe geochemical and C/O isotope data from samples from a stratigraphic section composited from two deep cored holes in the Chambishi Basin. A more detailed C/O isotope study of the Nkana deposit is described by Croaker (this volume).

Future Work

Several additional sample sets have been analysed at ACME, or are currently undergoing analysis. These include samples from'stratigraphic' drill-holes from the Mufulira area (L80, MW107 and DDH219), and KLB145 from Konkola . Much of the geochemical and isotopic work is deliberately focused in the Chambishi Basin reflecting the focus of P544 sedimentological and structural work in this area. Geochemical and isotopic analyses for C/O and S for samples from fences of

holes from Chambishi SE deposit, Mwambashi deposit (Selley et al., this volume), and Chambishi deposit will be discussed in the P544 final reports. A subset of these samples will be analysed for both organic and inorganic C.

Reference

Krom, M. D. and R. A. Berner, 1983. A rapid method for the determination of organic and carbonate carbon in geological samples. Journal of Sedimentary Petrology **53**: 660-663.

Table 1: Elements measured and detection limits for the services from the three laboratories used to analyse P544 Zambian samples.

	Becquerel: RNAA	UTAS: XRF & pyrolysis C	ACME: modified 4B/4B
SiO2		0.01	0.02
TiO2		0.04	0.01
Al2O3		0.04	0.03
Fe2O3	0.02	0.0002	0.04
MnO		0.01	0.01
MgO		0.007	0.01
CaO	1	0.0006	0.01
Na2O	0.01	0.018	0.01
K2O	0.2	0.0003	0.04
P2O5		0.01	0.01
Cr2O3	0.0005	0.0001	0.001
Loss on Ignition		0.01	0.01
Ctotal		0.01	0.01
Cinorganic		0.01	
Corganic		0.01	
Ag	5	3	0.1
As	1		1
Au	0.005		
Ba	100	4	0.5
Bi		2	0.1
Br	1		
Cd			0.1
Co	1	2	0.5
Cr	5	1	
Cs	1		0.1
Cu		2	0.1
Ga			0.5
Hf	0.5		0.5
Ir	20		
Mo	5	1	0.1
Nb			0.5
Ni		1	0.1
Pb		1.5	0.1
Rb	20	1	0.5
S		20	100
Sb	0.2		0.1
Sc	0.1	2	1
Se	5		
Sn			1
Sr		1	0.5

	Becquerel: RNAA	UTAS: XRF & pyrolysis C	ACME: modified 4B/4B
Ta	1		0.1
Te	5		
Th	0.5	1.5	0.1
Tl		1.5	0.1
U	2	1	0.1
V		1.5	5
W	2	2	1
Y		1	0.1
Yb	0.5		
Zn	100	1	1
Zr	500	1	0.5
La	0.5		0.5
Ce	2		0.5
Pr			0.02
Nd			0.4
Sm	0.2		0.1
Eu	0.5		0.05
Gd			0.05
Tb			0.01
Dy			0.05
Ho			0.05
Er			0.05
Tm			0.05
Yb	0.5		0.05
Lu	0.2		0.01

Slide 1

Zambian Copper Belt Geochemistry:
Part I Introduction

Peter McGoldrick

Slide 2

Geochemistry (& isotopes) yield information that can:

- be used as empirical guides to ore or favourable horizons
- have implications for ore-forming processes

Slide 3

Questions:

- are the different Zambian Cu deposits geochemically distinct?
- can we use geochemical and isotopic signatures to design vectors to hidden deposits?
- what implications does the chemistry of the ores have for ore forming and metal transporting process?
- are there chemical or isotopic signatures that can be used for chemostratigraphic correlations?

Slide 4

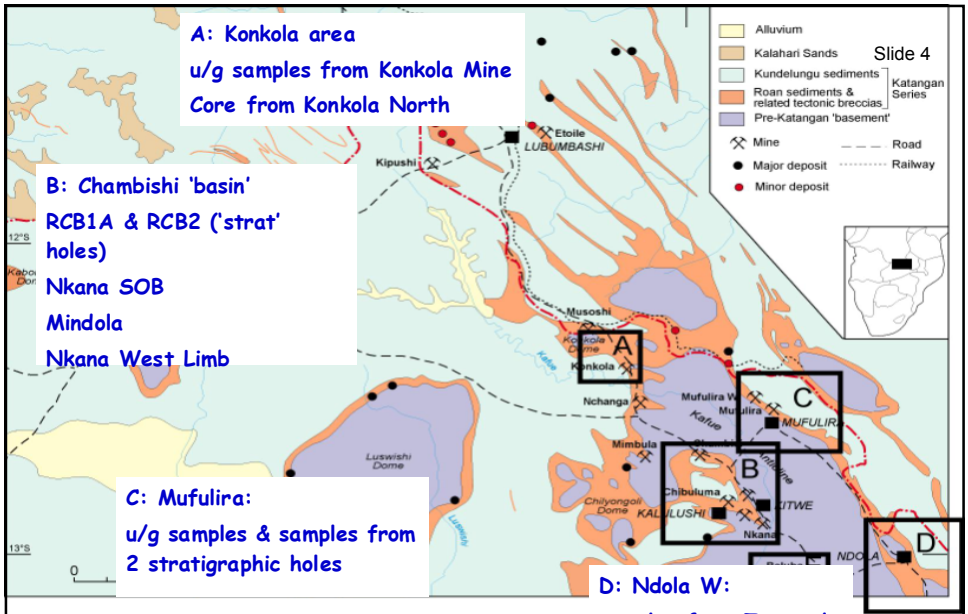

Sample locations

AMIRA P544 Meeting Golden November 1st 2002

Slide 5

Analytical techniques:

- Different sample sets analysed at three different labs for different element groups
- University of Tasmania: XRF major & trace analyses, pyrolysis C
- Becqueral: 'Au+28' procedure (mainly for Au to 5ppb & some REE
- ACME Vancouver: modified 4A/4B 40 element ICP procedure

Slide 6

This meeting

- chalcophile element geochemistry of mineralised and barren argillite ('Ore Shale', 'Ore Formation' etc)
- chemostratigraphy and C/O isotopes in Roan sediments frommthe Chambishi basin

Zambian Copperbelt geochemistry II: 'Ore Shale' geochemistry

Peter McGoldrick
Centre for Ore Deposit Research, University of Tasmania

Summary

This report describes geochemical character of the 'Ore Shale' from Nkana-Mindola and Konkola deposits and makes comparison between mineralised and unmineralised argillites from these areas. As well as Cu and Co, the element- association characterising mineralisaton includes Ag, Bi, Au and possibly Mo and U. In contrast, several chalcophile elements (As, Sb, Ni, Pb, Tl and Zn) are present at levels at, or below, 'average shale' abundances. Some of the darkest coloured argillites actually contain little organic C. These observations, together with the variable Au tenor of the mineralised argillites, are consistent with oxidised fluids being responsible for metal transport, and reaction with organic matter being a metal trapping mechanism.

In samples from the Konkola 'barren gap', of the ore association elements, only Co remains at levels seen in mineralised samples.

Introduction

The so-called 'Ore Shale' is the major Cu-bearing host in many of the ZCB deposits and it contains variable amounts of Cu, Fe and Co sulfides, and is carbonaceous in parts. It can be lithologically diverse, but commonly comprises variably metamorphosed and deformed grey to black siltstones and shales ('argillites'). The dark argillites are mostly siliciclastics, but carbonate-rich lateral facies equivalents are present in some places (e.g., Mindola – Croaker, this volume). It ranges from zero to about 10 m true thickness, but can be up to 30 m in structurally thickened zones.

Regionally, it is an important marker and represents a significant change in basin configuration (Selley et al., this volume; Broughton, this volume).

Argillite lithologies are present at stratigraphically higher levels in the Roan and Mwashia in the ZCB (e.g., Broughton – this volume & references therein), and, although they occasionally contain Cu sulfides (e.g., the 'Upper Ore Shale' at Konkola – see Pollington and Bull, this volume), they do not contain known economic concentrations of Cu or Co.

This report documents for the first time detailed, high precision, multi-element geochemistry of 'Ore Shale' argillites from a number of locations in the ZCB. These data shed light on several important questions that address key aims of project P544. These include:

(i) Is there a suite of chalcophile elements that characterise the 'Ore Shale' other than Cu, Co (and S)?
(ii) Do these ore-associated elements persist at elevated levels in unmineralised argillites?
(iii) What implications does the 'metal tenor' of 'Ore Shale' mineralisation have for transport and trap processes?
(iv) Can the 'Ore Shale' argillites be distinguished chemically and/or isotopically from other Katangan argillites?

Sample Sets

The data sets discussed in this report come from drill core from the Nkana-Mindola deposit in the south east Chambishi Basin, and from Konkola mine (slide 3). A third large set of "Ore Shale' samples from drill core from the Konkola North deposit are discussed in a short report by Pollington and McGoldrick (this volume), and will be the subject of a more extensive report at a later date.

The Nkana-Mindola samples comprise 16 mineralised and 15 unmineralised (arbitrarily defined as more than or less than 1000 ppm Cu, respectively) one metre composite samples from underground drill hole NS009 in SOB (South Orebody) – see slide 4. Seventeen mineralised argillites from drill holes MX184 and MX188 through Mindola orebobody (slide 4), and 19 samples from drill core from the west limb of the Nkana Syncline (slide 7). The west limb is not known to contain significant Cu mineralisation.

It was not practical to 'grab' sample the Nkana-Mindola drill-holes, a practise employed for other lithogeochemical work in P544. First Quantum-Mopani supplied splits of the coarse rejects, or assay pulps of one metre drill intersections, which were subsequently analysed at the University of Tasmania, or ACME Laboratories in Vancouver (see below). This meant that variable amounts (up to several percent) of vein material (quartz-calcite ± minor sulfides at SOB (slide 5), or dolomite-calcite ± minor sulfides at Mindola (slide 6)) were incorporated with argillite in some samples. It is not possible to geochemically recognise the presence of vein material in any of our analyses, hence, they can not be taken into account in the interpretation presented here. However, if the vein constituents are locally derived (Croaker, this volume) then small amounts of vein material should not inordinately bias the whole rock analyses.

The Konkola deposit is a classic 'Ore Shale'-hosted, giant Cu orebody that wraps around the nose of in the western ZCB (Sweeney and Binda, 1989). Samples discussed here come from underground workings accessed from No. 3 Shaft in the nose of the Kirila Bomwe Anticline (slide 8), and from an old surface drill-hole (KLB67) that penetrated the 'barren gap' separating the 'northern' and 'southern' orebodies at Konkola (Broughton, 2002).

A much larger sample set of 'Ore Shale' and hangingwall samples has been obtained from the Konkola North deposit as part of Nicky Pollington's ongoing PhD studies. It had been planned to use 'Ore Shale' argillites from this data set for comparative purposes to the Nkana-Mindola and Konkola samples previously described. However, most of her 'Ore Shale' samples show evidence for moderate to strong oxidation ('deep leaching') which makes comparison to the other fresh samples difficult. Hence, these results are not considered in this report, but form the basis for a later short report (Pollington and McGoldrick, this volume).

Analytical techniques

Samples discussed here were analysed at either the University of Tasmania, or ACME Vancouver, and Au analyses were performed by Becqueral, Sydney (see the previous report (McGoldrick, this volume) for details).

Results and Discussion

For the purpose of illustration a group of chalcophile and/or possible ore-related elements have been chosen for a series of simple cross-plots (slides 10 to 30). In all cases the data are depicted as three or five samples sets. These are:

- Nkana all 'shales': the Nkana SOB NS009 samples
- Mindola: mineralised argillites from MX184 and MX188
- Konkola: six mineralised underground samples
- Konkola BG: eleven samples from KLB67 through the Konkola 'barren gap'.

On most of the plots there is compositional information for 'typical' shales compiled from the literature. These are a commonly cited 'average shale' and 'black shale' published by Vine and Tourtelot

(1970), and an average 'Aussie 'oil' shale' from the Bowen Basin compiled by Patterson et al., (1986). Not all the elements considered here are available in each of these compilations, and in some instances, a best estimate from earlier literature sources was used, or, in the case of Au, RNAA data from analyses of northern Australian Palaeoproterozoic shales (McGoldrick: various sources).

Ore elements: Fe, S, Cu and Co

In all but the Konkola barren gap (KBG) samples, Fe and S are well correlated are well correlated (slide 11). The KBG samples have similar amounts of Fe to the other argillite sample sets, but are essentially lacking in S. The Cu and S relationships are more complex, with the four of the six Konkola underground (KU) samples having high Cu for a given S content when compared to Cu mineralised Nkana and Mindola samples. Also, many Nkana and Mindola samples are S-rich, but low in Cu (slide 12).

Cobalt and S are not correlated in Cu-mineralised samples (slide 13), but virtually all mineralised samples, and the KBG samples, have Co levels elevated well above typical shales (slides 14, 15). Nkana west limb (NWL) samples have the lowest Co values, with many at or lower than typical shales.

Discussion

The Fe and S relationships are consistent with pyrite and Cu-Fe sulfides being the main hosts for these two elements in most samples, and 'barren' Fe-sulfide-rich argillites can be clearly distinguished in the Nkana-Mindola group. The Cu-rich character of several KU samples is consistent with chalcocite being the present in these samples. It is not clear why most samples are so enriched in Co, but for Nkana, Mindola and Konkola this is clearly an ore signature. Hence, it is noteworthy that the KBG samples are also enriched in Co.

Bismuth and silver

Slides 16-18 show Bi and S, and Ag and S relationships for all five sample groups, and as with Co, the three mineralised groups show elevated Bi compared to typical shales, however, the KBG samples do not contain measureable Bi or Ag. Copper and Ag (slide 18) are well correlated for the Nkana and Mindola mineralised samples, but the Konkola samples are more equivocal, as a Ag-Cu correlation may be masked by the poor sensitivity of the XRF technique used to measure Ag in the KU samples.

Discussion

As for Co, it appears that Bi and Ag are ore association elements, with barren argillites from NWL and the KBG lacking Ag enrichment.

Gold

The Au content of the mineralised argillite samples range from less than 5 ppb (the detection limit of the INAA technique used for analysis) to nearly 40 ppb in one of the KU samples (slides 19, 20). The Nkana SOB samples, the KBG and NWL samples are all below detection limit for Au. High Au samples (nominally > 10 ppb – but see discussion) are present in the Mindola and KU sample sets, but shows no simple relationship with Cu tenor.

Discussion

Clearly many argillite samples are strongly enriched in Au compared to the 1 or 2 ppb likely to be present in a typical shale, and it can be argued that Au is an ore association element. Furthermore, it is noteworthy that the most Au-rich samples are the chalcocite-bearing Konkola ores.

Zinc, lead and arsenic

These elements are all present at levels that are mostly around, or less than, 'typical' shale abundances. Most samples have Zn contents of below 50 ppm, with some of the more S-rich Nkana samples ranging up to 380 ppm Zn. Lead is mostly less than 10 ppm, and As less than 15 ppm (again with the exception of a few S-rich Nkana samples which have upto 380 ppm As). The KBG samples have very low levels of all three of these elements.

Discussion

On the strength of these observations none of these elements can be considered to be part of the 'ore signature'. Elevated Zn and As in some Nkana samples is consistent with minor enrichment of these metals in (?diagenetic) Fe sulfides.

Nickel, vanadium and molybdenum

Nickel (slide 26) is at or below levels typical of shales and black shales. Vanadium (slide 25) shows a scatter to slightly higher than 'typical' black shale values, with no clear separation of barren and mineralised samples. Molybdenum (slide 27) has a similar pattern to V, with a group of high Mo samples (mainly from Nkana), but the Mo enrichment over 'typical' black shales is arguably greater than that shown by V.

Discussion

These three elements can become extremely enriched in organic matter-rich black shales e.g., 'oil shales (Coveny et al., 1992), However, in the ZCB argillites none of these elements are enriched to the degree expected for former 'oil shales', although, a small contribution from organic matter (particularly for V) cannot be excluded.

On the other hand, Ni is not enriched at all, hence, it is arguable that high Mo (the most enriched of these three metals) reflects to the same processes that produced Cu, Co, Bi, Ag and Au enrichment in these rocks.

Uranium and thorium

Most samples contain 'typical' shale levels of U of around 2-3 ppm, although a few samples, including four from NWL have U levels more than five to fifteen times higher than this. Thorium shows a scatter of values around the 'average shale' value of 12 ppm, with three Konkola samples having the highest values (about three times 'average shale'), and much of the U scatter may also reflect this.

Discussion

The Th data are quite consistent with a spread of values reflecting variations in the heavy mineral abundance and diversity in these samples. In contrast, the highest U values (particularly those from the NWL samples) may indicate U forms a distal enrichment to the Nkana lodes (see below for further discussion). More work is needed to confirm this interpretation.

Other elements: thallium and organic carbon

A somewhat unexpected result of this geochemical study was that Tl was at or below 1 ppm in all the argillite samples analysed. These are 'typical' background Tl levels in many Proterozoic sedimentary rocks.

A small number of samples from Nkana and Konkola have been analysed for total C and organic C. Samples from the arenite-hosted Mufullira deposit were also available for comparison (slide 33). Although total C is present at levels up to several weight percent, the organic C content of the argillites (0.7 wt % and 0.1 wt% from Nkana and Konkola, respectively) is very low.

Discussion

Many base metal deposits contain large amounts of Tl, and have large primary dispersion halos of this element (e.g., Large and McGoldrick, 1998). Thallium was apparently transported in the ore-forming fluid and fixed in sulfides of K-silicates at the site of ore deposition. In the ZCB there is no shortage of sulfides and/or K-silicate minerals in and around the orebodies, so it can be argued that the metal-carrying fluid did not transport Tl. Univalent Tl is quite soluble over a range of Eh-pH conditions, but trivalent Tl (only stable under very oxidising conditions) tends to be sequestered into Fe-oxyhydroxide phases (McGoldrick and Keays, 1981). Hence, the lack of Tl in the ZCB may implicate very oxidised fluids in metal transport.

Modelling by Haynes, (1987), and Cooke et al., (2000) indicates oxidised saline brines are very good at transporting Cu, Co and Ag, even at low temperatures. Gold transport in oxidised fluids requires a combination of high salinity and/or high Eh and/or high temperatures (Huston and large, 1989)

Furthermore, such oxidised fluids would tend to destroy (oxidise) organic matter in their flow paths,

under high water-rock ratio conditions. The apparent low organic C, now present in the ZCB argillites, may indicate such a process has occurred, and implicate oxidation of organic matter as a mechanism for precipitating ore metals from solution.

Conclusions

Several important empirical observations can be made from the argillite geochemical data. These include that:

- Cu, Co, Ag, Bi and Au (?Mo) are 'ore-association' elements
- compared to 'average shale Cu is 100 to 1000x, Ag up to100x, Co up to 50x, Bi up to 20x, Au between 1 to 10x
- U is anomalous in 'distal' samples at Nkana and hence may be a broad halo-forming 'ore-association' element
- As, Sb, Ni, Pb, Tl and Zn in mineralised argillites are at levels less than, or equal to 'average shales'
- Of the 'ore-association' elements only Co is present at anomalous levels in both unmineralised *and* barren-gap samples
- Some black 'Ore Shales' are devoid of organic C

Furthermore, there are a number of important inferences concerning ore-forming processes to be drawn from the argillite geochemical data. For instance:

- Cu, Co, U, Au (?and Bi & Mo) are an 'oxidised' fluid signature
- low Tl is consistent with an oxidised ore fluid
- low organic C in some deposits may indicate destruction of original sedimentary organic matter or hydrocarbons during ore precipitation
- the presence of Au in some parts of some deposits has implications for metal transport and ore deposition

References

Broughton, David, 2002, Comparative study of drill cores from the Konkola North Orebody and Barren Gap, CODES/CSM AMIRA Project P544 – Proterozoic sediment-hosted copper deposits, June 2002 report, p.19-35.

Cooke, D. R., Bull, S. W., Large, R.R. and McGoldrick, P.J., 2000, The importance of oxidised brines for the formation of Australian Proterozoic stratiform sediment-hosted Pb-Zn (Sedex) deposits: Economic Geology v.95, p.1-17.

Coveny, R. M., and Muowchick, J. B., 1992, Field relations, origins, and resource implicaitons for platiniferous molybdenum-nickel ores in black shales of south China: Exploration and Mining Geology v1. p. 21-28.

Huston, D. L. and R. R. Large (1989). "A chemical model for the concentration of gold in volcanogenic massive sulphide deposits." Ore Geol Reviews 4: 171-200.

Haynes, D. W. (1987). "Stratiform copper deposits hosted by low energy sediments: III. Aspects of metal transport." Economic Geology 82: 635-648.

Large, R. R. and P. J. McGoldrick (1998). "Lithogeochemical halos and geochemical vectors to stratiform sediment-hosted Zn-Pb-Ag deposits. Part 1: Lady Loretta deposit, Queensland." Journal of Geochemical Exploration 63: 37-56.

McGoldrick, P. J. and R. R. Keays (1981). "Precious and volatile metals in the Perseverance nickel deposit gossan : implications for exploration in weathered terrains." Economic Geology 76: 1752-1763.

Patterson, J. H., Ramsden A. R., Dale, L.S., and Fardy, J.J., 1986, Geochemistry and mineralogical residences of trace elements in oil shales from Julia Creek, Queensland, Australia: Chemical Geology, v. 55, p.1-16.

Sweeney and Binda, 1989, The role of diagenesis in the formation of the Konkola Cu-Co orebody of the Zambain Copperbelt, Geological Association of Canada, Special Paper 36, p.499-518.

Vine, J. D. and Tourtelot, E. B., 1970, Geochemistry of black shale deposits - a summary report.: Economic Geology, v. 65, p.253-272.

Zambian Copper Belt Geochemistry:
Part II 'Ore Shale' geochemistry

Peter McGoldrick, Mawson Croaker &
David Broughton

Questions?

What are the ore-associated (chalcophile) elements?

Are there ore-associated elements present at elevated levels in low-Cu argillites that are indicators of mineralisation (halos)?

What implications does the metal tenor of the 'Ore Shale' mineralisation have for transport and trap processes?

Do the Lower Roan argillites have a chemistry that distinguishes them from other Katangan argillites?

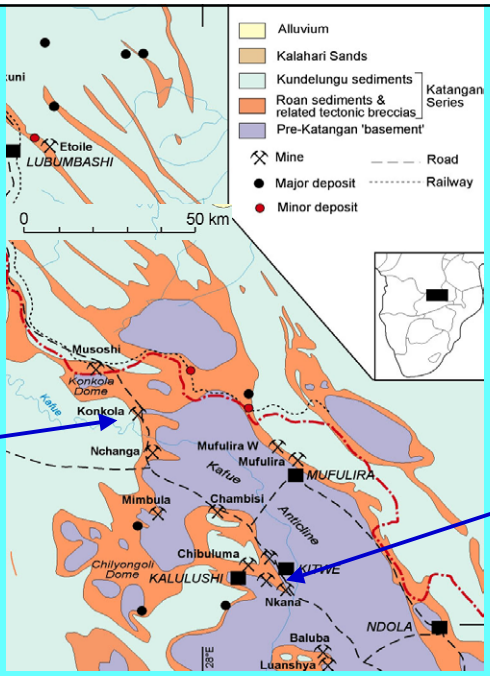

Konkola

Nkana/Mindola

Data sets

1. Nkana SOB
DDH NS009:
31 mineralised & unmineralised argillites

2. Mindola DDHs
MX184 & MX188:
17 mineralised argillites

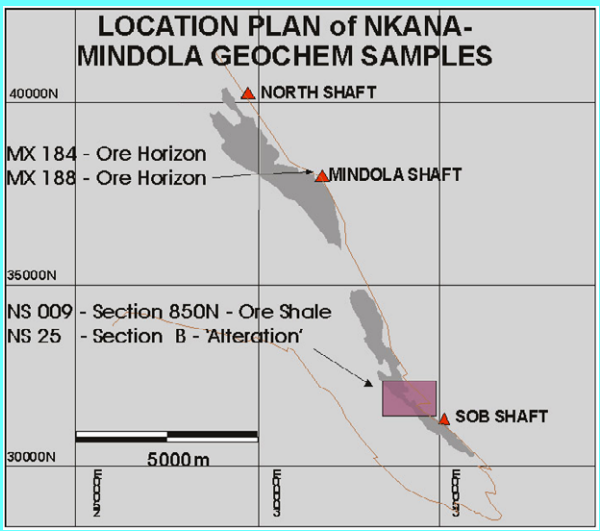

Nkana SOB

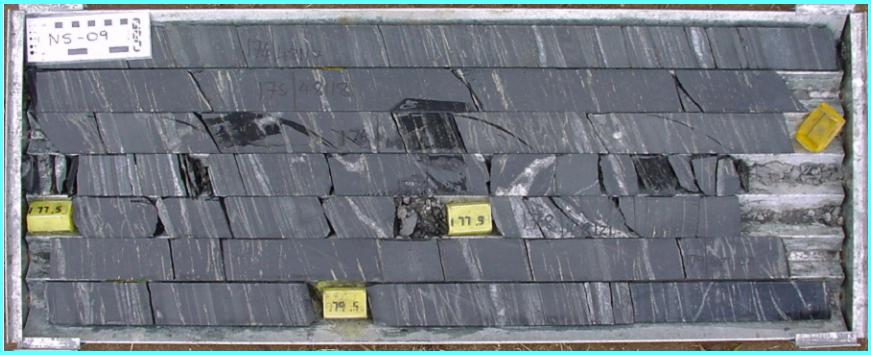

Typical black carbonaceous ore shale from NS009
So parallel to main cleavage
NB Quartz-calcite veins
Geochemistry samples ca. 1m composites

Mindola

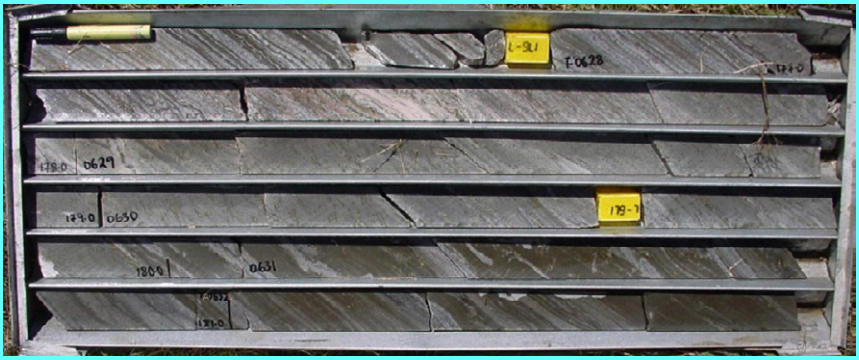

Ore Shale lithology from Mindola – dolomitic argillite, argillite, includes So-parallel carbonate veins

Geochemistry samples ca. 1m composites

Nkana: West Limb

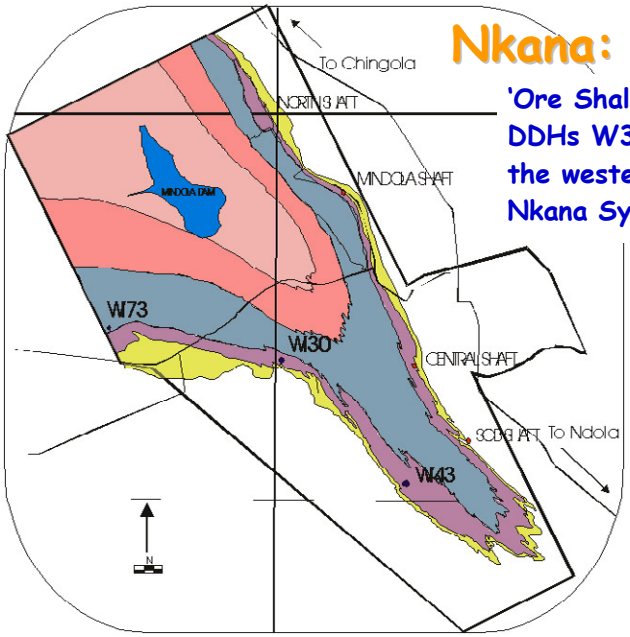

'Ore Shale' equivalent from DDHs W30 & W43 through the western limb of the Nkana Syncline

19 samples:

four with 0.1 to 0.6%Cu, others <0.1%Cu

Konkola

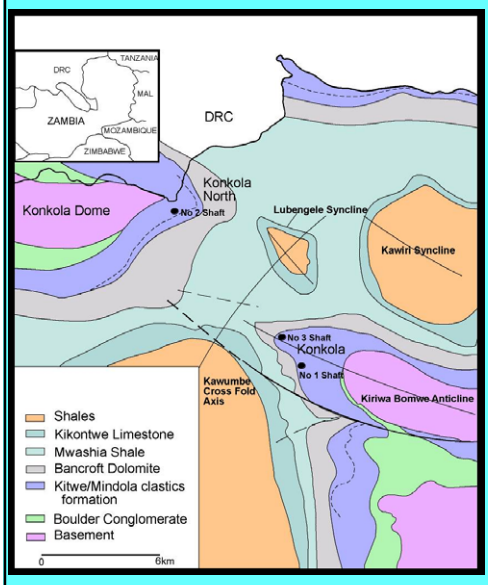

No. 3 shaft u/g samples:

6 samples

KLB67 Konkola Barren Gap:

11 samples

Elements

series of cross-plots comparing chalcophile minor & trace elements with S (and Cu)

Cu, Co, Bi, Ag, Au, Zn, Pb, As, V, Ni, Mo, U & Th

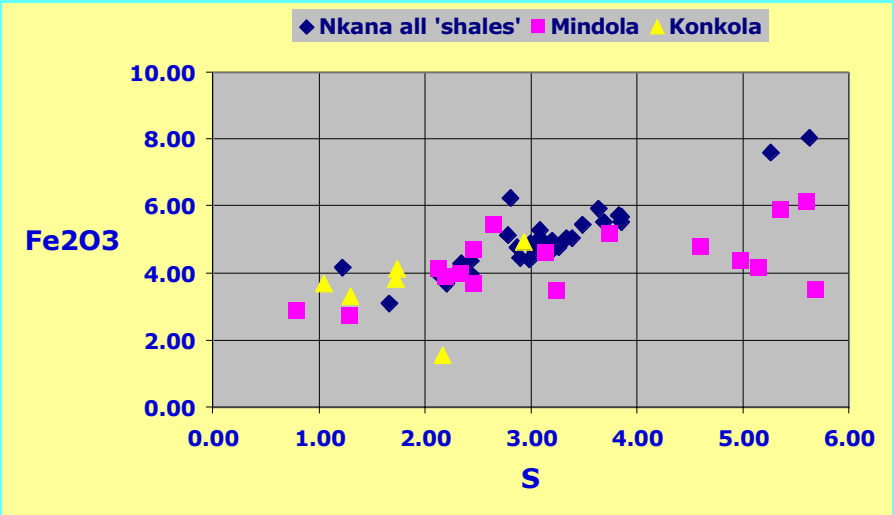

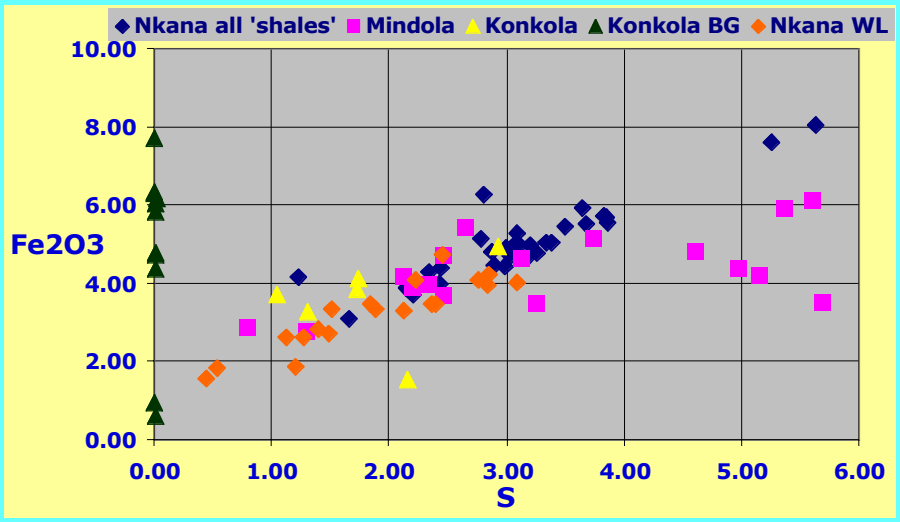

'average shale' = 35 ppm Cu
'black' shale = 70 ppm Cu
Aussie 'oil' shale = 110 ppm Cu

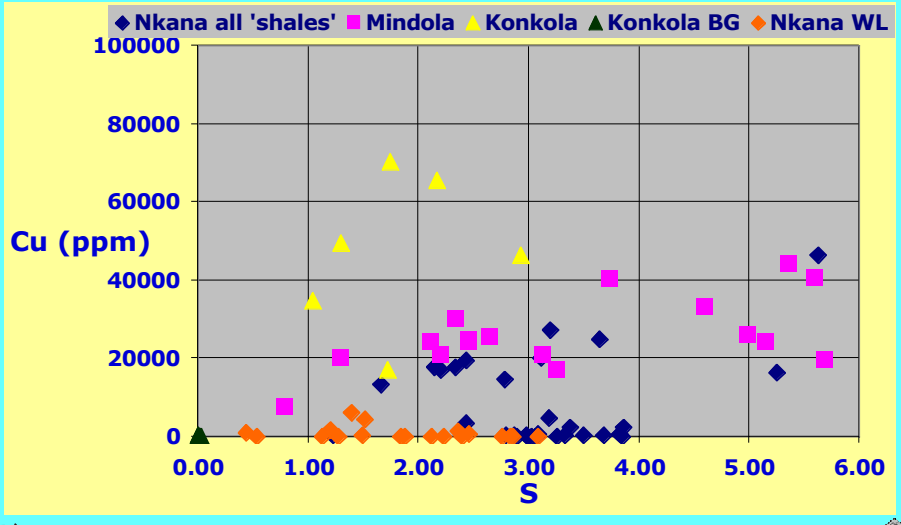

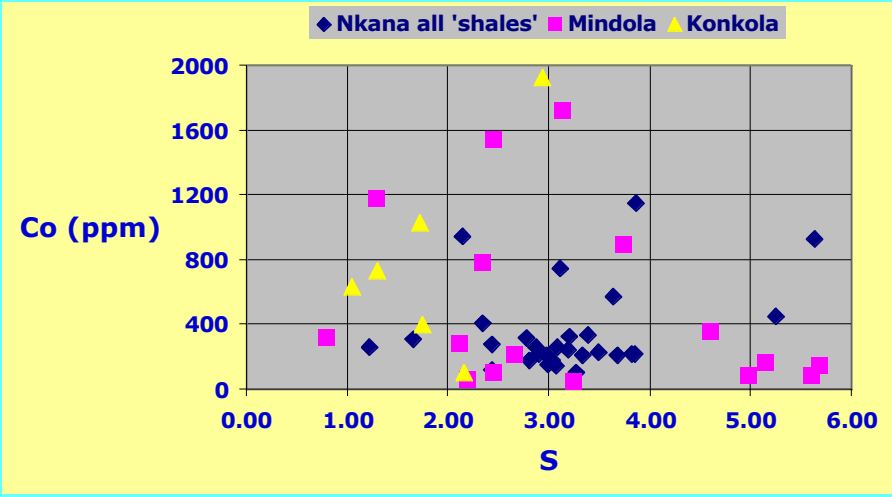
Nkana all 'shales'
Mindola
Konkola
Co (ppm)
2000
1600
1200
800
400
0
0.00
1.00
2.00
3.00
4.00
5.00
6.00
S

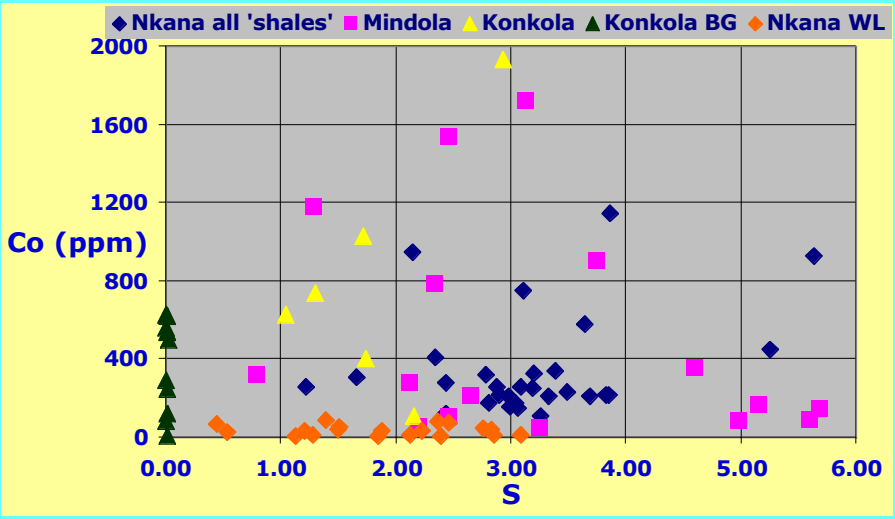
Nkana all 'shales'
Mindola
Konkola
Konkola BG
Nkana WL
Co (ppm)
2000
1600
1200
800
400
0
0.00
1.00
2.00
3.00
4.00
5.00
6.00
S

'average shale' = 20 ppm Co
'black' shale = 10 ppm Co
Aussie 'oil' shale = 9 ppm Co

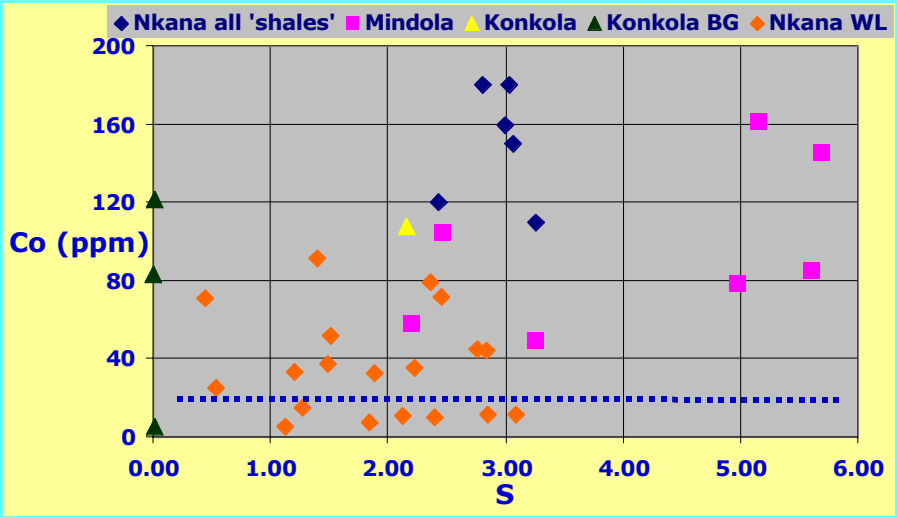

'average shale' = ~0.5 ppm Bi

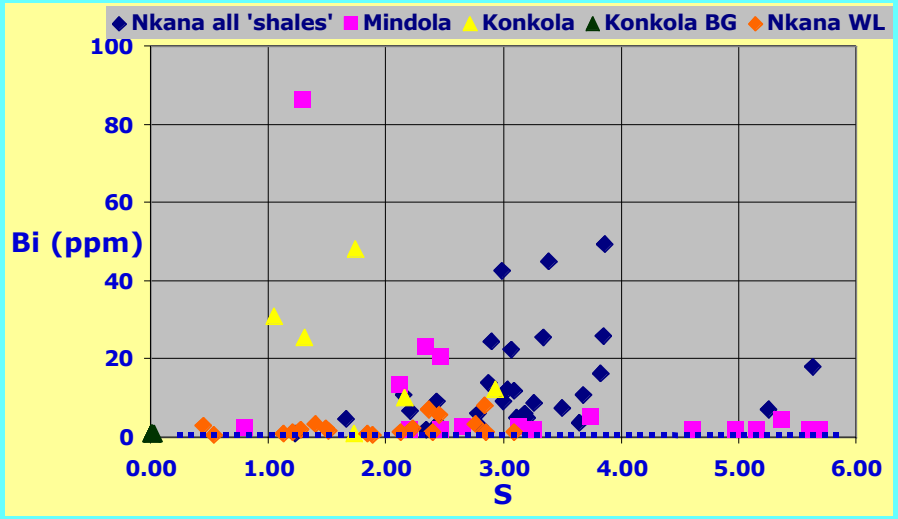

'average shale' = ~0.05 ppm Ag

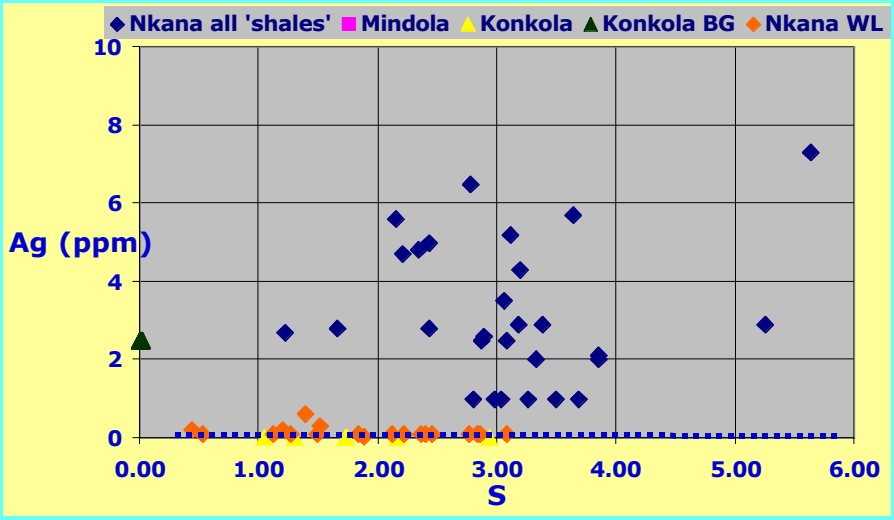

'average shale' = ~0.05 ppm Ag

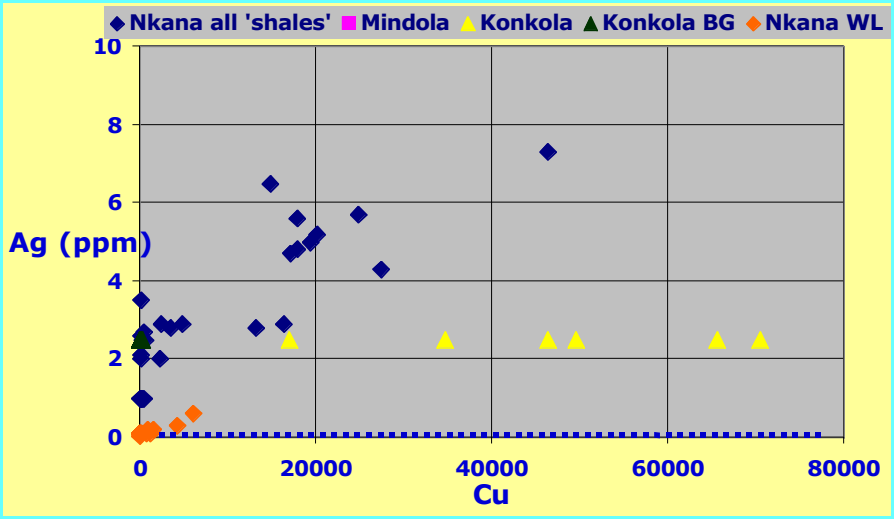

'average shale' = ~2 ppb Au

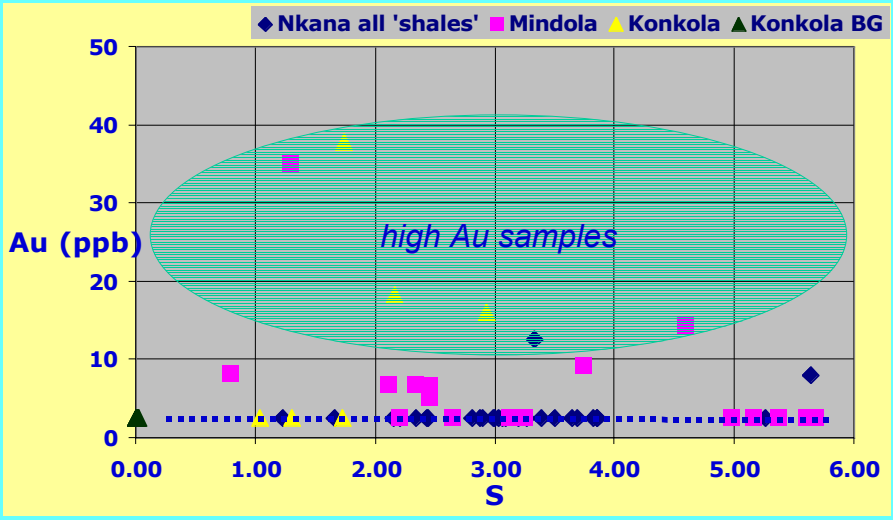

'average shale' = ~2 ppb Au

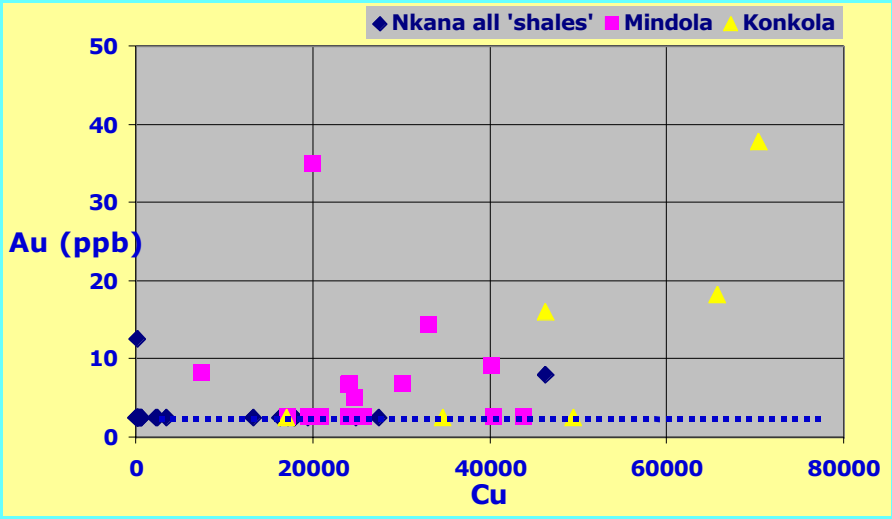

Slide 21

'average shale' = ~100 ppm Zn
Aussie 'oil' shale = ~800 ppm Zn

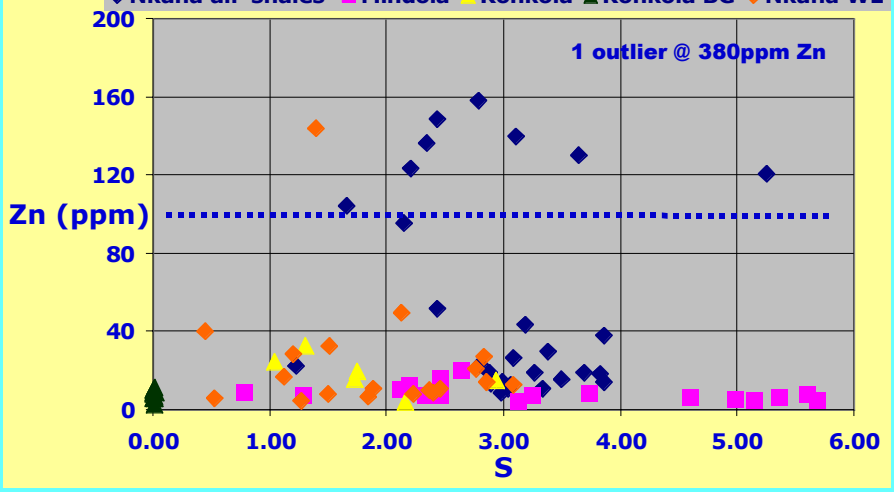

Slide 22

'average shale' = ~20 ppm Pb
'black' shale = ~20 ppm Pb

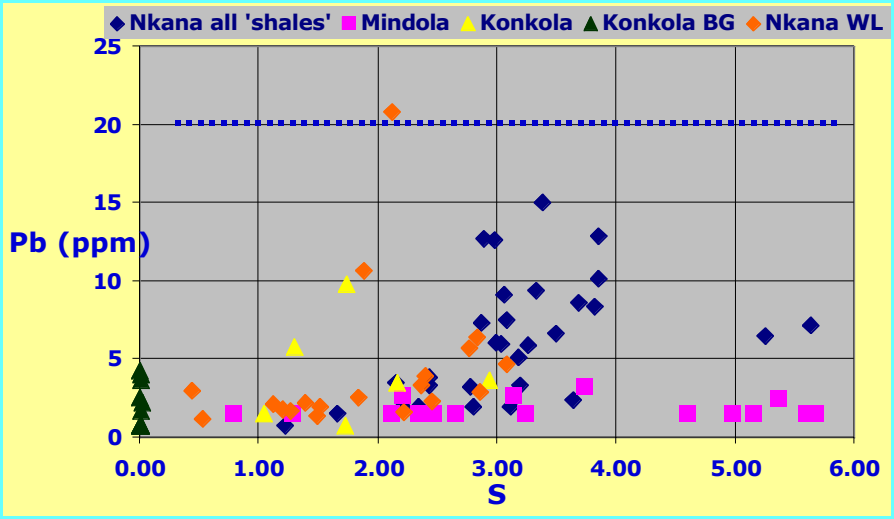

Slide 23

'average shale' = 13 ppm As
Aussie 'oil' shale = 50 ppm As

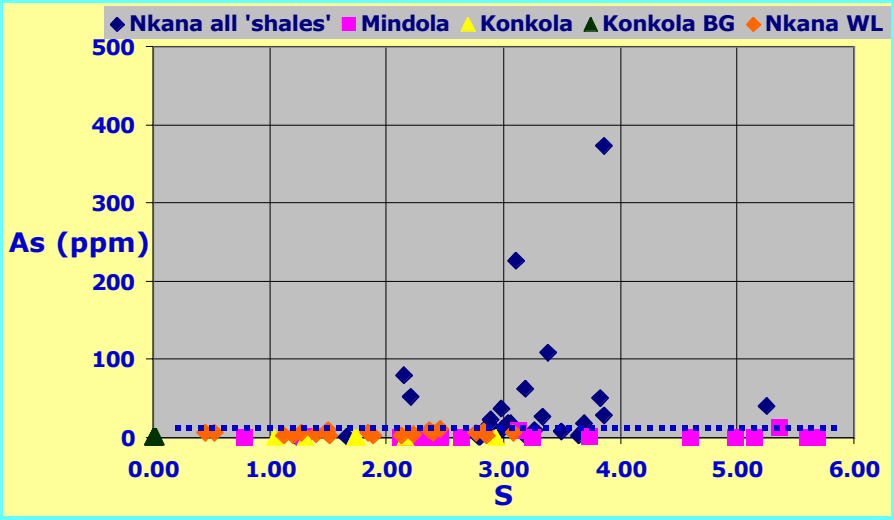

Slide 24

'average shale' = 13 ppm As
Aussie 'oil' shale = 50 ppm As

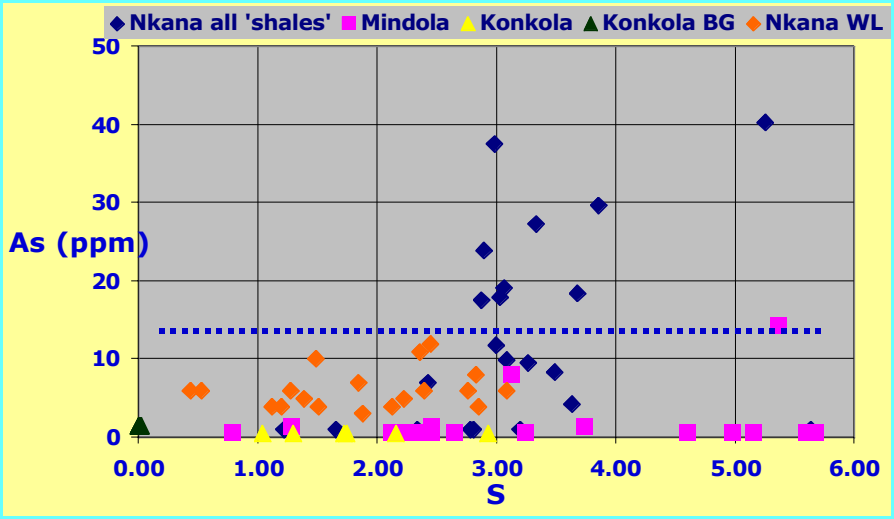

'average shale' = 98 ppm V
'black' shale = 150 ppm V
Aussie 'oil' shale = 2000 ppm V

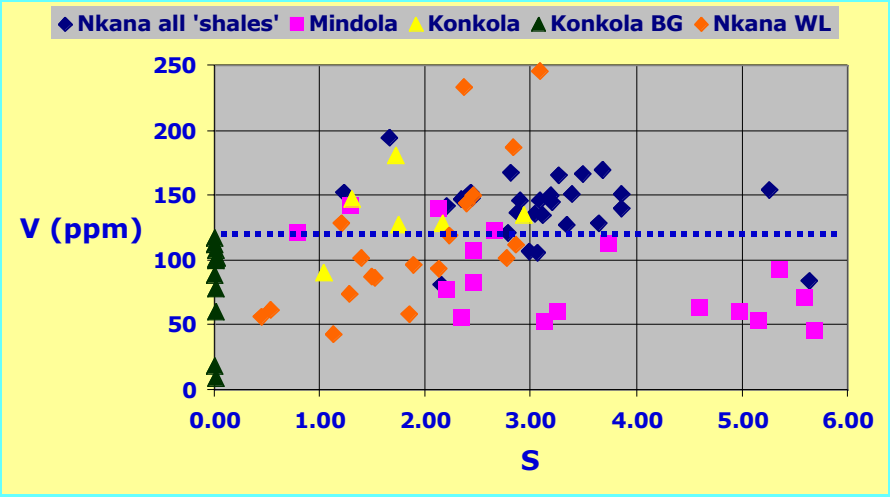

'average shale' = 42 ppm Ni
'black' shale = 50 ppm Ni
Aussie 'oil' shale = 160 ppm Ni

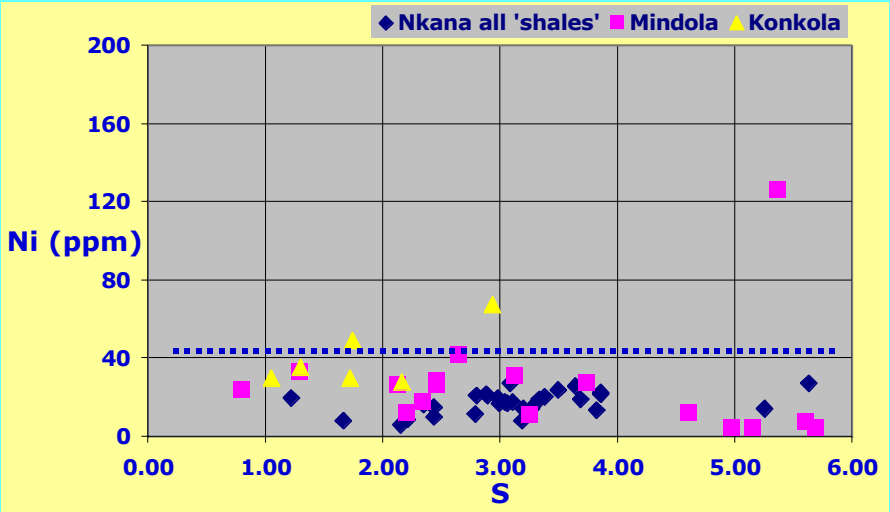

'average shale' = 0.7 ppm Mo
'black' shale = 10 ppm Mo
Aussie 'oil' shale = 270 ppm Mo

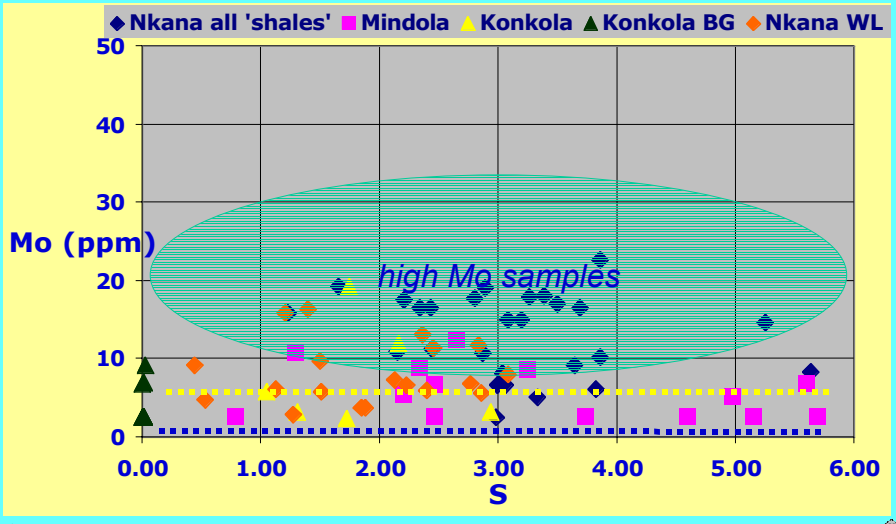

'average shale' = 2.5 ppm U
Aussie 'oil' shale = 30 ppm U

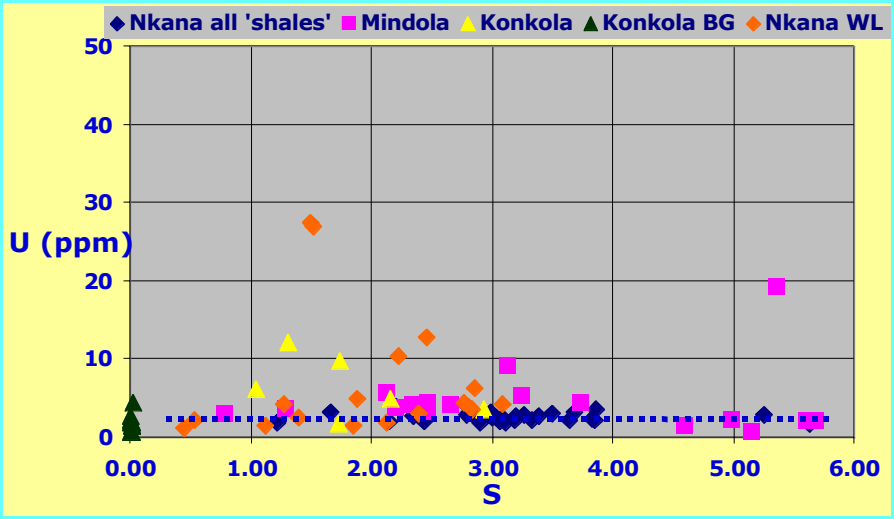

'average shale' = 2.5 ppm U
Aussie 'oil' shale = 30 ppm U

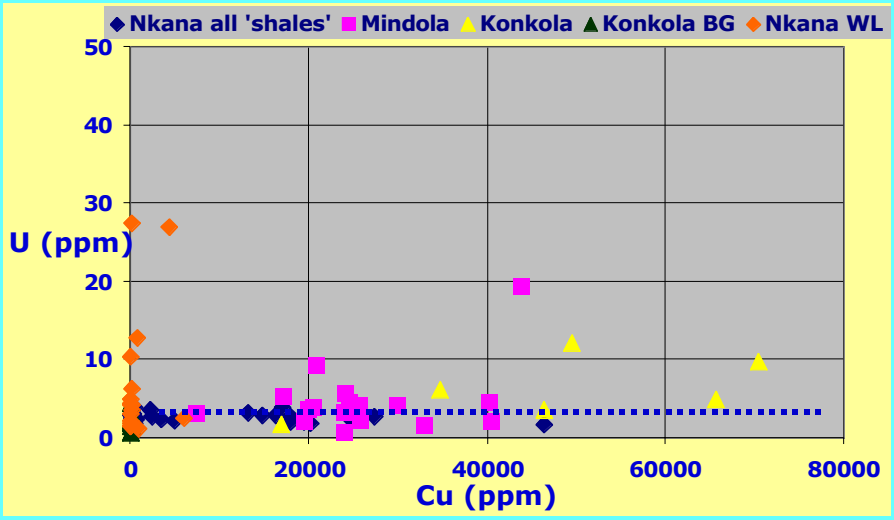

'average shale' = 12 ppm Th
Aussie 'oil' shale = 2.3 ppm Th

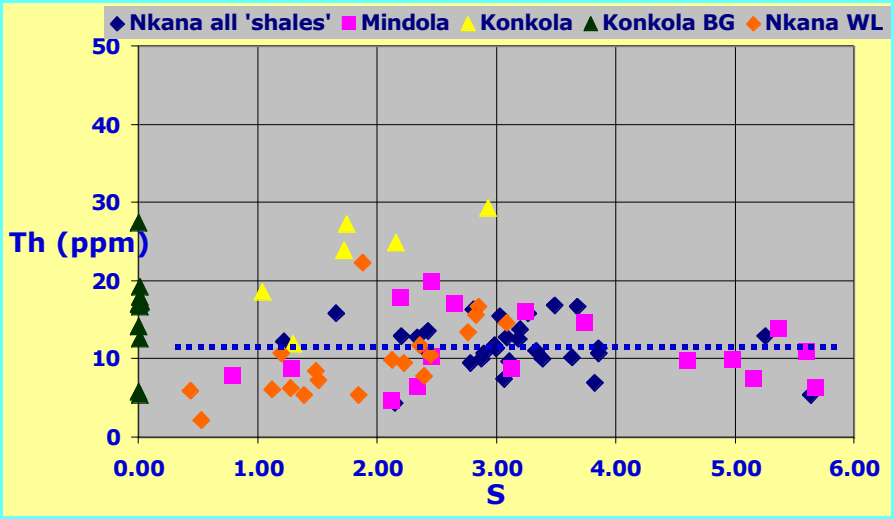

Thallium

All samples analysed by XRF were below detection limit (~1 ppm)

Samples analysed by ICP-MS were 0.1 to ~1 ppm

Ave. shale ~1 ppm

Organic Carbon

Limited number of analyses to date:

- 4 Nkana mill feed samples
- 7 Mufulira samples
- 6 Konkola u/g samples

Organic Carbon (con)

Nkana:

- total carbon 4.1 - 4.6 wt % ave: 4.2
- organic carbon 0.2 - 1.1 wt % ave: 0.7

Mufulira:

- total carbon 0.2 - 2.7 wt % ave: 1.1
- organic carbon 0.0 - 1.1 wt % ave: 0.4

Konkola:

- total carbon 0.0 - 1.8 wt % ave: 0.6
- organic carbon 0.0 - 0.2 wt % ave: 0.1

Conclusions I

- Cu, Co, Ag, Bi and Au (?Mo) are 'ore-association' elements:

cf 'average shale':

Cu - 100 to 1000x, Ag - ?100, Co - 50, Bi - ?20, Au - 1 to 10

- U is anomalous in ?'distal' samples at Nkana and may also be an 'ore-association' element (=broad halo)
- As, Sb, Ni, Pb, Tl and Zn in mineralised argillites are at levels < or = 'average shales'
- Of the 'ore-association' elements only Co is present at anomalous levels in both unmineralised *and* barren-gap samples
- Some black 'Ore Shales' are devoid of organic C

Clonclusions II

- Cu, Co, U, Au (?and Bi & Mo) are an 'oxidised' fluid signature
- low Tl is consistent with an oxidised ore fluid
- low organic C in some deposits (e.g., Konkola) may indicate all reductant was exhausted during ore precipitation
- variable Au tenor has implications for Au transport and ore-formation

Konkola North geochemistry: Preliminary observations

Nicky Pollington and Peter McGoldrick
Centre for Ore Deposit Research, University of Tasmania

Introduction

Three specific sampling programs were employed in this geochemical study at Konkola North:

1. Lithogeochemical samples to understand variations in geochemistry throughout the ore horizon.
2. Specific ore shale sampling of the different mineralised zones to determine if there is a geochemical characteristic which influences Cu mineral zonation.
3. Specific silt samples to determine if there is any difference between all the silts in the ore horizon and why the "Ore Shale" is copper mineralised and the others are barren or contain pyrite.

Samples were taken over two field seasons from the most recent drilling program of 50 holes carried out by AVMIN in 1998 (Slide 2).

Preliminary Geochemistry

About 150 samples have been taken in the Konkola North area and results have recently been received. For the purpose of this report an example of preliminary studies on these results will be presented. The first of these was to compare the lithogeochemical samples against the sedimentological logs which was carried out on three holes. Slide 3 shows Kn6 as an example of the holes which were sampled for lithogeochemistry and the simplified geology and facies (further details in Pollington and Bull, this volume).

Slide 4 shows some elements plotted against down hole position for Kn6. This slide shows that Co, Mo, Bi and U all follow the same distribution pattern as Cu. Further analyses not shown for the three holes indicate the following features:

- High K_2O in the ore horizon (average above 10% as compared to the world average of 3.2%) with apparently lower in Footwall.
- CaO and MgO only elevated in logged carbonate zones within the top part of the ore horizon.
- Al_2O_3 is patchy and defines weathered zones.
- Na_2O is low overall and discrete high patches define albite alteration.
- TiO_2 is erratic.
- TiO_2/Zr ratio is also erratic but is highest in the two mineralised horizons- the Ore Shale and the upper ore shale.
- K_2O_3/Al_2O_3 ratio suggestive of an indicator towards the ore shale in Kn6 but not as convincing in Kn35 and Kn1.
- Cu is variable throughout the ore horizon.
- Zn is low overall and shows little association with Cu.
- Co increases gradually towards the ore shale.
- Bi is low throughout however peaks distinctly with Cu.
- Mo, U and V are variable but also peak distinctly with Cu.

Some of the downhole data was confined within the ore shale as part of the comparative study (Slide 6). These data show a distinct variation of some chalcophile elements within the ore shale in a pattern which may suggest a supergene remobilisation of Copper. A number of holes were investigated however only S, Cu, Co and V are shown in Slide 6. The data from the other holes follows:

- Kn16 has a much higher Co content overall. Also MnO and P_2O_5 exhibit pronounced enrichment and S is depleted in the highest grade areas. This mineral assemblage is consistent with the observation of plumbogummites or Wad in the logging (Slide 7).
- KN19 has much lower Co, MnO and P_2O_5 values and less erratic distribution of most other elements shown. This is also consistent with the less weathered appearance. One sample from this set was observed to be much more intensely weathered when sampled (1133 m) and this exhibits depletion in Cu, S, Co, V and Ni, and enrichment in Zn, U, MnO and P_2O_5. The very high Bi peak is not associated with anything observed from logging and will be investigated with thin section analysis.
- Both holes exhibit a reduction in S towards the base of the ore shale and no corresponding drop in Cu. Kn19 has an enrichment of Cu towards the base. This is interpreted to be a result of the effect of deep circulating waters in the footwall aquifer.

The results from the ore shale samples which were taken in order to study the difference between the mineralised zones have also been received. These are specific samples and detailed petrography needs to be completed before the interpretation of these can begin. For the purpose of this report these samples were grouped into (1) sulphide mineralisation, (2) oxidised mineralisation and (3) barren ore shale. The chalcophile elements have been compared to those in "average world shales" (see McGoldrick, this volume). This is shown graphically in Slide 8, which are spider plots of the relative enrichment or depletion of the chalcophile elements with 1 being the average shale. These graphs show that the sulphide and oxide mineralisation exhibit similar patterns in the distribution of chalcophile elements. Also the barren ore shale exhibits the same pattern with less extreme variations. The ore shale is enriched in Ag, Au, Ba, Bi, Co, Cu, Mo, U and V, and depleted in As, Ni, Pb, Sb, and Zn.

Conclusions

1. Co, Au, Ag, Bi, U, Mo are associated with mineralising fluid.
2. Ore Shale
   - enriched in Ag, Au, Cu, Co, Mo, Bi, V, U
   - depleted in Ni, Pb, Sb, Zn.
3. Mild to intense supergene overprint complicates the geochemistry of the ore shale and detailed petrography is required before further data interpretation.
4. Supergene effects
   - depletion of S and enrichment of Cu (V?)
   - local development of MnO, P_2O_5 (±Cu and Co).

Zambian Copper Belt Geochemistry:
Part 2 Konkola North

Nicky Pollington, Peter McGoldrick &
David Selley
CODES

Konkola North with Geochemical Sample Locations

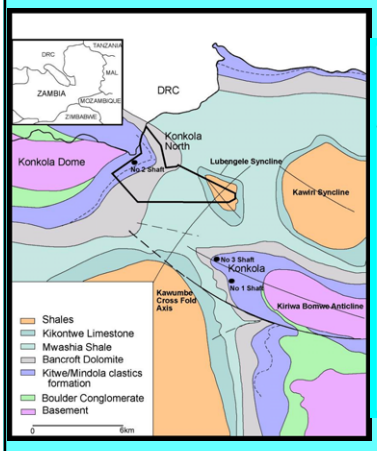

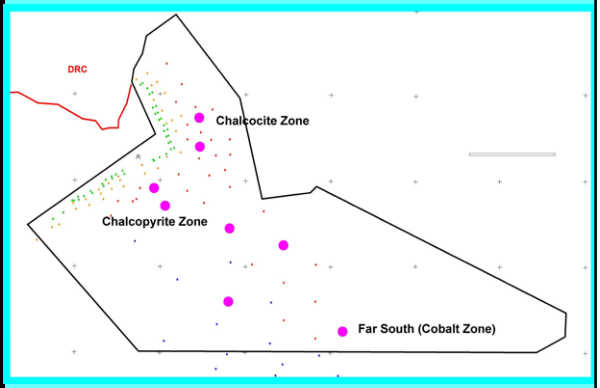

Simplified Geology for Kn6

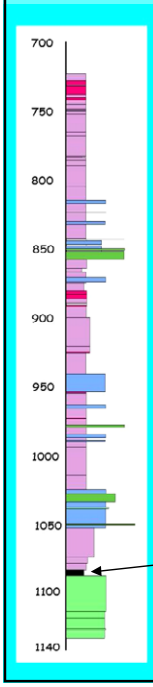

- Mwashia – fine dark silts
- Shale with Grit – fine dark silt with qtz and fspar grit
- Konkola Conglomerate
- "Upper Ore Zone" – dark silt with common py +- cpy
- Mixed Sequence – silt, sand, conglomerate
- Arkosic sandstone – conglomerate
- OS2 – mixed dark silt and sand
- "Ore Shale"
- Kafufya – sandstones and conglomerates

Konkola Conglomerate

Mixed Sequence

Ore Shale

Kafufya

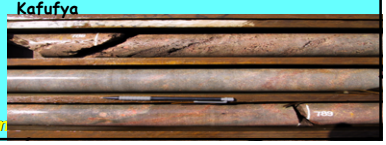

Argillite Geochemistry

- Database of over 150 multi element analyses has been compiled
- Chalcophile elements investigated for this presentation

  Cu, Co, Bi, Ag, Au, Zn, Pb, As, V, Ni, Mo, U, Th

- Downhole variations from Mwashia to Footwall
- Downhole variations within the Ore Shale
- Comparison to "Average Shale"

Lithogeochemistry of Ore Horizon in Kn6

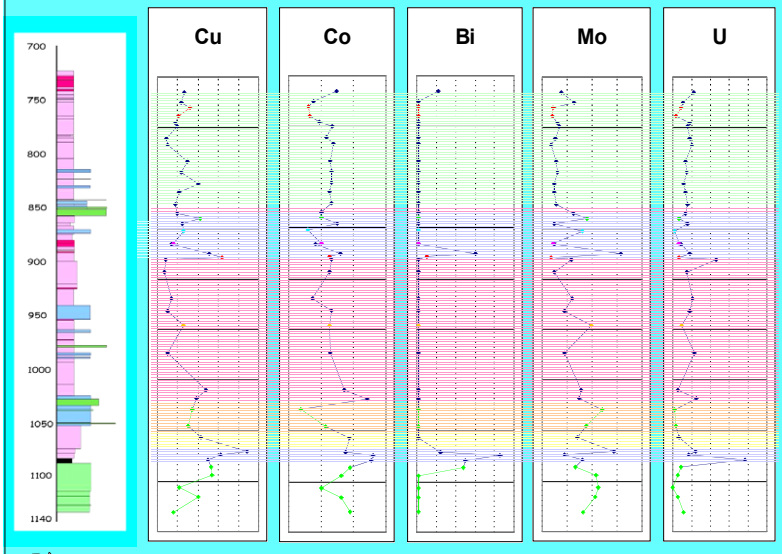

Ore Shale Downhole Variation

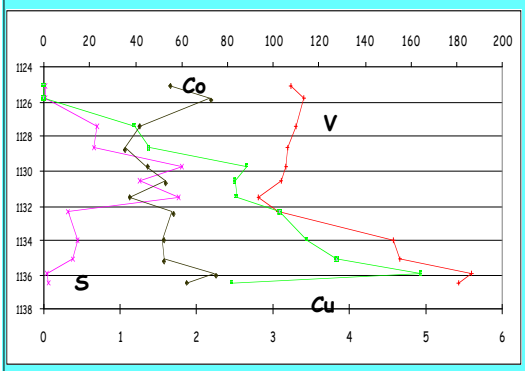

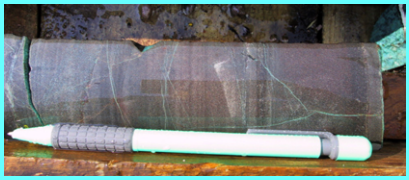

- S content variable within the ore shale
- Supergene minerals such as Mal common on contacts with footwall and hanginwall
- Commonly elevated Cu and reduced S at base where in contact with the footwall aquifer
- Elevated V appears to follow same pattern – related to same supergene effects(?)

Ore Shale Downhole variation- Far South

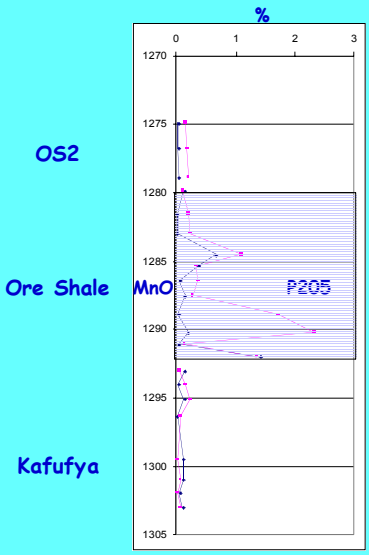

- MnO and P2O5 enriched in southern zone

Chalcophile Elements Normalised to "Average Shale"

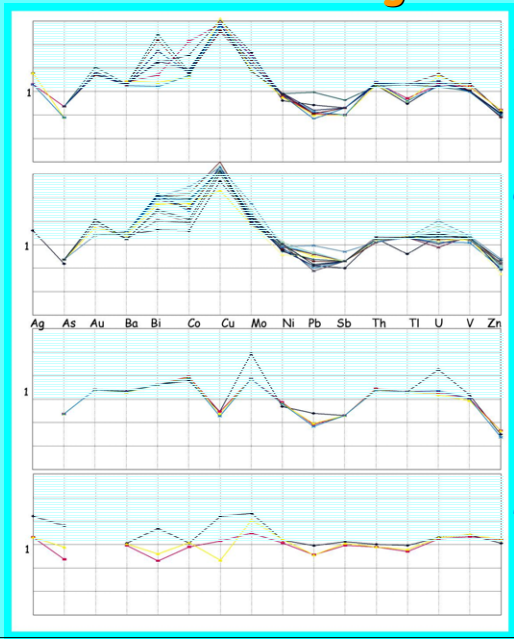

Sulphide Mineralised Ore Shale

+Ag, Au, Cu, Co, Mo, Bi, V, U,
-Ni, As, Pb, Sb, Zn

Oxidised Ore Shale

+Ag, Au, Cu, Co, Mo, Bi, V, U,
-Ni, As, Pb, Sb, Zn

Unmineralised Ore Shale

+Au, Co, Mo, Bi, V, U,
-As, Ni, Pb, Sb, Zn

Mwashia

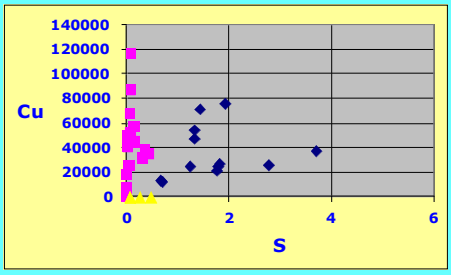

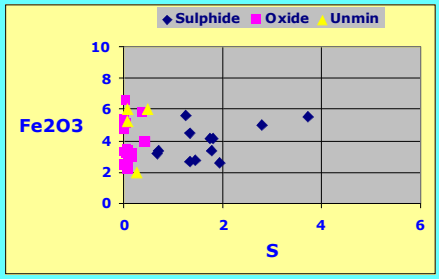

'average shale' = 35 ppm Cu

'average shale' = 20 ppm Co

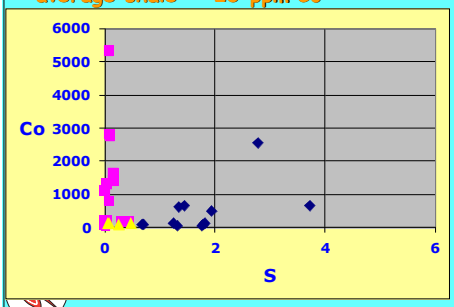

'average shale' = ~0.5 ppm Bi

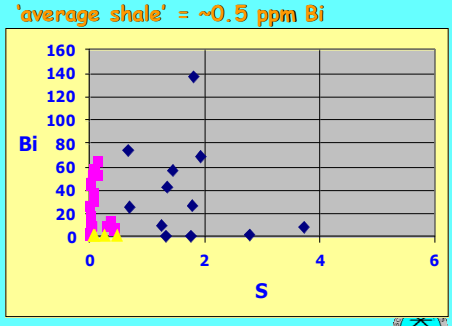

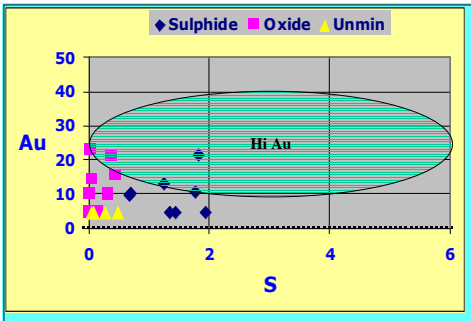

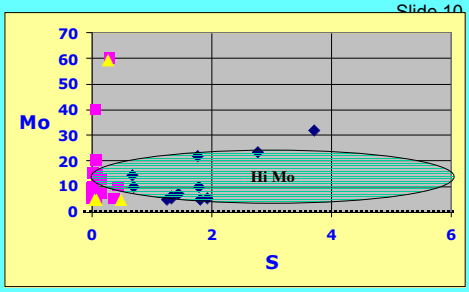

'average shale' = ~2 ppb Au

'average shale' = 0.7 ppm Mo

'average shale' = 2.5 ppm U

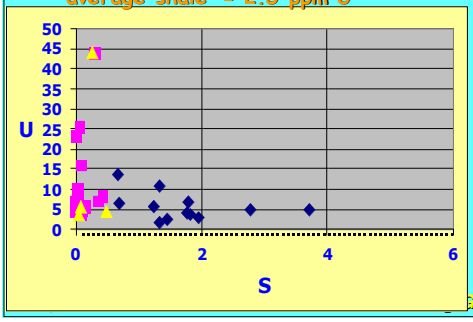

'average shale' = 12 ppm Th

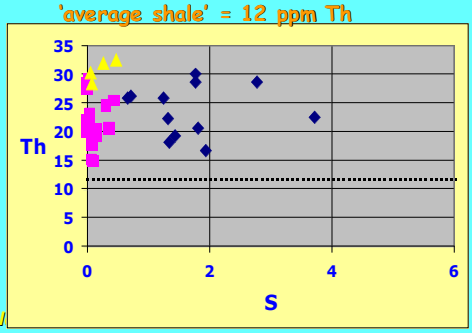

Summary

- Co, Au, Ag, Bi, U, Mo are associated with mineralising fluid
- Ore Shale
  - enriched in Ag, Au, Cu, Co, Mo, Bi, V, U
  - Depleted in Ni, Pb, Sb, Zn
- Mild to intense supergene overprint complicates the geochemistry of the ore shale and detailed petrography is required before further data interpretation
- Supergene effects
  - Depletion of S and enrichment of Cu (V?)
  - Local development of MnO, P2O5 (+- Cu and Co)

Zambian Copperbelt geochemistry III: Preliminary assessment of chemostratigraphy, alteration geochemistry and C-O isotopes in carbonates

Ross Large, Peter McGoldrick and Mawson Croaker
Centre for Ore Deposit Research, University of Tasmania

Summary

This report presents an assessment of geochemical and C/O isotope data from two drill cores in the Chambishi Basin that provide a continuous section through lower Mwashia and Roan rocks. Comparisons are made between 'shaley' rocks in these drill holes and 'Ore Shale' samples from Nkana (Croaker, - this volume; McGoldrick et al., this volume).

The data show that immobile elements (Ti/Zr ratios) in siliciclastic units may assist with correlations, and the 'Ore Shale' at Nkana has a distinct Ti/Zr ratio of 22–26. There are systematic variations in K, Na and Al_2O_3 in siliciclastics from RCB2 that define a halo of K-feldspar enrichment the hanging wall to the 'Ore Shale'. The 'Ore Shale' at Nkana and Konkola is enriched in K and depleted in Na compared to normal shales.

Carbonates and carbonate-rich units have more variable Ti/Zr ratios than the siliciclastics, but their C/O isotopes may provide a vector to ore. Carbonates proximal to ore have isotopically light C and light O, compared with other carbonates. This coupled C-O isotope depletion in carbonate is consistent with a moderate to high temperature fluid (150°–350°C), with $\delta^{18}O$ near zero (seawater?), interacting with organic carbon and sedimentary carbonate at the site of ore deposition (see also Croaker, this volume).

Introduction

The aims of this preliminary lithogeochemical study were four-fold:

1. To test whether there are significant chemostratigraphic variations in the Roan sequence, that may assist with stratigraphic correlations.

2. To test whether there are particular major or trace elements in the sediments that vary in proximity to copper mineralisation.

3. To assess potential lithogeochemical vectors to ore.

4. To study the variation in carbon and oxygen isotopes of different types of carbonates within and remote from mineralisation.

Samples for this study were collected from two stratigraphic holes RCB1A and RCB2 within the Chambishi Basin (slide 2 in the Powerpoint® presentation following this report). Lithogeochemical and isotopic comparisons were made with a series of samples collected from the ore shales and adjacent host rocks at Nkana-Mindola, along the southeast margin of the basin (slide 2).

Stratigraphic drill holes

RCB1A

This 812-m drill hole is collared in the Mwashia shales and siltstones, drills into the Upper Roan carbonates, siltstones and shales, and terminates in a dolerite intrusion with brecciated margins (slide 3). This hole did not intersect significant mineralisation and finished at least 500 m stratigraphically above the 'ore shale.' Forty samples where collected for analysis from this hole.

RCB2

Collared about 5 km northeast of RCB1A, this 1850m hole intersected the Upper Roan and Lower Roan (slide 3) including a 100-m thick zone of mineralised 'ore shale' from 1230 to 1330 m down-hole. The complete stratigraphic sequence above the ore shale was sampled and analysed (39 samples). Core through the mineralised section was jumbled and partly missing, and no samples of this section were collected for analysis. Samples through the sandstones and conglomerates below the mineralised section will be analysed for the next report.

In the stratigraphic logs in slide 3 colour coding is blue-carbonates, grey-shales and siltstones, brown-sandstones and orange-conglomerates and sandstones. Triangles are breccia zones.

Analytical Techniques

All samples from RCB1A and RCB2 were cleaned, crushed and milled using facilities in the School of Earth Sciences, University of Tasmania. Large samples were jaw-crushed, mixed, and carefully split. Smaller samples were crushed and split into two equal parts. One split from each sample was milled in a W-C ring mill and this powder was used for the multi-element analyses. A second split of each sample was milled in a Cr-steel mill, and this powder was used for W and Co determinations.

The powdered samples were analysed by XRF for a range of major and trace elements (see McGoldrick, this volume, for a list of all elements analysed) at the University of Tasmania.

Isotope determinations for C/O were carried out on whole rock powders containing more than approximately 10wt% carbonate. Analyses were made on a VG (Micromass) Optima mass spectrometer. The precision of analyses is ±0.2‰ for both C and O.

Chemostratigraphy of RCB2

Samples from RCB2 were divided into two groups for the down-hole chemostratigraphy plots (slides 6 to 18).

Group 1: siliclastics defined by loss on ignition LOI < 20 wt% (sandstones, conglomerates, siltstones and shales)

Group 2: carbonates defined by LOI ≥ 20 wt% (dolomites and dolomitic siltstones and sandstones)

Because LOI roughly equals CO_2 content in the Roan sediments, then LOI is a good measure of the carbonate content of the sediments. From the plot of LOI variation down-hole (slide 6) it is apparent that in the 400 m thickness of sediments above the 'ore shale' (800–1200 m down hole) the carbonate content of both sediment groups 1 and 2 decreases through the hanging wall sediments towards the 'ore shale'. This is interpreted as a result of variation in the sedimentary facies and may suggest a gradual shallowing of the basin above the 'ore shale'.

Immobile elements

A variety of immobile element ratios were plotted to test for chemostratgraphic variation. The only ratio which showed potential for systematic variation down-hole was Ti/Zr. The plot of TiO_2 vs Zr for all siliclastic samples analysed (slide 4), suggests the following:

- The 'ore shale' from Nkana has a tight distribution with Ti/Zr = 22 to 26. Also TiO_2 and Zr values are commonly low with TiO_2 < 0.8 wt% and Zr < 200 ppm.
- Upper Roan siliclastics are more variable with Ti/Zr = 12 to 38 (slides 4 and 8). Two distributions are suggested by the data; Ti/Zr ~ 18 and 35.
- Mwashia shales are more Ti-rich than the ore shale, with Ti/Zr = 30 to 36.

The tight distribution of Ti/Zr in the Nkana 'ore shale' needs checking with analyses from other ore shales throughout the Copper Belt. This will be reported at the next meeting.

Although the Ti/Zr is well constrained within the siliclastics, by contrast this ratio (and others we have tried) shows erratic down-hole variations in the carbonate samples (slide 8). For this reason it is

recommended that only the siliclastic units be sampled for chemostratigraphic correlations.

Alkali elements (Na_2O and K_2O)

Of all the major elements the alkalies show the most systematic down-hole variation and are worthy of some discussion.

The down-hole plot of Na_2O (slide 10) in both the carbonates (blue line) and the siliclastics (red line) indicates the following:

- Upper Roan siliclastics average around 1.8 wt% Na_2O. This equates to about 15 wt% albite. Whether this albite is detrital or metasomatic is yet to be determined.
- Discrete zones of metasomatic albite contain 5 to 7 wt% Na_2O (45–60 wt% albite). These zones are commonly associated with brecciation and alteration of siltstones and sandstones (e.g. 802 m in RCB2, slides 10 and 11)
- Carbonates commonly contain < 0.1 wt% Na_2O, except for a zone of albite-bearing carbonates at 530 to 640 in RCB2.

K_2O commonly exhibits and inverse pattern to Na_2O. Unlike sodium, which is only present in albite in the Roan sediments, potassium is present in biotite, muscovite and K-feldspar. The down-hole variation in K_2O shown in slide 13 indicates the following;

- Upper Roan siliclastics vary from 2.5 to 8 wt% K_2O with a mean of 4.2 wt%. This compares to a world average for shales of 3.2 wt% (McGoldrick, this volume)
- Carbonates are consistently low in K_2O, showing values of 0.1 to 2 wt%.
- There is an increase in K_2O from levels of less than 1 wt% to over 7 wt%, over a stratigraphic distance of 400m, towards the 'ore shale' in the hanging wall siliclastics.

The variation from 1 to 4 wt% K_2O probably relates to variations in the content of metamorphic biotite (after muscovite) and detrital K-feldspar, which are controlled by the primary sedimentary facies. However K_2O values in the range 4–8 wt% are very anomalous for these types of sediments, and thus probably relate to K-feldspar (and biotite?) metasomatism associated with the copper mineralising event.

A systematic pattern of increasing K-feldpar alteration in the sediments from 800 to 1200 m down-hole toward the 'ore shale' is strongly suggested by the K_2O/Al_2O_3 ratio (slide 15). This ratio varies from values close to zero (no K-bearing minerals), to over 0.6, where the rock contains 7.5 wt% K_2O, which equates to about 50 wt% K-feldspar. From slide 17 it is apparent that potassic sediments with K_2O/Al_2O_3 between 0.4 and 0.9 are rich in K-felspar $\pm$ biotite, whereas sediments with K_2O/Al_2O_3 below 0.4 are deficient in K-feldspar but will contain biotite $\pm$ sericite.

Trace elements

Most of the chalcophile trace elements shown no patterns that appear to relate to the proximity of the copper-bearing ore shale in RCB2. For example, except for anomalous values at about 450 m down-hole (slide 18), Cu shows a flat distribution, with values of less than 20 ppm over 700 m in the hanging wall of the 'ore shale'.

Zinc and cobalt exhibit patterns that require further investigation (slide 18). Zinc increases systematically from 10 to 40 ppm in the hanging wall sediments towards the 'ore shale' over a stratigraphic interval of 300 m. Cobalt increases over the same interval from about 2 to 30 ppm.

Chemostratigraphy of RCB1A

RCB1A was terminated in the Upper Roan at least 500 m above the ore shale.

Down-hole Ti/Zr ratio in the siliclastics shows a change from values above 26 to below 22 at a depth of around 400 m (slide 21). This may correspond to the contact between the Mwashia and the Upper Roan. Further work is required to verify whether Ti/Zr can be used to define this contact in other drill holes.

K_2O and K_2O/Al_2O_3 plots (slide 44) indicate that RCB1A did not penetrate deep enough through the Roan to detect the K-feldspar alteration, assumed to be related to ore, previously defined in RCB2 (slide 13).

Na_2O values in the siliclastics average around 2–3 wt%, and are slightly higher than the background values in RCB2. Three samples toward the bottom of the hole (600–800 m) show intense albite alteration and probably correlate with albite altered zones at similar depths in RCB2. It is interesting to note that the albite alteration extends into the dolerite in RCB1A, and thus is synchronous with, or post dates, dolerite intrusion.

Carbon and oxygen isotopes in carbonates

Sixty-two carbonate-rich sediments from RCB1A and RCB2 have been analysed for C and O isotopes, and the results compared with data from the Nkana-Mindola 'ore-shale' discussed in the following section. Where necessary, samples were drilled-out with a dentist drill to obtain relatively carbonate-rich portions. Analysis of the isotopes was undertaken in the Central Science Laboratory, University of Tasmania, using standard procedures.

RCB2

Down-hole plots of $\delta^{18}O$ and $\delta^{13}C$ in carbonate are shown in slide 24. Sedimentary carbonates in the Upper and Lower Roan exhibit values of $\delta^{18}O = 20$ to 28‰ with a mean of 24‰ and $\delta^{13}C = -2$ to +5‰ with a mean of +2.2‰. These values are compatible with the range of Proterozoic sedimentary and diagenetic carbonates recorded by other workers (e.g. Veizer et al., 1992; Large et al., 2001a).

Two zones in RCB2 (slide 24) show a major excursion from the normal sedimentary/diagenetic isotopic values.

1. Between 750 and 910 m down-hole, $\delta^{18}O$ values drop nearly 20‰ to values around +5‰. $\delta^{13}C$ values show a minor decrease of about 5‰ over the same interval. This interval is marked by carbonate-albite veining and patchy breccia textures, but contains no significant copper mineralisation.
2. Between 1100 and 1210 m, in the immediate hanging wall of the 'ore shale', the sedimentary carbonate shows a marked and systematic decrease in $\delta^{13}C$ values from +5 to –5‰. This is accompanied by a less systematic decrease in $\delta^{18}O$ values from 25 towards 15‰. As outlined below this coupled decrease in both $\delta^{18}O$ and $\delta^{13}C$ is considered to represent a hanging wall halo to the copper mineralisation and provides a vector to ore.

Comparison with carbonates in the 'ore shale' and footwall

Samples collected by Mawson Croaker from the 'ore shale' or Copperbelt Orebody Member (COM) at the Nkana-Mindola mine, exhibit distinctly lower $\delta^{13}C$ and $\delta^{18}O$ values than the sedimentary/diagenetic carbonates in RCB2 (slide 27). The trend of coupled decreasing $\delta^{18}O$ and $\delta^{13}C$ exhibited by the hanging wall samples in RCB2 trends toward the field of the ore-related carbonates in slide 27, strongly suggesting that these hanging wall samples represent an isotopic halo to the mineralisation.

Six carbonate-bearing sandstones from below the ore zone in drill hole NN42 show values that are close to the 'ore shale' carbonates, but with $\delta^{13}C$ values lying between the sedimentary carbonates and the 'ore shale' carbonates (slide 27).

A more detailed discussion of the C/O isotopes of carbonates in the Nkana-Mindola mine area is provided in the accompanying paper by Croaker (this volume).

RCB1A

Carbonate samples from the Upper Roan in RCB1A have similar values to those in RCB2 (slide 26). A minor negative excursion in $\delta^{13}C$ occurs at 500–600 m which may correspond to a zone of albite/carbonate alteration (slides 26 and 44). Four samples from the upper-most part of the drill hole, in the Mwashia, have a significantly lower $\delta^{13}C$ signature than the Upper Roan sediments. Further sampling of the Mwashia carbonates is required to check this difference.

Discussion and preliminary isotope interpretation

The coupled trend of decreasing $\delta^{18}O$ and $\delta^{13}C$ values passing from background sedimentary carbonates

towards the ore zone carbonates, revealed in this study of the Chambishi Basin, is similar to trends found in the halo zones of replacement Zn-Pb deposits such as Irish style, skarn style and MVT deposits (slide 29, Large et al., 2001a). This negative $\delta^{18}O$ trend is very different to the positive trend found in the halo of some north Australian SEDEX deposits (slide 29).

Isotope modelling of fluid–rock interaction between a hydrothermal fluid and pre-existing carbonate-bearing sediments (e.g. Zheng and Hoefs, 1993; Large et al., 2001a, slide 30) reveals that these coupled negative trends of $\delta^{18}O$ and $\delta^{13}C$ found in the halo of many replacement deposits result from the interaction of a moderately hot fluids (150° to 350°C), of low $\delta^{18}O$ composition (either seawater or meteoric water), with the carbonate-bearing host rocks.

The very negative $\delta^{13}C$ values of carbonates in the ore zone, is unlikely to be the result of simple hot fluid-rock interaction, but strongly suggests the involvement of organic carbon in the mineralization process. These strongly negative carbon isotopes probably result from the oxidation of organic carbon at the site of mineral deposition, with the evolved CO_2 incorporated into the ore-related carbonate.

Conclusions from the C/O isotope studies

- Sedimentary and diagenetic carbonates in the Upper Roan have $\delta^{18}O$ = 20 to 28‰ and $\delta^{13}C$ = 5 to 2‰, similar to Proterozoic carbonates reported elsewhere.
- Ore-related carbonates analysed to date, are strongly depleted in both ^{18}O and ^{13}C ($\delta^{18}O$ = 8 to 18‰ and $\delta^{13}C$ = –7 to –20‰), compared to the sedimentary and diagenetic carbonates
- A halo of both ^{18}O and ^{13}C depletion extends into the hanging wall sediments above the mineralised 'ore shale' for at least 100m in RCB2, and provides an excellent vector to ore.
- Alteration carbonates in the footwall sandstones and conglomerates also show significant depletion in ^{18}O and ^{13}C.
- Isotope modelling of the coupled C-O depletion associated with the copper mineralisation suggests
  - An ore fluid with $\delta^{18}O = 0 \pm 5$‰
  - Moderate to high temperatures: 150° to 350°C ?
  - Involvement of organic carbon oxidation in the ore forming process
- The strong ^{18}O depletion in the albite-carbonate breccia zones suggests involvement of a different fluid to that responsible for the copper mineralisation; possibly meteoric with $\delta^{18}O$ = ~–10‰.

Towards developing a Copper Belt lithogeochemical vector diagram

The development of alteration indices has become an important part of the process of applying lithogeochemistry in mineral exploration. VHMS alteration indices have been used for sometime now (e.g. Ishikawa et al., 1976; Galley, 1995), and SEDEX alteration indices have been recently developed (e.g.Large and McGoldrick, 1998).

Large et al. (2001b) have shown, how alteration indices can be combined to develop an alteration box plot or vector diagram for VHMS exploration. Vector diagrams of this type can be powerful tools in understanding the relationship between mineralogy, lithogeochemistry and intensity of alteration in zoned alteration systems related to ore deposits and should assist the exploration geologist in determining vectors to the centre of the ore system.

In this section we explore the possibility of developing a lithogeochemical vector diagram for exploration in the Copper Belt.

The VHMS alteration box plot

The alteration box plot is a combination of the Ishikawa alteration index (AI) plotted on the horizontal axis and the chlorite-carbonate-pyrite index (CCPI) plotted on the vertical axis (slide 34). Least altered volcanics plot toward the centre of the diagram, and hydrothermally altered volcanics plot at varying positions dependent on the principal hydrothermal minerals present. The mineral end members (albite, K-feldspar, sericite, chlorite, pyrite, dolomite, ankerite and epidote) plot along the boundaries of the box (Large et al., 2001b, fig 4).

The two selected alteration indices are based on the elements added and elements lost during the alteration process:

Ideal Alteration Index =

$$\frac{100(\text{major elements added})}{(\text{major elements added} + \text{major elements lost})}$$

$$AI = \frac{100\ (K_2O + MgO)}{(K_2O + MgO + Na_2O + CaO)}$$

(sericite and chlorite alteration)

$$CCPI = \frac{100\ (MgO + FeO)}{(MgO + FeO + Na_2O + K_2O)}$$

(chlorite, pyrite and Fe-Mg carbonate alt.)

where FeO is total ($FeO + Fe_2O_3$) content of the rock

In slide 43, as the volcanics become progressively hydrothermally altered, by initially sericite, and then chlorite and pyrite, the plotted compositions move out of the least altered box and head toward to top right-hand corner of the diagram, marked as the 'ore centre'. A diagonal line across the box plot joining epidote and K-feldspar divides the plot area into two fields. The lower left-hand field includes least altered and diagenetically altered samples with the assemblage plagioclase±K-felspar±calcite±e pidote; the upper right-hand field includes all the hydrothermally altered samples with the assemblage sericite±chlorite±pyrite±Fe-Mg carbonate.

Application to the Copper Belt

In order to apply this approach to the Zambian Copper Belt we need to first define the difference between the background least altered mineral assemblage and the ore-related mineral assemblage, and then secondly to select the major rock-forming elements added and lost during the mineralisation process.

Based on the previous petrographic studies by Darnley (1960) and our own observations on both the petrography and lithogeochemistry of the Roan sediments, the following assumptions are made:

- Least altered Roan siliclastics, distal from mineralisation, have the assemblage quartz-biotite-albite-dolomite-K-feldspar-sericite-chlorite. All these minerals were principally detrital components, except for biotite, which is metamorphic in origin.
- Mineralised shale and siliclastics are enriched in one or more potassic minerals; biotite, K-feldspar, sericite. They are commonly depleted in albite and have lost Na_2O during the mineralising process. This statement is not universally correct. For example some footwall ore bodies at Chibuluma show abundant evidence of albitisation (Selley, 2001)
- Carbonate in the sediments and ores is principally dolomite, although calcite and magnesite are present in minor amounts.

Sedimentary copper alteration indices

From the above it is concluded that the only major element changes related to alteration and mineralisation of the ''ore shale' are addition of K_2O and loss of Na_2O accompanying the replacement of albite by K-felspar (and biotite or sericite?). Our petrographic and geochemical studies do not indicate significant mass changes in any other major rock forming elements.

Based on this conclusion two alteration indices are proposed:

$$\text{SC AI Mk2} = \frac{100\ (K_2O)}{(K_2O + (10 \times Na_2O)}$$

This index measures the degree of replacement of albite by the potassic minerals K-feldspar, biotite and sericite. Na_2O is multiplied by a factor of 10 due the commonly very low levels of Na_2O in the mineralised ore shales.

$$\text{SC AI Mk5} = \frac{100\ (FeO + MgO)}{(FeO + MgO + Na_2O + K_2O + (Al_2O_3)/4)}$$

This index separates the carbonate and siliclastic sedimentary facies. Carbonate facies have values of 80 to 100 whereas siliclastic facies have values of 30 to 70.

Copper Belt lithogeochemical vector diagram

The diagram generated by plotting these two indices against one another is shown in slides 37 and 38. The minerals albite, K-felspar, sericite, biotite and carbonate-talc-chlorite plot around the margins of the diagram.

Least altered siliclastics from RCB1A and RCB2 plot in a fairly tight box with CSAI Mk2 = 10 to 30 and CSAI Mk5 = 40 to 70 (slide 37). Sediments that have undergone sodium metasomatism (albitisation) plot to the left of the least altered box, and those that have undergone potassium metasomatism (or sodium depletion) plot to the right of the least altered box (slide 37). The world average shale, from McGoldrick (this volume) plots toward the centre of the least altered field.

Carbonate-rich sediments from RCB1A and RCB2 have a greater spread, with significantly higher CSAI Mk5 values.

In slide 38 the mineralised 'ore shales' from Nkana are shown to plot in a discrete field well to the right of the Upper and Lower Roan sediments from RCB1A and RCB2. A value of SCAI Mk2 = 50 separates the background Roan sediments from the mineralised sediments.

This first attempt to develop a Copper Belt vector diagram seems to be relatively successful, however it only depends on the exchange between sodium and potassium in the sediments, and requires testing on a range of different Copper Belt deposits before it can be accepted as a viable tool for exploration .

Importance of feldspar in understanding alteration and mineralisation in the Copper Belt.

In our previous work all feldspar alteration was assumed to be albite. However this lithogeochemical study has demonstrated that both K-feldspar alteration and albitisation are common in the Roan sediments. The felspar paragenesis is likely to be fairly complex as our recent work, based on petrography, staining and geochemistry, indicates that detrital, diagenetic and metasomatic forms of both albite **and** K-feldspar are present in the sediments.

Our preliminary conclusions about the felspar relationships are:

- Roan siliclastics contain from 5 to 25 wt% detrital/diagenetic albite and minor detrital K-felspar
- Albite is commonly replaced by K-feldspar during the main copper mineralisation of the ore shale.

  $$NaAlSi_3O_8 + K^+ \Rightarrow KAlSi_3O_8 + Na^+$$

  Ore shales commonly contain 30 to 50 wt% K-felspar+biotite$\pm$sericite
- A second generation of metasomatic albite, focussed along faults, breccia zones and permeable horizons is related to a later hydrothermal event. This later event may (e.g. Chibuluma) or may-not (Nkana, Konkola North) have associated Cu mineralisation
- Preliminary C/O isotope studies indicate that the K-metasomatism and Na-metasomatism may be related to different fluids.

Further petrographic, staining and geochemical studies will be undertaken to test these ideas.

Conclusions

1. Immobile element ratios (Ti/Zr) may assist with stratigraphic correlations of siliclastic units in the Roan and Mwashia. However carbonate-bearing sediments show erratic values
2. The 'ore shale' at Nkana has a unique Ti/Zr ratio of 22-26
3. There maybe a hanging wall halo to ore, defined by K_2O/Al_2O_3 ratio, due to K-metasomatism causing K-felspar enrichment in the sediments. Co and Zn may also be enriched in the potassic halo, but this requires verification.
4. There appears to be a clear C-O isotope depletion halo in the carbonate-bearing sediments surrounding ore.

5. C and O isotopes in sedimentary and vein carbonates may provide a useful vector to ore.
6. At least two different alteration fluids have effected the sequence; having different C-O isotope characteristics.
7. The coupled C-O isotope depletion in carbonate associated with the mineralising event suggests a moderate to high temperature fluid (150°–350°C), with $\delta^{18}O$ near zero (seawater?), interacting with organic carbon at the site of ore deposition.
8. The ore shales are typically depleted in Na and enriched in K compared with normal shales. At Nkana and Konkola North the copper mineralising event is accompanied by extensive K-felspar alteration.
9. There is good potential to develop a litho-geochemical vector diagram, based on feldspar alteration, that may be useful for exploration.

References

Darnley, A.G., 1960, Petrology of some Rhodesian Copperbelt Orebodies and Associated Rocks: Trans. Inst. Min. Metall., v 69, p. 137-173.

Galley, A.G., 1995, Target vectoring using lithogeochemistry: applications to the exploration for volcanic hosted massive sulfide deposits: CIM Bulletin, v. 88, no, 990, p.15-25.

Ishikawa, Y., Sawaguchi, T., Iwaya, S. and Horiuchi, M., 1976, Delineation of prospecting targets for Kuroko deposits based on modes of volcanism of underlying dacite and alteration halos: Mining Geology, v. 26, p. 105 – 117 (in Japanese with English abstract).

Large, R.R., Bull, S.W., and McGoldrick, P.J., 2000, Lithogeochemical halos and geochemical vectors to stratiform sediment hosted Zn-Pb-Ag deposits. Part 2: HYC Deposit, McArthur River, Northern Territory: Journal of Geochemical Exploration, v 68, p. 105 – 126

Large, R.R., Bull, S.W., and Winefield, P.R., 2001a, Carbon and oxygen isotopic halo in carbonates related to the McArthur River (HYC) Zn-Pb-Ag deposit: implications for sedimentation, ore genesis and mineral exploration. *Economic Geology*,v. 96, p. 1567-1593.

Large, R.R., Gemmell, J. B., Paulick, H., and Huston, D. L., 2001b, The alteration box plot: a simple approach to understanding the relationship between alteration mineralogy and lithogeochemistry associated with VHMS deposits. *Economic Geology*, v. 96, p. 957-972

Large, R.R. & McGoldrick, P.J., 1998. Lithogeochemical halos and geochemical vectors to stratiform sediment hosted Zn-Pb-Ag deposits, Part 1. Lady Loretta Deposit, Queensland. *Journal of Geochemical Exploration*, v. 63, p. 37-56.

McCrae, L.M., 1950, The isotope chemistry of carbonates and the palaeotemperature scale, Journal of Chemistry and Physics, 18, 849-857.

Selley, D., 2001, Mineral zonation and controls on fluid pathways at Chibuluma West: AMIRA Report; P544 Proterozoic sediment hosted copper deposits, May 2002, Centre for ore Deposit Research, University of Tasmania, p12.1 – 12.15.

Veizer, J., Plumb, K. A., Clayton, R. N., Hinton, R. W. and Grotzinger, J. P. 1992. Geochemistry of Precambrian carbonates: V. Late Palaeoproterozoic seawater. C Geochemica et Cosmochimica Acta, v. 56, p. 2487-2501.

Zheng, Y.F. and Hoefs, J., 1993, Carbon and Oxygen isotope covariations in hydrothermal calcites: Mineralium Deposita, v. 28, p. 79 – 89.

Zambian Copper Belt Geochemistry:
Part III; Preliminary assessment of chemostratigraphy and alteration geochemistry

Ross Large, Peter McGoldrick &
Mawson Croaker

Chemostratigraphy tested in two Chambishi basin drill holes: RCB1A and RCB2

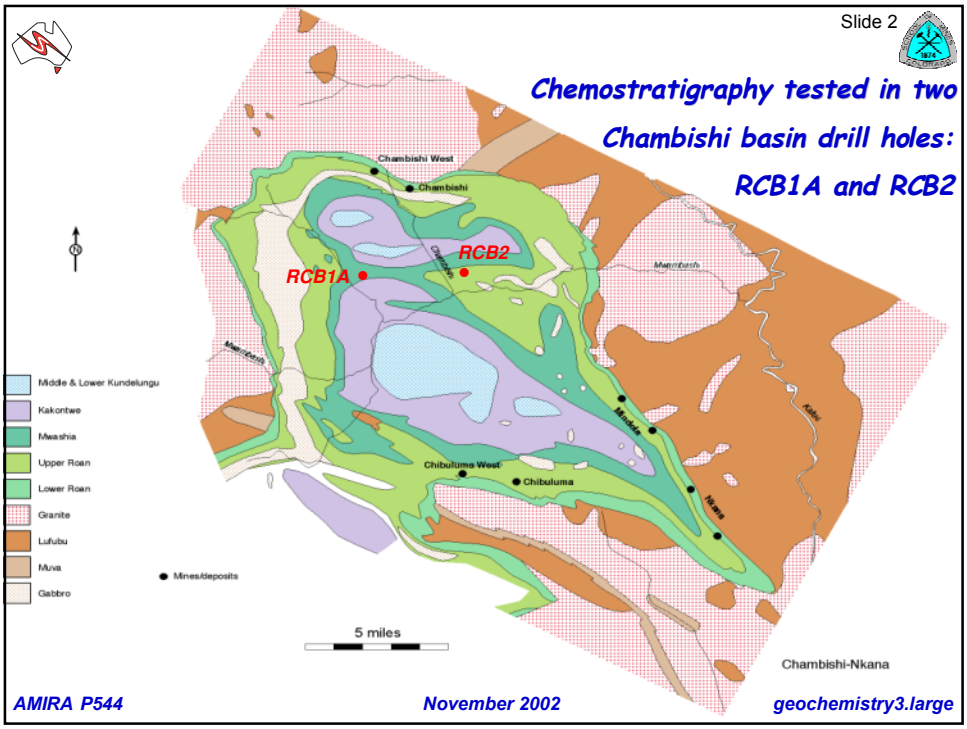

RCB1A

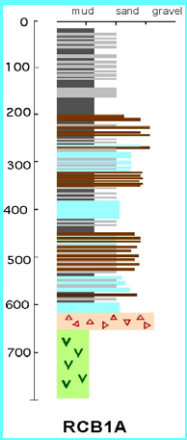

collared in Mwashia

RCB2

collared in Upper Roan

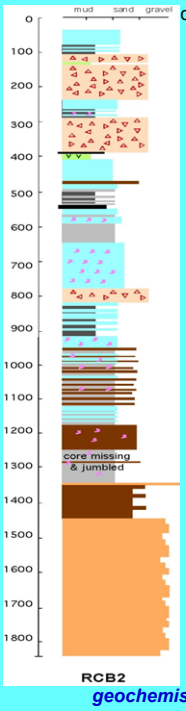

Immobile Elements

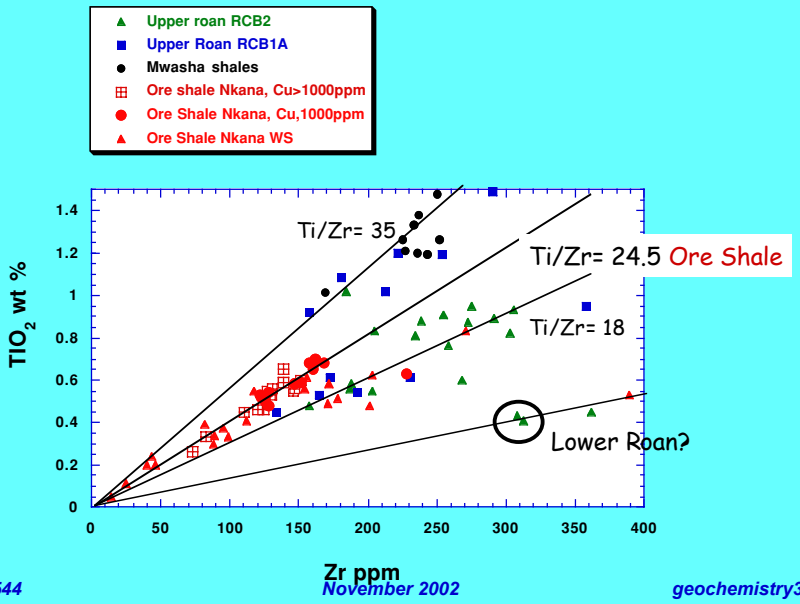

Ti - Zr patterns

- Ore Shale commonly has a tight distribution: Ti/Zr = 22-26, Ti < 0.8wt%, Zr < 200ppm
- Upper Roan siliciclastics are more variable: Ti/Zr = 12-38, two distributions are suggested by the data, Ti/Zr ~ 18 and 35
- Mwashia shales are more Ti-rich than Ore Shales, with Ti/Zr = 30 to 36

Lithogeochemistry of Upper Roan in RCB2

Carbonate content

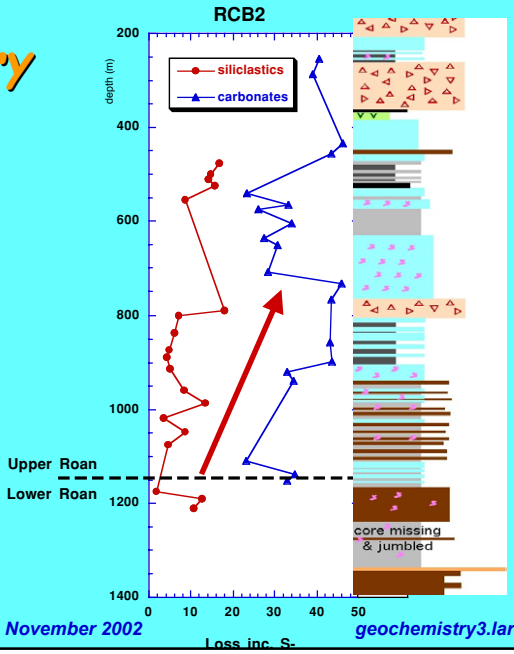

RCB2: Carbonate Variation

- Data set split into two groups:
  - Siliciclastics, LOI < 20 wt%
  - Carbonates, LOI > 20 wt%
- Carbonate content increases systematically up stratigraphy through the Upper Roan above the Ore Shale.

Lithogeochemistry of Upper Roan in RCB2

Ti/Zr variation

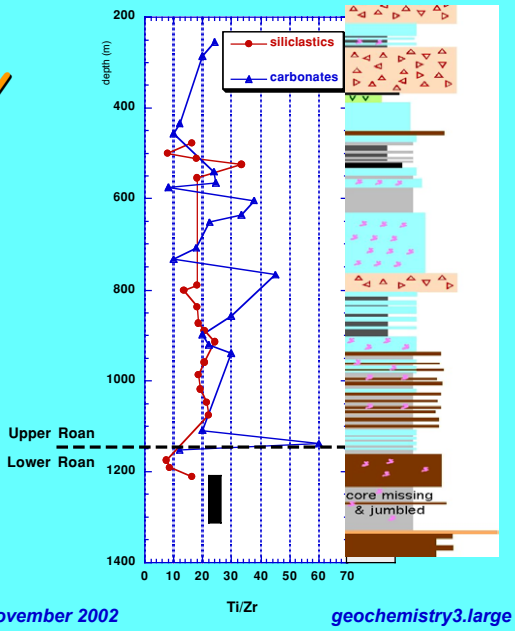

Ti - Zr patterns

- Immobile elements in carbonates are erratic - only use shales for lithostratigraphic correlations

Lithogeochemistry of Upper Roan in RCB2

Na_2O variation

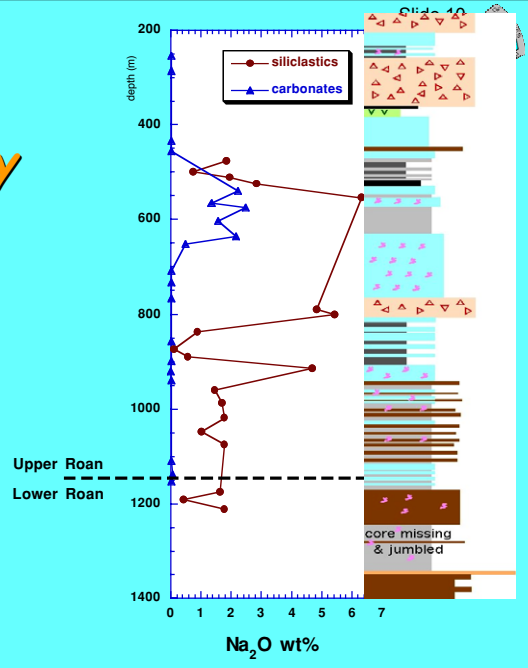

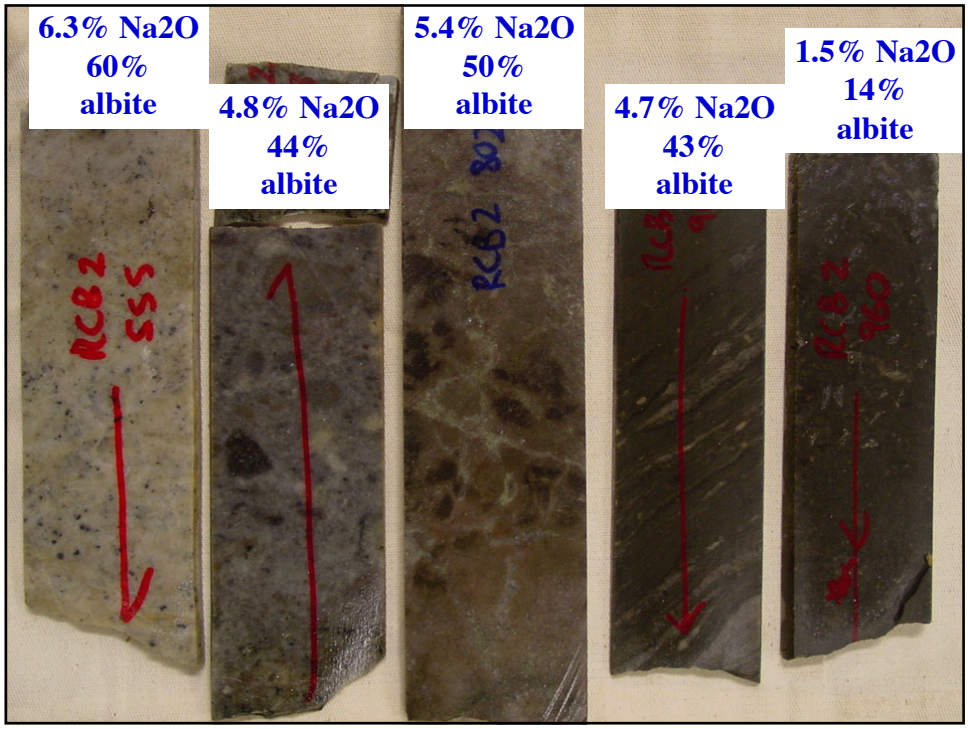

RCB2: Na_2O

- Upper Roan siliciclastics average around 1.8 wt% Na_2O
- This equates to ~ 15 wt% albite in siliciclastics
- Discrete zones of albite alteration contain 5-7 wt% Na_2O (45-60 wt% albite)
- Carbonates commonly contain < 0.1 wt% Na_2O, except for a zone of albite-rich carbonates at 530-640m in RCB2

Lithogeochemistry of Upper Roan in RCB2

K_2O variation

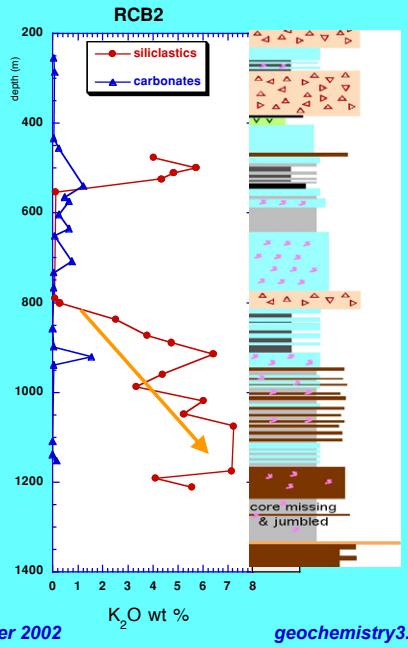

RCB2: K_2O

- Upper Roan siliclastics vary from 2.5 to 8 wt% K_2O (mean: 4.2 wt%)
- This compares to a world average for shales of 3.2 wt%
- Carbonates contain low K_2O: 0.1 to 2 wt%
- There appears to be an increase in K_2O toward the ore shale in the HW siliclastics
- The HW enrichment in K_2O (4-8wt%) is anomalous - could it be due to alteration?

Lithogeochemistry of Upper Roan in RCB2

K_2O/Al_2O_3 variation

vector to ore?
vector to 'favourable' horizon?

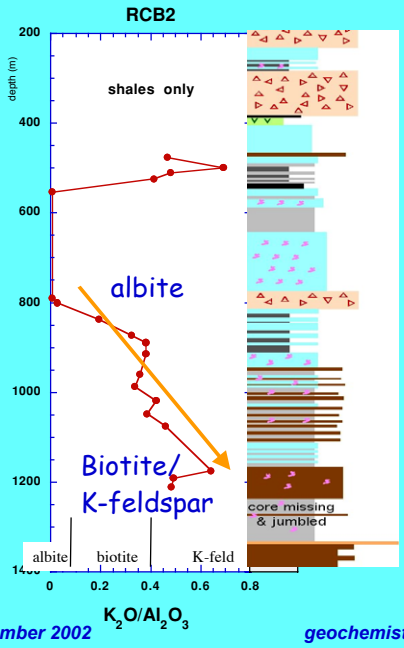

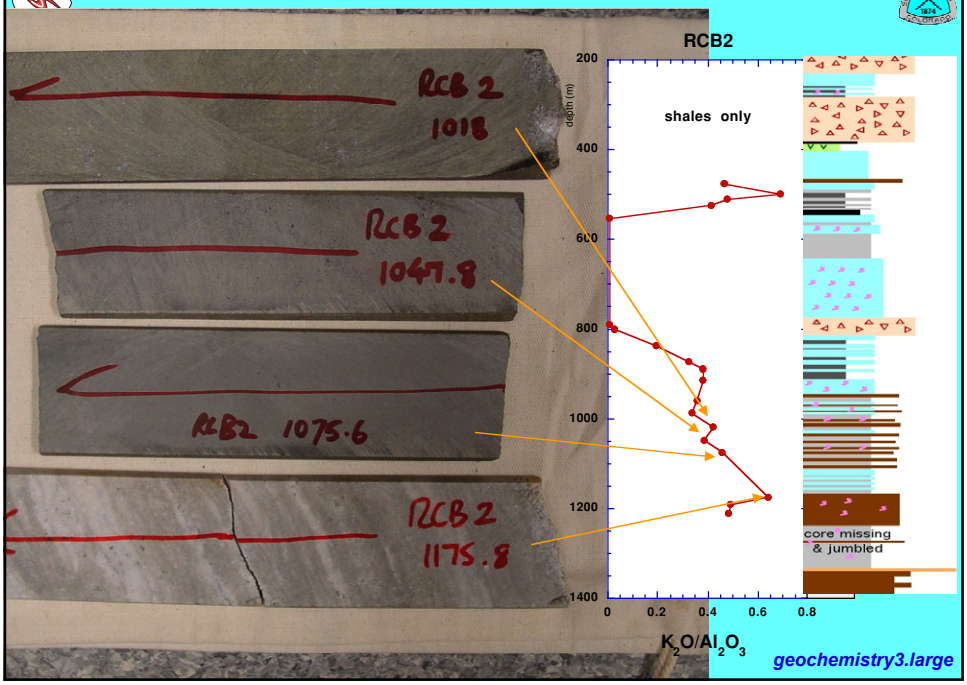

K_2O - Al_2O_3 variation in siliciclastics

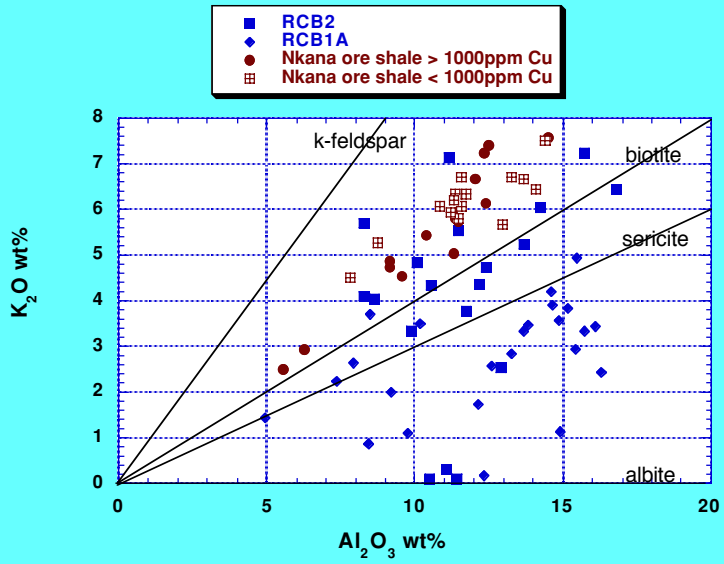

Cu Zn Co

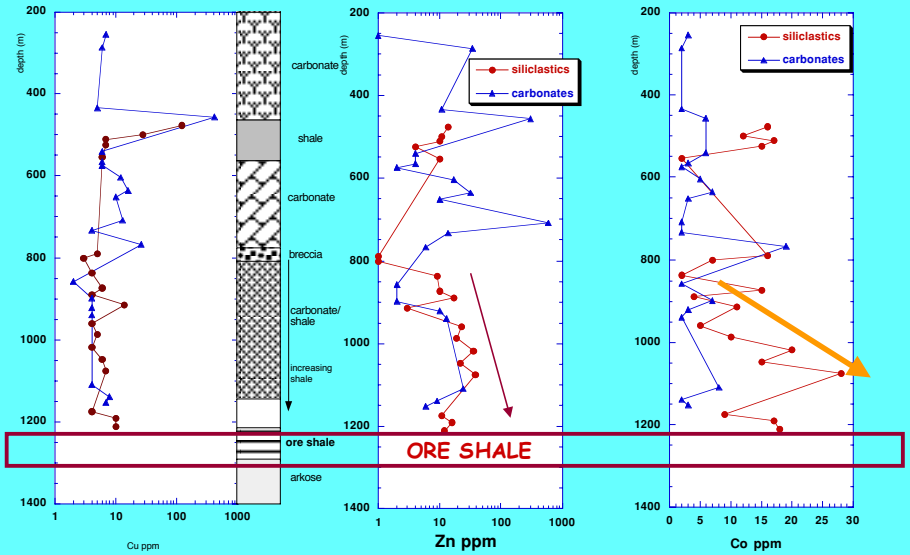

Variation of Cu, Zn and Co in HW

- There is no Cu halo in hangingwall sediments to ore shale.
- Zn and Co show a gradual increase toward the Lower Roan contact
- Additional studies required to test these variations

Possible HW vectors to ore

- K_2O/Al_2O_3 ratio in siliciclastics
- Zn in siliclastics
- Co in siliclastics

Lithogeochemistry of Upper Roan in RCB1A

Ti/Zr variation

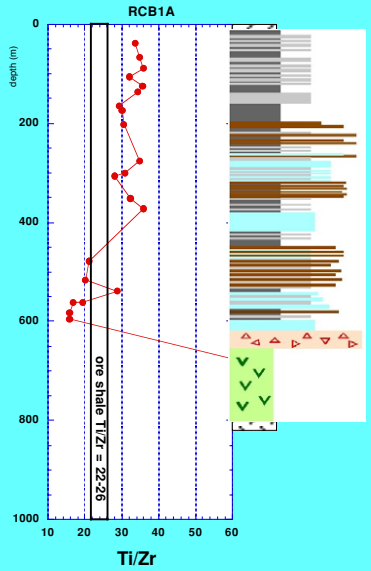

Lithogeochemistry of Upper Roan in RCB1A

Ti/Zr variation

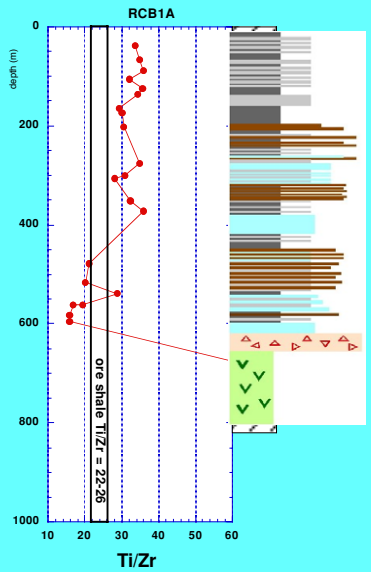

C and O isotopes in carbonates

- Carbonate-rich horizons in RCB1A and RCB2 were analysed for C & O isotopes at the University of Tasmania, CSL
- Carbonate altered footwall arkoses from drill hole NN42 were also analysed
- A set of carbonate-rich samples from the Nkana ore zone have been analysed by Mawson Croaker, and will be reported separately

O and C Isotopes of Carbonates RCB2

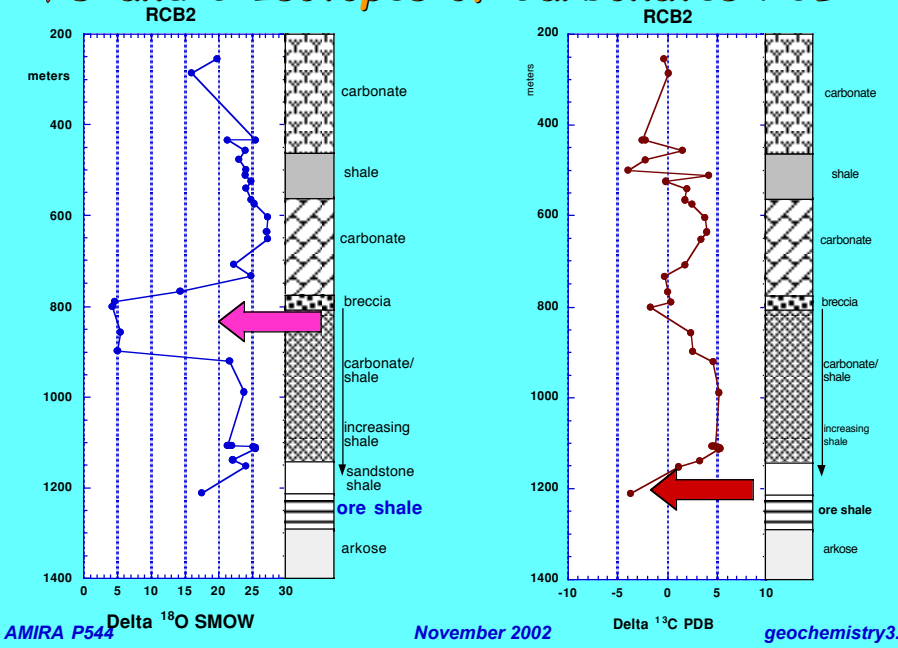

O and C Isotopes of Carbonates RCB2

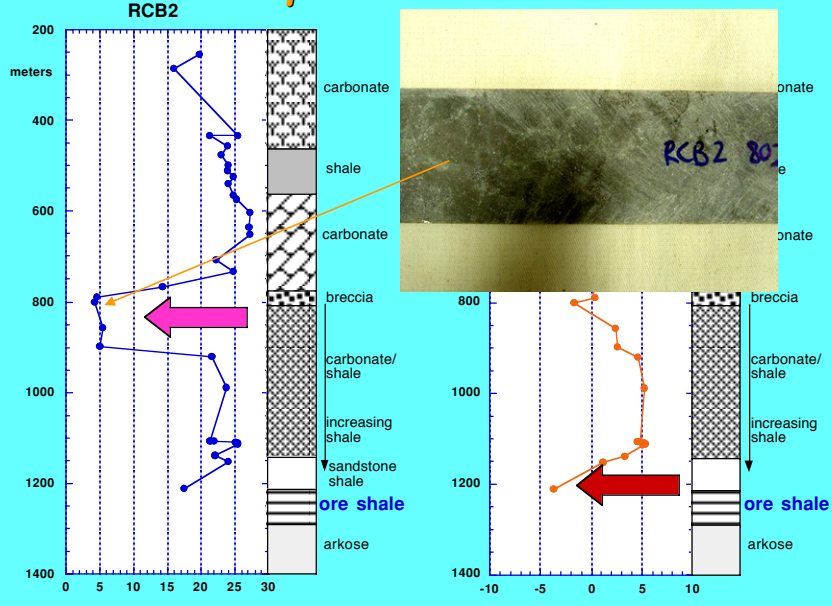

O and C Isotopes of Carbonates RCB1A

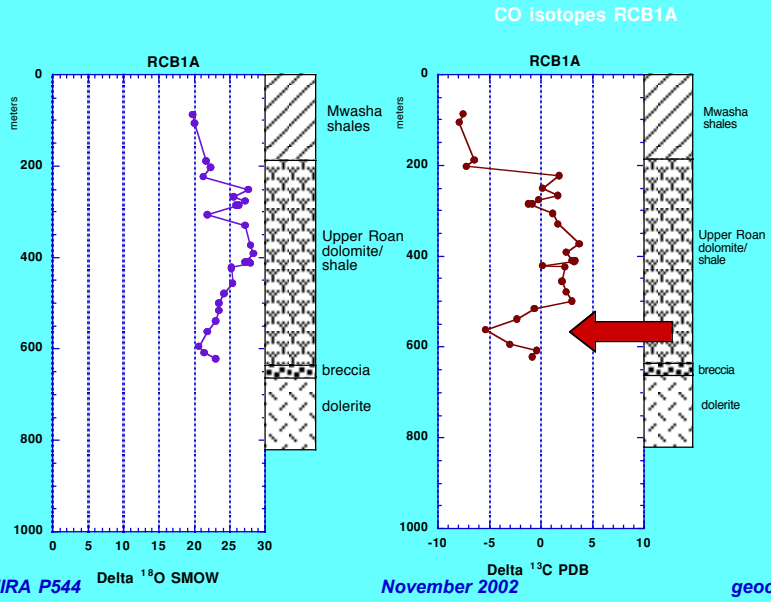

C-O isotope relationships

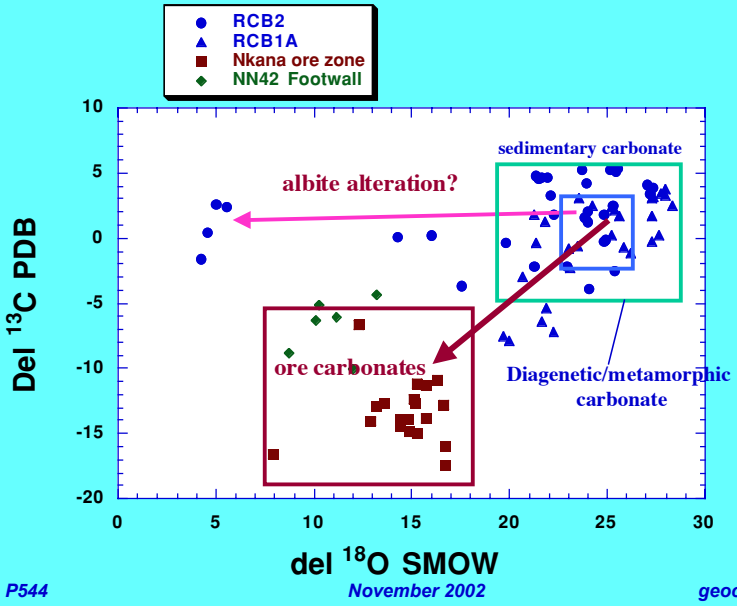

Comments on C-O isotopes

- Sedimentary & diagenetic carbonates have $d^{18}O$ = 20-28 permil, $d^{13}C$ = +5 to -2 permil, similar to early Prot. Sedimentary/diagenetic values
- Ore-related carbonates are strongly depleted in both ^{18}O and ^{13}C ($d^{18}O$ = 8-18 permil, $d^{13}C$ = -5 to -20 permil)
- A halo of ^{18}O and ^{13}C depletion extends into the HW sediments above the ore shale for at least 100m
- Further work needed to study footwall carbonates, but they appear to have the ore signature

Isotope Interpretation

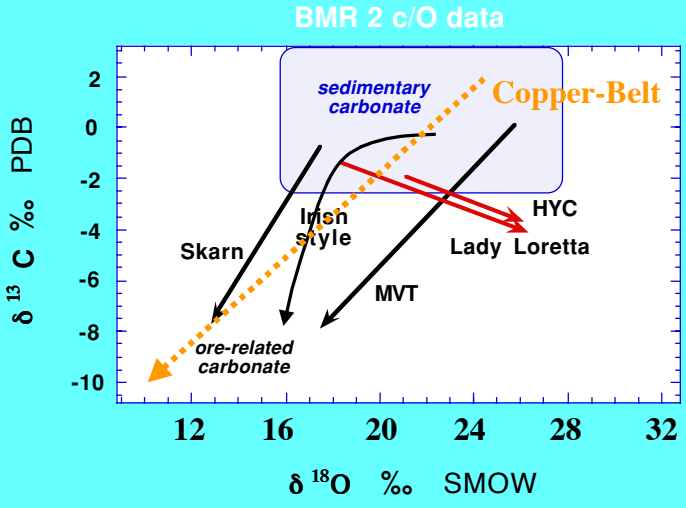

Isotope Modelling

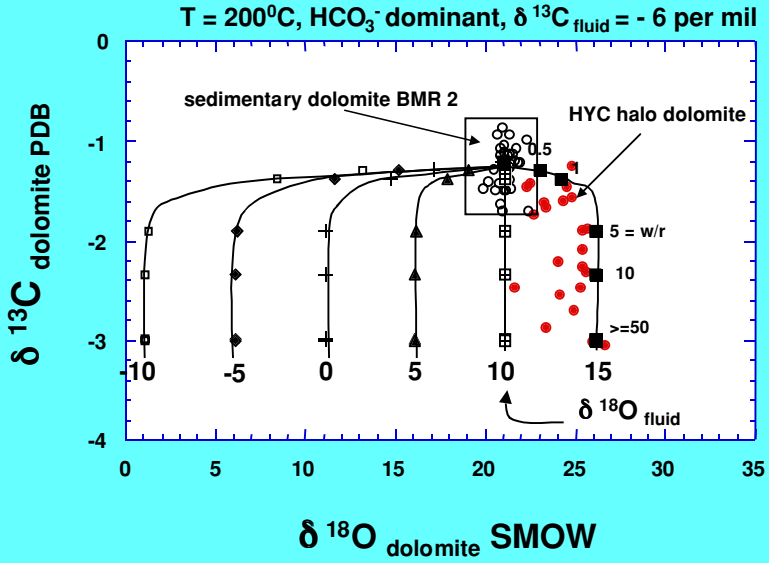

Preliminary isotope Interp

- The coupled C-O depletion associated with the mineralising event suggests:
  - A fluid with $d^{18}O$ = 0 ± 5 permil
  - Moderate to high temperatures 150 - 350 °C
  - Involvement of organic carbon oxidation in the ore forming process
- The strong oxygen depletion in the albite-carbonate breccia zone suggests involvement of a much lighter ^{18}O fluid; probably meteoric ($d^{18}O$ = -10 permil?)

O and C Isotopes of Carbonates RCB2

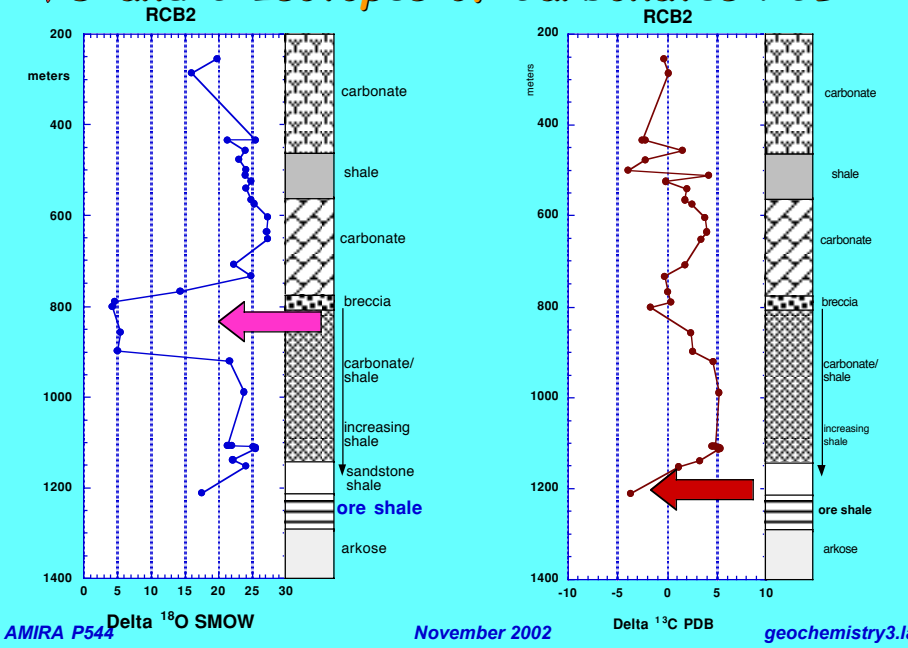

Towards Developing a Copper Belt Lithogeochem Vector Diagram

VHMS Alteration Box Plot

Large, Gemmell, Herrman, Paulick & Huston (2001)

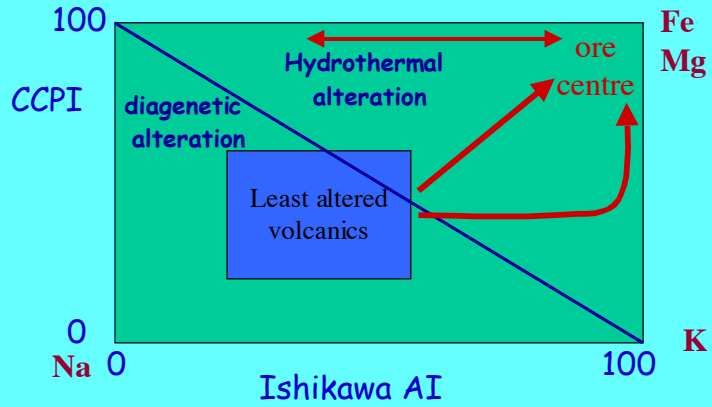

Copper Belt mineral associations

after Darnley (1960)

- Background unmineralized Roan siliciclastics contain biotite, K-feldspar, albite, quartz, sericite and chlorite
- Mineralised shale and siliciclastics commonly contain no albite (low Na_2O), and are enriched in one or more potassic minerals (biotite, K-feldspar or sericite). BUT, some fw orebodies contain albite
- Carbonates are principally dolomite, but some calcite and magnesite is also present

Enriched and Depleted elements

- Enriched in ore zones : K_2O, and……..?
- Depleted in ore zones: Na_2O, and……..?
- SC AI Mk2 = $\dfrac{K_2O \times 100}{K_2O + (10 \times Na_2O)}$
- SC AI Mk5 = $\dfrac{(FeO + MgO) \times 100}{(FeO + MgO + Na_2O + K_2O + Al_2O_3/4)}$

Roan Siliciclastics and Carbonates

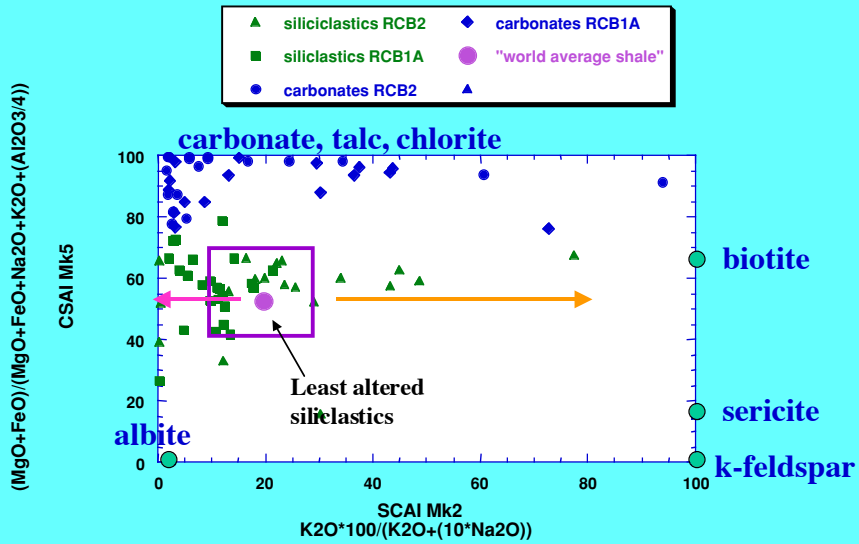

Ore Shales at Nkana

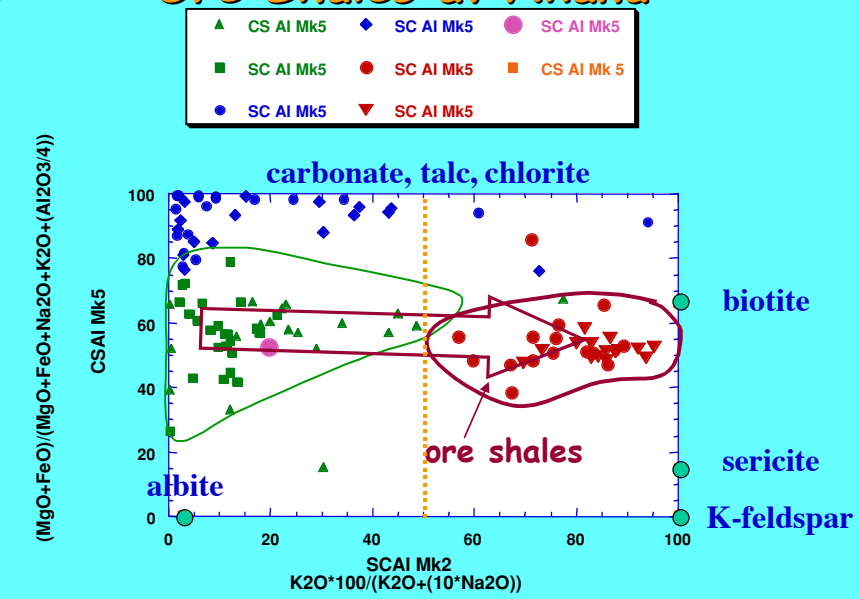

Feldspar is the Key

- Roan silciclastics contain from 5 to 25 wt% detrital/diagenetic albite
- This albite is commonly replaced by K-feldspar during the Cu mineralisation of the Ore Shale

$$NaAlSi_3O_8 + K^+ = KAlSi_3O_8 + Na^+$$

- A second generation of metasomatic albite, focussed along faults and breccia zones, is related to a later hydrothermal event (Darnley, 1960)
- Further petrographic and staining studies are needed to confirm these relationships

Preliminary Conclusions

- Immobile element ratios (Ti/Zr) can assist stratigraphic correlations
- The ore shale at Nkana has a unique Ti/Zr ratio
- There may be a hangingwall halo to ore, defined by K_2O/Al_2O_3, Co and Zn in the siliclastics
- There appears to be a clear C-O isotope depletion halo in the carbonates surrounding ore
- C and O isotopes in carbonates may provide a useful vector to ore

C-O isotope relationships

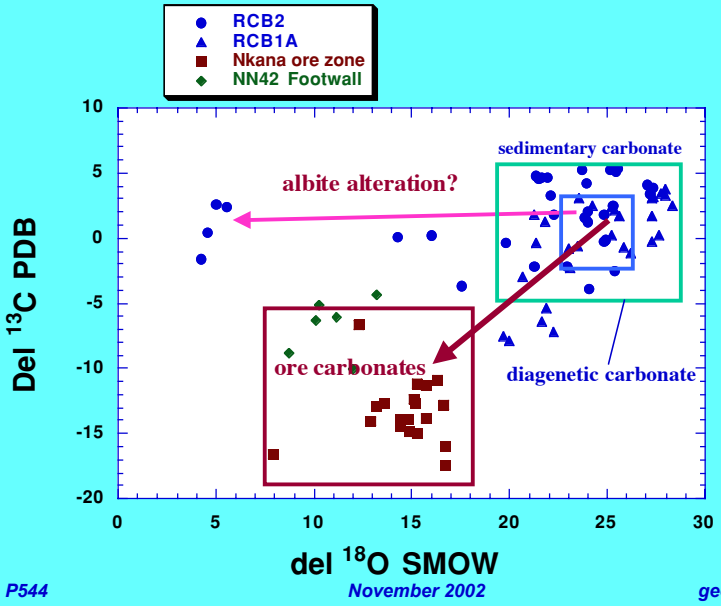

Preliminary Conclusions

- At least two different alteration fluids have effected the sequence; having different C-O isotope characteristics
- The ore shales are typically depleted in Na and enriched in K compared with normal shales (based on Nkana and Konkola North data)
- There is good potential to develop a lithogeochemical vector diagram, based on feldspar alteration, that may be useful for exploration

end

K_2O RCB1A Na_2O

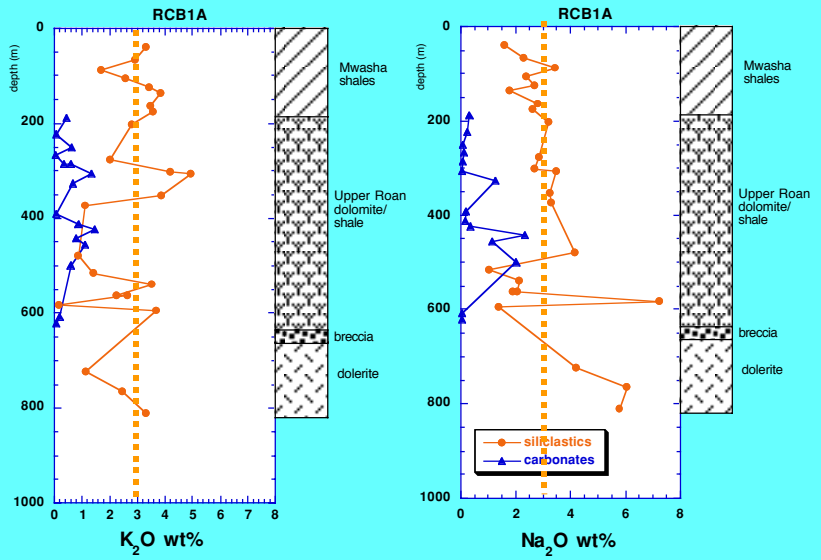

Comment on Na_2O and K_2O

- In the uppermost Roan and Mwasha intersected in RCB1A, the siliclastics average 3.1% Na_2O and 2.7% K_2O
- The stratigraphically lower siliclastics in the Roan (RCB2), closer to the ores, contain a lower mean Na_2O (2.2%) and higher mean K_2O (4.2%) content

Chambishi Basin Progress Report 2: Basin geometry and its control on mineralisation at Mwambashi B

David Selley, Stuart Bull, Robert Scott & David Cooke
Centre for Ore Deposit Research, University of Tasmania

Summary

Sedimentation of Lower Roan in the Chambishi Basin was controlled by WNW-trending half graben structures and subordinate NW- to NNW-trending transfer zones. At the onset of extension, the basin geometry was highly compartmentalised, resulting in lateral facies variation of predominantly arenaceous lithotypes and complex sediment dispersal patterns. Subaerial depositional environments typify this early phase of basin growth (Mindola Clastics Formation), however an upward transition to marine conditions is recorded within depocentre maxima. Transfer zones were the principal sites of locally derived, coarse-grained sediment input, which accumulated in restricted depocentres characterised by lateral pinch outs and limited accommodation development. Stratigraphy in the region of transfer zones is condensed and anomalously coarse-grained. The combination of 3-D pinch outs and quality reservoir strata in these regions made them optimal trap sites for migrating hydrocarbons.

Upward transition to finer-grained, predominantly marine lithofacies of the basal Kitwe Formation is abrupt and records a fundamental change in basin configuration involving widespread sediment starvation. Depositional compartments became broader and more rapidly subsident, perhaps in response to a regional extensional pulse. Strata transgressed older basin compartments, providing a regional seal on an underlying system of semi-connected, permeable sandstone bodies.

The Rokana Evaporites and Nchanga Quartzite members mark a transition to cyclical marginal marine-subaerial sedimentation that may relate to crustal rebound following the initial extensional pulse. Tectonic quiescence, typical of the sag phase of crustal extension is recorded by the platformal carbonate-dominated succession of the Chambishi Dolomites Member.

Cu mineralisation at Chibuluma West, Mwambashi B and parts of Chambishi occurs below the level of the Ore Shale. It is concentrated towards the top of clean, permeable arenaceous units, with indistinct geological footwalls, but sharp upper contacts with less permeable media. Host arenites occur within restricted depocentres and have pronounced feldspathic alteration. The architecture of host packages is consistent with that of a hydrocarbon reservoir. A strong spatial association of Cu-sulphides with radiogenic heavy mineral phases at Chibuluma West, may be considered indirect evidence of former hydrocarbons.

We speculate that the permeable pathways and reservoirs utilised by migrating hydrocarbons, remained 'open' during subsequent passage of hydrothermal metal-bearing brines. Thus fluids directly responsible for mineralisation must have been introduced prior to complete consolidation of the MCF (ie. pre-peak metamorphism).

Introduction

This report summarises results of the ongoing Chambishi Basin study. We have built upon our initial studies at the Chibuluma West deposit (Selley & Bull, 2001; Selley & Cooke, 2001) and incorporated key findings from Mawson Croaker's PhD study of the Nkana system, as well as work on arenite-hosted

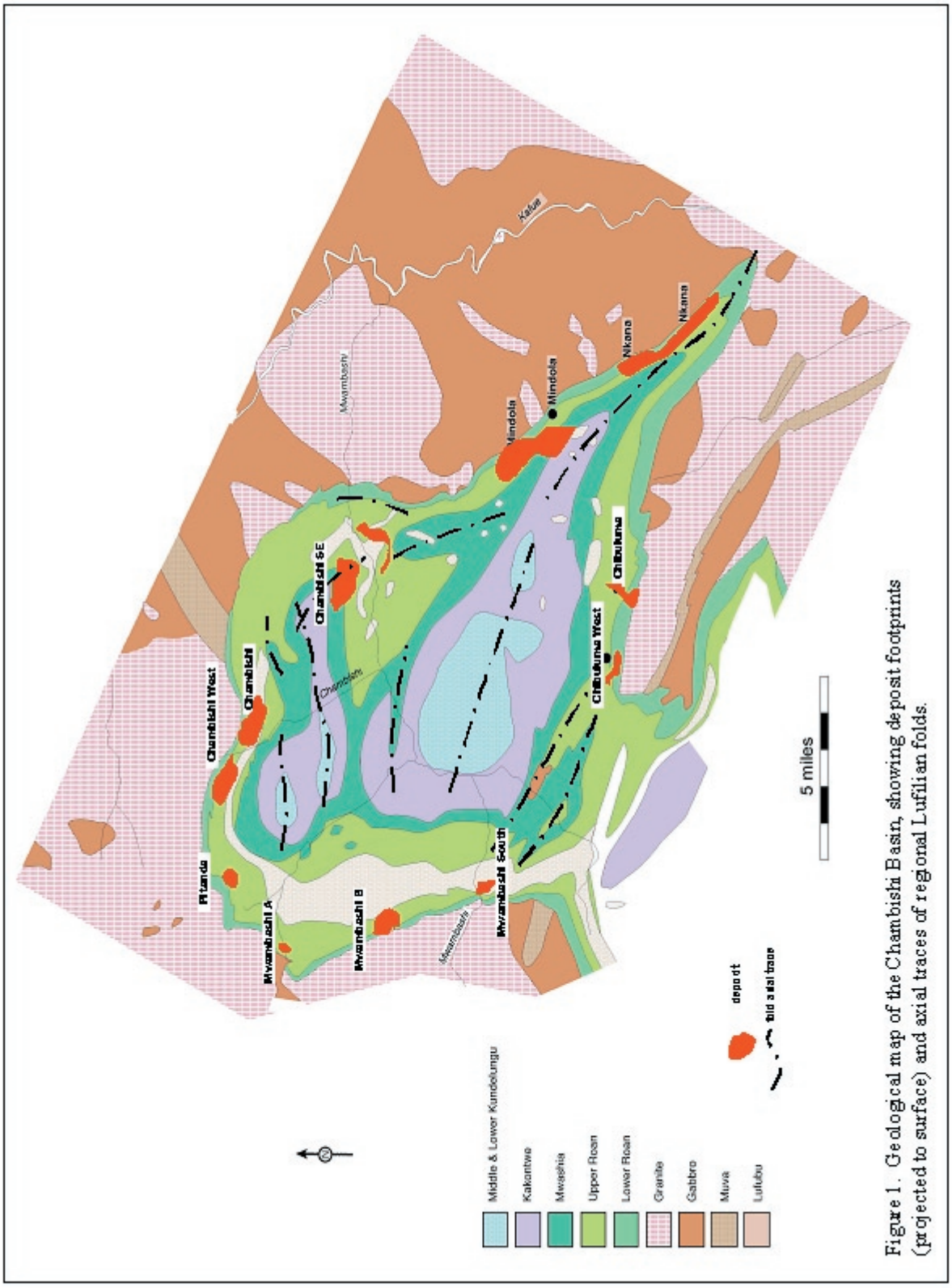

Figure 1. Geological map of the Chambishi Basin, showing deposit footprints (projected to surface) and axial traces of regional Lufilian folds.

mineralisation from the eastern margin of the Kafue Anticline (Scott, 2001; Scott, this volume; Broughton, this volume). The Chambishi Basin (fig. 1) was selected as an area of detailed research as it contains a number of elements critical to understanding Copperbelt mineralisation. Firstly, mine exposure and/or high density drill hole coverage is widespread about the periphery of the 'basin', providing a unique opportunity to constrain 3-D facies variation (hence basin architecture) throughout the Lower Roan. Secondly, much of drilling was continued to basement (uncommon throughout much of the Copperbelt) and as such provides invaluable information regarding basin growth at the onset of Katangan sedimentation. Consequently, important aspects of basin architecture, such as pronounced basement topography during accumulation of the Mindola Clastics Formation, as well as significant facies variation at the level of the Copperbelt Orebody Member are well documented (e.g. Annells, 1984) at a variety of scales and provide an excellent framework within which to refine basin evolutionary models. Thirdly, deposits are highly variable in terms of tonnage, grade, precious metal content, stratigraphic position, structural complexity and alteration assemblage. How do these attributes vary within the contexts of basin geometry and evolution? Finally, existing geological maps demonstrate the domainal nature of macroscopic Lufilian fold patterns. Domains of relatively simple E–W to WNW fold trends are juxtaposed with domains of clear interference of WNW and NNW trending fold generations. Do these Lufilian fold domains record the influence of basin architecture developed at the onset of Katangan sedimentation? Can fold patterns be used as proxies for basin geometry?

Principal aims of the study are to:

1. Resolve the history of basin growth throughout deposition of the Lower Roan.
2. Provide geochronological constraints on alteration and mineralisation.
3. Constrain inversion history: number of events, style of deformation, kinematics and geometry,
4. Identify influences (if any) of Lower Roan basin architecture on Lufilian fold geometry.
5. Investigate the variation in style, stratigraphic position and structural position of Cu-Co mineralisation within the context of a basin evolutionary model.

Throughout the past 12 months, field work has concentrated on 'footwall-hosted' mineralisation at Mwambashi B, situated at the western margin of the Chambishi Basin (fig. 1). The results of this work provide the focus for this report. Additional logging of core was carried out at Chambishi and Chambishi SE deposits, but is yet to be processed in full. Considerable effort was also made to compile a comprehensive geological database from historical sections and plans derived from exploration drilling about the periphery of the Chambishi Basin: i.e. Mwambashi A, B & South, Pitanda, Chambishi and Chambishi SE deposit and prospect licences. Sections were constructed at scales ranging 1:500 to 1:2000 and provide detailed, accurate summaries of facies types, thickness variation and Cu-Co grade distribution. At Chibuluma West and Mwambashi B, these historical data have been integrated with our own logging to determine basin evolution and geometric/facies controls on mineralisation. Work at Chambishi SE has been initially to reinterpret historical sections.

The report begins with a summary of major results from work undertaken at Chibuluma West. More comprehensive discussion of data and interpretation can be found in Selley & Cooke (2001 & 2002) and Selley & Bull (2001), however we considered it useful to reiterate findings here in order to highlight similarities between Chibuluma West and Mwambashi B.

Key findings of Chibuluma West study

(Selley & Cooke, 2001 & 2002; Selley & Bull, 2001 & 2002)

Basin architecture

- Chibuluma West occupies an inverted half-graben system, within which a condensed sequence of Lower Roan strata accumulated. Mineralisation is hosted by relatively clean 'footwall' lithotypes, occurring immediately below the lithostratigraphic equivalents of the Kafue Arenites Member (fig. 2). Ore Shale and siliciclastic-dominated 'hangingwall' facies of the Kitwe Formation are absent. Loss

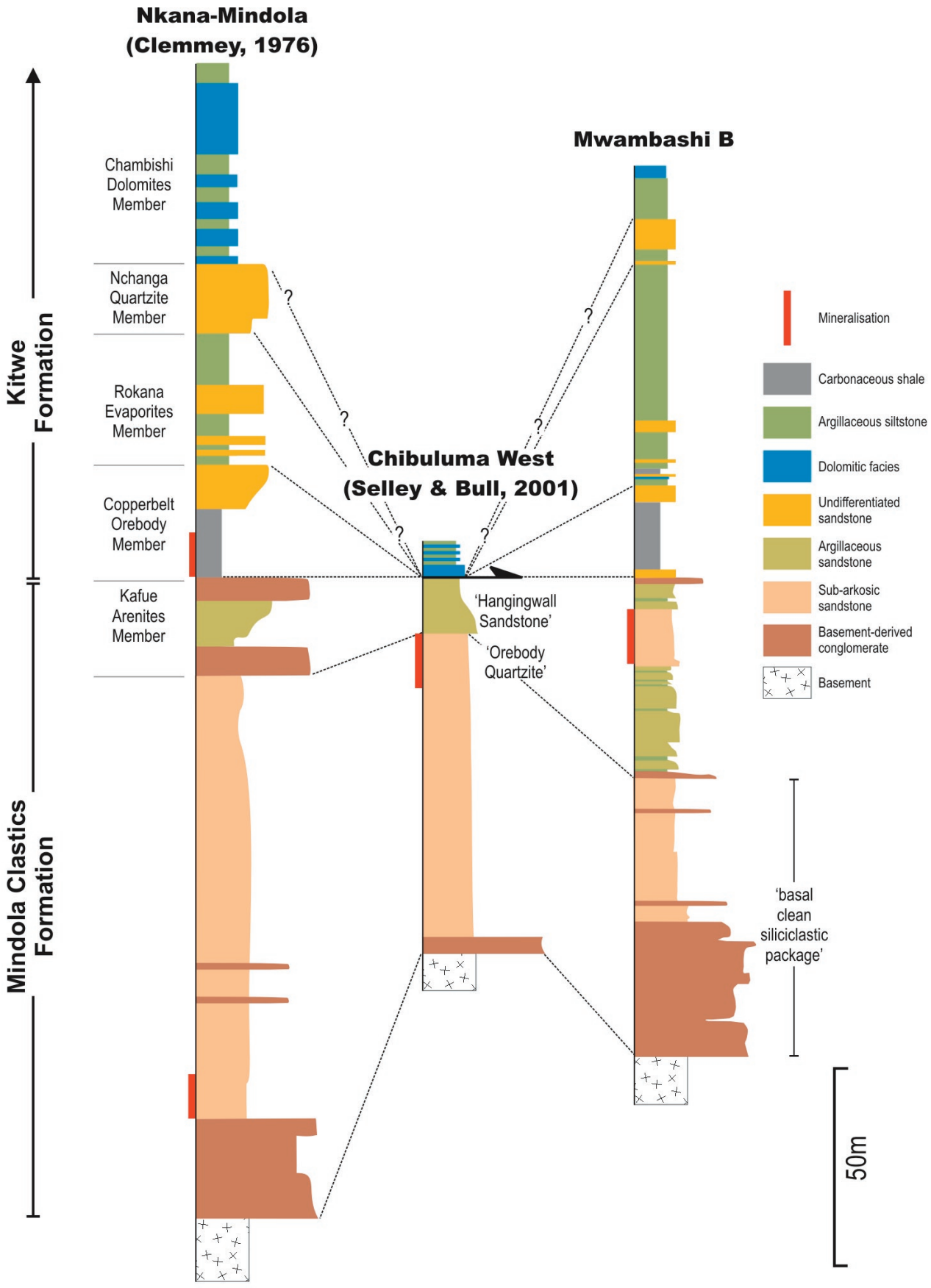

Figure 2. Comparative stratigraphic sections of the Lower Roan from the southern Chambishi Basin. Stratigraphic nomenclature based on Clemmey (1976).

of stratigraphy is probably the result of non-deposition/erosion, however tectonic removal cannot be discounted.

- Sub-basins occupy WNW-trending synclinal cores separated by NNE-dipping growth faults. Footwall tilt blocks are basement-cored, presently inverted and emplaced as narrow, high amplitude inliers within lower levels of the Roan stratigraphy.
- Compartmentalisation of the half-graben system becomes more pronounced to the west, where syn-depositional fault density and displacement increased (leading to more pronounced footwall uplift).
- The half graben system terminates to the west against a NNW-trending basement ridge, interpreted as a transfer zone during initial basin growth.
- Facies variation within the Mindola Clastics Formation is most pronounced vertically. An abrupt change from a lower succession of relatively clean, parallel and cross stratified, heavy mineral bearing sandstone to a 'dirty' poorly-sorted, crudely stratified, upward-fining arkose-siltstone package, records a transition from dominantly fluviatile to subaqueous sedimentation. This transgressive shift indicates greater rates of subsidence relative to sediment input with time.
- Upper levels of the stratigraphy are notably fine-grained relative to the 'footwall' and comprise chloritic and/or feldspathically altered siltstones and carbonates more typical of highest stratigraphic levels of the Lower Roan (i.e. Chambishi Dolomites Member) or Upper Roan.
- Fine-grained 'hangingwall' units apparently transgress intrabasinal footwall highs (i.e. basement topography), indicating deposition coincident with an abrupt broadening of the basin system.
- The folded contact of the arenaceous 'footwall' and finer-grained 'hangingwall' packages is ubiquitously sheared, indicating decoupling between the compartmentalised and 'layer-cake' portions of the basin infill, probably at the onset of basin inversion.

Mineralisation

Cu-Co Distribution

- Although grossly stratabound, the Cu orebody is strongly focussed about the periphery of the early sub-basins (i.e. where host strata pinch-out or terminate against intrabasinal basement highs), thickening broadly to the west as the system becomes more confined.
- In profile, the Cu assay hangingwall coincides with the transition from clean sub-arkosic sandstone to poorly-sorted sandstone. However, no obvious primary compositional or textural features distinguish the ore horizon from the Cu assay footwall.
- The main Cu and Co orebodies are partitioned into different levels of the stratigraphy (locally separated by a narrow barren zone): Cu is concentrated within the uppermost portion of the clean sub-arkosic sandstone, whereas Co grade is most significant within the upper poorly-sorted, matrix rich arkose.
- Although broadly separated, highest grade Cu within the main ore zones coincides with elevated Co.
- Vertical distribution of metals is broadly reflected in sulphide composition: the Cu zone is bornite rich at the base, passing upward to chalcopyrite-dominant domains; an abrupt increase in pyrite occurs at the top of the Cu orebody and persists up into the Co orebody.

Alteration & grain-scale textures

- The ore zone and upper part of the barren footwall is characterised by strong recrystallisation of the original detrital framework, leading to a grain-scale mosaic of intergrown quartz and feldspar, with subordinate calcite, tremolite, tourmaline, biotite and chlorite. By contrast, original detrital textures are well preserved within the weakly recrystallised Hangingwall Sandstone, where biotite, calcite and chlorite are the dominant non-detrital phases.
- Simple and consistent sulphide paragenesis was recognised within all mineralised samples: pyrite → carrollite → chalcopyrite → chalcopyrite + bornite.

- A strong spatial association exists between Cu- and Fe-sulfides, and stratiform and transgressive cm-scale domains of feldspar metasomatism (albite?). Tremolite has antithetic spatial distribution with albite and sulfides.
- Symmetrical sulphide zoning occurs about feldspathic domains: pyrite ± carrollite + chalcopyrite concentrated in cores, bornite + chalcopyrite at peripheries.
- Feldspathic domains are loci of grain-scale fracture. Evidence of significant displacement associated with cataclasis is generally lacking. However, rare evidence does exist for syn-kinematic precipitation of feldspar, quartz and sulphides. By contrast, grain-scale strain associated with sulphides at the periphery of feldspathic domains is lacking, where globular intergrowths of bornite and chalcopyrite apparently occupy inter-granular pore-space.
- There is a common association of feldspathic alteration and sulphide concentration with 'heavy mineral bands'. Although detrital tourmaline and zircon are present in these bands, Th-bearing phases (i.e. monazite and huttonite) are most conspicuous and often have intimate grain-scale textural relationships with sulphides.
- Initial petrographic studies indicate Th-bearing phases occur in increased abundance within the ore zone relative to the barren footwall. Furthermore, monazites within the ore zone appear chemically distinct (Th-depleted) from those in the footwall.

Sulphur isotopes

- Sulphides from Chibuluma have the heaviest average sulphur isotopic compositions of any stratiform Copperbelt deposit (Dechow and Jensen, 1965).
- There is a gross up-stratigraphic increase in $\delta^{34}S$ content of sediment-hosted sulphides, similar to other Copperbelt deposits (Annels, 1989). However, sulphides in mylonitic basement rocks have elevated sulphur compositions, comparable to those within central and upper parts of the sediment-hosted system. The upward increase in $\delta^{34}S$ cannot be accounted for by progressive depletion of $\delta^{32}S$ from a fluid reservoir passing up-stratigraphy with time (e.g. Annels, *op. cit*.).
- Initial results reveal correlation between vertical sulphide zonation patterns and ^{34}S compositions of both pyrite and chalcopyrite, on a local scale at least. Heaviest values coincide with the highest-grade, pyrite + carrollite + chalcopyrite interval and decrease within the chalcopyrite ± bornite dominant upper and lower fringes. These data are consistent with, but do not prove influx of fluid and along bedding sub-parallel fracture zones.
- Although the above relationship between increased Cu grade and $\delta^{34}S$ composition applies locally, it is not valid for the entire ore zone: a high grade interval near the base of the orebody is most $\delta^{32}S$ enriched. Thus a simple, direct correlation between sulphur isotopic compositions of individual grains and Cu grade is yet to be demonstrated.
- $\delta^{34}S$ values are too heavy to be accounted for by biogenic sulphate reduction (assuming Late Proterozoic aqueous sulphate ranging between 11 and 23‰: Hitzman, 2000). Thermochemical sulphate reduction or decomposition of organic matter to generate H_2S gas may have provided alternative sulphur sources.
- The variation in sulphur isotopic signatures throughout the Copperbelt (and within individual deposits: e.g. Chambishi, Hitzman, 2001) potentially indicates that different sulphur reservoirs were present at different trap sites (e.g. sour gas, pre-existing sulphides, aqueous sulphate or pore-filling anhydrite). These sulphur reservoirs may have existed contemporaneously, or evolved, or were introduced at different times in the basin's history.

Geochronology

- Within the Cu ore zone, monazites (and huttonite grains) are commonly rimmed or partly overgrown by albite and/or sulphides and thus have the potential to provide maximum age constraints on the timing of mineralisation.
- Dating of monazites using the CHIME technique at the University of Tasmania was significantly hampered by their low initial Th content (leading to below detection Pb in 43% of analyses). Low Th-monazites were restricted to the ore zone and are

of probable hydrothermal origin. Despite problems with near- and sub-detection Pb abundances, 99% of ore zone monazite data conform to a single isochron of 500 ± 42Ma. Two high-Th grains were identified within the barren footwall, returning accurate detrital (2045 ± 108Ma, 1616 ± 50Ma, 1162 ± 120Ma) and Lufilian metamorphic ages respectively (463 ± 32Ma).

- Partitioning of 500 ± 42Ma hydrothermal (low Th) monazites within the ore zone, supports an interpretation of syn-orogenic fluid influx. The fluid(s) was focussed below the interface between clean sub-arkosic sandstone and an overlying poorly-sorted hangingwall sandstone-siltstone aquiclude package.
- No evidence has been found of diagenetic phases of mineralisation/alteration. The paragenetically earliest sulphide phase (i.e. pyrite) was observed in one instance to enclose a hydrothermal monazite grain dated at 450 ± 126Ma. Similarly albite, which has an intimate spatial association within sulphides, was observed to enclose monazite dated at 554 ± 86Ma. (all ages reported with 2σ errors)

Mwambashi B

Mwambashi B is a presently unexploited arenite-hosted ('footwall') Cu-Co deposit located on the western margin of the Chambishi Basin (fig. 1). It was discovered in the 1960s, with recent infill drilling by Anglovaal indicating a resource of 8.4 Mt @ 2.63% Cu and 0.08% Co (Kirkpatrick, 1997).

Although 'footwall-hosted', the stratigraphic position of Mwambashi B Cu ore is distinct from that of the Chibuluma West deposit (fig. 2). For the most part, mineralisation is hosted within the Kafue Arenites Member (i.e. hangingwall of Chibuluma West). Furthermore, Mwambashi lies northward of the WNW-trending 'Ore Shale pinch-out' zone (as defined by Annels, 1989), with well preserved, albeit weakly mineralised intervals of Copperbelt Orebody and Rokana Evaporite members. Lateral facies variation is pronounced, at least to the upper level of the Copperbelt Orebody Member, attesting to a more complex basin geometry and growth history relative to Chibuluma West.

Similarities do exist between the two deposits however, including: (1) relatively clean host facies type capped by more argillaceous units, (2) accumulation of the host package within a highly restricted sub-basin, (3) fundamental basin reconfiguration at the top of the Mindola Clastics Formation, (4) increased feldspathic alteration within mineralised intervals, and (5) similar paragenetic relationships between sulphide phases.

Stratigraphy and Facies Associations

Mindola Clastics Formation (MCF)

The basic two-fold stratigraphic subdivision of the MCF defined at Nkana-Mindola and Chibuluma West remains broadly applicable at Mwambashi B (fig. 2). The subdivision is based primarily on an abrupt vertical transition to argillaceous strata (fig. 3), which is interpreted to reflect a regional change in sedimentary environment (or phase of basin development). The lower member (herein referred to as the *basal clean siliciclastic package*) comprises relatively clean arenaceous and rudaceous units with alluvial fan- braided fluvial affinities. Overlying argillaceous sandstones, siltstones and conglomerate facies are correlated on litho-stratigraphic grounds with the Kafue Arenites Member (KAM) and record a change to probable subaqueous environment and fan-delta sedimentation (cf. Chibuluma West). A local provenance appears to persist throughout accumulation of the MCF in this region, with immature monomictic, granite-derived debris occurring at numerous positions within the stratigraphy.

Significant thickness and lateral facies variation occurs throughout the deposit, and within regions where the MFC become condensed, the two-fold stratigraphy becomes less distinct (fig. 3). In these regions, rates of sediment input remained high relative to the rate of generation of accommodation space, such that subaerial fan-dominated sedimentation persisted to the level of the Copperbelt Orebody Member. In the following section we highlight the main vertical facies associations.

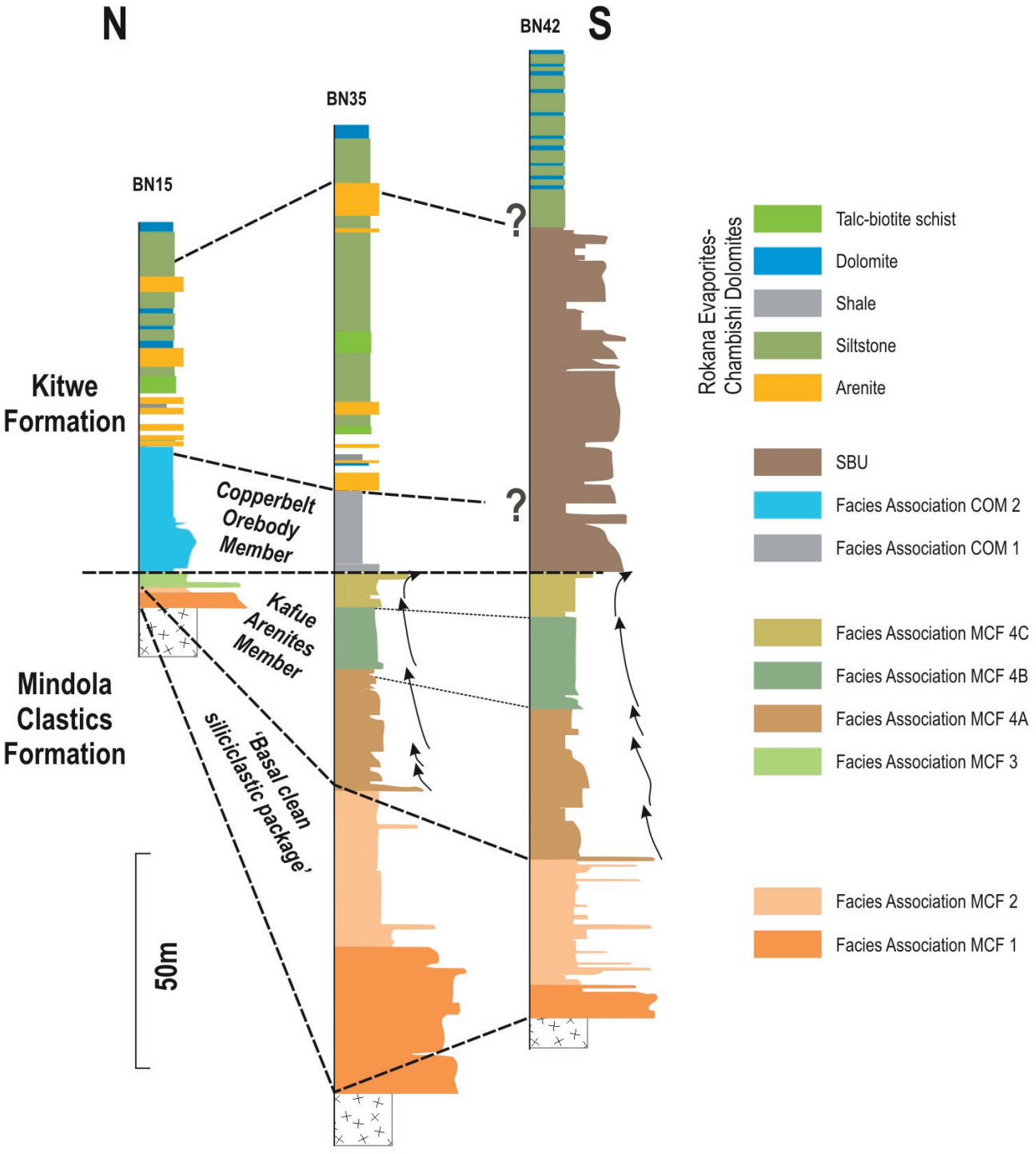

Figure 3. Selected sections showing end members of vertical and lateral facies variation throughout Lower Roan at Mwambashi B. Sections hung on interpreted base of Copperbelt Orebody Member.

Basal clean siliciclastic package

The basal part of the sequence comprises two main facies associations (fig.3). These are distinguished primarily on median grainsize and depositional process. Broadly, these criteria vary in a vertical sense, with most drill holes intersecting upward fining successions, however pronounced lateral facies variation occurs locally in areas interpreted to have been proximal to active growth faults. Thickness variation (70–0 m overall) is most pronounced within lower, coarser-grained portions of the package.

Facies association MCF 1 is characterised by poorly organised, matrix-supported, monomictic granule to boulder conglomerate, with subordinate intervals of massive to crudely stratified arkose (figs 3, 4a). Clasts are invariably derived from the local granitic basement, and are generally rounded to sub-rounded, set within a medium-grained arkosic matrix. Conglomerate beds are generally tabular and distinct upward coarsening occurs in some cases. Rare granule to pebble conglomerate beds less than 1m in thickness with low matrix component display erosional bases and upward fining internal structure. Cross-stratification may be developed within the sandier upper portions of such intervals.

Matrix-poor, monomictic pebble to boulder conglomerate units with distinctive angular clast morphology occur at the base of the sequence in a small number of holes (fig. 4b). They occur up to 30 m in thickness and have very limited lateral extent.

Interpretation: The facies association records complex interplay of debris flow, stream flow and rock-fall processes that is typical of proximal parts of an alluvial fan system. The dominance of debris flow depositional processes is demonstrated by the abundant matrix-rich conglomerates, particularly those with upward coarsening internal structure. Channellised, normally graded conglomerates and more tabular sandstone intervals record streamflow sedimentation. Upward fining trends may reflect channel abandonment or waning of flood events. Localised matrix-poor angular clast breccias were emplaced as talus cones adjacent to active fault scarps.

Facies association MCF 2 is characterised by a dominance of sandstone, with subordinate thin conglomerate bands (figs 3, 4c). Sandstones are typically moderately well-sorted, matrix-poor arkoses and sub-arkoses, with overall subtle vertical grainsize variation. Their internal structure is variable, including massive, parallel- and small-scale cross-stratification. Internal stratification is usually defined by heavy mineral lamination or more clay rich seams, but in some cases is defined by prominent grain-size contrast and concentration of granule seams. Granule and pebble lags at the base of beds occur locally. Conglomerates are matrix rich, with indistinct upper and lower margins.

Interpretation: Predominance of streamflow and/or sheetflood processes is demonstrated by abundance of parallel and cross-stratification. Evidence of channellisation is rare, perhaps due to the limitations of drill core, but indicated locally by gravely channel-floor lags. Such depositional processes are typical of middle to outer fan environments, but are also compatible with more basin axial directed braided fluvial systems.

Kafue Arenites Member

Resurgence of tectonic activity during deposition of the upper portion of the MCF is indicated by an abrupt change in facies association (hence depositional conditions). The onset of this event is heralded in a few holes by influx of conglomerate or grit, which in a regional sense, may correlate with the Lower Conglomerate at Nkana (cf. Croaker, this volume). The KAM is characterised by an increased argillaceous component and more diversified facies association compared to the underlying *basal clean siliciclastic package*. Siltstone and mudstone become volumetrically significant facies types, however there is an overall coarsening of grainsize relative to the fluviatile-outer fan facies association of upper portions of the *basal clean siliciclastic package*.

Thickness of the KAM varies from 65 to 0 m. Thicker successions generally coincide with thicker parts of the *basal clean siliciclastic package* (fig. 3), indicating that the architecture of the controlling faults and associated depocentres remained largely unchanged during accumulation of the MCF. This

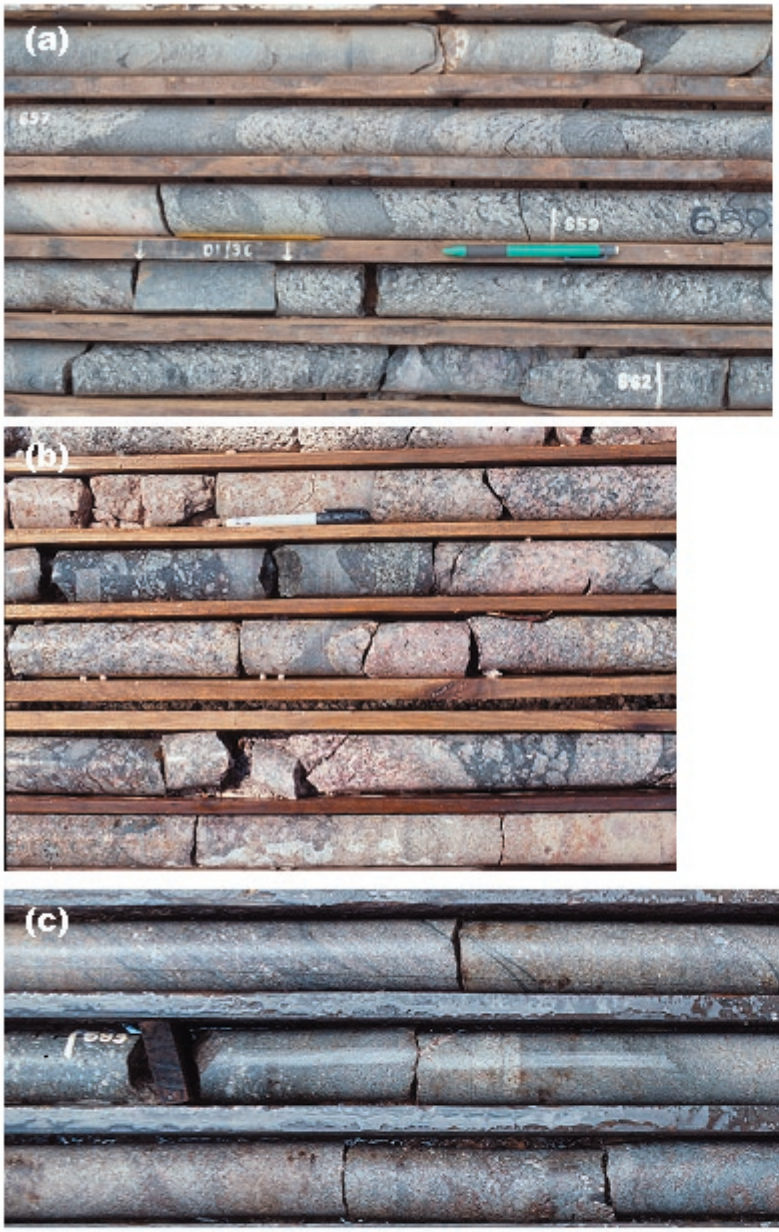

Figure 4. Facies association MCF 1 & 2.

(a) Facies association MCF 1 matrix supported, monogenetic granite clast conglomerate of debris flow origin.

(b) Facies association MCF 1 matrix poor granite clast breccia. Note highly angular habit of clasts. Very limited lateral extent, probable deposition via rock fall processes.

(c) Facies association MCF2 cross-stratified sandstone, gritty sandstone, with thin intervals of granite-derived pebbly sandstone.

interpretation is in accordance with the persistence of a local-derived granitic provenance throughout the sequence.

Within thicker portions of the MCF, distinct 10–15-m thick vertical megasequences are developed (fig. 3). A broad transition occurs from upward thinning and fining cycles towards the base to upward thickening and coarsening cycles near the top. Basal megasequences are interpreted to record progressive waning of relief following discrete tectonic pulses, whereas upper coarsening and thickening cycles are interpreted to record a progressive increase in fault activity and rate of sediment input, climaxing in an abrupt change in basin configuration at the top of the MCF. An internal structure is less clearly defined in areas of condensed section, where arenaceous-dominated deposits with affinities to the *basal clean siliciclastic package* appear more randomly punctuated by pulses of coarse-grained debris. Facies associations developed within condensed and expanded parts of the member are discussed separately below: facies associations MCF 3 & 4 respectively.

Facies Association MCF 3 is defined within condensed portions of the KAM (fig. 3), where measured sections have a maximum thickness of 20 m. It comprises roughly equal volumes of moderately-sorted sandstone and poorly-sorted gritty sandstone to conglomerate. Facies types are similar to those of facies associations 1 and 2, however biotite content appear slightly lower than in the latter, suggesting lower original argillaceous components. Moderately-sorted sandstone facies display parallel and cross stratification, and are matrix-poor. Coarser-grained facies include normally graded granule conglomerate and grit beds with erosional basal contacts, and internally structureless, immature pebbly sandstone to cobble conglomerate.

Interpretation: Facies types within condensed sections indicate persistence of the subaerial alluvial fan environments that characterises the lower member of the MCF. Lack of evidence of subaqueous sedimentation, a feature observed throughout much of the thicker sections (see below), combined with the coarse-grained, immature nature of the facies, indicate high rates of sedimentation relative to rates of accommodation development. Condensed, relatively argillite-poor portions of the KAM are interpreted to coincide with areas of greatest sediment input.

Facies Association MCF 4A comprises argillaceous sandstone, siltstone, mudstone and minor conglomerate. It occurs within lower levels of thicker Kafue Arenite Member sections (i.e. >50 m). Measured sections reveal at least two upward fining and thinning megasequences with conglomeratic (both matrix- and clast-supported) to coarse-grained sandstone bases and siltstone-dominated tops (fig. 3). Basal coarse-grained facies local display upward coarsening and thickening profiles. The bulk of the each megasequence consists of tabular to repetitive upward fining sandstone-dominated cycles ranging 30 cm to 4 m in thickness. Tabular sandstone beds are moderately to poorly-sorted, medium to coarse-grained, and crudely stratified to internally massive (fig. 5a). Domains of relict, distorted parallel- and cross-stratification, and dismembered siltstone layers within predominantly massive units indicate that the internal character resulted in part, at least, from post-depositional homogenisation of originally stratified beds (fig. 5b). Lack of strain within such units implies that homogenisation occurred prior to complete lithification. Normally graded units have erosional to planar bases and pass upward from poorly-sorted gritty sandstone to laminated siltstone and fine sandstone. Cross- and parallel stratification is developed within lower portions of thicker sandy intervals.

Siltstone-dominated intervals at the top of megasequences are up to 5 m in thickness and are laterally extensive. The correlative potential of these units was recognised by Mwale (2001), who argued they could provide useful stratigraphic markers. Facies types include parallel-laminated siltstone and mudstone, and thinly interbedded siltstone-sandstone couplets. Sandstone beds range from <1cm to 10 cm, with tabular to lenticular forms, the latter locally resembling starved ripples. They are massive to normally graded, with common ripple- and cross-lamination (fig. 5c). Clastic dykes, contorted lamellae and homogenised silt-sand intervals provide evidence of liquefaction and/or fluidisation processes.

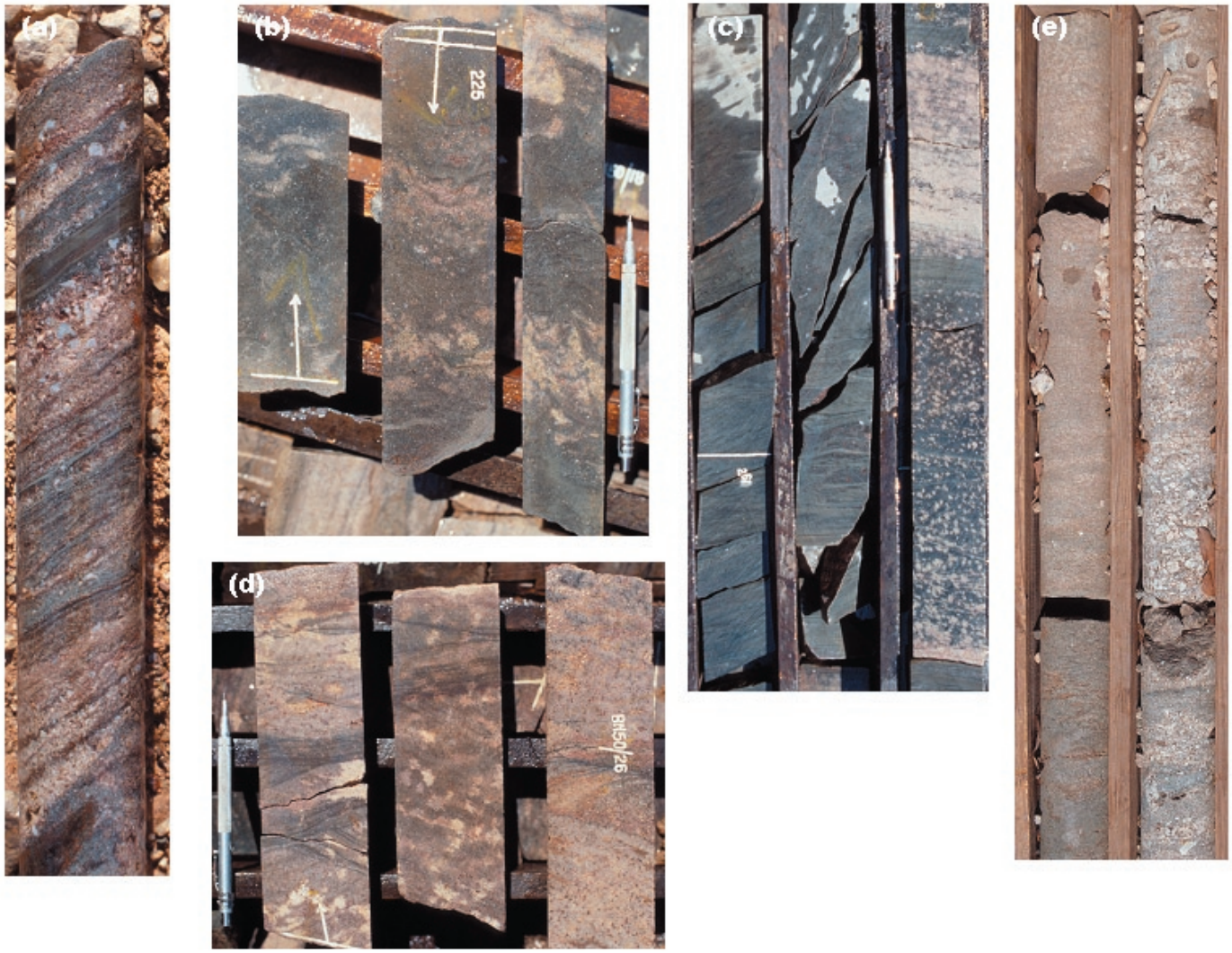

Figure 5. Facies association 4 of the MCF.

(a) Facies association 4A poorly sorted, parallel-stratified tabular sandstone.

(b) Facies association 4A partly homogenised biotitic sandstone and siltstone.

(c) Facies association 4A siltstone-shale. Normally graded sandstone intervals with relict low angle cross-stratification.

(d) Facies association 4B well sorted, matrix poor arkosic sandstone. Well developed cross-stratification and heavy mineral lamination.

(e) Facies association 4C upward coarsening cycle (left to right). Granite clast conglomerate marks top of MCF.

Interpretation: The dominant fining and thinning upward character of megasequences indicates they record episodes of fan retreat at localities distal to local sediment input points (i.e. condensed inner and middle fan environments of facies association 3). Evidence of progradation is indicated by subordinate coarsening and thickening upward profiles at the base of megasequences in some drill holes.

Sandstone facies were deposited within a braided channel environment, as indicated by multiple, second-order fining upward cycles, which most probably reflect lateral migration of transient channel systems. The laterally continuous geometry of siltstone-dominated intervals at the top of megasequences is unlikely to be explained by inter-channel sedimentation (i.e. overbank deposits within a meandering or braided fluvial system) and is interpreted to indicate progressive starvation of clastic input. The structure of sandstone-siltstone couplets, in particular lenticular bed morphology and small-scale cross-stratification, is considered typical of a lower delta plain depositional environment. The abundance of liquefaction/fluidisation related textures throughout facies association MCF 4A is also characteristic of deltaic environments where water-laden strata are subject to rapid sediment loading during episodic tectonic/flood events.

Facies Association MCF 4B occurs within middle to upper portions of thick KAM sections (fig. 3). It comprises a tabular, laterally extensive15–20 m-thick interval of clean, matrix-poor arkose very similar to facies association MCF 2 and fine-grained portions of facies association MCF 3. Subtle upward fining is enhanced by a narrow gravely to cobbly sandstone internal at the base in some drill holes. The bulk of the interval is parallel- and/or cross-stratified, with lamination commonly defined by bark haematitic lamellae (fig. 5d).

Interpretation: This facies association marks a regressive trend to subaerial fluviatile, outer fan or perhaps littoral sedimentation. Renewed fault activity is indicated by coarse-grained lithofacies at the base.

Facies Association MCF 4C involves a 3–10 m-thick, coarsening and thickening upward megasequence at the top of the KAM (fig. 3). It is correlated regionally with the Footwall Conglomerate defined at Nkana-Mindola (fig. 2), Chambishi and Konkola.

Lower portions of the megasequence resemble facies association MCF 4A. They comprise intervals of medium-grained, tabular to normally graded argillaceous sandstone and minor siltstone which thicken upward locally from 30 cm to 3 m. Liquefaction is evident in some drill holes, whereas parallel and cross-stratification is preserved in others. The top of the megasequence comprises a 1–2 m thick, poorly-sorted and generally clast-supported, granite-derived granule to pebble conglomerate (fig. 5e). The conglomerate is massive in most drill hole intersections, however crude parallel stratification is locally developed.

Interpretation: The abrupt basal transition from clean fluviatile sandstones of facies association MCF 4B to argillaceous sandstones is interpreted to record basin floor subsidence and a trangressive trend towards subaqueous sedimentation. Overall, however, progradation of alluvial fan deposits over a probable channellised upper delta plain environment is indicated by the upward coarsening and thickening profile of the megasequence. This basin filling event utilised older source regions as indicated by the persistent local granitic provenance, but heralds the onset of a fundamental phase of basin reconfiguration recorded by the abrupt change in facies association across the Mindola Clastics–Kitwe formation boundary.

Kitwe Formation (KW)

The KW records a change to predominantly subaqueous marine (?) sedimentation, as indicated by increased abundance of shale and carbonate. It has been defined at Nkana-Mindola as comprising four lithostratigraphically distinct members: Copperbelt Orebody, Rokana Evaporites, Nchanga Quartzite and Antelope Clastics members (fig. 2: Clemmey, 1976). A similar stratigraphy is recognised at Mwambashi B, albeit obscured in part by deep weathering and alteration.

We deviate slightly from Clemmey's *(op. cit.)* subdivision at the level of the Copperbelt Orebody

Member (COM). At Nkana-Mindola, the uppermost portion this member is defined by a distinctive upward coarsening cycle (fig. 2) and includes the first significant arenite unit deposited above the typically siltstone-dominated 'Ore Shale' interval. This transitional upper contact of the COM is not clear at Mwambashi B, and we consider the first arenite unit to have closer affinities with the overlying Rokana Evaporites Member.

Copperbelt Orebody Member

The COM is mainly well preserved, occurring below the level of strong oxidation in drill holes logged for this study. In stark contrast to the underlying MCF, lateral thickness variation is subtle (15–40 m), a feature which typifies the regional Copperbelt stratigraphy (figs 3, 6). However, evidence of lateral facies variation does occur (and has been well documented by previous geologists), and in a local sense mimics the more pronounced facies and thickness variation within underlying units. This is most convincingly demonstrated within the predominantly fine-grained portions of the COM (i.e. those units traditionally termed 'Ore Shale'), where two distinct facies associations occur. Dark grey carbonaceous siltstone is the dominant lithotype within the volumetrically most significant of these facies associations, and overlies the main part of the orebody. At the northern periphery of the orebody, dark grey siltstone passes abruptly into a slightly condensed package of brecciated and altered dolomitic lithofacies (figs 3, 6). We suspect that this lateral facies variation within the COM at Mwambashi B is analogous to that developed at Nkana-Mindola (see Croaker, this volume). In both systems, higher levels of alteration (and possibly also strain) in areas of dolomitic facies obscure the true nature of the protolith.

The lateral transition from 'carbonaceous' to 'dolomitic' facies associations coincides with an along strike pinch-out of the MCF. That is, the dolomitic facies association to the north of the main orebody lies directly on basement. However, this spatial link between facies (and to a lesser extent, thickness) variation within each unit does not hold throughout the deposit, because in areas of down-dip pinch-out of the MCF, basement is overlain by the carbonaceous facies association of the COM.

Potential lateral facies variation at the level of the COM also occurs ~3 km south of the deposit. Two isolated drill holes from this region (BN 42 and BN43) failed to intersect typical 'Ore Shale' facies. In the drill core logged for this study (BN42), the MCF appears complete, but is overlain by a highly altered package of breccias (figs 3, 6; herein termed the 'southern breccia unit' (SBU). The thickness of the breccia package is roughly compatible with the combined thickness of the COM and Rokana Evaporites members above the main orebody.

The following section provides additional detail regarding the facies associations of the COM. The SBU will be discussed separately as it transgresses the COM-Rokana Evaporites Member contact.

Facies Association COM 1 consists predominantly of dark-grey siltstone and mudstone. A distinctive and laterally continuous vertical profile occurs in most drill holes comprising four principal lithofacies (A–D) with overall upward thinning and fining character (fig. 7a). The basal lithofacies (A) consists of pale grey sericitic and/or carbonate matrix sandstone with minor conglomerate and breccia, generally less than 3 m in thickness. Relatively high degree of strain at this level results from tectonic decoupling between the COM and underlying units, a feature which is enhanced where the MFC is either thin or absent. This deformation partly obscures the protolith and in particular creates difficulty in discriminating between breccias of tectonic and sedimentary origin. Moreover, it is presently unclear as to whether the increased carbonate and/or sericite component is primary or the result of alteration. Further petrographic work is required to resolve these problems. However, despite the tectonic (and possibly alteration) overprint, a broadly upward fining profile is preserved (fig. 7a, d). Lowermost sandstones are poorly-sorted and stratified, with predominantly fine- to grit-sized, texturally immature quartz fragments 'floating' within a fine-grained matrix (fig. 7eii). The quartz framework is texturally analogous to that within the immediately underlying MCF and implies a similar granite-derived provenance (compare figs. 7eii & 7eiii). Up-section,

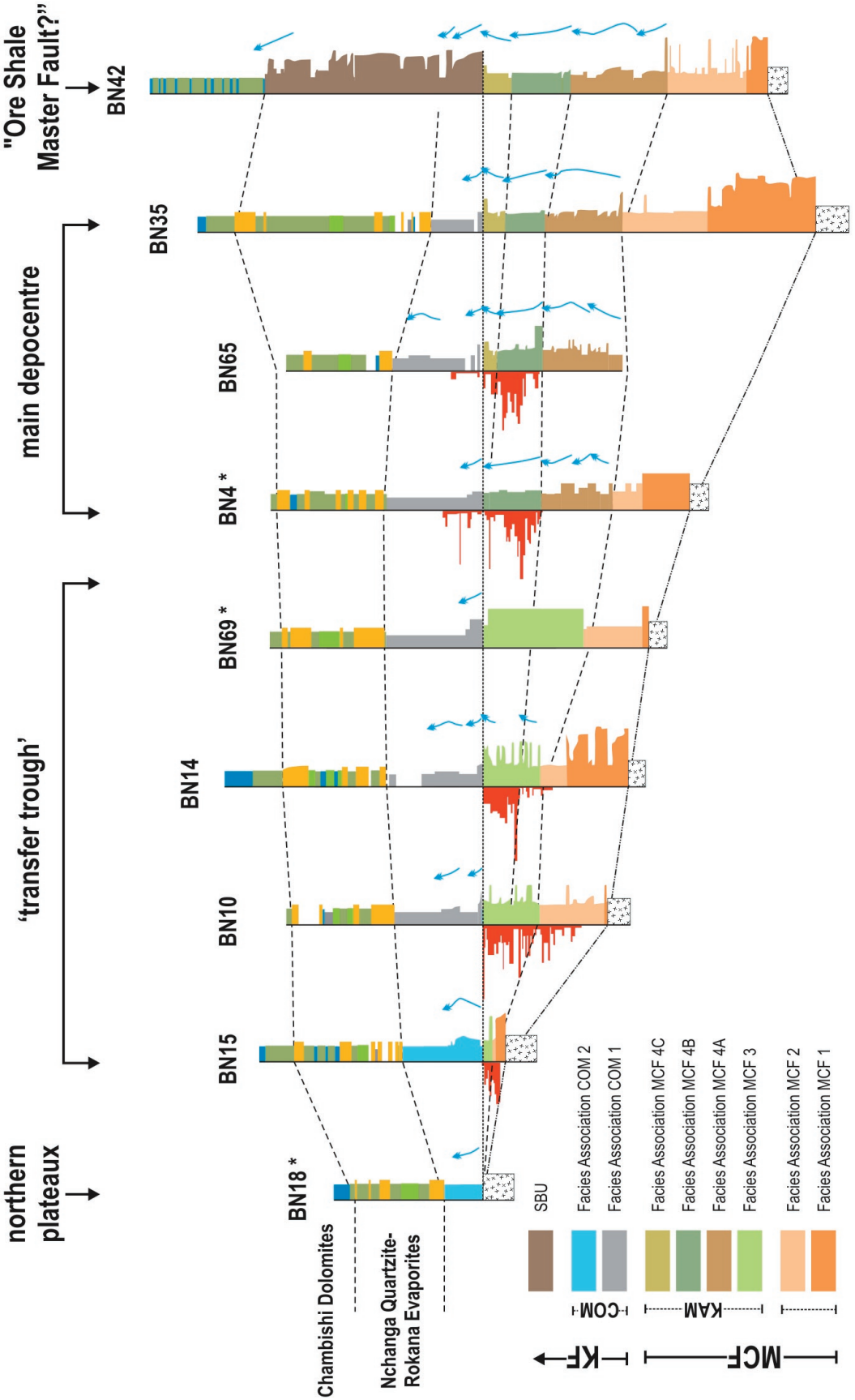

Figure 6. N-S longitudinal section showing position and relative grade of Cu mineralisation.
BN* denotes section from historical logs. Refer to Figure 3 for facies types in Rokana Evaporites and higher members. Refer to Figure 10 for location of traverse.

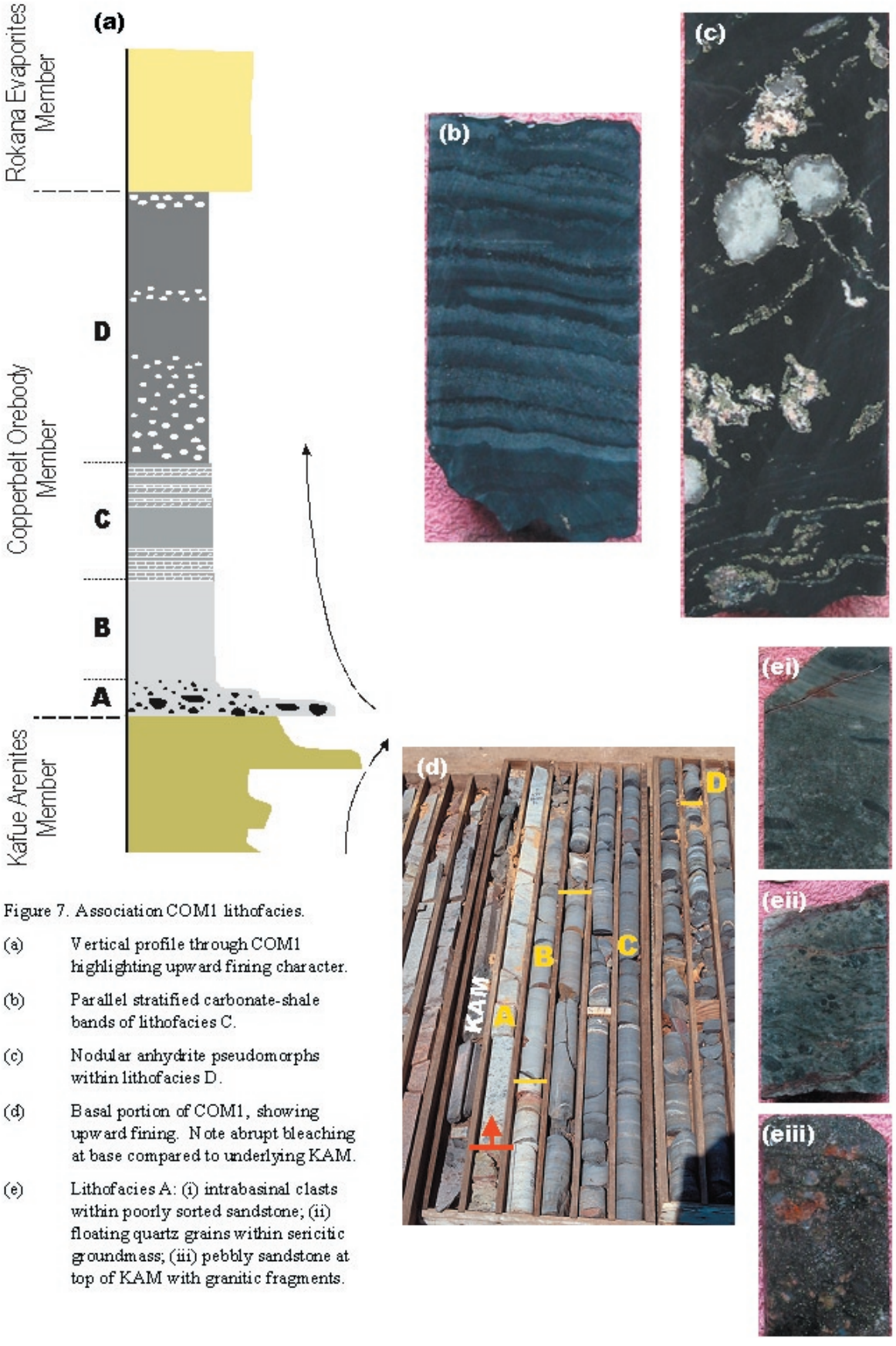

Figure 7. Association COM1 lithofacies.

(a) Vertical profile through COM1 highlighting upward fining character.

(b) Parallel stratified carbonate-shale bands of lithofacies C.

(c) Nodular anhydrite pseudomorphs within lithofacies D.

(d) Basal portion of COM1, showing upward fining. Note abrupt bleaching at base compared to underlying KAM.

(e) Lithofacies A: (i) intrabasinal clasts within poorly sorted sandstone; (ii) floating quartz grains within sericitic groundmass; (iii) pebbly sandstone at top of KAM with granitic fragments.

massive to normally-graded, fine- to medium-grained sandstone beds from 0.5–10 cm in thickness occur interbedded with pale grey siltstone. Although better sorted that underlying units, sandstone intervals remain matrix-rich in some cases and display diffuse margins with enclosing siltstone. Sub-rounded to angular mudstone fragments within thicker sandstone beds or breccia units are also apparent towards the top of lithofacies A (fig. 7ei).

The sandstone-dominated base passes rapidly upward into a transitional unit (lithofacies B) 2–4 m in thickness, of pale grey, massive to crudely banded and rarely parallel-laminated siltstone (fig. 7a, d). Banding occurs on the scale of 0.1-5mm and is defined by subtle changes in colour, which may reflect variable carbonate content. No obvious grainsize variation occurs throughout this interval. The transition from lithofacies B to C (7–12 m in thickness) is defined by a progressive darkening, coupled with the development of well-defined, parallel laminations and predominantly sub-centimetre scale bedding. Stratification is defined by alternation of pale grey carbonate-rich (primarily calcite) and dark grey siliceous siltstone and shale (fig. 7a, b, d). Disseminated pyrite occurs throughout. Carbonate-rich bands are generally tabular, but include wavy to lensoidal forms. Fine-grained carbonate-rich bands have mainly sharp margins. However coarsening upward, apparently due to recrystallisation, occurs in many cases (particularly near the top of the interval where strain is often intensified), resulting in diffuse or fibrous vein-like upper contacts with overlying dark grey siltstone. In some cases, entire carbonate-rich bands appear recrystallised and may locally transgress primary layering. Intervening dark grey siltstones and shale bands are predominantly massive, but delicate parallel lamination occurs rarely.

Lithofacies D comprises dark grey laminated siltstone and shale, with apparently lesser carbonate content relative to lithofacies C. It ranges 16–18 m in thickness in most drill holes, however an anomalously thin (8 m) interval was measured in one drill hole. Distinctive sub-tabular and laterally extensive nodular domains occur concentrated at the base and top of the interval (fig. 7a, c). Nodules have ellipsoidal forms, with aligned long axes ranging 0.1–3 cm in length (coarsest examples occur at the top of the package). They consist of calcite with minor quartz and feldspar and are commonly enclosed within a thin veneer of pyrite. Quartz crystals occur locally as radiating needles or rosettes, with pyramidal terminations implying replacive growth or infilling of partial voids. Lamellae within the enclosing siltstone are contorted or in some cases obliterated. This deformation almost certainly includes the effects of late-stage tectonism. However, textures indicative of displacive nodule growth such as deflection of lamellae around nodule margins and in particular homogenisation of the enclosing siltstone imply growth of nodules prior to consolidation of the host medium.

Interpretation: The abrupt reduction in grainsize across the MCF-COM boundary marks the onset of a period of starvation of coarse clastic sediment. Overall, the apparent upward reduction in carbonate content, coupled with the upward fining character of lithofacies A & B potentially records rapid, but progressive subsidence and transgression of local source areas to the MCF.

Rapid retrogradation of the fan-delta systems that fed the upper portion of the MCF, is indicated by the thinning and fining upward trend at the base of the package. The matrix-rich nature of the basal sandstones, combined with normal grading in some cases, suggests emplacement by mass flow processes. However, as mentioned previously, we are presently unsure as to whether the sericite and/or carbonate dominated matrix is primary or related to alteration. Considering the similarity between the detrital quartz framework of the lowermost gritty sandstones to immediately underlying arkosic conglomerates and sandstones of the MCF, it could be argued that protoliths were fundamentally the same and that the contact between the two packages is in fact a secondary alteration front. For example, the present 'quartz-in-sericitic-groundmass' texture of some lithofacies A sandstones may record infiltration of an acidic fluid along the basal zone of decoupling and wholesale degradation of a primary feldspathic framework component. If further petrographic studies show this to have been the case, we may have to

modify our interpretation of the precise basal position of the COM. Regardless of this problem however, the appearance of mudstone fragments towards the top of lithofacies A indicates the onset of intrabasinal reworking and contrasts with the persistent basement-derived provenance of the MCF.

The dominant parallel stratified character of lithofacies B-D, combined with the lack of evidence for tractional reworking or periods of emergence (i.e. ripple lamination, desiccation cracks, intraclast breccias), supports a sub-wave base depositional environment, wherein the bulk of the fine-grained clastic component settled out of suspension.

Nodular domains within lithofacies D are both texturally and compositionally analogous to nodular intervals situated at the mineralised base of the COM at Chambishi SE (Annels, 1974). For the latter deposit, Annels argued that nodules originated as early diagenetic displacive anhydrite and demonstrated progressive replacement by calcite, quartz and sulphide during the mineralising process. We are yet to demonstrate an original anhydrite composition for the nodules at Mwambashi B, however evidence of early diagenetic displacive growth and the replacive character of their present constituents, supports such an interpretation.

The presence of former anhydrite provides a constraint on the depositional environment, as sulfate-bearing brines are formed in significant volumes only in evaporitic marginal marine settings. However, there is no indication that facies association COM1 formed in an evaporitic environment (for the reasons outlined above), and therefore anhydrite precipitation must have been associated with influx of exotic hypersaline groundwaters. Possible evaporitic source environments include the laterally equivalent lithofacies association COM2 (see below) and/or the overlying Rokana Evaporites Member. Dense hypersaline brines formed during deposition of either of these units could have percolated downward and/or laterally into the partly consolidated COM1 strata. Thus concentration of former anhydrite nodules at the top and base of lithofacies D is probably a reflection of the early diagenetic hydrological system: i.e. retention of higher permeabilities within upper carbonate-poor levels of the package.

Facies Association COM2 comprises predominantly 'dolomitic' lithofacies situated at the northern periphery of the deposit. In two holes logged for this study, the package thins northward from 30 m to 14 m over a strike length of 250 m (fig. 6). It comprises three main lithofacies, the lower two of which are similar to those situated towards the base of facies association COM1 (i.e. lithofacies A & B). Thickness variation between the two logged intervals occurs mainly within this lower part of the package.

Lithofacies A equivalent varies between 14 and 6 m in thickness, and is characterised by pale green to grey, massive to normally graded, poorly-sorted, coarse-grained dolomitic sandstone (fig. 8a, bi). In contrast to facies association COM1, a crudely symmetrical vertical profile is developed in the thicker of the sections, with an upward coarsening and thickening base and an upward fining and thinning top. A 1m thick talc-carbonate schist occurs within a shear zone at the base.

The overlying transitional zone (lithofacies B equivalent) comprises pale grey dolomitic, siliceous and/or talcose siltstone. It is largely brecciated with some textures, including angular plate breccias, potentially of sedimentary origin (fig. 8bii). However, other breccia textures involving highly angular to well-rounded, silicified monomictic fragments set within a sheared talcose matrix are almost certainly of post-depositional origin (i.e. tectonic, hydraulic or solution collapse breccias: fig. 8biii).

The uppermost lithofacies (E) is similarly brecciated throughout, but comprises highly angular, dark grey, silicified dolomite ('cherty dolomite'), set within a talc-poor siliceous matrix. Of particular significance is the preservation of delicate crenulate lamellae within clasts, which closely resemble microbial lamination (fig. 8biv). Direct correlation of lower lithofacies between the facies association COM1 & COM2 would make this interval a lateral equivalent of dark grey siltstone dominated lithofacies C & D. It thins northward from 8 m to 6 m in the two logged drill holes and compares with roughly 25 m for the combined thickness of lithofacies C & D.

Interpretation: High degree of alteration and strain throughout facies association COM2 hampers interpretation of sedimentary processes. The spatial

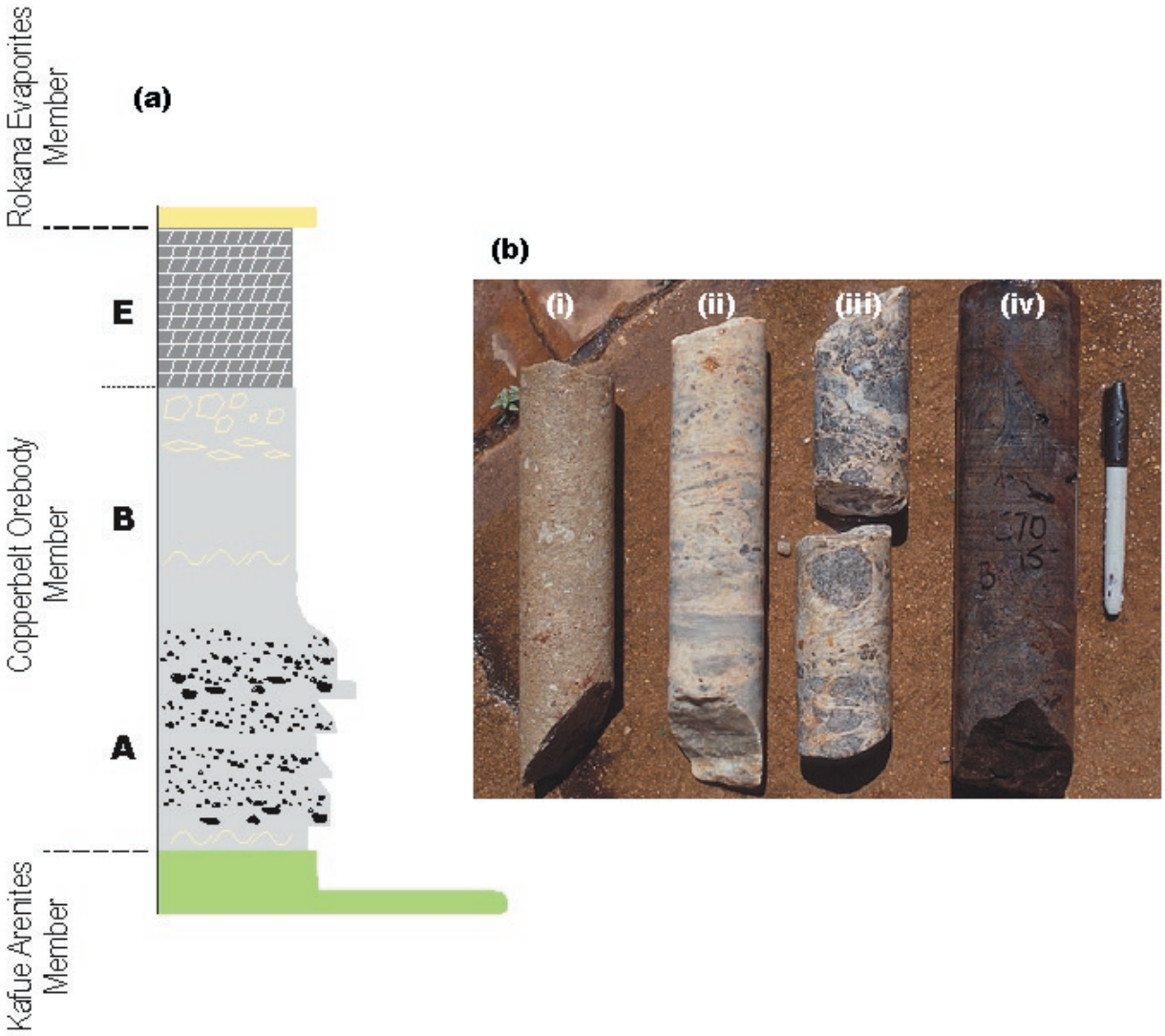

Figure 8. Association COM2 lithofacies.

(a) Vertical profile through COM2 showing 3-fold subdivision.

(b) Facies types: (i) Lithofacies A sericite-carbonate altered gritty sandstone; (ii) Lithofacies B dolomitic breccia of possible sedimentary origin; (iii) Lithofacies B dolomitic breccia of probable tectonic origin; (iii) Lithofacies E dark silicified and brecciated dolostone, with relict cryptalgal lamination.

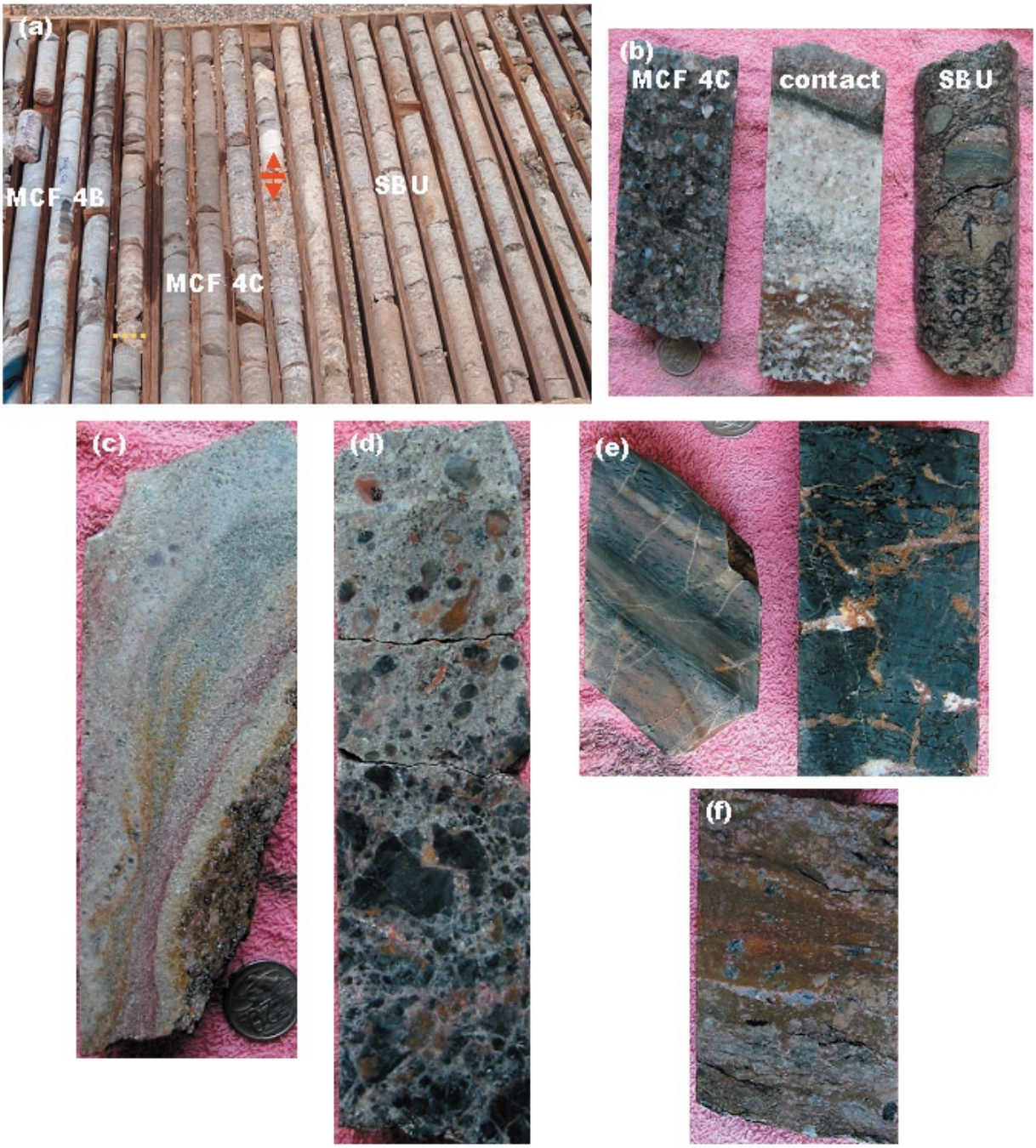

Figure 9. Textural and compositional features of the SBU.

(a) Contact between the MCF and SBU in BN42. Note that the MCF is complete, also abrupt increase of alteration (bleaching) above the contact.

(b) Detail of the MCF-SBU contact: facies association MCF 4C granite clast conglomerate (left); intensely albitised interval on contact (centre); rounded heavy mineral bearing sandstone clasts within the basal SBU (right).

(c) Apparent preservation of relict stratification: interbeds of well-sorted sandstone and poorly-sorted grit.

(d) Transitional contact of crackle breccia with local jigzaw-fit texture and pebbly sandstone.

(e) Scapolite-bearing dolomitic siltstone and weakly brecciated chloritic siltstone overlying SBU (possible Chambishi Dolomite Member equivalent.

(f) Cubic halite pseudomorphs concentrated at upper contact of SBU.

relationship between facies association COM1 & 2, combined with distinct lateral facies and thickness variation between the two packages, do however allow us to speculate on the local depositional environment.

Thickness contrasts are very apparent between the lower portions of facies association COM1 & 2, with lithofacies A sandstones thickening from a maximum of 4 m in the former to 14 m in the latter. Furthermore, the upward coarsening and thickening profile in facies association COM2 is distinct from the subtle upward fining and thinning profile in facies association COM1. This transition is potentially explained by limited seaward progradation of a variety of possible littoral sandstone environments, including shoreline/barrier island, channellised deltaic facies or subtidal sandstone units. Shoreline and/or barrier island environments are the least likely of these scenarios, as the sandstones lack internal stratification and their normally graded profiles are more indicative of channellised or mass-flow sedimentation.

Abrupt lateral thickness variation within lithofacies A may alternatively be explained if our interpretation of the base of the COM is incorrect for the thicker of the association COM2 intersections. The upward coarsening and thickening profile developed in this intersection may be better correlated with the uppermost MCF, with the precise position of the basal contact being obscured by strain and alteration (as discussed in the preceding section).

The most important lateral facies change between facies association COM1 & 2 occurs at the top of the packages. Apparent preservation of microbial lamination within lithofacies E indicates an abrupt shallowing of depositional environment relative to equivalent siliciclastic shales and siltstones of lithofacies C & D. This interpretation accords with the traditional model of alternating siliciclastic 'Ore Shale' depocentres and adjacent carbonate-dominated 'biohermal' facies. In favour of this interpretation, is the fact that packages enclosing facies association COM2 (i.e. underlying MCF and overlying Rokana Evaporites Member) are also condensed (figs 3, 6). This relationship would imply that the northern periphery of the orebody remained an area of limited accommodation space throughout deposition of the Lower Roan, and thus explain the persistence of shallow water or possibly emergent conditions in this region.

At this stage we offer the above interpretation provisionally. We cannot entirely discount that thickness and apparent facies variation within the COM results from a combination of deformation and alteration. The principal problem we face is that unequivocal evidence of shallow water conditions during deposition of facies 2 is lacking (due mainly to the alteration/deformation overprint). It is hoped that future whole rock geochemical studies will aid in resolving this problem. Initial studies of this type elsewhere throughout the Copperbelt indicate that typically immobile trace element ratios are largely unaffected by alteration. Thus the higher siliciclastic component apparent within facies association COM1 relative to that of COM2 should be reflected in the trace element abundances and ratios of the two units.

Southern Breccia Unit

The SBU overlies a thick, intact succession of MCF and is 80 m thick in the drill hole logged for this study (fig. 3). A close spatial association occurs between breccia units and intrusive gabbroic bodies, the latter occurring at slightly higher stratigraphic levels over the main part of the deposit. The basal contact is abrupt, but partly obscured by intense alteration (fig. 8a, b). It involves a relatively fine-grained, massive 1m thick albitic interval (fig. 8b), which lies directly on considerably less altered (mainly feldspar-calcite) pebbly sandstone. The underlying conglomeratic unit is massive and of monomictic granite clast composition (fig. 8b). It typifies the uppermost unit of facies association MCF 4C.

Lithotypes contained within the breccia package display some similarities to parts of the underlying MCF. Specifically, breccias are predominantly matrix-supported, lacking in a clear internal structure, and possess a high degree of clast rounding (fig. 8b). They resemble the pebbly mass-flow units within facies association MCF 1 & 3. Furthermore, vertical grainsize variation of the coarser framework component produces broad upward fining profiles (~10 m in

thickness) within parts of the breccia (fig. 3). Most convincing evidence of sedimentary fragmentation occurs within these upward fining sections, where thin pebbly sandstone bands appear to alternate with medium-grained, massive sandstone beds (fig. 8c).

Pronounced differences also occur between the MCF and the SBU. Most conspicuously, the level of alteration is much greater within the latter (fig. 8a). Pervasive carbonate-talc-albite-scapolite alteration occurs within the SBU, primarily within the matrix, but also commonly partitioned into narrow zones wherein primary textures are obliterated. Secondly, the locally derived granitic framework component, which typifies coarse-grained lithofacies of the MFC, appears absent within the SBU. The dominant resolvable clast component throughout the SBU is quartzitic sandstone of probable intrabasinal origin (fig. 8b). Such clasts are mainly internally massive, but in some cases preserve dark heavy mineral lamination. This change in clast provenance occurs immediately above the base of the breccia. Potential source units include much of the MFC, but also lateral equivalents within the Rokana Evaporites Member (see below).

Strain also intensifies within the SBU relative to the MCF. Domains containing strong shear fabrics, themselves folded, occur at a number of levels throughout the breccia. Monomictic crackle breccias displaying jigsaw-fit textures coincident with finer-grained dolomitic intervals (fig. 8d) are indicative of a more brittle style of post-depositional overprint. These breccia units appear tabular and have transitional contacts with enclosing pebbly sandstone facies.

The uppermost portion of the SBU displays rapid upward fining before passing abruptly into fine-grained dolomitic, chloritic and scapolitic siltstones and shales (fig. 8e). Cubic pseudomorphs interpreted to be after halite occur at the upper contact (fig. 8f). Weak crackle brecciation persists into the overlying siltstone-dominated package, which is tentatively correlated with the Chambishi Dolomites Member (fig. 2).

Interpretation: Understanding the mechanism(s) of fragmentation is critical to the interpretation of the SBU. A number of features are consistent with a sedimentary origin, however these do not preclude a multi-phase genesis involving subsequent components of tectonic and/or solution collapse related fragmentation.

The gross geometry of the SBU is considered to discount a tectonic origin involving significant lateral displacement. Its overall thickness is compatible with the combined thickness of the COM and Rokana Evaporites Member, suggesting that structural thickening or thinning has been insignificant. Furthermore, the underlying MCF is intact and lacks evidence of significant strain. However, due to the intensity of alteration at the basal contact, we cannot unequivocally preclude a component of shear without further petrographic work.

Factors that favour a sedimentary fragmentation process are: (1) the rounded habit of the bulk of the clastic component, (2) predominantly matrix-rich character, (3) the lack of obvious grain-scale deformation throughout much of the sandy matrix, (4) the development of a crude internal structure involving relict upward fining cycles, (5) preservation of apparent fine-scale stratification, and (6) the lack of clast types typical of the COM towards the base. These features are consistent with, but not exclusively indicative of a mass flow emplacement mechanism. For example, well-rounded clasts can be generated via *in situ* fragmentation, as shown in facies association COM 2 (fig. 8biii). However, the lack of mesoscopic cataclastic textures throughout the sandy matrix would indicate that if fragmentation was of a post-depositional origin, it must have proceeded in part at least via particulate flow. Thus deformation would have to have occurred prior to consolidation, either early in the rock's history, or under conditions which prevented effective cementation. The latter is potentially explained by the presence of saline brines, which may have had the ability to preserve porosity well into late diagenesis. Supporting this interpretation is the widespread abundance of scapolite, both within the SBU and overlying siltstones, as well as the evidence of former halite at the upper contact.

In situ fragmentation is indicated locally by the monomictic crackle breccia intervals. These are very difficult to explain by sedimentary processes (possible emplacement as talus blocks) and their lithological

distinction from enclosing pebbly sandstones suggest dismemberment of a once intact stratigraphic succession. Persistence of weak crackle breccia textures into the Chambishi Dolomites Member indicate that this episode of fragmentation affected a significant thickness of stratigraphy.

Elements of the SBU outlined above indicate that it was unlikely to have formed by sedimentary processes alone. At this stage, we favour a model involving modification of a package comprising intercalated mass flow conglomerates, sandstone and minor dolomite. Post-depositional fragmentation was potentially driven by dissolution of intergranular or bodies of salt (possibly in the vicinity of hot gabbroic bodies), an interpretation which may explain the elevated alteration within the SBU compared to the MCF. This interpretation is in accordance with that of Broughton (this volume), who recognised breccia units with similar composition and texture at higher levels of the stratigraphy.

Rokana Evaporites Member (REM)

The REM was deeply weathered in our logged drill holes, and as such was not studied in detail. It is further obscured by elevated strain and alteration (carbonate-talc-biotite-chlorite) relative to lower stratigraphic intervals. Where best preserved, protoliths included alternations of massive to cross-stratified sandstone, narrow intervals of siltstone and shale, and minor dolomite. No evidence of former evaporites was noted. Superficially, this facies association most closely resembles facies association MCF 4A. In contrast to the MCF however, lateral facies variation is lacking, with sandstone units possessing laterally extensive, tabular forms. Shale intervals are similarly correlatible over broad areas and partly resemble fine-grained siliciclastic portions of the COM. The repetitive character of the facies association indicates fluctuating rates of clastic input, within a marginal to marine environment.

Basin architecture

Introduction

Pronounced lateral and vertical thickness and facies variation throughout Lower Roan provide excellent constraints on the evolution of basin geometry to the level of the COM at least. In a vertical sense, variation in stratigraphic architecture reveals two principal phases of basin growth. The initial phase, as recorded by the MCF, is typical of modern rift settings. It is characterised by a highly compartmentalised geometry controlled by a complex array of active extensional faults. Sediment dispersal systems during this period were similarly complex. The largely monomictic clast assemblage dominated by granitic material identical to that of the immediately underlying basement indicates persistent contribution from local source areas. However, rapid lateral facies changes throughout the MCF (but particularly at the level of the KAM) reveal interplay of transverse drainage systems supplying coarse-grained debris across or between active fault segments (i.e. facies associations MCF1, 3, 4C), and finer-grained facies associations derived from probable axial drainages (i.e. facies associations MCF2, 4A, 4B).

Fundamental basin re-configuration occurred at the onset of Kitwe Formation sedimentation. The COM in particular records abrupt death of the local fault system that controlled accumulation of the MCF and consequent starvation of coarse clastic sediment input. Stratigraphic architecture at this time is characterised by broadly layer-lake geometries, even with the resumption of arenaceous sedimentation within the REM.

In the following sections, we provide details of the basin geometry during both of these basin phases, but concentrate on the mineralised portion of the stratigraphy: i.e. initial rifting and accumulation of the MCF. The data and interpretation presented here represent an integration of our own core logging with those preserved in historical sections and reports. They are in the form of an isopach map of the MCF as well as a series of cross sections throughout the main part of the deposit. Inversion-related strains are not significant. Although strata dip fairly uniformly

at 35° to the northeast, fold wavelengths are much broader than the width of the well-preserved basin compartments. As a result we considered there to be little advantage in restoring cross sections. It should be noted however, that the interpreted fault traces shown on the isopach map are projected to surface from unrestored sections and thus deviate slightly from their original geometry where oblique to the overall NW strike of layering. Thickness calculations have taken into account minor basement-involved thrusting (identified previously in one hole, i.e. BN 53 (Kirkpatrick, 1997) and reconfirmed in this study), as well as low wavelength folding developed locally in the MCF. Decoupling has also occurred at the MCF-KF boundary (as with Chibuluma West), however transport appears limited as the intensity of layer-parallel shear varies significantly even between adjacent drill holes. Effects of this decoupling include asymmetric folding within the COM (with amplitudes up to 10 m) and are most pronounced where the MCF is thin or absent.

Basin evolution during accumulation of the Mindola Clastics Formation

Isopachs of the MCF are shown in Figure 10. They reveal a roughly NW-trending, compartmentalised depocentre with a distinct asymmetry indicating gradual increase in accommodation space towards the SW. The detailed geometry of the depocentre is best demonstrated within the central part of the deposit, where drill hole density is greatest. Here, thickness variation within the MCF defines a complex array of discontinuous troughs and adjacent elevated basement blocks. As it will become clear from the following description of facies architecture, this thickness variation is a direct consequence of syn-depositional basin geometry and not an erosional phenomenon. The principal basin element within the central part of the deposit is a highly restricted and mildly subsident trough with NW-trend. The trough effectively bisects a broadly WNW- to NW-trending basement ridge, which forms the northern margin to the main depocentre and separates it from a second, less-well defined (due to limited drilling) depocentre to the northeast. Accommodation space in the central trough, as indicated by variation in thickness, dies out progressively at either end of its axis onto elevated basement blocks. Its north-eastern margin is defined by more abrupt pinch out against a broad basement plateau, whereas a narrow 'channel' of thickened MCF to the west indicates the position of an opening to the thicker parts of the depocentre.

The complex, compartmentalised character of MCF depocentres outlined above resulted from the interplay of discontinuous, but systematic fault segments. Domains of accommodation and adjacent uplifted areas *evolved during sedimentation* due to lateral and vertical variation in displacement along this fault array, rather than passive infilling of a pre-depositional and non-systematic basement topography. The position, orientation and displacement history of syn-depositional fault segments are defined by the combination of: (1) the three-dimensional geometry of sedimentary packages, and (2) facies variation within these packages. The first of these key indicators has been discussed briefly above with reference to MCF isopachs, whereas facies variation is demonstrated on the sections in figure 11. These data reveal a primary basin architecture controlled by three E-W to NW-trending fault segments, with hangingwall blocks downthrown to the north. The polarity of these fault segments is best demonstrated in the southernmost example, where an asymmetric half graben geometry is defined by progressive southward thickening of the MCF from 0 m to >110 m away from the central WNW-trending basement ridge. To the west, where the MCF occurs at relatively shallow levels, the NW strike of the fault segment is defined clearly by abrupt thickness variation from high density auger, percussion and diamond drilling. To the south however, drill holes are lacking, but extrapolation of the fault to the ESE is constrained to some degree by the distribution of basal talus breccia in the inferred hangingwall, which indicates proximity to an active fault scarp.

Less-well constrained are the geometries of roughly E-W trending faults located along the northern edge of the central WNW-trending basement ridge and at the northern limit of the deposit (fig. 10). Although drilling is fairly sparse in these regions, available data are best explained by an abrupt, fault-controlled

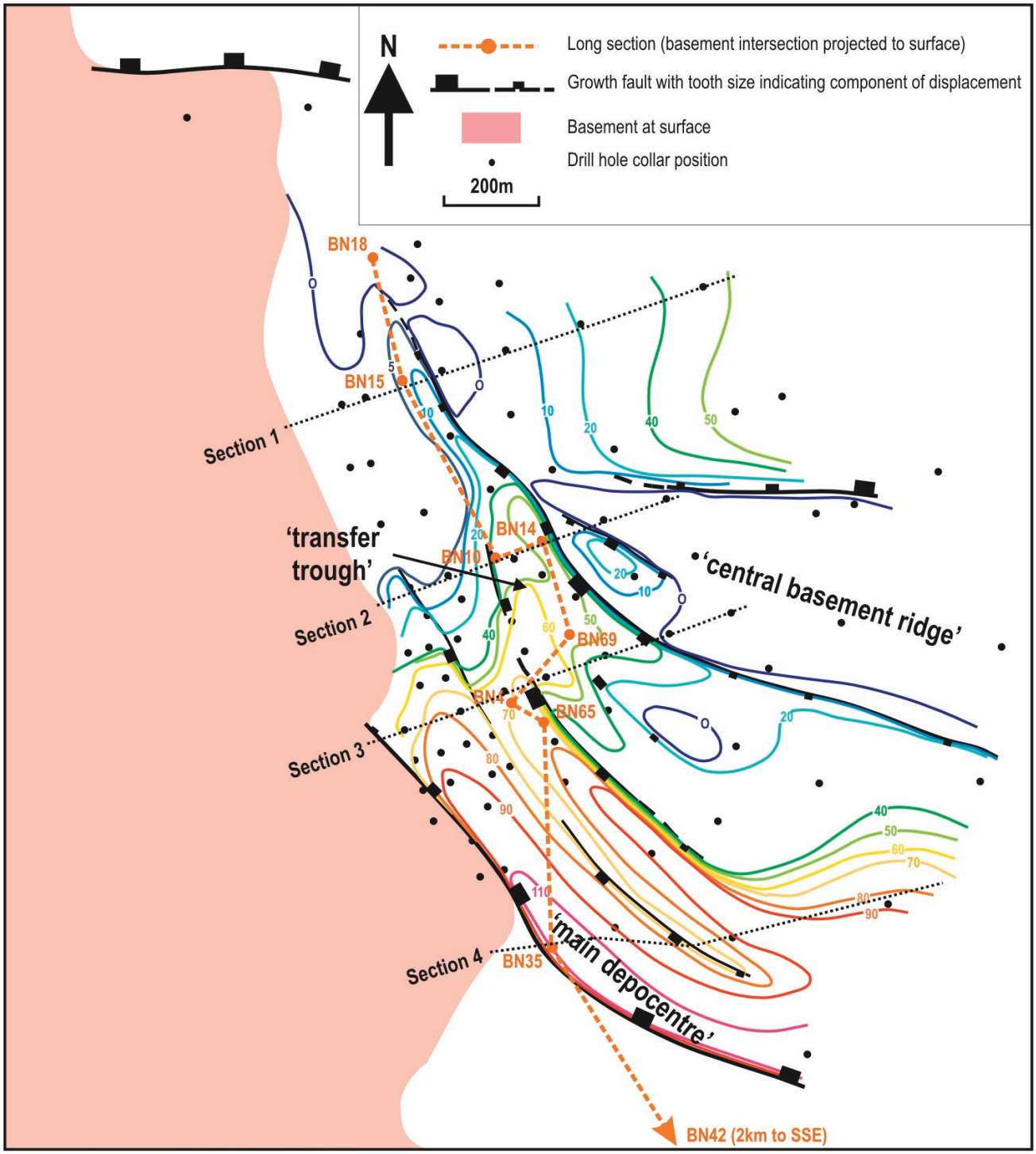

Figure 10. Isopach map of the Mindola Clastics Formation, showing interpreted basin geometry.

thickness increase immediately northward of each of these interpreted structures. Displacement along the central fault segment appears to dissipate westward, where the structure dies out against the central basement ridge.

Within the central portion of the deposit, an array of secondary NW- to NNW-trending fault segments lie obliquely with respect to the primary W- to NW-trending set (fig. 10). In addition to this misorientation in strike, the secondary set converge down-dip with the primary set, with hangingwall blocks downthrown to the southwest (fig. 11). This fault array is interpreted as a convergent transfer or linkage system, which accommodated extension between tips of primary fault segments. This is demonstrated by the fact that maximum displacement and generation of accommodation space along the transfer system coincides with the point at which displacement died out along the central E-W trending fault segment (fig. 10).

The small, restricted NW-trending trough located within the central part of the deposit (outlined at the beginning of this section) was thus controlled by lateral variation in displacement along the oblique transfer zone. Facies architecture within this trough is unique, and characterised by persistent influx of coarse-grained, texturally immature debris under predominantly subaerial conditions. These features are demonstrated on the series of cross sections in figure 11, wherein it can be seen that the portion of the MCF contained within the restricted trough was dominated by proximal alluvial fan sedimentation (sections 1–3). By contrast, as the trough opens to the south and west, deeper water conditions developed, particularly at higher levels of the stratigraphy (i.e. KAM: sections 3, 4). This is indicated by the abrupt lateral transition to finer-grained, subaqueously deposited lithofacies (i.e. facies association MCF 4A) within the thicker parts of the main depocentre. Sections 1 & 2 highlight the confined nature of the trough, as well as the progressive northward dissipation in displacement along the main NNW-trending fault segment and accompanying reduction in accommodation space. In particular, facies architecture in section 2 demonstrates the pronounced W-dipping half graben geometry, with its distinctive asymmetric profile. Talus breccias and debris flow conglomerates (facies associations MCF 1 & 3) are partitioned into the thickened part of the MCF in the immediate hangingwall of the main WSW-dipping transfer segment. On the western side of the trough where rates of accommodation were reduced on the hangingwall block, the MCF is considerably thinner and finer-grained.

Basin evolution during accumulation of the Kitwe Formation

Transition from the MCF to KF is abrupt and recorded regionally, with the sudden upward reduction in grainsize characterised on this contact at Mwambashi B developed similarly throughout the western flank of the Kafue Anticline. Thus the KF records a distinct phase in the evolution of the Katangan system and probably coincides with a fundamental reorganisation of fault geometries. The onset of this event is likely to have been recorded by the uppermost units of the MCF, where the progradation of facies association MCF 4C conglomerates herald a new phase of tectonism. This unit is also recognised on a regional scale as the 'footwall conglomerates' to the host sequences at Nkana-Mindola, Chambishi and Konkola.

Contrast in facies architecture between the MCF and KF is demonstrated in the cross sections of figure 1 and the long section of figure 6. With the exception of section 4, the KF is starkly layer-cake in its geometry compared to the underlying MCF. The basal COM clearly transgresses older basin compartments, indicating wholesale death of the complex fault system that controlled MCF deposition. Subtle thickness variation within the COM, particularly above elevated basement blocks, resulted from local folding and thrusting during the inversion event. The lack of original thickness variation across older basin-bounding structures clearly indicates fault inactivity, rather than simple flooding of former static intrabasinal highs. Further evidence for basin reconfiguration is shown by the change in provenance across the MCF-KW boundary, which records sudden cessation of influence of local, structurally controlled basement source areas.

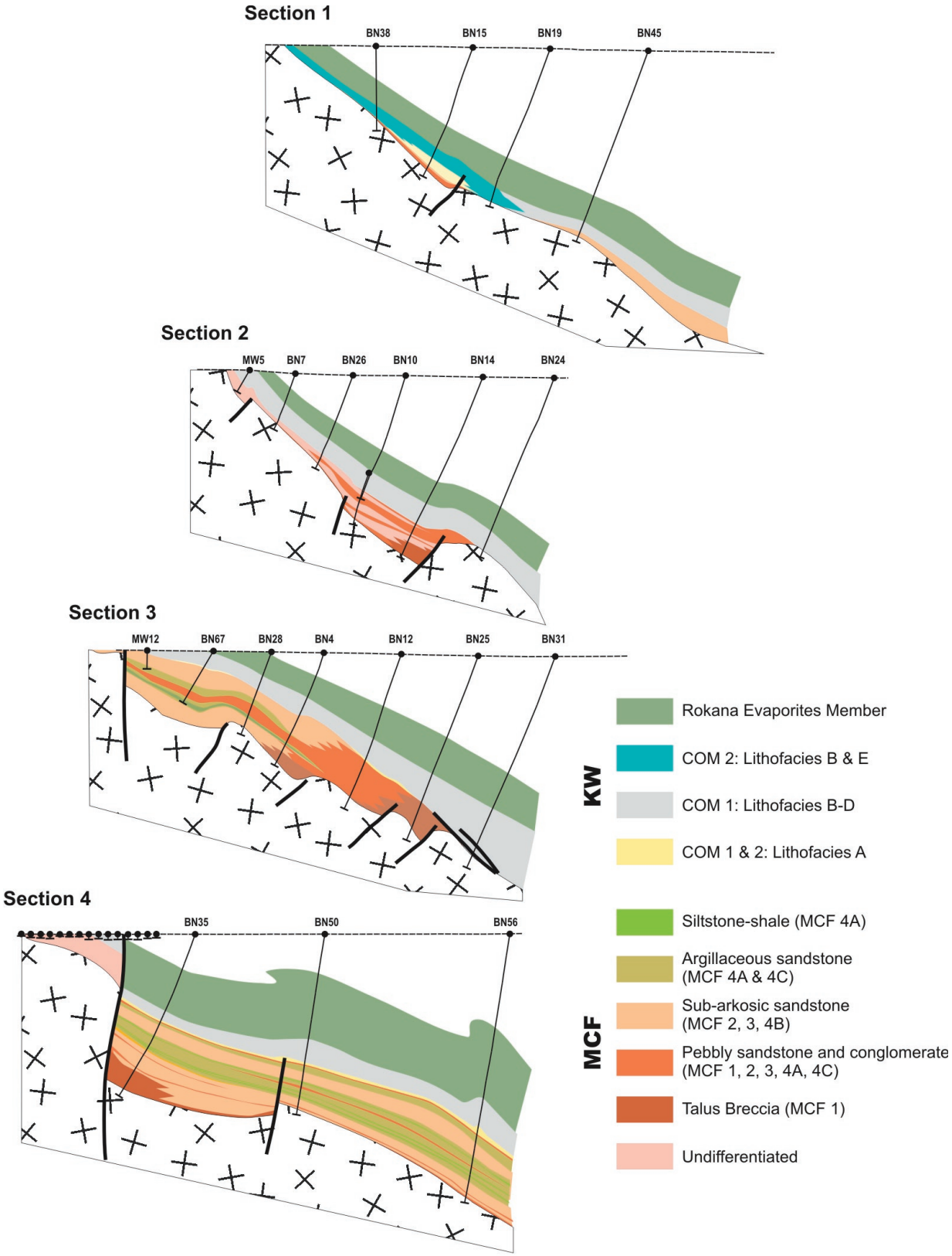

Figure 11. Cross sections through the Mwambashi B deposit, showing lateral and vertical variation in facies architecture.

Although a large number of faults became inactive during deposition of the KF, continued active tectonism is indicated by the prograding clastic wedge at the top of the MCF. Moreover, the abrupt transition to sub-wave base sedimentation recorded by shale-dominated facies association COM 1 indicates greater rates of basin subsidence. Thus the fine-grained nature of the COM in particular does not indicate sedimentation during a period of tectonic quiescence, but rather starvation of the basin system of coarse clastic sediment input. The narrow upward fining cycle at the base of the COM (i.e. lithofacies A) records the rapid decline in influence of the local fault generated source areas for the coarse clastic debris that have controlled sedimentation until this time.

Emergent conditions persisted locally at the onset of the KF, as indicated by platformal facies association COM 2. Condensed dolomitic facies with apparent preservation of cryptal lamination are restricted to the northern end of the deposit and coincide with an emergent inter-basinal domain during MCF sedimentation (section 1, fig. 11; fig. 6). Thus despite the overall basin reconfiguration, 'ghosts' of the MCF basin framework are reflected in KF facies architecture. However, this relationship does not hold for the entire deposit, as eastern portions of the central basement ridge, emergent during MCF deposition, are overlain by thick sequences of deeper water facies (sections 2, 3, fig. 11).

The overlying Rokana Evaporites Member is similarly layer-cake in terms of its facies architecture, despite a return to periods of coarser-grained sediment influx. There is no evidence to indicate reactivation of the older fault system (i.e. reactivation of intrabasinal source areas), and it is probable the basin-bounding structures were the same as those that controlled depocentre generation during COM sedimentation. The overall coarsening upward cycle at the top of the COM (i.e. progradational sequence set), obscured by strain and alteration at Mwambashi B, but well preserved at Mindola and Konkola (Pollington and Bull, this volume), thus probably relates to increased rates of sediment input relative to basin subsidence. These two factors competed episodically to produce laterally extensive, regressive vertical cycles of shale, dolomite/evaporite and sandstone (e.g. Broughton, this volume).

The enigmatic southern breccia unit potentially defines the position of a basin bounding structure during deposition of the KF (fig. 6). This interpretation is supported by the conglomeratic character of the unit, combined with the lack of clast types typical of the COM near the base of the unit. Furthermore, the breccia is situated close to a prominent WNW-trending lineament in certain geophysical datasets, which clearly offsets units on either side.

Comparison of basin evolution to typical rift environments

Arrays of fault segments, with limited lateral continuity and linkage at tips by oblique transfer zones, typify the structural geometry developed at the initial stages of rifting (Gawthorpe and Leeder, 2000). As extension progresses, faults propagate laterally at their tips, increasing their strike length and providing greater connectivity between adjacent segments. Within increasing strike length, each segment is capable of accommodation higher rates and components of vertical displacement, resulting in enhanced subsidence of the hangingwall block, but importantly greater uplift of the footwall block. Thus deepest parts of depocentres often coincide with adjacent areas of greatest uplift. The overall result is a complex, undulating basement topography.

Fault evolution has an important bearing not only on the generation of accommodation space, but also on sediment dispersal patterns. At early stages of basin growth, minor components of sediment input are directed transversely to the incipient depocentres, in the form of talus cones and/or small alluvial fans fed from immediately adjacent canyonised footwall blocks. However, the bulk of the sediment input is derived from further field drainage systems, which meander throughout the disconnected depocentres, ultimately feeding them via more axially-oriented drainages. Numerous uplifted footwall blocks provide abundant, widely dispersed local source regions for these inter-depocentre drainages. They are directed through zones of subdued uplift and hence away from portions of fault segments with large vertical

displacements. Lower topographic regions occur at the tips of fault segments or along mildly subsident, but active transfer arrays. Thus transfer zones are characterised by high rates of sediment input, but relatively low rates of accommodation development (Morely et al., 1990; Gawthorpe and Hurst, 1993). Facies associations within transfer zones are therefore dominated by prograding, coarse-grained clastic wedges, whereas retrogressive vertical sediment profiles incorporating finer, deeper water sequences occur in depocentre maxima. This pattern is clearly demonstrated in the Mwambashi B facies architecture, where coarse-grained, subaerially deposited lithofacies of the KAM are partitioned into the restricted trough adjacent to the interpreted transfer array. By contrast, finer-grained subaqueous deposits occur within thicker, more subsident portions of the main depocentre (seen most profoundly in section 3 of figure 11).

With continuing maturity of the basin system, lateral propagation of fault segments results in more effective linkage, ultimately forming extensive through-going structures. Strain becomes partitioned into a small number of these extensive fault systems, resulting in focussed and increased displacement rates at the expense of a much larger number of disconnected fault segments. This period in basin development is therefore marked by widespread fault death, combined with enlargement and coalescence of older depocentres (Gawthorpe and Leeder, 2000). The collapse of the compartmentalised fault system means that intrabasinal source areas become flooded and/or inactive. Furthermore, basin-marginal source areas retreat abruptly to the through-going fault zones, the high degree of connectivity of which results in increased and more laterally extensive footwall uplift. The effect of the basin reconfiguration is to completely restructure sediment dispersal patterns, such that footwall-sourced drainages can no longer enter the rapidly subsiding depocentre. In other words, the basin, although broadening and deepening, becomes starved of the previously abundant footwall sourced material.

We propose that this type of evolution from a compartmentalised basin configuration to an extensive, sediment starved basin system via progressive fault linkage accounts for the abrupt change in facies architecture recorded across the MCF-KF boundary. This model is particularly attractive as it accounts for: (1) abrupt decrease in grainsize, (2) change in provenance and loss of intrabasinal source areas, (3) transition to layer-cake stratigraphic architecture, and (4) increased rates of subsidence at this stratigraphic level. Also expected, perhaps on a more regional scale, is the development of broader hangingwall fed coarse-clastic systems, interfingering within finer axial fed systems within depocentre maxima. The REM potentially records this component of the basin fill, and as such may be in part equivalent to the COM. If so, the upper contact of the COM may be diachronous in a regional sense.

The major problem with the fault linkage model, is the widespread, remarkably abrupt and apparently regionally synchronous transition from the MCF to the KF. Under a stable stress field, the evolution from a compartmentalised basin system to an extensive system might be expected to be progressive and regionally diachronous rather than catastrophic and geologically instantaneous. Our observations would favour the latter, and hence may require a fundamental change in the far field stresses at the onset of the KF. One possible scenario to account for this is a sudden increase in the rate of crustal extension. This extensional pulse could generate the basin reconfiguration and increased subsidence seen at the base of KF. Resumption of emergent environments during REM deposition may reflect a period of post-extensional rebound, during which basin geometry remained stable, but the elevated rates of sedimentation due to regional uplift outweighed the rate of subsidence. Alternatively, an abrupt reorientation of far field stresses at the onset of KF sedimentation may have resulted in partitioning of strain into a small number of suitably oriented fault zones, or reactivation of favourable structural orientations within the basement.

Mineralisation and alteration

In this section we deal primarily with the macro-scale distribution of Cu mineralisation with respect to facies architecture and basin geometry. Petrographic work

is at a very early stage and as such will be discussed only briefly.

Stratigraphic controls on Cu mineralisation

High grade Cu mineralisation is largely restricted to arenaceous and less commonly rudaceous units within the upper portion of the MCF (fig. 6). The COM, although thick and well preserved, is effectively devoid of economic grades. In the rare cases where the COM has been sampled for assay, Cu grades are typically less than 0.5%. The abrupt transition from coarse-grained units of the MCF to sericitic and dolomitic grits and siltstones of the basal COM, forms the geological hangingwall to the orebody in most mineralised drill hole intersections. Minor low grade Cu has been identified within altered arenaceous units at the base of the REM, and is in part at least of supragene origin.

Disseminated chalcopyrite is largely stratabound and partitioned into a relatively clean, heavy mineral bearing, sub-arkosic sandstone interval near the top of the KAM (facies association MCF 3). In thicker portions of the MCF, this interval (facies association MCF 4B) is clearly distinct from its enclosing facies due to its high degree of sorting, well-developed parallel and cross-stratification and low argillaceous component. This relationship is well demonstrated in drill hole BN65 (fig. 6), where Cu values tail off rapidly immediately above and below this stratigraphic interval. Where the MCF is condensed and argillaceous component is ubiquitously low, Cu mineralisation occurs in a variety of lithofacies including matrix supported conglomerate and massive sandstone. Granite clasts within debris flow units are commonly mineralised, often with higher concentration of sulphides compared to the enclosing arenaceous matrix. However, most consistent high grade intersections within condensed portions of the MCF remain within well stratified, moderately-sorted sandstone intervals, interpreted as lithostratigraphic correlates of facies association MCF 4B (fig. 12). Although the geological hangingwall is sharply defined in such intersections by the basal intercalated grits and siltstones of the COM, the geological footwall is less distinct. The latter coincides roughly with the interpreted base of the KAM, however sporadic high grade intervals continue down into well-stratified sandstones of the 'basal clean siliciclastic package' (facies association 2). The lowermost conglomeratic portion of the 'basal clean siliciclastic package' (facies association 1) is rarely mineralised, except where the MCF is extremely condensed.

Pyrite is the dominant sulphide phase within the COM. It is unlikely to be entirely of diagenetic origin, as it occurs concentrated within fibrous calcite veins as well as disseminated throughout silty intervals and within nodular anhydrite pseudomorphs. The basal sericite-dolomite interval is often highly pyritic, particularly where intensely sheared. In one drill hole examined (BN53), a narrow bornite-chalcopyrite zone occurs within the sheared base of the COM and overlies barren (but pyritic) MCF.

Cu-rich intervals of the MCF are characterised by intense bleaching and calcite alteration (fig. 12 b–d). In hand specimen, this bleaching resembles the intense albite-quartz alteration associated with mineralisation at Chibuluma West. However, limited petrographic studies indicate that although albite is present, potassium feldspar (a phase largely absent within the ore zone at Chibuluma West) is the dominant feldspathic phase, and is in part at least of metasomatic origin. In thickened portions of the MFC, this feldspar-quartz bleaching contrasts markedly with the dark, biotite-rich nature of the enclosing strata.

Although Cu mineralisation has a strong spatial (and presumably genetic) association with feldspathic bleaching, the latter persists well into barren intervals. The principal control on the distribution of feldspathic bleaching appears to be lithotype: i.e. moderately clean and sorted sandstones. For example, at the southern, barren edge of the deposit, the clean arenaceous host horizon remains intensely altered, despite the lack of sulphides. Figure 13 shows progressive increase of alteration intensity from above and below the level of the host horizon. As the basal contact is approached, stratabound bleached intervals increase in thickness and frequency, with each interval coinciding with slightly coarser layers within the predominantly argillaceous 'footwall'. Relatively clean, heavy mineral bearing arenaceous units within the usually barren

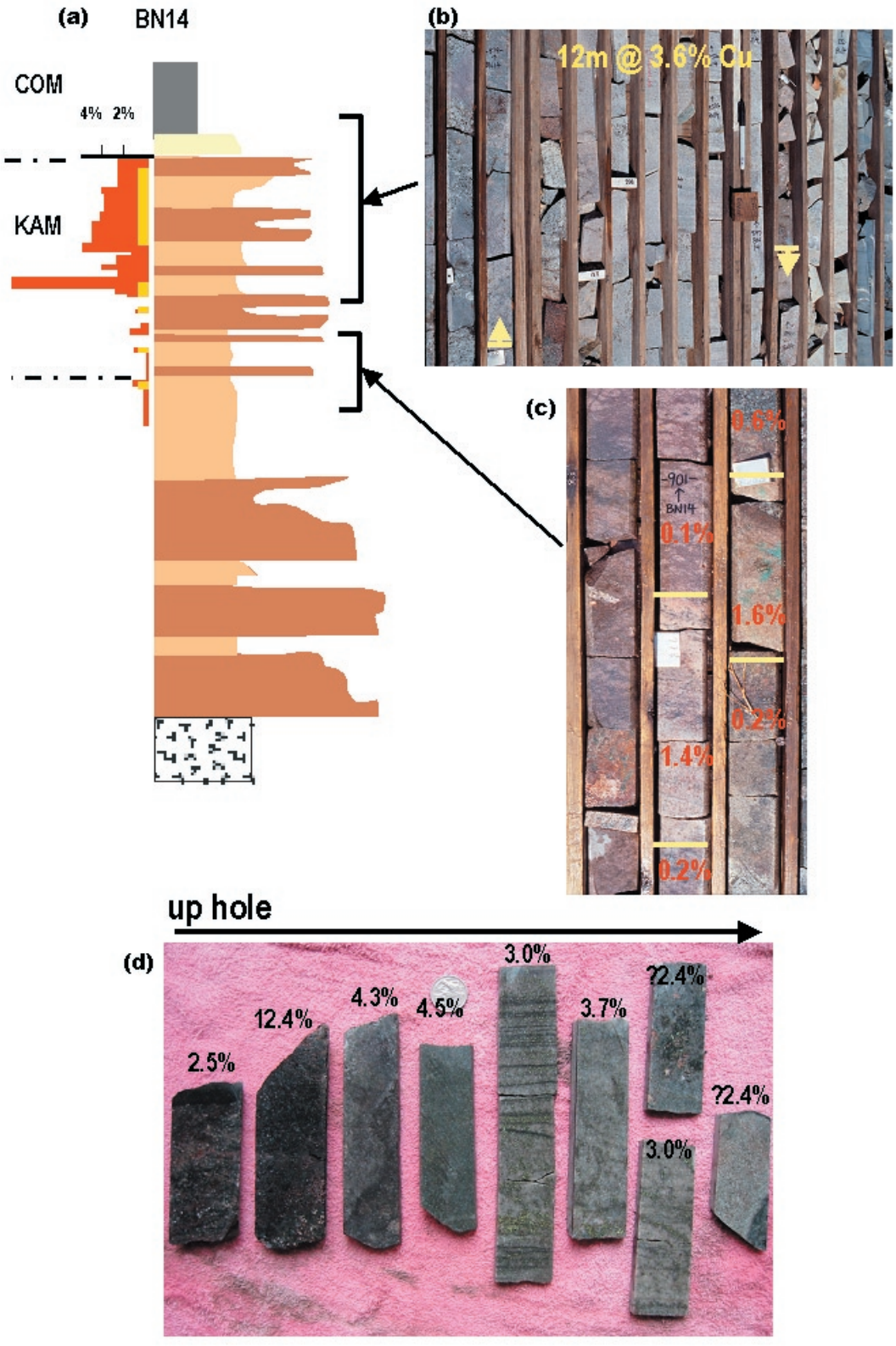

Figure 12. Vertical distribution of copper and associated alteration within BN14; an intersection within the condensed portion of the MCF.
(a) Vertical section through BN14, showing strong partitioning of mineralisation within the uppermost MCF.
(b) Concentration of copper grade within well-stratified, matrix-poor sub-arkoses. Note also elevated levels of bleaching within the mineralised interval, interpreted to reflect feldspathic alteration.
(c) Strong spatial association of elevated copper grades with discrete bleached intervals at the base the ore zone.
(d) Detail of the mineralised interval in (b), showing progressive destruction of primary textures up-hole.

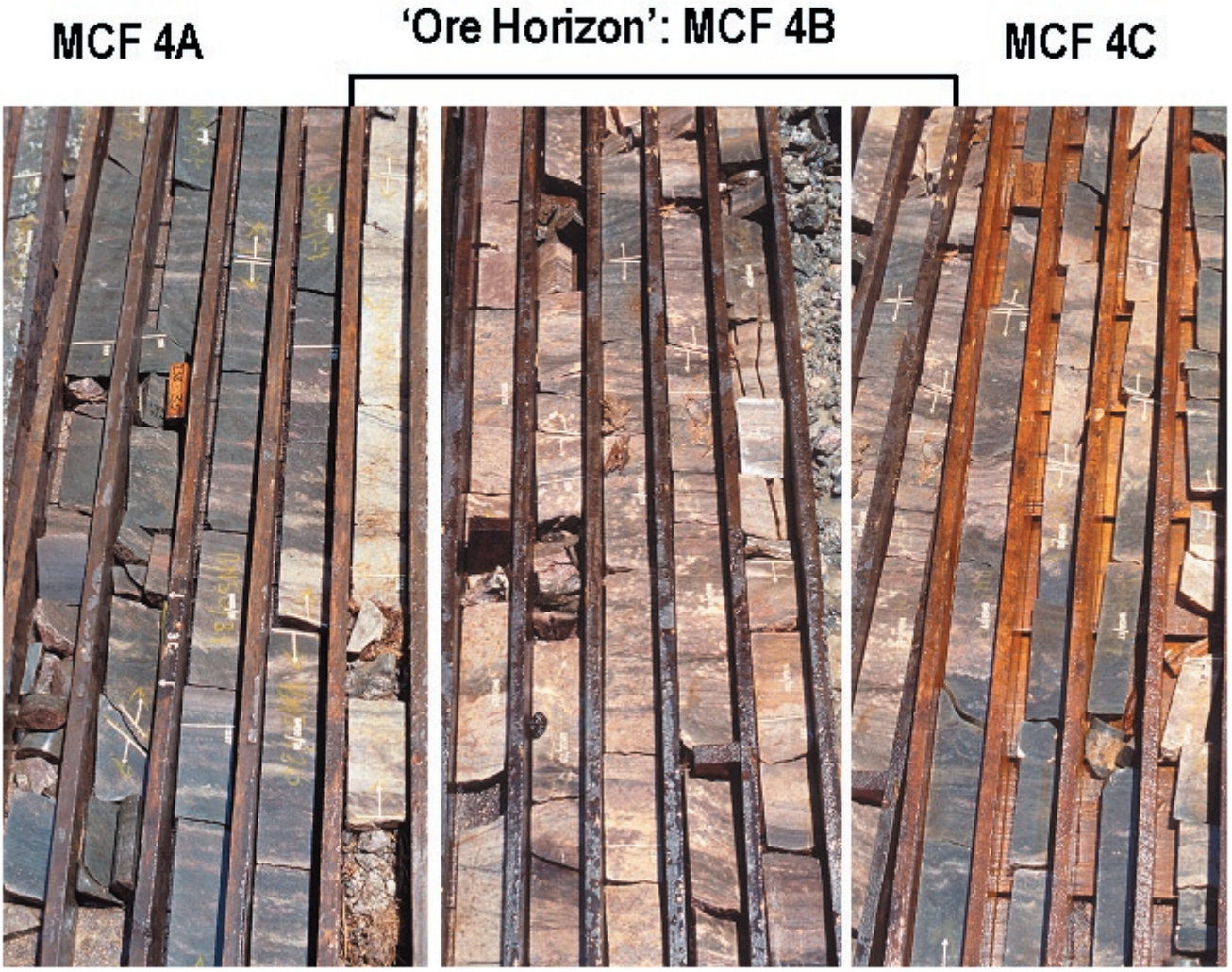

Figure 13. Feldspathic alteration within a barren intersection of the 'ore horizon' (BN50).

'basal clean siliciclastic package' are also characterised by quartz-feldspar-calcite alteration, with additional growth of haematite along heavy mineral bands. Partitioning of silicate alteration into clean arenites presumably relates to their higher porosity and permeability relative to enclosing argillaceous units (including the COM). These units would have been efficient aquifers during early burial and diagenesis prior to the occlusion of primary porosity, which may give a crude indication of the time of fluid infiltration and alteration.

It would appear, therefore, that the distribution of silicate alteration phases is more directly linked to lithotype than is the distribution of sulphides. That is, clean, well-sorted sandstone units are ubiquitously silicate altered, whereas Cu mineralisation is mainly confined to such lithotypes occurring at higher stratigraphic levels. Furthermore, sulphide alteration has more limited lateral extent throughout discrete stratigraphic units, which lack obvious variation in their original detrital component. If the assertion of a genetic association of feldspathic alteration and metal bearing fluids is correct (based on the sulphide-feldspar spatial relationship in mineralised intervals), why are not all feldspathically altered sandstones also mineralised? The lack of a direct association between silicate alteration and sulphide distribution within units of superficially homogenous texture and composition indicates that permeability and the composition of the detrital component are not the only contributing factors in the precipitation of metals.

Control of basin geometry on Cu distribution

The problems raised above are perhaps explained by viewing the distribution of Cu mineralisation within the basin framework. Figure 14 shows a vertical projection of average Cu grade interfaced with a similar projection of isopachs of the MCF. It clearly demonstrates a close spatial relationship between elevated average Cu grade and condensed portions of the MCF situated on the northern hangingwall block of the main NW-trending depocentre. Moreover, highest average Cu grades define a roughly NNW-trending corridor coincident with the series of confined, transfer-related troughs situated in the central part of the deposit. This relationship is demonstrated even more convincingly when viewing mineralisation as metre% contours (fig. 15). The discrepancy between the average Cu grade and metre% values in the northern extremity of the main NNW-trending trough results from extreme thinning of the host sequence in this region. Thus although high grades persist to the limit of the trough, the mineralised interval is not sufficiently thick to produce significant metre% values. It is also interesting to note that moderate and high average Cu grades extend locally onto the central basement ridge where preserved MCF is lacking. It these regions, mineralisation is contained within sheared basal COM and underlying granitic basement.

Partitioning of Cu mineralisation within the transfer-related trough system highlights the favourability of condensed, argillite-poor packages as hosts. This three-fold relationship between facies-type, basin geometry and Cu distribution is also shown in figure 6. Here it can be seen that although Cu persists into thicker argillite-bearing MCF successions, the upper host horizon is significantly mineralised only near the 'mouth' of the transfer-related trough system. It would appear therefore, that the funnel-like geometry of the trough system, and possibly also the enhanced permeability of clean, coarse-grained units contained therein, were important factors in focussing fluids during mineralisation. Supporting this interpretation is the fact that the COM is mineralised (albeit confined largely to shear zones at the base) mainly at the MCF pinch-out zones at the periphery of the transfer zone. Enhanced structurally-induced permeability at the base of the COM where in contact with basement, may have provided a means of outflow for fluids funnelled into the trough system. This may also explain the anomalously high level of alteration within condensed dolomitic COM facies (facies association COM 2) at the northern fringe of the deposit.

Possible involvement of hydrocarbons

Although the confined basin geometry potentially provided a means of fluid focussing, it still does not account for the precipitation of sulphides. We

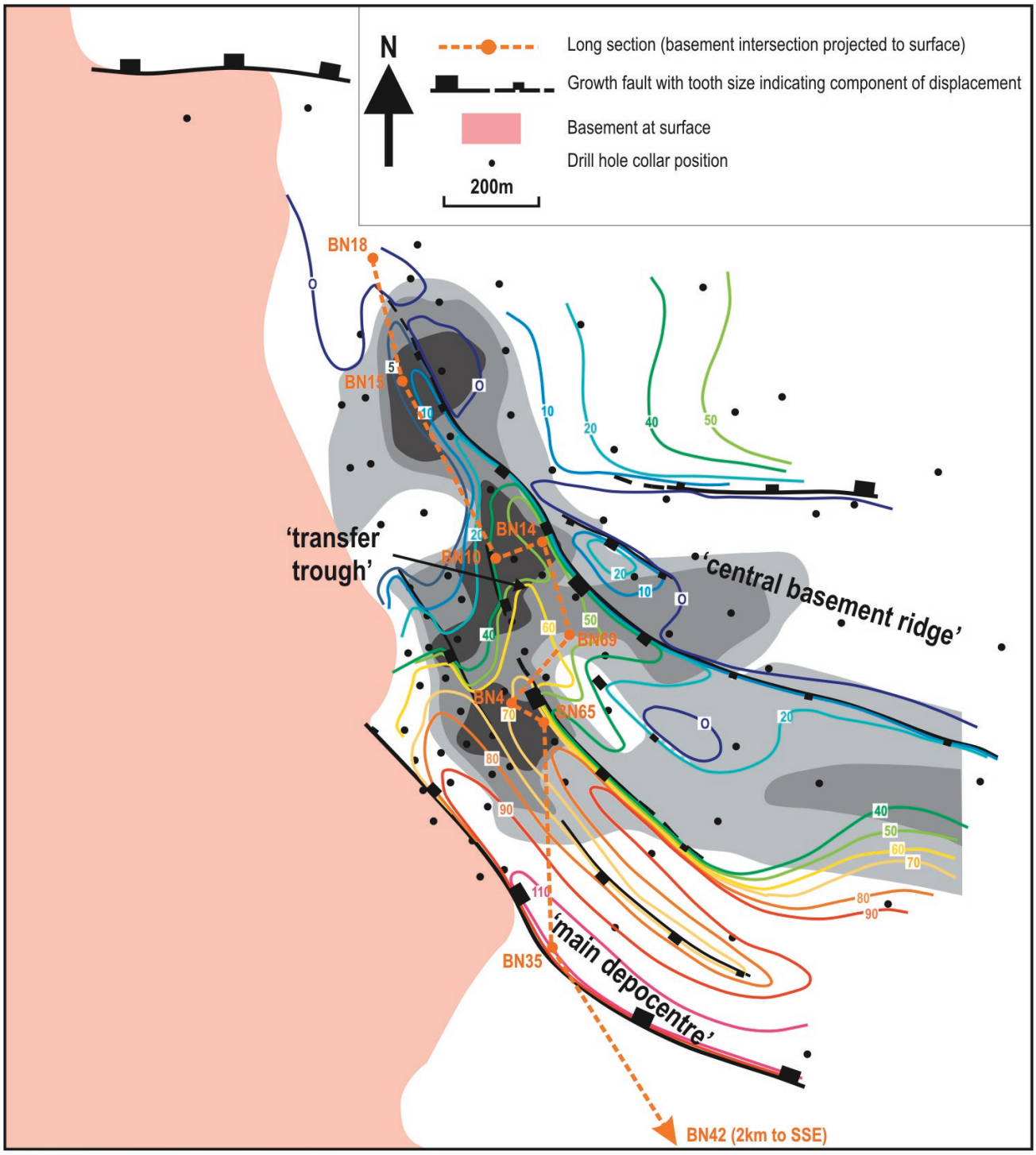

Figure 14. Geometry of the MCF sub-basin system overlain on average copper grade. Grade contoured at 1, 2 & 3% cut-offs: unmodified from Mwale (2001).

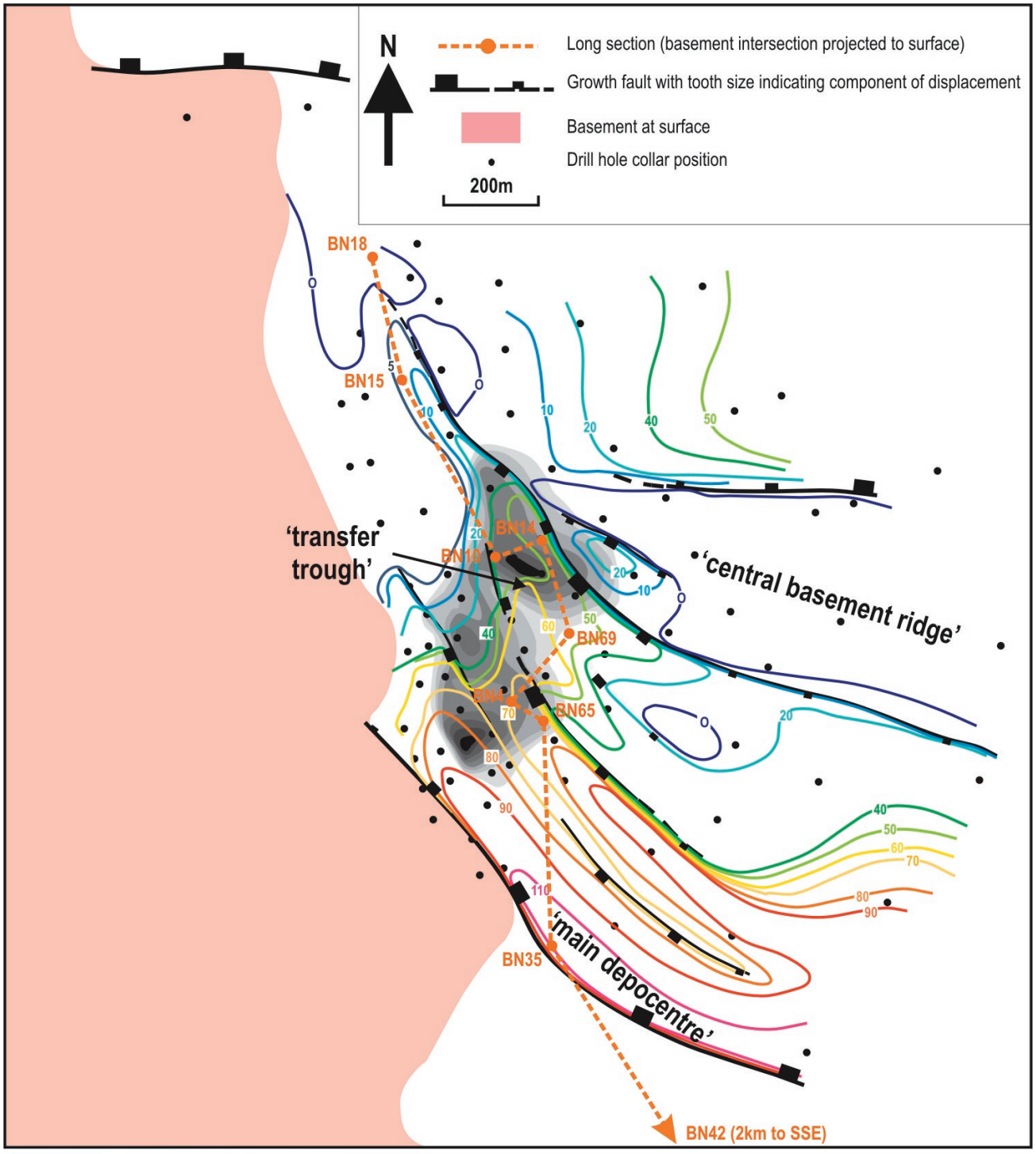

Figure 15. Geometry of the MCF sub-basin system overlain on metre% copper. Contour intervals at 10m%, ranging 10-80m%: unmodified from Mwale (2001).

hypothesise that the former presence of hydrocarbons played a role in this regard. The basin geometry and associated facies architecture within the transfer system would have provided an excellent physical hydrocarbon trap during burial induced source rock maturation and migration of hydrocarbons. That is, a restricted porous and permeable compartment (i.e. reservoir) bounded laterally and at its base by less permeable basement rocks, and at its roof by the transgressive COM seal. Transfer zones form optimum sites for hydrocarbon accumulation as: (1) their high rates of sediment input vs accommodation development result in deposition of high quality, permeable and porous reservoir rocks, and (2) their complex fault geometries raise the potential for the development of local structural trap sites (Morley et al., 1990).

This hydrocarbon model is similar to that proposed for arenite-hosted Cu mineralisation at Mufulira by Annels (1979) and has also been postulated for Chibuluma West (Bull et al., 2001; Selley & Cooke, 2001). At Mufulira, Cu is hosted in part by a series of stacked carbonaceous arenite lenses, each capped by impermeable argillaceous or dolomitic units. Annels (*op cit.*) argued for accumulation of graphitic carbon via migration of hydrocarbons, the latter having reacted with diagenetic anhydrite to produce the reduced sulphur required to precipitate sulphides from metal-bearing brines. Trap sites were considered to be incipient anticlinal structures. Interestingly, Annels also recognised concentration of sericite, formed at the expense of detrital potassium feldspar, within and at the fringes of carbon-bearing units. This relationship may be analogous to the 'sericitic cap' at the base of the COM at Mwambashi B.

At Mwambashi B, we envisage a two-stage model involving initial migration and trapping of hydrocarbons and/or sour gas within permeable strata, and subsequent infiltration of oxidised, metal-bearing fluids along similar pathways. Acid released by the degradation of hydrocarbons on reaction with the oxidising fluid, is potentially recorded by the 'sericitic-cap' and the break-down of detrital K-feldspar. However, despite the attractiveness of the model, we have been unable as yet to find unequivocal evidence of former hydrocarbons. The lack of preserved organic matter within the host packages may be explained by introduction of hydrocarbon as a largely gaseous phase, of which little relict evidence would be expected.

One means of recognising former hydrocarbons is by detailed examination of radiogenic heavy mineral grains. The thermal aureole around Th and U bearing phases in particular, commonly results in polymerisation of hydrocarbons and the formation of insoluble bitumen at the grain margin (Rasmussen et al., 1989; Parnell et al., 1990; Buick et al., 1998). This process has the potential to explain the widely recognised association of Cu sulphides with heavy mineral bands in many of the Copperbelt deposits (i.e. localised concentration of reducing phases along heavy mineral bands).

Perhaps a more efficient way of testing for the former presence of hydrocarbons is the use of C isotopes. Zentilli *et al.* (1997) demonstrated for the cases of stratabound Cu deposits in Chile, that gangue carbonates were the product, in part, of oxidised hydrocarbons. $\delta^{13}C$ values for carbonates were found to be anomalously light, a feature they argued was consistent with reaction with a fluid rich in hydrocarbons.

Summary and Conclusions

Stratigraphy and Basin Evolution

The fundamental two-fold stratigraphy of the Lower Roan (i.e. Mindola Clastics Formation and overlying Kitwe Formation), defined by Clemmey (1976) at Nkana-Mindola, can be applied throughout the southern Chambishi Basin. The MCF records sedimentation within a complex compartmentalised basin framework, whose geometry and mode of fault evolution typifies the onset of rifting in recent extensional settings. The fault system that controlled basin development during deposition of the MCF at Mwambashi B, is geometrically analogous to that at Chibuluma West: i.e. WNW-trending primary half-grabens, with hangingwall blocks down-thrown to the N, and secondary NW- to NNW- trending transfer or

zones. This consistent fault configuration implies the development of systematic fault arrays during lower Katangan sedimentation, probably under regional NNE-SSW directed extension. However, predominance of fault orientations ranging WNW to NNW, may also in part reflect inheritance from similarly oriented (?Irumide) structures within the basement.

At both Mwambashi B and Chibuluma West, the interaction of half-graben and transfer structures, resulted in lateral facies variation (albeit subtle and Chibuluma West). The MCF became more condensed within the region of transfer zones, with dominance of coarse-grained, sub-aerially deposited lithofacies reflecting high rates of sediment input relative to accommodation development. These anomalously coarse-grained and matrix-poor lithofacies accumulated within highly restricted depocentres, characterised in 3-D by lateral pinch-outs of the MCF. This sub-basin geometry, combined with lateral and vertical variations in facies architecture, was important for inferred migration and trapping of gaseous hydrocarbons and subsequent focussing of metal-bearing hydrothermal fluids.

Vertical variation in stratigraphic architecture of the MCF is dominated by the upward trend from 'clean', sub-arkosic alluvial-fluvial sequences, towards less well-sorted, argillaceous arenites and minor siltstone (the latter most conspicuous at Mwambashi B). The paucity of 'clean' lithofacies at higher levels of the stratigraphy is interpreted to record a transgression to subaqueous sedimentation, possibly within a deltaic and/or littoral environment. This change in depositional environment was coincident with an abrupt increase in the rate of generation of accommodation space interpreted to reflect enhanced subsidence due to more effective fault linkage.

The transition to conspicuously finer-grained lithofacies of the basal KF is abrupt and records a fundamental change in basin configuration involving widespread starvation of coarse-grained clastic sediment. Depositional compartments suddenly became broader and more rapidly subsident. They were controlled by a small number of laterally extensive, or 'through-going' fault systems, whose continuity in strike and ubiquitously elevated footwall blocks prevented clastic input. The broad WNW-trending 'Ore Shale pinch out zone' identified by Annels (1989) in the southern Chambishi Basin, that also forms a locus for intrusion of younger gabbroic bodies, may represent such a structure. Older closely spaced fault networks that controlled the deposition of the MCF and whose interaction provided numerous sites of sediment sourcing and input, effectively died at the onset of KF sedimentation. Thus the KF transgresses former MCF basin compartments, providing a regional seal on an underlying system of semi-connected, permeable sandstone bodies.

The widespread fault death at the base of the KF, accompanied by dramatically increased efficiency of linkage of certain master fault systems, is best explained by a regionally recorded extensional pulse. The upward transition to cyclical marginal marine-subaerial sedimentation of the Rokana Evaporites and Nchanga Quartzite members may relate to crustal rebound following the initial extensional pulse. Tectonic quiescence, typical of the sag phase of crustal extension, is recorded by the overlying platformal carbonate-dominated succession of the Chambishi Dolomites Member.

Mineralisation

Common elements of the mineralised systems at Mwambashi B and Chibuluma West include:

- Host strata are relatively clean arenaceous and/or rudaceous units within the MCF.
- The geological hangingwall is well-defined: i.e. host strata are capped by more argillaceous lithotypes (COM or facies association at Mwambashi B and the Hangingwall Sandstone at Chibuluma West), that would have been relatively impermeable at the time of hydrothermal fluid influx.
- Mineralised intervals coincide with elevated feldspathic alteration: appears exclusively albitic at Chibuluma West, but mixed K-feldspar and albite at Mwambashi B.
- Copper distribution is strongly controlled by basin geometry, with localisation in more restricted depocentres.

These features are also present in the small 'footwall-hosted' deposit at Chambishi (fig. 16; Annels, 1989). In this case, high grade Cu mineralisation occurs within a restricted trough on the margin of a basement ridge separating the main east and west orebodies. The host sequence is wedge-shaped body of clean, strongly albitised sandstone, overlain by argillaceous sandstone. However, in contrast to Chibuluma and Mwambashi B, the 'footwall' orebody at Chambishi is subordinate to a much larger 'Ore Shale' hosted system. Interestingly, higher-grade portions of the 'Ore Shale' orebody directly overlie the 'footwall' orebody (fig. 16b), suggesting a genetic relationship between the two.

The most conspicuous feature of all 'footwall'-hosted deposits in the Chambishi Basin is their location within optimum hydrocarbon trap geometries. In each case, mineralisation is concentrated towards the top of clean, permeable packages, with indistinct geological footwalls, but sharp upper contacts with less permeable media. In addition to the upper seal, host sandstone bodies are bounded laterally and basally by less permeable basement lithotypes.

We are yet to demonstrate unequivocal evidence of the former presence of hydrocarbons at any of the deposits. However, the strong spatial association of Cu-sulphides with radiogenic heavy mineral phases (i.e. Th-rich) at Chibuluma West, may be considered indirect evidence of this association. Heavy mineral bands had the potential to stabilise and hence concentrate residual hydrocarbons, forming local sites of enhanced reducing conditions.

We speculate that the permeable pathways and reservoirs utilised by migrating hydrocarbons remained 'open' allowing the subsequent passage of hydrothermal metal-bearing brines. Thus fluids directly responsible for mineralisation must have been introduced prior to complete consolidation of the MCF (i.e. pre-peak metamorphism).

References

Annels, A. E. 1979. Mufulira greywacke and their associated sulphides. Trans. Inst. Ming. Metall. B88, 15-23.

Annels, A. E. 1989. Ore genesis in the Zambian Copperbelt, with particular reference to the northern sector of the Chambishi Basin. In: Boyle, R.W., Brown, A.C., Jefferson, C.W., Jowett, E.C., and Kirkham, R.V., eds., Sediment-hosted stratiform copper deposits: Geological association of Canada, Special Paper 36, p. 427-452.

Broughton, D. This volume

Buick, R., Rasmussen, B. & Krapez, B. 1998. Archaean oil: Evidence for extensive hydrocarbon generation and migration 2.5-3.5Ga. AAPG Bulletin, 82, 50-69.

Bull, S., Selley, D., Cooke D., Mackay, W., Large, R. & McGoldrick, P. 2001. Provisional stratigraphic correlation of three Cu mineralized basins; the Zambian Copperbelt, the Polish Kupferschiefer and the Adelaide Fold Belt. AMIRA / ARC Project P544 Proterozoic sediment-hosted copper deposits. Meeting 4, 233-246.

Clemmey, H. 1976. Aspects of stratigraphy, sedimentology and ore genesis on the Zambian Copperbelt. PhD dissertation, University of Leeds, UK. 365pp.

Croaker this volume

Dechow, E. & Jensen, M.L., 1965. Sulfur isotopes of some Central African sulfide deposits. Economic Geology, 60, 894-941.

Gawthorpe, R. L. & Hurst, J. M. 1993. Transfer zones in extensional basins: their structural style and influence on drainage development and stratigraphy. Journal of the Geological Society of London, 150, 1137-1152.

Gawthorpe, R. L. & Leeder, M. R. 2000. Tectono-sedimentary evolution of active extensional basins. Basin Research, 12, 195-218.

Kirkpatrick. 1997. Geological evaluation of the Mwambashi B Prospect, Chambishi Basin, Zambia. Avmin company report.

Morely, C. K., Nelson, R. A., Patton, T. L., & Munn, S. G. 1990. Transfer zones in the East African Rift System and their relevance to hydrocarbon exploration in rifts. AAPG Bulletin, 74, 1234-1253.

Mwale, J. 2001. Mwambashi pre-feasibility geology report. Avmin company report. 38pp.

Parnell, J., Monson, B. & Tosswill, R. J. Petrography of thoriferous hydrocarbon nodules in sandstones, and their significance for petroleum exploration. Journal of the Geological Society of London, 147, 837-842.

Pollington, N. & Bull, S. This volume.

Rasmussen, B., Glover, J. E. & Alexander, R. 1989. Hydrocarbon rims on monazite in Permian-Triassic arenites, northern Perth Basin, Western Australia: Pointers to the former presence of oil. Geology, 17, 115-118.

Selley, D. & Bull, S. W. 2001. Stratigraphy and basin geometry at the Chibuluma West copper-cobalt deposit, Zambia. AMIRA / ARC Project P544 Proterozoic sediment-hosted copper deposits. Meeting 4, 101-132.

Selley, D. & Cooke, D. 2001. Mineral zonation and sulfur isotope systematics at Chibuluma West copper-cobalt deposit, Zambia. AMIRA / ARC Project P544 Proterozoic sediment-hosted copper deposits. Meeting 4, 133-170.

Zentilli, M., Munizaga, F., Graves, M. C., Boric, R., Wilson, N., Mukhopadhyay, P. K. & Snowdon, L. R. 1997. Hydrocarbon involvement in the genesis of ore

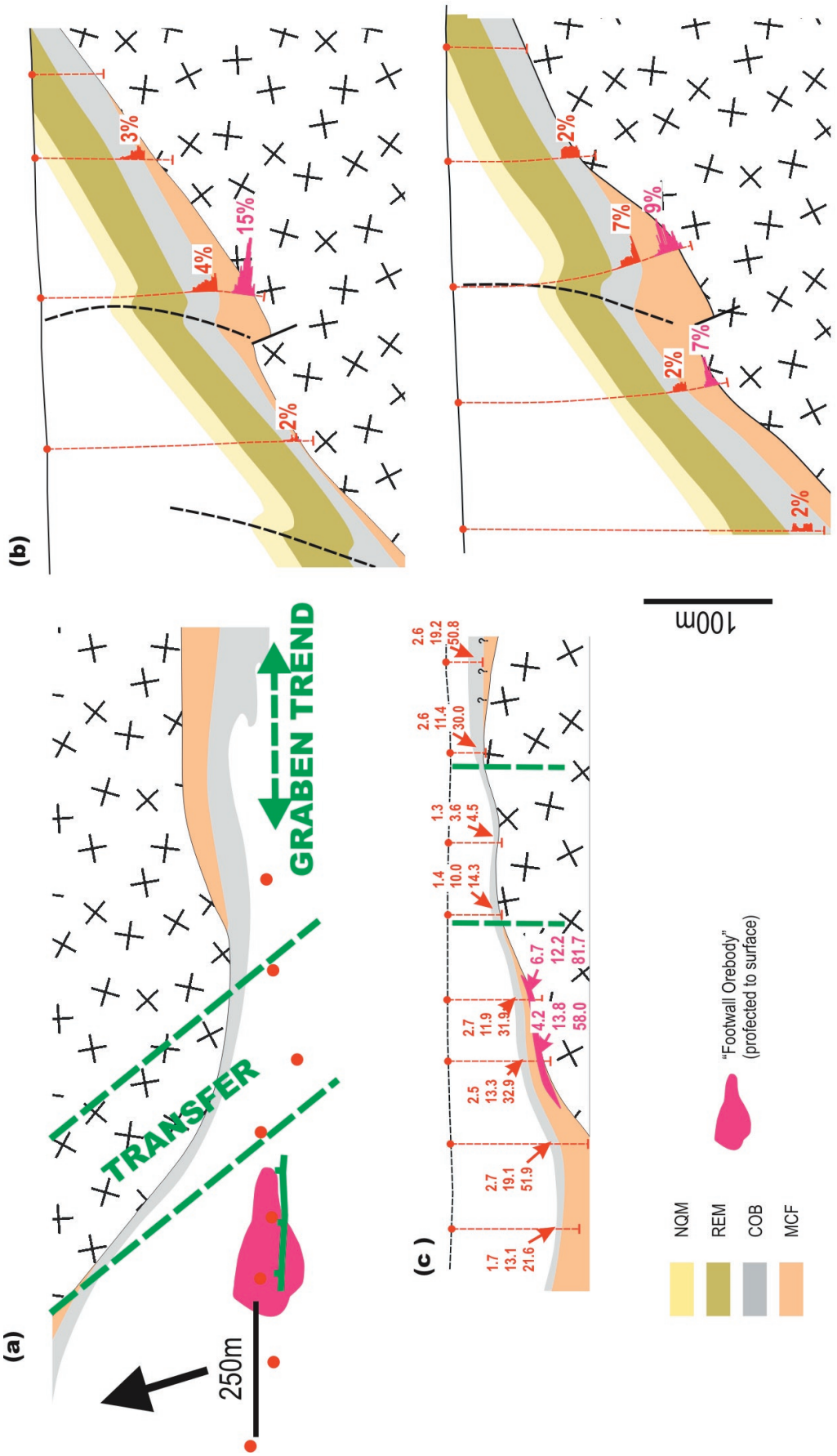

Figure 16. "Footwall" orebody at Chambishi (constructed from historical exploration sections).
(a) Plan view, showing location of footwall deposit on the western flank of a basement ridge, probably related to a transfer structure. Note pinch-out of the MCF on either flank of the ridge.
(b) Cross sections (upper situated immediately east of the lower section) showing localisation of "footwall" Cu within restricted N-dipping half-graben, which narrows and pinchs out to east. Note elevated Cu grades within the "Ore Shale"-hosted orebody, directly overlie the "footwall" orebody.
(c) W-E long section (left to right) showing distribution of "footwall" and "Ore Shale" mineralisation.

deposits: an example in Cretaceous stratabound (Manto-type) copper deposits of Central Chile. International Geology Reviews, 39, 1-21.

The geology and genesis of the Nkana-Mindola deposit, Zambia: Progress summary 2002

Mawson Croaker
Centre for Ore Deposit Research, University of Tasmania

The well mineralised and economic Nkana-Mindola (NKM) system within the Chambishi Basin (Fig.1) was targeted for this study as: (1) deformation intensity changes along strike; (2) significant vertical and lateral facies variations within the Lower Roan have been documented; and (3) copper sulphides assemblages change along strike. The principal objective of this study will be:

- To constrain the genesis of copper mineralisation at NKM by investigating stratigraphic, sedimentological, structural, petrological and geochemical aspects of the Neoproterozoic mineralised system.

The NKM deposit includes Mindola North Shaft, Mindola Shaft, Central Shaft, SOB Shaft and the West Limb (Figs 1, 2). The NKM copper system has a strike length of approximately 33 km, of which approximately 16 km strike length is the focus of current mining operations or has been exploited during the previous sixty years of mining operations. Mining operations have been continuous from surface to a current depth of 5500 ft at Mindola and 3960 ft at SOB Shaft. All economic resources are currently from sulphide orebodies hosted by the ore shale along the north- eastern limb of the Nkana syncline. Several significant observations and preliminary ideas can been drawn from work to date.

Stratigraphic, sedimentology and basin architecture

Broad stratigraphic and sedimentological analysis across the NKM area has been completed. Significant observations and preliminary outcomes of work to date:

- Identified the same principle stratigraphic division as devised by Clemmey (1976, 1978) as being the most effective division of the Lower Roan and generally concur with his descriptions of the facies particularly of the Copperbelt Orebody Member (COM, 'Ore Shale').
- Significant variations in thickness and facies of Mindola Clastic Formation (MCF, footwall sequence) is interpreted to indicate deposition within small compartmentalised basins. Numerous pieces of sedimentology and structural data suggest faulted margins to MCF. This interpretation is similar style to that identified by Selley and Bull (2001) and Selley et al. (2002) elsewhere in the Chambishi Basin.
- Lateral facies variation occurs throughout the COM, particularly within the lower 15 m.
- Available data suggests limited lateral facies and depositional thickness variations in Kitwe Formation (hangingwall sequence).
- Abrupt changes in the overall NW strike of the basement-Lower Roan contact coincide with facies and thickness changes of the MCF. Such changes are currently interpreted to mark basin margins, however no sense of the original orientation of basin structures are yet to be accurately determined.

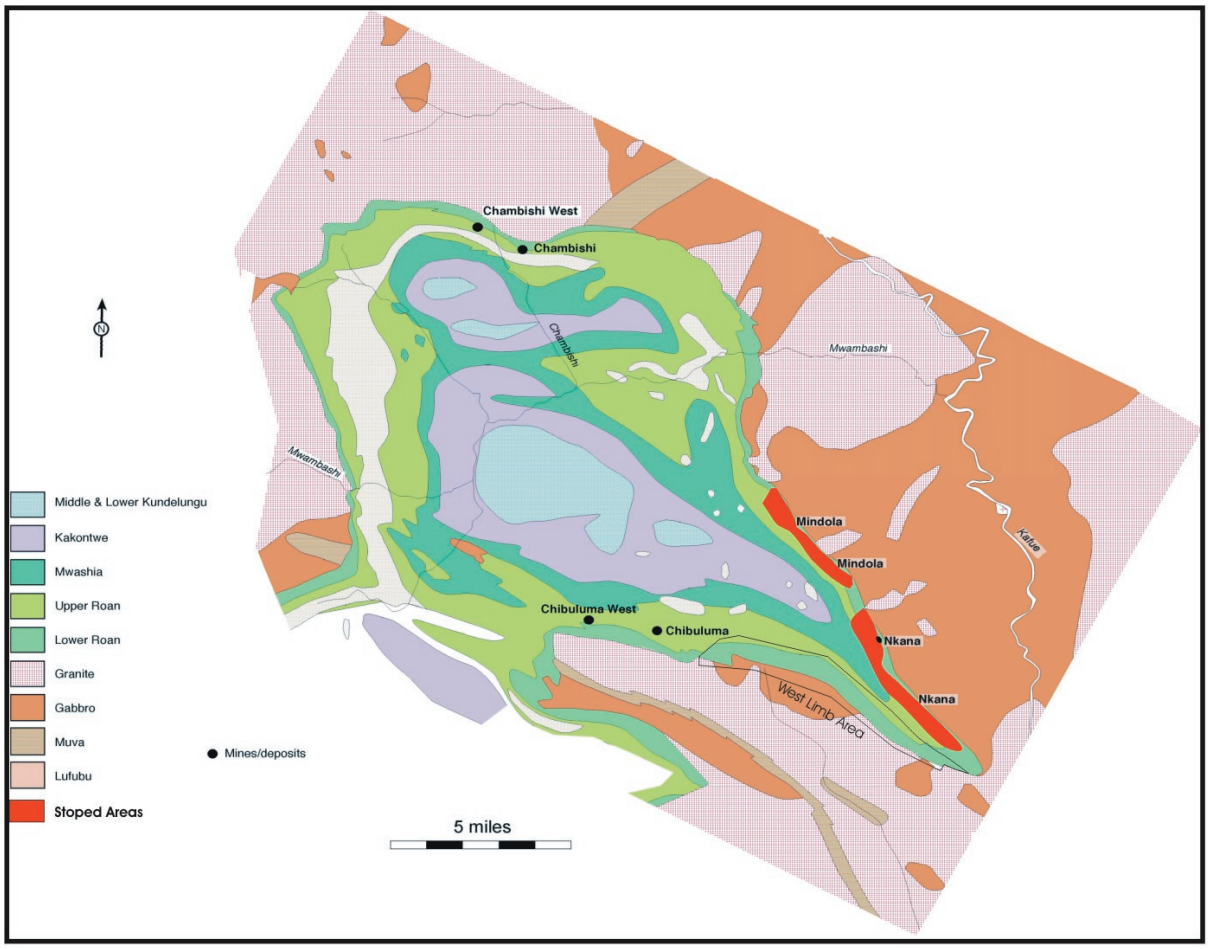

Figure 1. General location plan of the Nkana-Mindola area in the Chambishi Basin. All economic mineralisation is confined to the northeastern limb of Nkana Syncline.

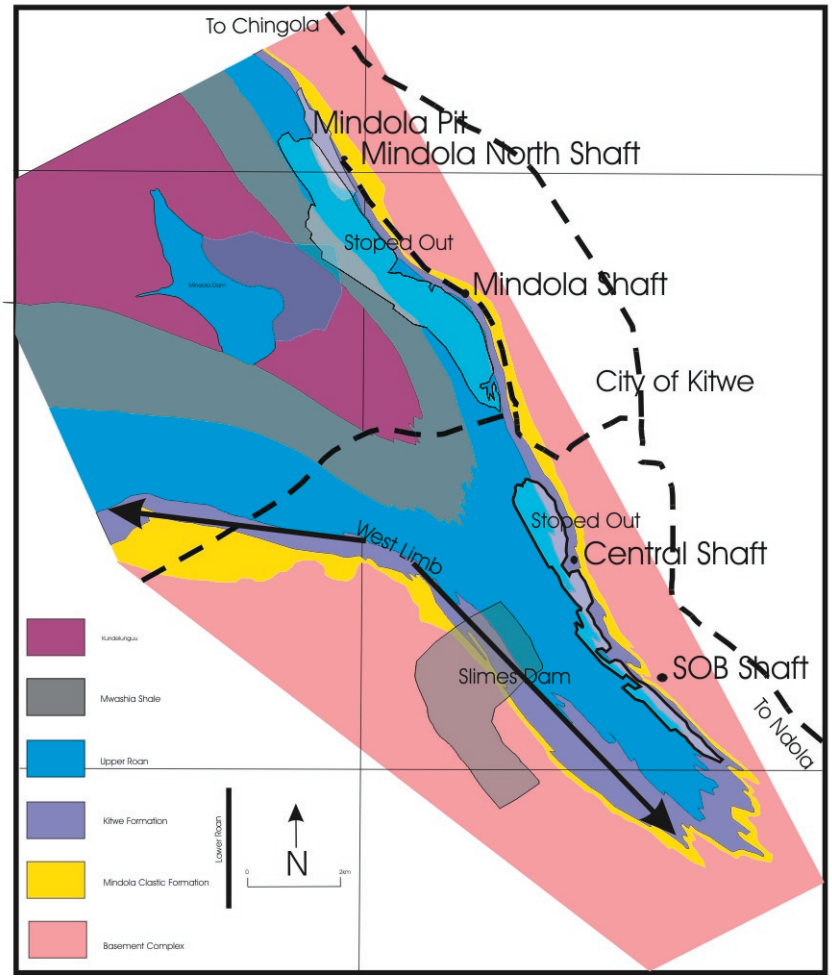

Figure 2. Geological map of the Nkana-Mindola area, with the location of the four operating shafts.

Inversion related structure

The focus of this work is the Nkana Synclinorium Project area (Fig. 3) at SOB as well as Central Shaft, primarily due to the complex nature of the Lufilian folding, as well as drillcore access and ongoing underground development. To date observations include:

- Significant strain partitioning between the footwall sequence and shale horizons, with the broad structural geometry more clearly defined by the footwall sequence. Macro- and microstructural work identified two main cleavages and a less well defined early cleavage in some samples. Significant dissolution and late shearing within the shale packages has considerably complicated the structure.
- No large scale decollement surface has been recognised.
- Geometry of overall orebodies are the same as the broad fold geometries, however significant thickening and thinning have occurred related to later folding.

A short field season during the second year of the PhD in 2003 is planned to undertake further detailed mapping of new crosscuts and drives within the Nkana Synclinorium Project area.

Mineralisation and 'alteration'

The focus of the detailed alteration work is also focussed within the Nkana Synclinorium Project area. To date observations include:

- Copper mineralisation and cobalt mineralisation are not always directly related.
- Several phases of 'alteration' / 'metasomatism' have been identified. Princpal alteration phases include

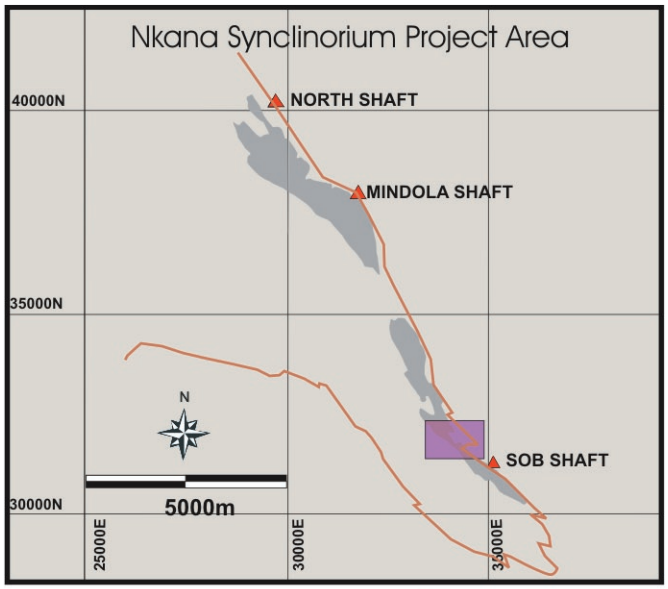

Figure 3. Simplified plan map outlining the basement geometry and a simplified cross section at the south end of the Nkana Synclinorium Project area. Detailed work on inversion structure, mineralisation distribution and alteration is focus on the Nkana Synclinorium Area. The Nkana Synclinorium Area is tightly folded and all mineralisation is hosted within the upper sandstone and dolomitic sandstone of the footwall and the Ore Shale. The geometry of the basement has a significant control on Lufilian fold geometries of the Lower Roan. The geometry of the mineralisation is grossly stratabound and would tend to indicate the main mineralisation phase was pre or early main Lufilian fold event.

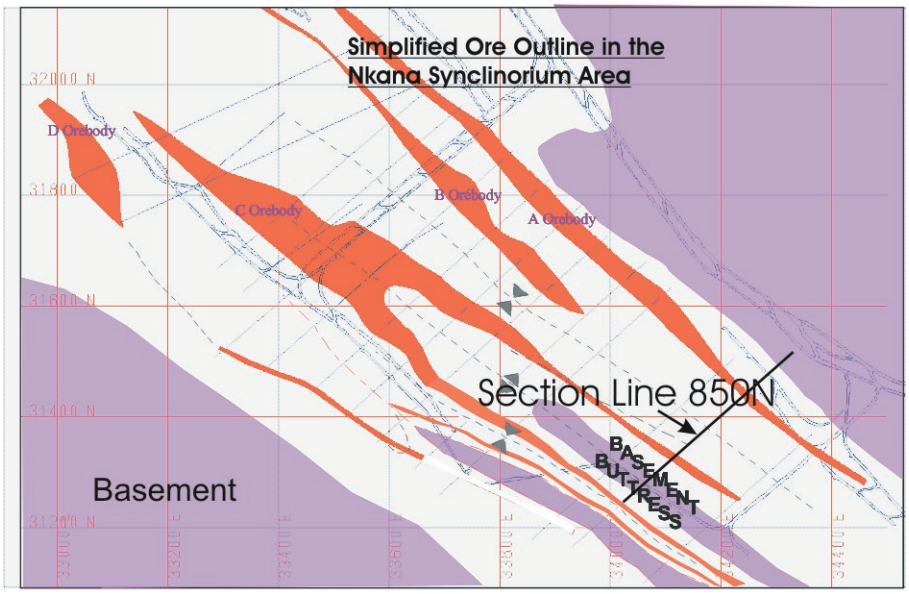

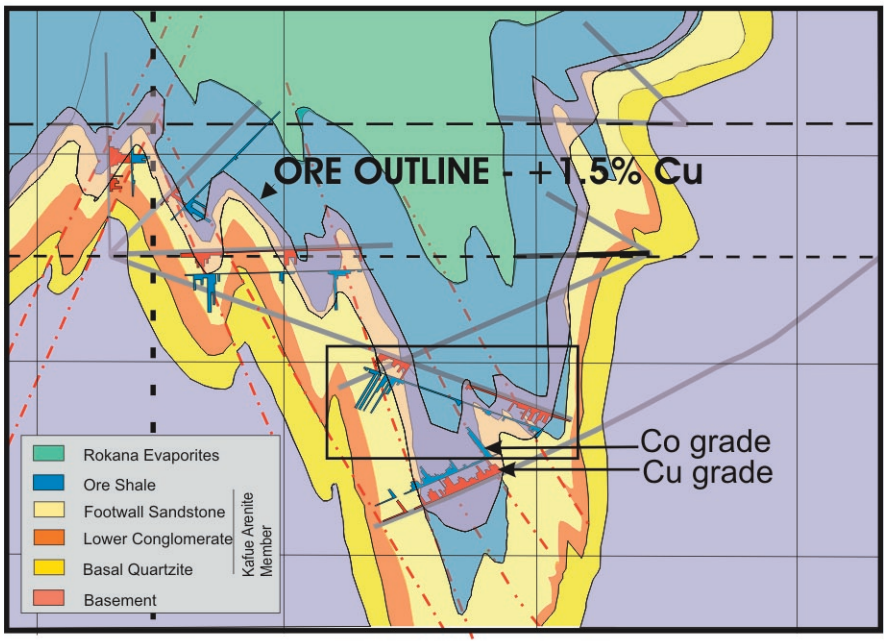

dolomite, calcite, albite and biotite.
- Close correlation of cobalt rich zones and carbonate rich alteration zones.
- Vertical changes in the distribution of copper mineralisation in the COM have been observed, however no systematic laterally have been recognised.
- Extensive remobilisation?/introduction? of anhydrite into the lower Footwall Sandstones at SOB.

Geochemistry and stable isotopes

Geochemical studies are primarily aimed at the level of the Ore Shale. An important aspect of this study is to determine whether lateral and/or vertical variation in the host lithologies, alteration style and grade are revealed in geochemical studies. Whole-rock analysis for major and trace elements have been obtained for 97 samples from NKM including samples from the uneconomic west limb area.

- No significant vertical and lateral changes in the geochemistry are identified between samples from Mindola, SOB and the unmineralised west limb Copperbelt Orebody Member.
- No significant lithochemical changes between mineralised Ore Shale lithologies and 'alteration' are identified.
- Ti/Zr ratios in the COM at Nkana are different from other areas in the Copperbelt.
- All mineralised samples (COM, alteration and veins) have similar carbon and oxygen isotopic values, with a noted depletion of carbon and oxygen compared to sedimentary carbonate.
- Carbon and oxygen values from barren dolomite lithologies of the COM are different to those from the mineralised samples.
- Carbon and oxygen values from the Ore Shale and mineralised veins in the Ore Shale at NKM are similar to those reported for Konkola by Swenney (1987).

Acknowledgements

The successful completion of two field seasons to date in Zambia has happened through the logistical and geological help provided by numerous people and companies in Zamiba. Particular thanks to Gavin Ferguson, Dave Armstrong, Wellington Mukumba, Giddy Mwale and all the shaft geologists, samplers and shift bosses across the four operating shafts at Mopani Copper Mines. Hugh Carruthers and Mike Stuart of First Quantum Minerals have provided extensive geological knowledge and guidance, as well as a great deal of practical and logistical support. Peter Mann and his staff at ZamAnglo for assisting with accommodation in 2002 and allowing 'Spider' to keep up with all the mechanical repairs to the 'Love Bus'.

Chambishi Basin progress report 3: Stratigraphy and sedimentology of Nkana-Mindola deposit

Mawson Croaker
Centre for Ore Deposit Research, University of Tasmania

Summary

This section provides a description and initial interpretation of the sedimentology and basin geometry at Nkana-Mindola at the time of deposition of the Lower Roan sequence. Basin architecture will provides a useful framework within which to examine relationships between deformation, distribution of Cu-Co mineralisation plus sulphide phases, geochemical halos, alteration and metasomatic processes. This integrated approach will allow for identification of the key processes involved in the formation of 'Ore Shale' hosted sedimentary copper deposits: *ie.* whether by early diagenetic, synorogenic, late hydrothermal or a combination of these mechanisms.

Previous sedimentology at Nkana-Mindola

This work does not represent the first sedimentology study based on the NKM area. Clemmey (1976, 1978) provided the first comprehensive descriptive study of the Lower Roan stratigraphy based upon work undertaken at Mindola Shaft, Mindola Pit and to a lesser degree at the southern end of the NKM area (Central Shaft and SOB Shaft) (Figs 1, 2). Much of this work remains unpublished in his PhD dissertation. This work emphasised on the sedimentology of the Copperbelt Orebody Member 'Ore Shale' as this hosts greater than 90% of all resources at NKM. Clemmey (1976) also described and interpreted the depositional environment of other members of the Lower Roan. A synthesis of this work is presented, and observations to date as part of this study generally support the descriptive work of Clemmey (1976).

With mining operations at NKM continuous for the last 70 years, a wealth of geological data existed in the form of mine sections, mine plans and mine reports. This dataset is now incomplete, however valuable remains available from sections of the NKM and are used within this study to complement and enhance data collected as part of this project.

Assumptions and limitations of this study

In this report I will use the stratigraphic division devised by Clemmey (1976) (Fig. 3). Recognition of differences and possible improvements, where necessary, will be addressed at a later stage upon completion of detailed facies work on the hangingwall sequence, petrographic studies and in context of the whole Chambishi Basin study as part of the P544 project.

Despite the extensive underground workings at NKM, severe limitations on the type and quality of both historical and present day geological data collection have been encountered during underground work. Ground conditions, white washing of walls, dirty walls, ventilation restrictions and the necessary rock support infrastructure restricts viewing of many rocks faces along drives and cross cuts. As with all mining operations the requirement to keep waste handling to a minimum restricts available underground exposures of the footwall and hangingwall sequences, particular at Mindola and Mindola North Shaft areas. Furthermore preservation of drill core and detailed geological logs, sections and plans is limited, particularly outside known economic mineralisation. No drill core within the NKM area has

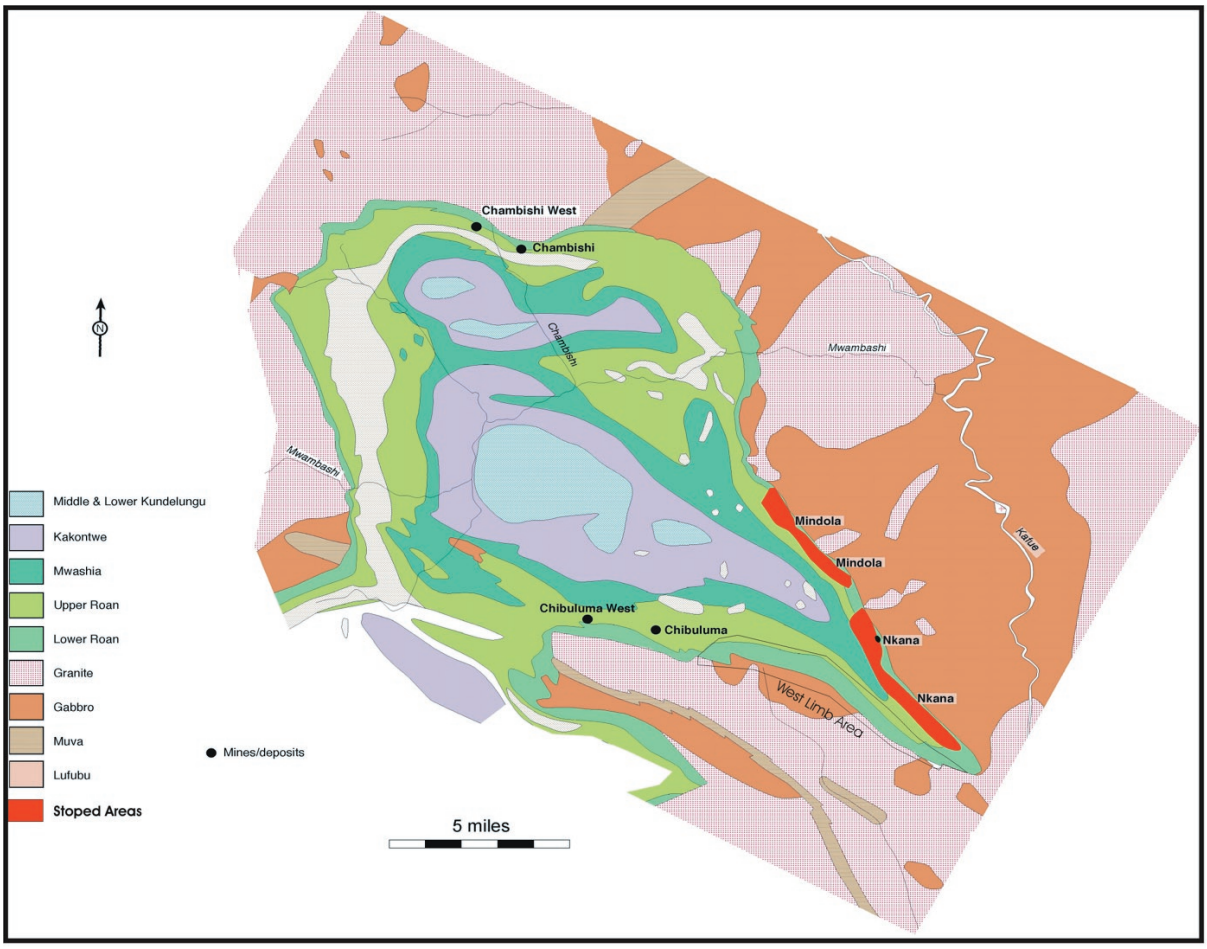

Figure 1. General location plan of the Nkana-Mindola area in the Chambishi Basin. All economic mineralisation is confined to the northeastern limb of Nkana Syncline.

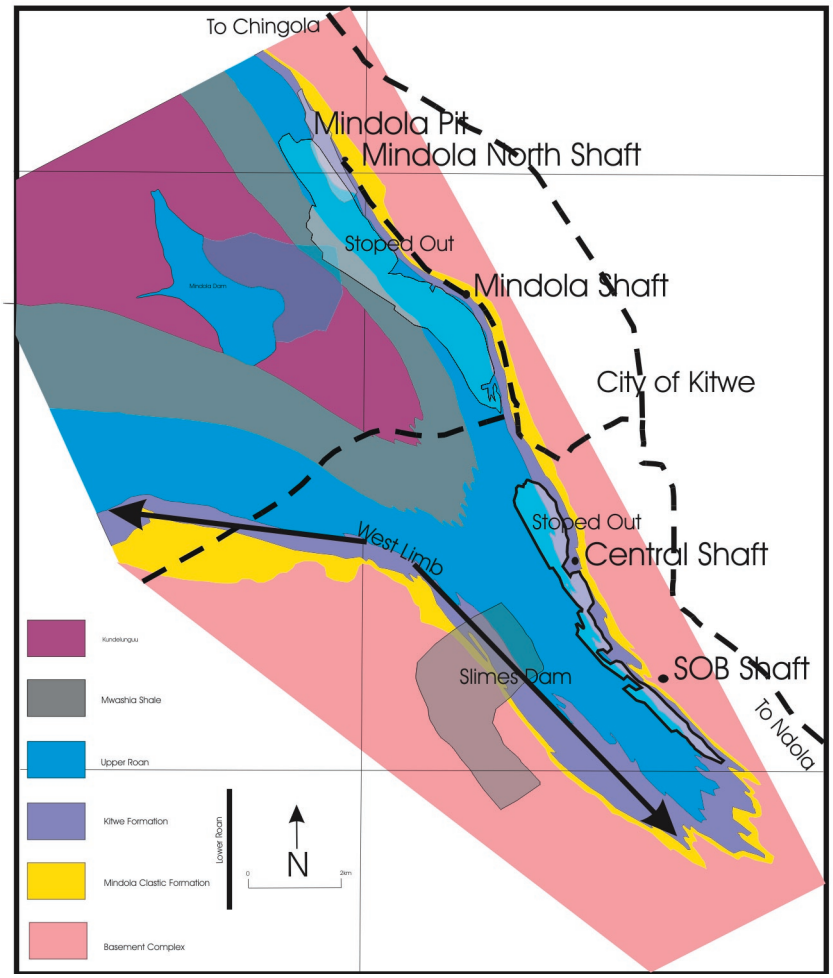

Figure 2. Geological map of the Nkana-Mindola area, with the location of the four operating shafts. Changes in the thickness of the Mindola Clastic Formation are readily observed on both side of the syncline. Thickness variations in the Kitwe Formation are less pronounced, and commonly related to structural thickening. Detailed surface maps used for this study are ZCCM geological maps compiled from augering and pit maps undertaken during the 1950s to 1990s.

Figure 3. Stratigraphic and Mine nomenclature used at Nkana Mindola. The stratigraphic nomenclature used in this report is adopted from Clemmey (1976) and all discussion will refer to this terminology.

Lithofacies Associations defined by Clemmey (1974, 1976) for Mindola Clastic Formation.	**Character**	**Depositional Environment**
Facies Association 1 - Poorly stratified, poorly sorted in fine matrix (Alluvial Fan)		
1a – paleosol	Fragments of basement within a fine to very grained chloritic siltstone-sandstone	Represents palaesol
1b – Massive unstratified	Sharp basal contact, boulders angular to subrounded up to 1 m in size, 0 – 10 m thick, fining upward sequence	Debris flow in arid environment – proximal sections of fan deposits.
1c – Matrix supported clasts	No further information	Alluvial Fan deposits
1d – Angular blocks in fine grained matrix	No further information	Alluvial Fan deposits
1e type A - Bedded gravel deposits	No further information	Alluvial Fan deposits
1e type B – Bedded, clast poor, argillaceous matrix.	No further information	Alluvial Fan deposits
Facies association 2 – Conglomerate, coarse grained matrix. (Pedimont Deposits)		
2	Well rounded, poorly sorted, boulder to pebble sized clasts in arkosic matrix, minor evidence of bedding in finer grained beds, 0 to 16 m thick, thickest in areas underlying paleovalley, thins against palaeotopography, lower erosional contact, maybe capped by shale horizon.	intraformation pedimentation and lag deposit.
Facies Association 3 – Finer Grained, moderate to well sorted, distinct bedding (Piedmont fluvio/lacustrine environment)		
3a – Type A cycles	Gradational, well bedded, minor laminated argillaceous, minor flaser bedding	Debris flow prograding into distal or simple low energy environment. Three possibilities: fluvial-deltaic; offshore bar-spit to barriers island; progradation of piedmont fan lobes into flood plain or lacustrine
3a – Type B cycles	Sandy facies type compared to Type A cycles, condensed sections	Braided river environment
3a – Type C cycles	Order of magnitude 16 to 18 m, upward coarsen cycle, planar and trough cross stratification, silt horizon commonly pinch ut laterally,	Braided river environment, lack of bank stability, reworking of proximal fan head
3b	Silt and mud grain size, three mina lithological types – argillaceous quartzite, laminated argillites and massive greywacke type, dessication noted.	Lacustrine and/or distal playa and/or piedmont flood plain sediments
3c – minor carbonate beds	Top of coarsening upwards cycles, lower reddened dolomite unit and silicificed anhydrite unit, unit is a transition from 3b.	
3d	Combination of facies 3a Type C and associated 3b.	Braided stream piedmont deposits.

4a.

4b.

Figure 4a and 4b. Breccia facies identified on the 3360L and 1250L at SOB shafts overlying basement. Only very poor and limited exposures are accessible at the present time.

yet been discovered with an intact, relatively undeformed complete hangingwall sequence. My study of the hangingwall sequence has been restricted to the Mindola Pit area and highly deformed portions of the lower hangingwall sequence at SOB. However is supplemented by information in Clemmey (1976) and from old drill logs, maps and mine reports.

Methods

Sedimentology data included in this study were collated through a number of methods. Sedimentology data were compiled from traverses, reconnaissance mapping and detailed mapping of production cross cuts, stopes and drives at Mindola North Shaft (1050L, 500L, 610L, 780L) , Mindola Shaft (4180L, 4440L, 5510L) Central Shaft (2320L, 2370L, 3130L) and SOB Shaft (790L, 1250L, 1810L, 2370L, 2880L, 3140L, 3130L, 3360L). These data were supplemented with detailed logs of specific new holes from Mindola Deep Project and Synclinorium Project Area, traverses through the Mindola Pit and logging of preserved drill cores. An extensive review of old log sheets, mine plans and sections, and monthly geological reports dating back to the 1940s has been undertaken.

Further work is still ongoing to analyse and integrate new data with the old mine plans and sections to help reveal a more accurate picture of the basin architecture, particular for the West Limb area and portions of the highly deformed north eastern limb around SOB Shaft. Detailed analysis of the sedimentology to date has focused on the lower parts of the stratigraphy.

For the purposes of this report I will briefly describe the stratigraphy of the Lower Roan using the subdivision of Clemmey (1976) as a framework. A specific section outlining clastic facies identified to date within the basal Mindola Clastic Formation is presented and a general review of the Lower Roan depositional cycle from work to date and Clemmey (1976) is discussed. Detailed facies analysis of the upper Lower Roan is still in progress.

Stratigraphy of the Lower Roan

The Lower Roan constituents a package of rocks divided into the Mindola Clastic Formation and the Kitwe Formation (Clemmey, 1976) (Fig. 3). The basal Mindola Clastic Formation unconformably overlies the basement complex and varies between 0 m and 150 m-thick and is subdivided into two members. The overlying approximately 150 m-thick siliciclastic-carbonate Kitwe Formation is divided into five members. Mine terminology recognises six units within the MCF and approximately 14 units within the Kitwe Formation (Fig. 3).

Mindola Clastic Formation (MCF)

Commonly referred to as the footwall sequence at NKM, the formation is divided into two members by Clemmey (1976) (Fig. 3). The lower unnamed basal member (herein termed the Basal Quartzite) is predominately composed of grey massive and crossbedded quartzites and sandstone, bi-modal cross-bedded quartzites, minor basal breccia units and thin, discontinuous matrix supported conglomerate units unconformably overlying the basement complex. The upper Kafue Arenites Member (KAM) is commonly recognised by 4–8 m-thick basal conglomeratic unit, locally referred to as the Lower Conglomerate, and by a sequence of small to medium scale cross bedded, medium- to coarse-grained sandstones and siltstones. The sandstones are typically arkoses, greywackes and quartz arenites. Significant thickness and facies variations characterise the MCF.

Clastic Lithofacies and Lithofacies Associations of the Mindola Clastic Formation

The recognition of individual lithofacies alone does not allow for accurate interpretation of the depositional environment however, distinctive vertical lithofacies associations do provide a meaningful method for interpreting depositional cycles. The relationship of these distinctive associations forms the basis for stratigraphic sub-division. One limiting factor of this NKM study, particular for the conglomeratic and sandstone facies, is the inability to assess accurately lateral relationships of different facies assemblages

particular in high strain zones. Clastic lithofacies association recognised within the MCF at NKM are discussed below and work by Clemmey (1976) is summarised in Table 1.

Basal Quartzite Member

Lithofacies Association 1. Unstratified massive breccia facies. (Lithofacies 1A and 1B)(Fig. 4a , 4b)

Lithofacies association 1 has several different breccia clast types (granite, genesis and minor micaceous quartzite) and from data available is interpreted to have a very limited lateral extent. No representative vertical profiles of any breccia facies have been logged during this study, however two different breccia lithofacies have been observed (Table 1, Fig. 4a , 4b).

Lithofacies 1A is interpreted to represent a proximal alluvial fan setting or talus breccia deposit. Both are commonly deposited along the edges of faulted basin margins during pronounced episodes of tectonic uplift. Lithofacies 1B, a matrix rich breccia, is interpreted as a proximal alluvial fan deposit or maybe considered an avalanche deposit

Lithofacies Association 2. White to grey, large scale cross-bedded and horizontal stratified quartzites. (Lithofacies 2I and 2H)

Lithofacies association 2 is a sequence of large-scale cross-bedded quartzite cycles, only identified in the lower portion of the MCF. This lithofacies association is recognised at the lower portion of the basal quartzite member and is similar to facies association 4 identified by Clemmey (1976) (Fig. 5b).

Lithofacies association 2 is interpreted as similar to Clemmey's (1976) facies association 4 and is interpreted likewise as an aeolian depositional environment. The bi modal petrographic nature of the quartzite also supports an aeolian environment.

Lithofacies Association 3. Massive coarse-grained sandstone and cross bedded sandstone (Lithofacies 3A, 3C or 3D) (Fig. 5a)

Recognised as predominantly beds of massive sandstone, this lithofacies association is approximately 5 m to 8 m-thick and has been only been laterally traced for 300 m to date. It is identified readily across NKM.

Lithofacies association 3 represents a braided-sheet flood fluvial deposit. A thin, pebble to cobble, matrix supported conglomerate unit has been observed on the 5520L Mindola as part of lithofacies association 3 and is interpreted as a short-lived high-energy pebbly sheet flood deposit.

Kafue Arenite Member

Conlgomerate Lithofacies Association 4 (Figs 6, 7)

Lithofacies association 4 is subdivided into two facies associations, both are only recognised in the basal Lower Conglomerate unit of the KFM (Figs 6a, 6b, 7a–c). This unit is common across NKM, however it does thin and pinch out in certain areas. No systematic lateral changes have been documented to date. Lithofacies association 4a is a massive pebble to cobble conglomerate composed of lithofacies 2A, 2B while lithofacies association 4b is a massive to stratified pebble to cobble conglomerate composed of lithofacies 2A, 2C. The distinction between the two is based upon evidence of the stratification of some conglomerate beds in lithofacies association 4b.

Lithofacies association 4a has been interpreted to represent wet, proximal to mid-fan sheet flood alluvial deposits while lithofacies association 4b has also been interpreted to suggest a similar wet, proximal to mid fan-sheet flood alluvial deposits, however the stratification is interpreted to indicate minor channelisation of the alluvial fan, possibly in a more distal setting.

Table 1. Thirteen clastic lithofacies have been identified within the Mindola Clastic Formation. Each lithofacies does not represent an unqiue depositional environment, however when assessed in association with adjacent lithofacies provide a link to the deposition environment.

Lithofacies Code	Lithofacies	Grain Size	Sedimentary structures and geometry	Depositional Environment	Occurrence
Breccia Facies					
1A	Massive clast dominant breccia	Max clasts 1.2m; clast range from 0.3m to 1.2m	No stratification	Rockfall to rock avalanche deposit – Talus breccia to very proximal alluvial fan.	Rare, Basal breccia (MCF) 1250L SOB Shaft
1B	Matric supported breccia fragments (chloritic sandstone matrix)	Max clast 1 m Clasts irregular sized and angular	No stratification		Rare, Basal breccia (MCF) 2370L SOB, 3360L SOB
Conglomerate Facies					
2A	Matrix supported, polymicitc conglomerate	Pebble to cobble, max clast size ca. 17 cm.	No stratification, erosional basal surface, lateral continuous for > 50 m, max 2 m thick.	Debris flow – alluvial fan, water-flow dominated, plastic debris flows, thinner deposits represent pseudoplastic debris flow and stream channel flow.	Very Common, Lower Conglomerate (MCF) across NKM
2B	Clast Supported polymicitic conglomerate	Pebble to cobble, max clast ca. 15 cm. Sub rounded-subangular clasts	No stratification, erosional basal surface, laterally traced for min. 20 m	Same as above –debris flow either proximal fan or mid to distal fan (Sheet flood deposits)	Lower Conglomerate (MCF)
2C	Poorly stratified matrix supported conglomerate	Pebble, maximum clast size 5 cm.	Poorly developed cross beds, beds max. 2m thick, lateral persistent ca. 30 to 50 m.	Minor channelisation alluvial fans, mid to distal fan.	Common, Footwall conglomerate and very rare occurrence in Lower Conglomerate (MCF)
2D	Stratified, matrix supported conglomerate	Pebble, with minor very coarse-grained sandstone lenses.	Planar stratified, lateral impersistent, max. thickness ca. 50 cm	Gravel bars or channelisation of alluvial fan system.	Rare, Footwall conglomerate, (MCF)
Sandstone - Siltstone Facies					
3A	Massive Sandstone	m-vc grained	20 cm to 2 m thick, some fining upward grading	Lower flow regime, sheet flood conditions.	MCF
3B	Horizontal stratified sandstone	m-vc grained, minor heavy mineral concentration along basal portion.	10 cm to 80 cm thick	Formed under upper flow regime conditions for mss, c to vcss generally formed under lower flow regime conditions.	MCF
3C	Trough cross bedded sandstone	m-vc grained	5 cm to 40 cm, rare 70 cm to 1 m thick sets	Sinuous crested and linguoid dunes, formed during low and high flow conditions – majority thought to occur under high flow conditions.	MCF
3D	Tabular cross bedded sandstone	f to vc grained	5 cm to 30 cm,reactiviation surfaces along foresets, heavy mineral conc. along forsets	Migration of sand bars, sandy transverse bars and migrating bars under low flow conditions	MCF
3E	Laminated sandstone-siltstone	Silt to medium ss	Maximum 10 thick sets, fining upward cycle, parallel continuous and discontinuous surfaces	Traction transport mechanism, either plane bed transport upper flow regime or lower flow regime.	MCF
3F	Ripple cross laminated sandstone	vf to f ss	Ripples, maximum 2 cm thick, minor heavy mineral concentration along foresets.	Ripples – lower flow regime.	Rare MCF
3G	Wedged shaped cross laminated sandstone.	fss to css – distinct light grey banded quartzites.	Up to 3 m in size, some small ripples observed along surfaces.	Tranverse aeolian sand dunes.	Lower portion of MCF

Figure 5. a). Massive quartzite, no visible bedding or sedimentary structures typical of lithofacies Basal Quartzite Member lithofacies association 3. b). Cross bedded quartzite and coarse-grained sandstone of the Basal Quartzite Member. Minor heavy mineral concentration along the forests of some cross beds. Minor intervals of intense albitic flooding. c). Biotite quartzite lithology occurring within the lithofacies association 3. d). Contact between Basal Quartzite Member and the Kafue Arenite Member marked by the lower conglomerate unit.

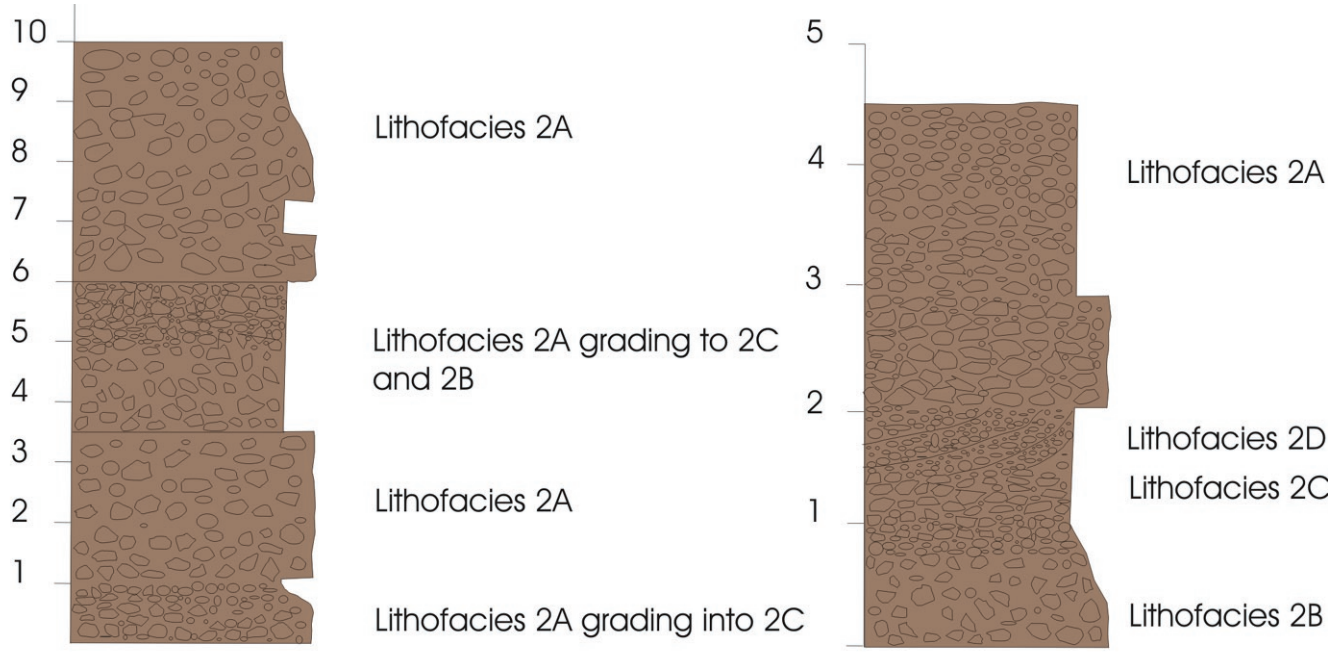

Figure 6a & 6b. Lithofacies Association 2a and 2b representing alluvial fan depositional environment. Poorly stratified beds (lithofacies 2c and 2d) are possible evidence for distal, channelisation of alluvial fan.

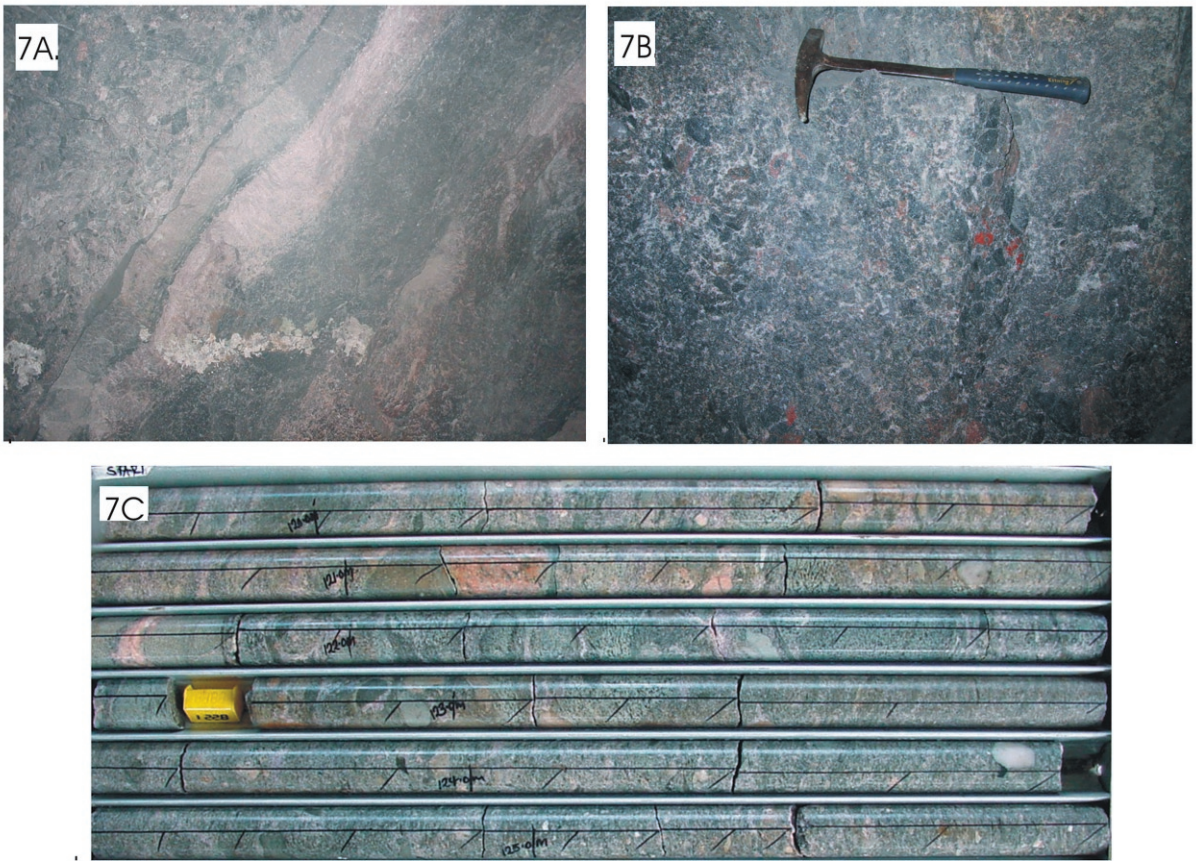

Figure 7a. Lithofacies 2a within the Lower Conglomerate unit of the Kafue Arenite Member at SOB Shaft (3360L) in contact with the overlying Footwall Sandstone unit. The contact is maybe marked by an intense 10 cm to 30 cm thick zone of anhydrite and/or albite flooding.
c). Conglomeratic lithofacies of lithofacies association 2a and 3b. Intense anhydrite flooding of the interstitial matrix-cement of the conglomeratic lithofacies is common at SOB.

Kafue Arenite Member - Conglomerate, sandstone and siltstone lithofacies association 5

Association 5a. Interbedded massive and cross bedded sandstone. (Fining upward - Lithofacies 3A, 3B, 3C and 3D) (Figs 8, 9a)

The typical cycle of association 5a is approximately 3 m thick, consisting of a basal massive sandstone grading upward to medium-grained, cross bedded sandstones. Repetition of two or three cycles is common, with the basal contact marked by very coarse-grained to pebbly sandstone.

Lithofacies association 5a is interpreted as fluvial environment, similar to that expected in low sinuosity braided river environment or from channel abandonment on an alluvial fan.

Lithofacies Association 5b. Interbedded sandstone, cross bedded sandstone and thin siltstone (Coarsen upwards – Lithofacies 3C, 3D, 3B and 3E) (Fig.8)

This sequence will typical have a very fine-grained sandstone or siltstone basal portion with a gradual coarsen upward cycle. The upper coarse- to very coarse-grained sandstones are arkosic and to greywacke in composition. Lithofacies association 5b commonly occurs as stacked, repetitive cycles up to 10 m thick.

This vertical succession is typical of fluvio-delta environment, commonly formed during prograding deltaic lobes.

Lithofacies Association 5c. Interbedded fine- to medium-grained sandstone and siltstone. (Lithofacies 3C, 3D and 3D) (Figs 8, 9b, 9c)

Lithofacies association 5c is an interbedded fine- to medium-grained cross-bedded sandstone and siltstone cycle. The cycle has thickness variations between 3 m to 6 m and an overall subtle fining upward trend is observed in some packages. Within the KAM, this association is commonly overlain by interbedded sandstone and cross-bedded sandstone units.

Lithofacies association 5c is interpreted as fluvial dominated distributary channels in a deltaic environment.

Lithofacies Association 5d. Interbedded sandstone, cross bedded sandstone to pebble conglomerate. (Coarsen upwards – Lithofacies 3B, 3C, 3D, 2C and 2D) (Figs 8, 9d).

Lithofacies association 5d has only been identified within the upper portion of the MCF. This cycle is very similar to association 3b, however it is has a distinct conglomeratic upper lithofacies. This pebbly, matrix supported conglomerate, with small discontinuous lenses of very coarse-grained sandstone commonly has scoured bases in the order of 50 cm to 2 m wide.

I interpret this vertical succession the same as lithofacies association 5b (fluvial-deltaic environment), however the coarser-grained upper conglomerate lithofacies is interpreted as lag deposits, possibly indicating episodic higher fluvial flow regime confine to different geographic areas of the fluivo-deltaic system.

Kitwe Formation

Copperbelt Orebody Member (Mine terminology - 'Ore Shale')

Unlike the coarse-grained and the variable thickness of the Mindola Clastic Formation, individual laterally continuous units of the siltstone, dolomitic siltstone and interbedded shale-siltstone and black carbonaceous shale characterise the Copperbelt Orebody Member (COM) which is the basal member of the Kitwe Formation.

Two distinctly different, laterally equivalent units can be recognised within the COM at NKM (Fig. 10a; Table 3). An interbedded siltstone-dolomitic siltstone package at the northern end of NKM is stratigraphically equivalent to a grey to black interbedded carbonaceous-carbonate shale-siltstone package towards the south and west (Fig. 10b, 10c). Above each unit is a light to dark grey, carbonate-rich, carbonaceous pyritic siltstone that is identified throughout the area. No significant thickness variations are recognised. The upper portion of the COM is an upward coarsen package of fine- to medium-grained sandstone and siltstone. This cycle

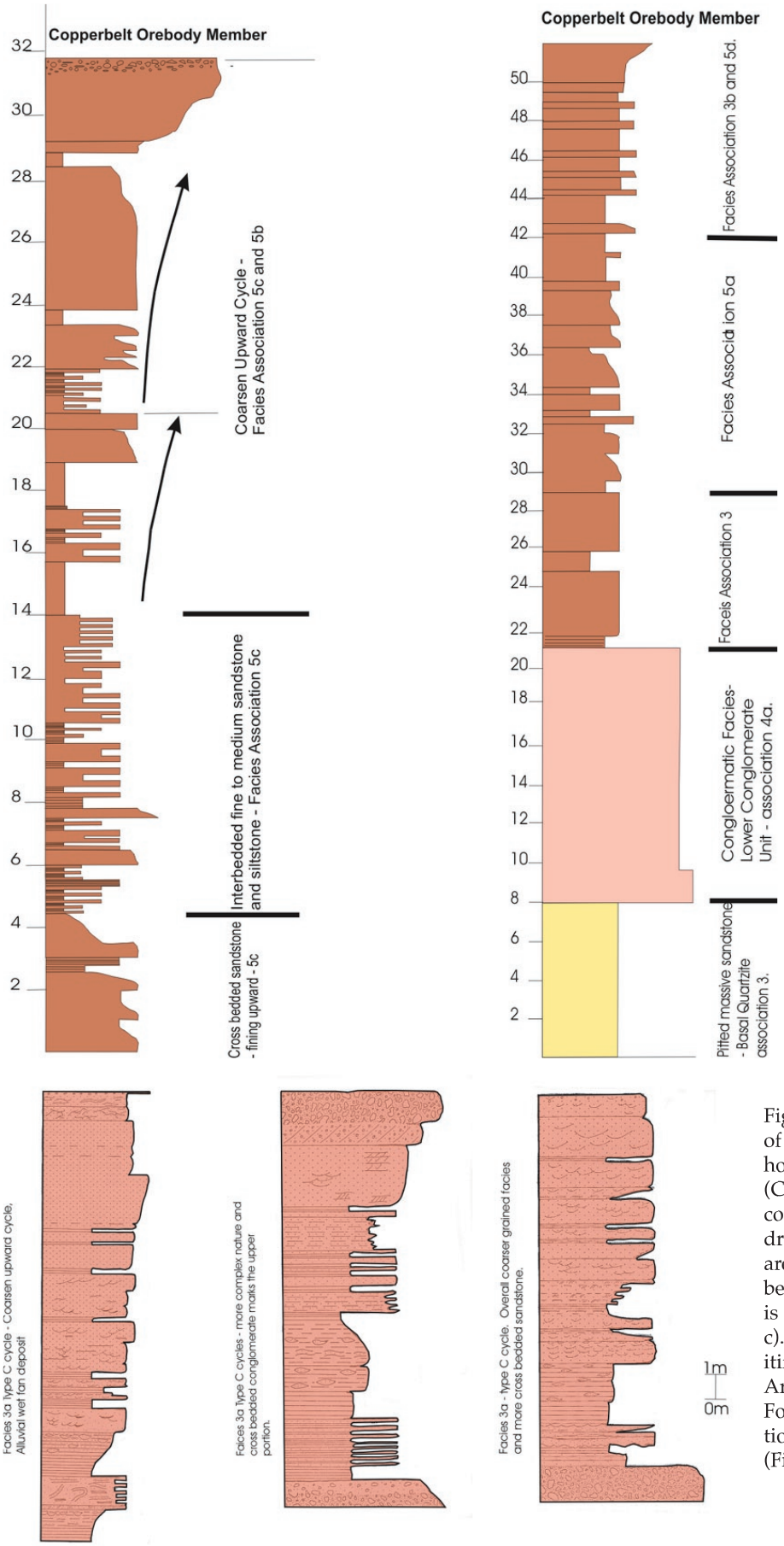

Figure 8a and 8b.Stratigraphic sections of Mindola Clastic Formation from drillholes MX 195 (Mindola Shaft) and CE490 (Central Shaft). The overall upward coarsen package is recognised in both drillholes and the internal differences are typical of the Kafue Arenite Member. The lower portion of the drillhole is a grey to white, silicified sandstone. c). Clastic lithofacies associations identified by Clemmey (1976) for the Kafue Arenite Member of the Mindola Clastic Formation. Similar lithofacies associations are identified as part of this study (Figure 8a and 8b).

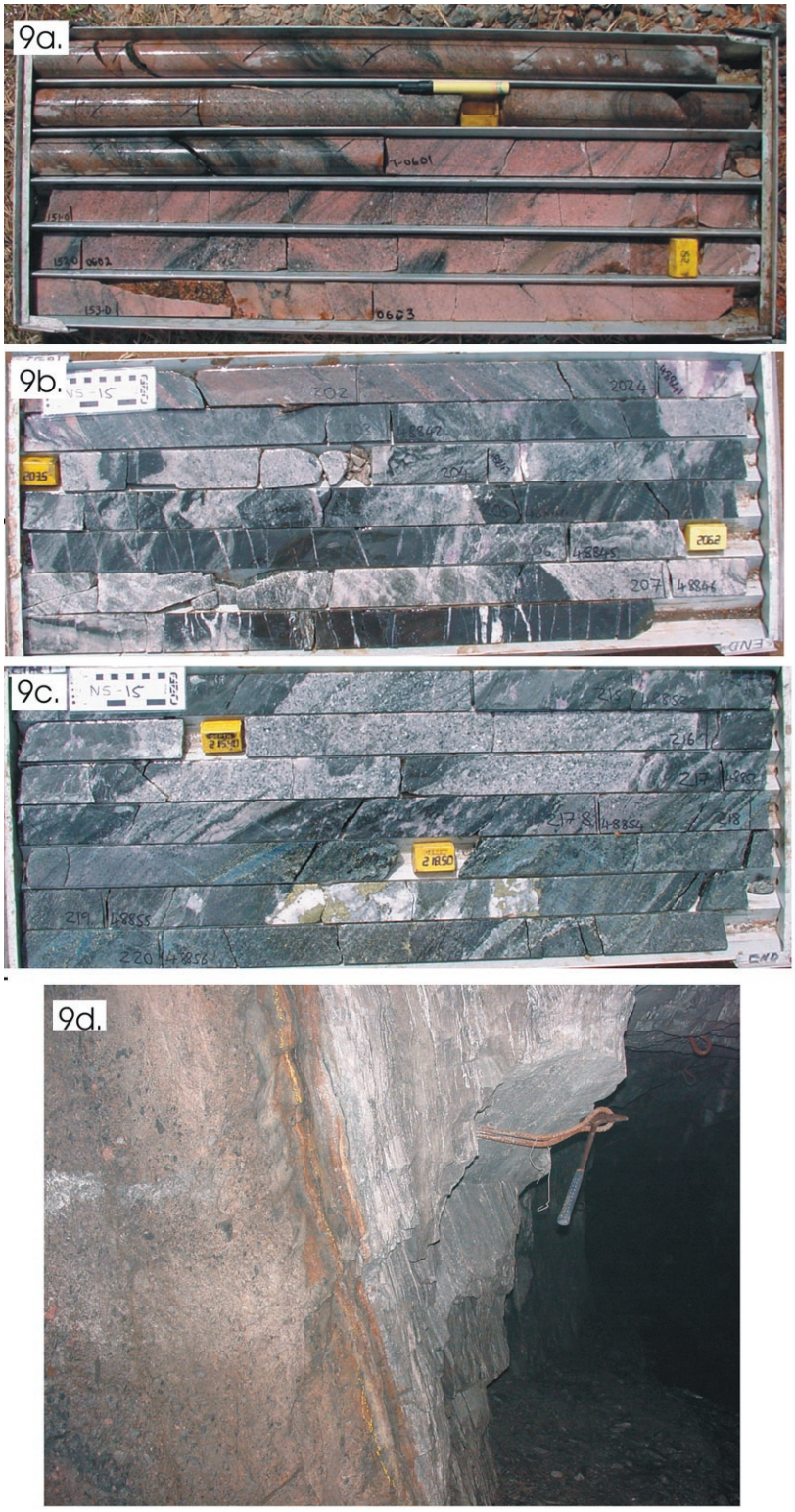

Figure 9. a). Small scale coarsen upward cycles of the upper Kafue Arenite Member at Mindola. b) Intensely veined interbedded sandstone and siltstone of the Kafue Arenite Member at SOB, minor anhydrite rich intervals do occur, however are not laterally persistent. c). Very coasrse grained to pebbly sandstone of the upper of the Kafue Arenite Member at SOB with minor disseminated chalcopyrite and pyrite and cross-cutting quartz-calcite-chalcopyrite veins. Anhydrite flooded zones and isolated blebs common. d). Contact between the upper conglomeratic facies of the Kafue Arenite Member (lithofacies association 5d) and the overlying Copperbelt Orebody Member.

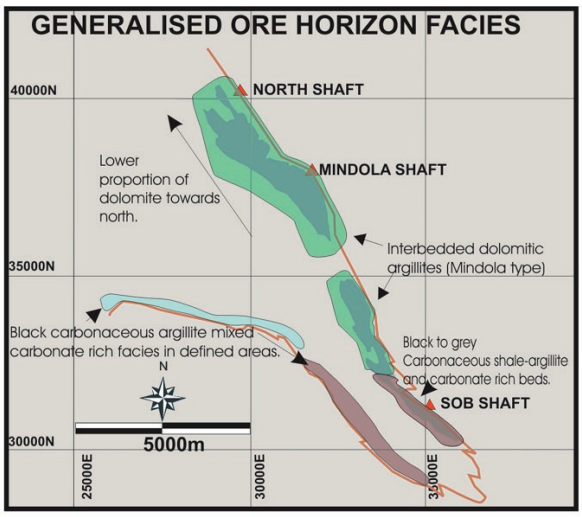

A.

B.

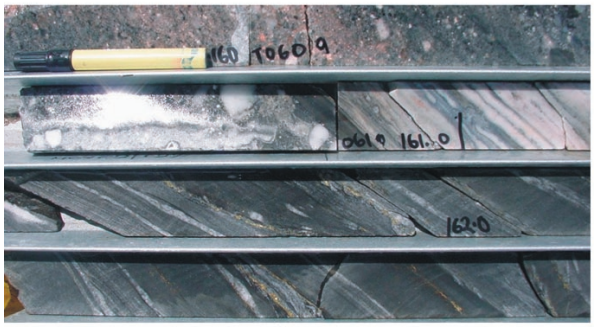

C.

D.

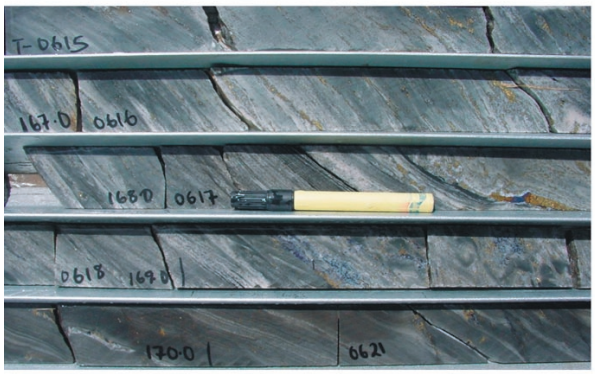

E.

Figure 10. a). Geographic distribution of the different facies of the Copperbelt Orebody Member (COM) at Nkana-Mindola. b). Lower portion of the COM within the Mindola Pit with dolomite rich beds interbedded with argillite. Dolomite pseudomorphs are also recognised in the Mindola Pit. c). Contact between the conglomerate of the Kafue Arenite Member and COM at Mindola. d). Talc-tremolite altered COM and more massive argillite with minor calcite veins. Minor chalcopyrite and pyrite disseminated throughout. e). Dolomitic argillite and argillite interbedded and bedding parallel veins in Units 2 and 3 at Mindoa. Relationship of the bedding parallel veins and dolomite rich beds remains unclear at this stage. Intense bedding parallel shearing and isoclinally folded individual beds are common at Mindola.

is very similar to lithofacies association 3b recognised in the KAM of the MCF. Laterally discontinuous carbonate dominant facies characterise lower portion of the COM at several localities along at NKM, and these coincident with the Kitwe Barren Gap and small SOB barren zone (Fig. 14). The carbonate rich facies grade laterally into the typical siltstone-shale facies and commonly directly overlie basement.

As previously mentioned, work by Clemmey (1976, 1978) provides a very detailed description and interpretation of the Copperbelt Orebody Member (COM). To date this study concurs with the overall facies description presented by Clemmey (1976, 1978). However, some future petrographic work may be able to define facies variations within the fine grained units and conclusively identify between sedimentary and metamorphic textures. Interpretation of the facies is still ongoing, within the context of the whole Kitwe Formation. Table 2 and Figure 11 summarise the lithofacies identified by Clemmey (1976, 1978) within the COM at Mindola and Mindola North Shaft. All rock packages overlying the COM are locally referred in mine terminology to as the Hangingwall Sequence.

Rokana Evaporites Member (REM)

Overlying the COM, is a sequence of interbedded siltstones, very fine to fine grained sandstones and thin dolomitic siltstone beds (Figs 12, 13a). This package can be traced for approximately 1 km strike length in the Mindola Pit, and is easily recognised within the steep pit walls. Surface mapping by ZCCM geologists at NKM, has identified this unit throughout the area and thickness variations are mainly interpreted as resulting from structural thickening and thinning. This study was restricted to examining the REM in steep, weathered pit walls and the pit floor at the northern end of the pit. The upper contact with the overlying Nchanga Quartzite Member (NQM) is marked by an approximately 4 m-thick interbedded medium- to fine-grained sandstone and siltstone cycle. Clemmey (1976) recognises very similar lithologies and facies to the COM.

Nchanga Quartzite Member (NQM)

The base of the Nchanga Quartzite Member (NQM) (Fig. 12) is marked by a 20–30 cm-thick silicified carbonate bed, with distinct internal dome shaped and polygonal structures. Overlying this bed, are medium- to coarse-grained, cross bedded dolomitic sandstones and interbedded sandstone and siltstones, very similar to lithofacies association 3b and 3e recognised in the MCF. Approximately ten metres above the basal contact, is a 90 cm-thick, medium- to coarse-grained sandstone bed characterised by soft sediment deformation. Overlying this bed is an approximately 3.5 m-thick cycle of planar stratified and cross-bedded sandstone with a significant dolomite composition in some beds. This cycle is overlain by a 4 m-thick, very large-scale cross-bedded, medium- to coarse-grained sandstone bed. Within the Mindola Pit this bed is traced laterally for approximately 500 m, however at the southern end of the Mindola Pit a planar stratified sandstone bed is identified at the same stratigraphic level. The upper approximately 8 m-thick package is a rapidly thinning and fining upward cycle of massive sandstone, cross bedded sandstone and interbedded sandstone-siltstone.

Chambishi Dolomite Member (CDM)

The approximately 45 m-thick Chambishi Dolomite Member (CDM), with 2–10 cm-thick beds traceable for at least 1 km, is readily identified by a distinct brown colouration and thin and thick bedded carbonate beds interbedded with white to pink, very weathered siltstone and sandstone beds (Figs 12, 13b). The basal contact is identified by a 5 cm to 10 cm-thick silicified carbonate bed that is laterally continuous for a minimum of 500 m strike length. Four depositional cycles are interpreted to date within the CDM. The approximately 10 m-thick basal cycle consists of medium- to fine-grained massive and cross bedded sandstones, siltstones and 2–10 cm-thick silicified carbonate beds (Fig. 13d). The basal cycle is overlain by a 18 m-thick sandstone and siltstone cycle, with two intervals of 2–10 cm-thick, repetitive silicified carbonate beds interbedded with siltstone and sandstone within the 18 m-thick cycle. Ripples

Table 2. Clemmey (1976, 1978) recognised several distinct lithofacies associations within the Mindola Clastic Formation and these are very similar to those identified as part of this study. For this reason I have adopted the stratigraphic division devised by Clemmey (1976).

Lithofacies Code	Lithofacies	Grain Size	Sedimentary structures and geometry	Depositional Environment	Occurrence
Breccia Facies					
1A	Massive clast dominant breccia	Max clasts 1.2m; clast range from 0.3m to 1.2m	No stratification	Rockfall to rock avalanche deposit – Talus breccia to very proximal alluvial fan.	Rare, Basal breccia (M 1250L SOB Shaft
1B	Matric supported breccia fragments (chloritic sandstone matrix)	Max clast 1 m Clasts irregular sized and angular	No stratification		Rare, Basal breccia (M 2370L SOB, 3360L SC
Conglomerate Facies					
2A	Matrix supported, polymicitc conglomerate	Pebble to cobble, max clast size ca. 17 cm.	No stratification, erosional basal surface, lateral continuous for > 50 m, max 2 m thick.	Debris flow – alluvial fan, water-flow dominated, plastic debris flows, thinner deposits represent pseudoplastic debris flow and stream channel flow.	Very Common, Lower Conglomerate (MCF) across NKM
2B	Clast Supported polymicitic conglomerate	Pebble to cobble, max clast ca. 15 cm. Sub rounded-subangular clasts	No stratification, erosional basal surface, laterally traced for min. 20 m	Same as above –debris flow either proximal fan or mid to distal fan (Sheet flood deposits)	Lower Conglomerate (I
2C	Poorly stratified matrix supported conglomerate	Pebble, maximum clast size 5 cm.	Poorly developed cross beds, beds max. 2m thick, lateral persistent ca. 30 to 50 m.	Minor channelisation alluvial fans, mid to distal fan.	Common, Footwall conglomerate and very occurrence in Lower Conglomerate (MCF)
2D	Stratified, matrix supported conglomerate	Pebble, with minor very coarse-grained sandstone lenses.	Planar stratified, lateral impersistent, max. thickness ca. 50 cm	Gravel bars or channelisation of alluvial fan system.	Rare, Footwall conglon (MCF)
Sandstone - Siltstone Facies					
3A	Massive Sandstone	m-vc grained	20 cm to 2 m thick, some fining upward grading	Lower flow regime, sheet flood conditions.	MCF
3B	Horizontal stratified sandstone	m-vc grained, minor heavy mineral concentration along basal portion.	10 cm to 80 cm thick	Formed under upper flow regime conditions for mss, c to vcss generally formed under lower flow regime conditions.	MCF
3C	Trough cross bedded sandstone	m-vc grained	5 cm to 40 cm, rare 70 cm to 1 m thick sets	Sinuous crested and linguoid dunes, formed during low and high flow conditions – majority thought to occur under high flow conditions.	MCF
3D	Tabular cross bedded sandstone	f to vc grained	5 cm to 30 cm,reactiviation surfaces along foresets, heavy mineral conc. along forsets	Migration of sand bars, sandy transverse bars and migrating bars under low flow conditions	MCF
3E	Laminated sandstone-siltstone	Silt to medium ss	Maximum 10 thick sets, fining upward cycle, parallel continuous and discontinuous surfaces	Traction transport mechanism, either plane bed transport upper flow regime or lower flow regime.	MCF
3F	Ripple cross laminated sandstone	vf to f ss	Ripples, maximum 2 cm thick, minor heavy mineral concentration along foresets.	Ripples – lower flow regime.	Rare MCF
3G	Wedged shaped cross laminated sandstone.	fss to css – distinct light grey banded quartzites.	Up to 3 m in size, some small ripples observed along surfaces.	Tranverse aeolian sand dunes.	Lower portion of MCF

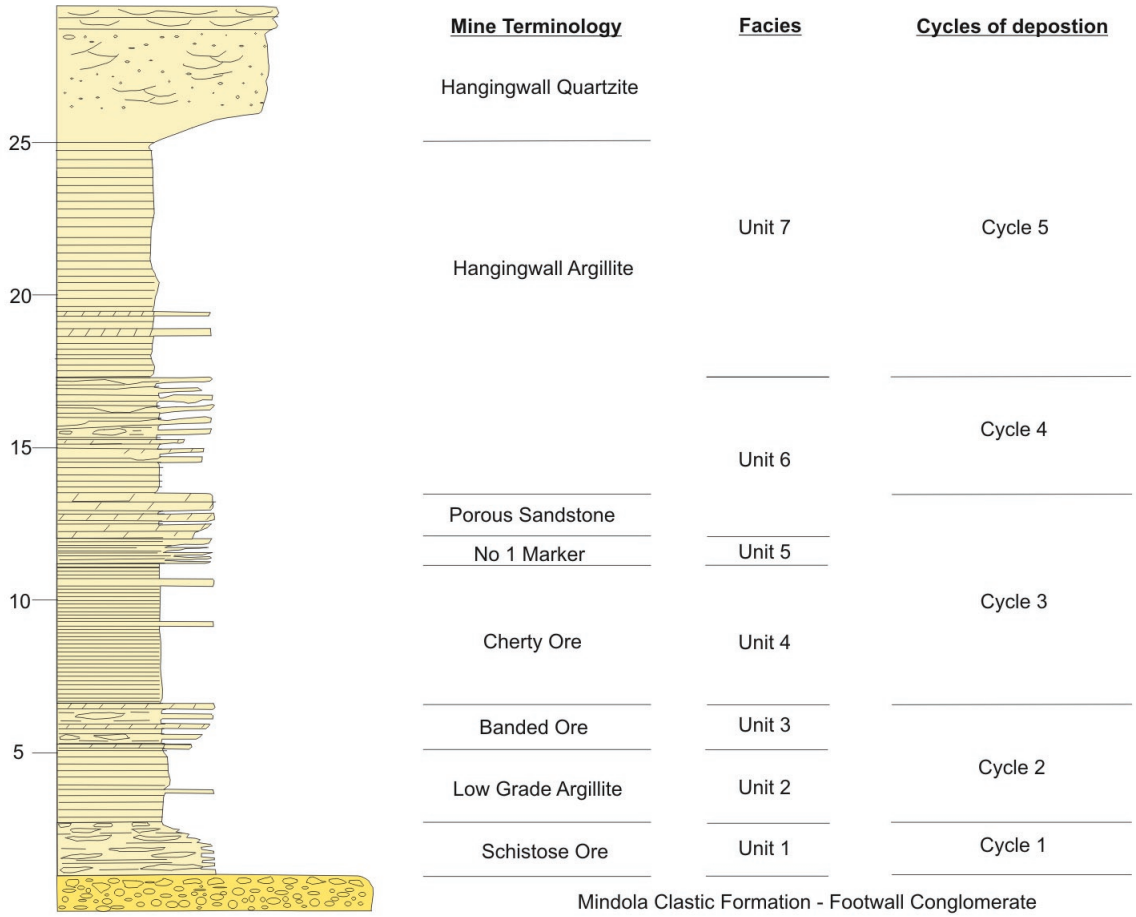

Figure 11. Summary diagram compiled from Clemmey (1976, 1978) of the main facies associations identified within the Copperbelt Orebody Member for the NKM area and recognised during this study.

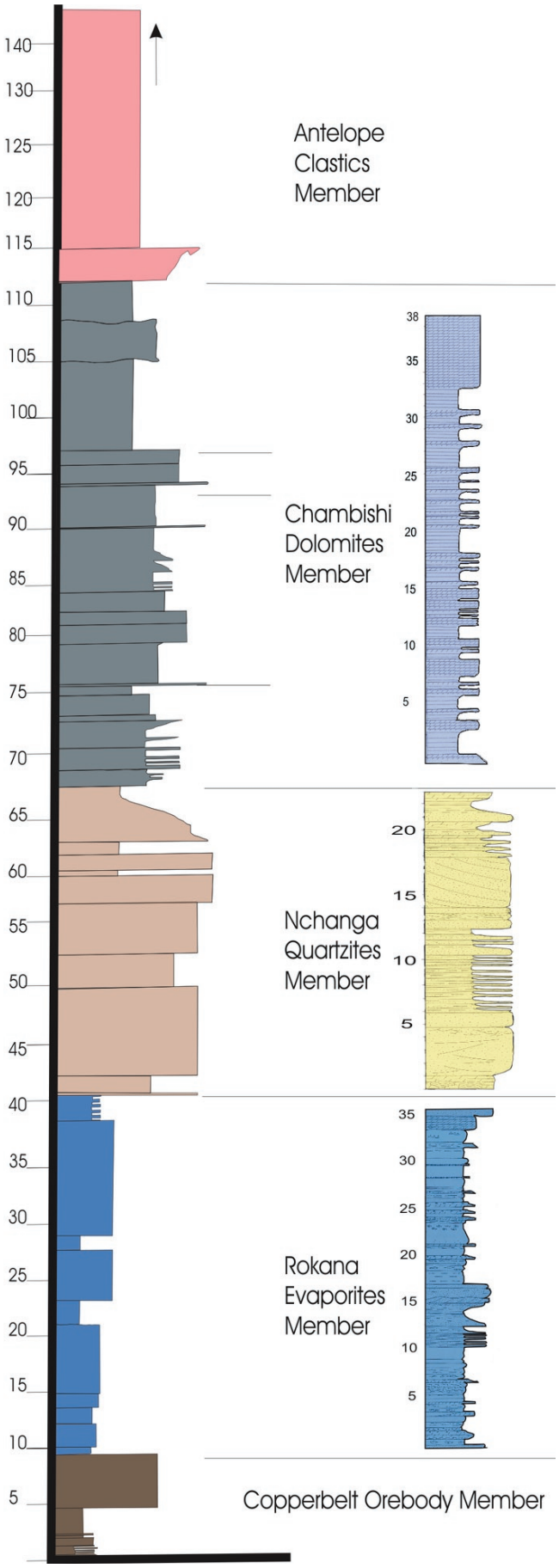

13a.

13b.

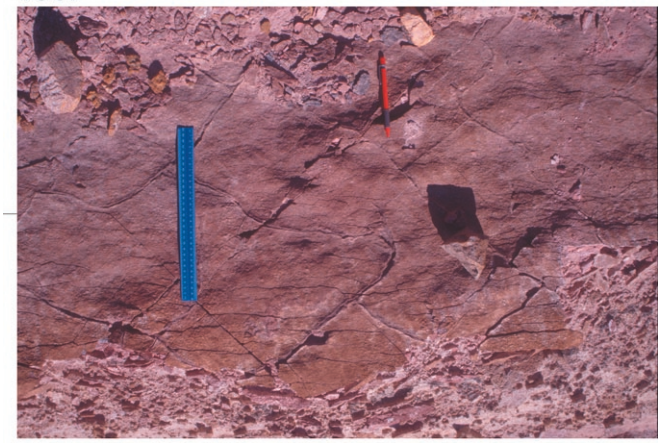

13c.

Figure 13a and b. Exposure of the Chambishi Dolomite Member in the Mindola Pit. Thin silificied carbonate beds are interbedded with medium-grained sandstones and siltstones.
13c. Dessication cracks are identified within the Chambishi Dolomite Member.

Figure 12. Measured stratigraphic of the Kitwe Formation at the Mindola Pit. The Mindola Pit is the only preserved exposure of relatively undeformed Kitwe Formation anywhere at Nkana-Mindola. The subdivisioin of the Kitwe Formation as devised by Clemmey (1976) as been adopted for the purpose of this report. The small stratigraphic sections included in Figure 12 are from Clemmey (1976).

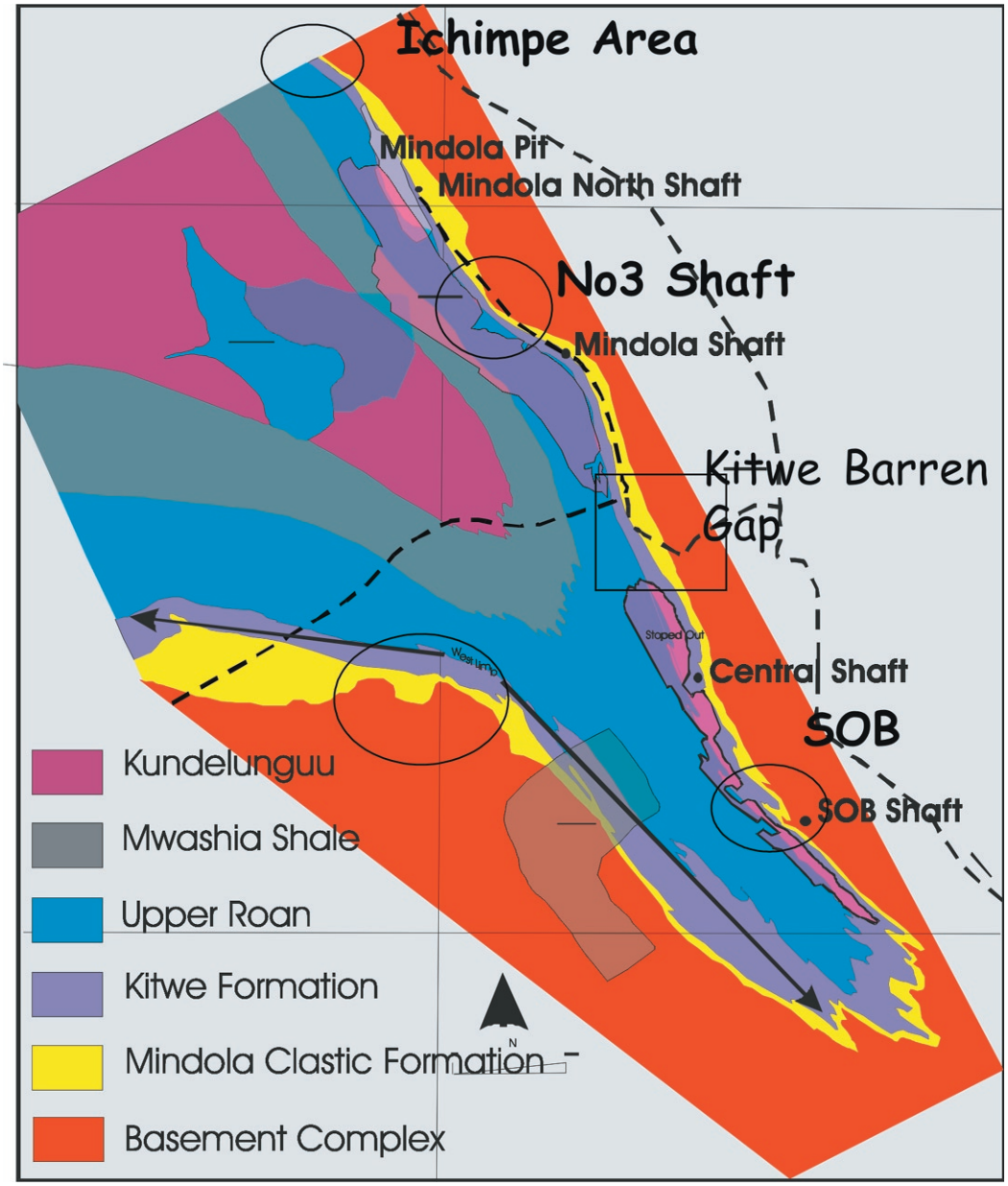

Figure 14. The distribution of breccia and conglomerate facies within the Mindola Clastic Formation is used as guide to define margins to the small, footwall basins. This work demonstrates that on the NE limb of the Nkana Syncline facies changes in the footwall sequence coincident with abrupt changes in the overall NW strike of the Basement-Lower Roan contact. Each of the significant changes in strike and facies changes coincide with 'barren' zones in the Copperbelt Orebody Member.

and desiccation cracks are observed as part of this cycle (Fig. 13c). The succeeding ca. 7 m-thick cycle is repetition of the basal cycle. The upper 15 m-thick cycle is recognised by massive, brown to cream 1 –3 m-thick carbonate beds, with internal very fine (5mm to 2 cm-thick) wavy and parallel laminations, as well as contorted, ball like structures. The upper contact of the CDM is marked by 3 m-thick massive dolomitic sandstone-siltstone bed.

Roan Clastic Member (RCM)

The abrupt change from the massive carbonate beds of the upper Chambishi Dolomite Member to interbedded siltstones and fine-grained sandstone marks the basal portion of the Roan Clastic Member, sometimes referred to as shale with grit. This highly weathered, white to pink, leached member is very poorly preserved in the Mindola Pit, therefore very limited sedimentology information was observed in outcrop apart from thin, irregular siltstone, shale and very fine grained sandstone beds and small scale sedimentary dykes (Fig. 12). Clemmey (1976) describes small to medium scale cross bedding, isolated dune and ripple trains, steep angle climbing ripples, desiccation cracks and small scale soft sediment deformation structures. Bedding parallel shearing is common throughout the unit leading to tectonic disruption of the beds and difficultly in identifying some of the sedimentary verus tectonic related disruptive structures.

Basin evolution of the Lower Roan at NKM – Depositional Model to date

Stage 1 – Basin initiation

Considerable thickness variations have been recognised in the MCF at NKM area. The basal portion of the package is commonly marked by a breccia and conglomeratic facies interpreted as indicating proximal to mid alluvial fan depositional environment and typical of facies deposited during tectonically active periods. The breccias are discontinuous and have a very confined geographic distribution. The clean grey to white quartzites and sandstones are indicative of distal alluvial fan-braided fluvial system and some large scale cross bedded quartzite units and bi-modal nature are indicative of an aeolian environment. Overall a broad fining upward cycle represents the Basal Quartzite Member. The lower basal portion of the MCF was deposited in an arid, alluvial-fluvial environment, with the basal breccia facies interpreted as indicating active fault margins.

The Kafue Arenite Member, with a relatively common lower conglomerate unit and cycles of fining and coarsen upward siltstones-sandstones, I interpret to indicate an early localised, proximal to mid alluvial fan environment with an upward transition to a fluvial-deltaic environment. The upward coarsen dolomitic sandstones with varying amounts anhydrite recognised in the southern area of NKM, are interpreted to represent small isolated pools in an arid environment. More work is required to understand the nature of the dolomitic sandstone and anhydrite 'beds' within the Kafue Arenite Member.

Constraints on the basin architecture, particularly the 3D geometry of original basin structures is very limited to date, reflecting the lack of basement control at the northern end of the NKM area and the progressively higher strain towards the south at Central and SOB Shafts. Work is still ongoing. Despite this, work by Selley and Bull (2001) and Selley et al. (2002) within the Chambishi Basin has been able to provide clear and accurate basin constraints on the deposition of the footwall sequence. Drawing on conclusions from this work, the distribution facies particularly breccia and conglomerate facies at NKM, mapping data to date and existing mine plans and reports I interpret the footwall sequence at NKM to be deposited in small, tectonically active, rift basins of approximate 2 to 3 km width. Significant and abrupt changes in the overall NW striking basement-Lower Roan contact are coincident with thinning or pinching out of the MCF and mapped facies variations. As such I can approximate the size of these basins, however the present day orientation of the interpreted basin margin structures does not represent original basin orientation.

Stage 2 – Basin reconfiguration

Identified by Copperbelt Orebody Member, initiation of stage 2 marks the deposition of a package of siltstones, carbonates, evaporites and very fine-grained sandstones indicating a significant lower energy depositional environment compared to the MCF. The Copperbelt Orebody Member marks a significant change in the basin development and size, which is maintained for the whole Kitwe Formation. Unlike the thickness variations and laterally discontinuous facies of the MCF, individual beds and units of the COM is traced for kilometres at NKM with no significant thickness variations, however lateral facies variations are observed. The distinct change to fine-grained facies, laterally continuous units and only relatively minor thickness variations compared to thickness variations of the MCF I interpret to indicate a significant basin reconfiguration and not just simple major transgression. The fundamental difference between the basin architecture of the MCF and the Kitwe Formation is relatively small, tectonically active basins control the deposition of the MCF, whereas the Kitwe Formation was deposited within a larger basin, with no evidence of any significant coarse-grained facies (e.g. conglomeratic facies) and no locally restricted breccia and conglomerate type facies typical of fault controlled basin margins.

This sedimentary succession is broadly repeated in the Rokana Evaporites Member (Clemmey, 1976) and for the purpose of this report is treated as such. The upwards coarsen upper portion of the COM is interpreted to record a progressively higher energy environment, possibly relating to tectonic activity or marine regression. Clemmey (1976, 1978) interprets both members as deposited in marine-lacustrine environment with siliciclastic sabkhas developed within isolated environments and the overall coarsen upward character reflecting progressive increase higher energy environment.

Stage 3 Minor basin activity and quiescent period

Recognised by the sandstone dominant Nchanga Quartzite Member, this coarser grained succession is interpreted as a shallow marine to near shoreline environment at the onset of a basin reactivation stage. The fining and thinning upper portion I currently interpret to indicate a shallow marine environment, possibly lagoonal. The basal silicified carbonate bed of the CDM is interpreted as evidence of low energy marine environment. Desiccation cracks and ripples do indicate periods of aerial and subaerial exposure during deposition of the carbonate-siliciclastic CDM. The sandstone dominant facies of the middle CDM are interpreted as higher energy marine environment, where as the thick, bedded carbonates of the upper CDM suggest a relative long period of sea level rise. No anhydrite is observed in the upper portion of the CDM. The carbonate dominant cycle of the CDM is interpreted as a shallow marine-carbonate platform environment, similar to that of the present day Shark Bay, Western Australia.

Stage 4 Basin reactivation

The abrupt change from the thick carbonate beds of the upper CDM to the thinly bedded siltstones and sandstones of the Roan Clastic Member is interpreted to represent a basin reactivation period and return to a shallow marine, possibly fluvio-deltaic environment.

This very simplified depositional model of the Lower Roan sequence still requires considerable refinement especially for the Upper Kitwe Formation, however several important observations have been made from work to date including:

- Small, separate basins control the deposition of the coarse-grained alluvial-fluvial dominant Mindola Clastic Formation.
- Sedimentary facies can be used to assist in defining limits to the footwall basins.
- The Kitwe Formation (hangingwall sequence) marks a significant basin reconfiguration not just a marine transgression. The small basins controlling footwall deposition no longer exist, and a more expansive basin now controls sedimentation. No evidence of basin margins to the hangingwall sequence has been identified to date at NKM.
- The Kitwe Formation is a siliciclastic-carbonate sequence indicative of a shallow marine(or

Table 3. Clemmey (1976, 1978) recognised seven distinct units within the Copperbelt Orebody Member. These distinct units are readily identified in the field.

UNIT	SEDIMENTARY STRUCTURES	INTERPRETATION.	OCCURRENCE
Mindola and northern Central Shaft COM Facies			
1	Dolomitic laminae and fine grained siliciclastic, desiccation cracks, gas bubbles and dolomite crystal pseudomorphs, wavy bedding and small channels	Low intertidal facies – marine environment however lacustrine still possible.	Schistose Ore – northern Central Shaft and Mindola area.
2	Erosional basal contact, massive and marinated silts 5 to 20 cm thick, bas bubble bursts, syneresis cracks.	Continuing transgression of tidal flats.	Low Grade argillite - northern Central Shaft and Mindola area.
3	Interbedded silts and 1 to 5 cm thick dolomites, desiccation cracks, rain textures, gypsum crystal mats, anhydrite lath mush, gelatinous stromatolites	Seasonal lagoon and shallow lake edge – require a fairly stable subaqueous environment.	Banded Ore - northern Central Shaft and Mindola area.
4	Massive and laminate silts, syneresis cracks and minor bas bubble bursts, minor basal channels, overall minor evidence of significant basal erosional surface, lower carbonate content compared to Unit 2.	Transgression, basal channel scours	Cherty Ore - northern Central Shaft and Mindola area.
5	Dolomite increasing upward cycle with thin silt layer at top.	Shoreline prograding – development of sabkas, lacustrine environment.	No 1 Marker, very lateral continuous
6	Interbedded dolomite and sandy dolomite, erosional channel, flaser bedding, laterally discontinuous, flat algal mats to tight algal buns. Vertical and lateral highly variable.	Increase depositional energy, progressive shallowing of water.	Porous Sandstone – lateral discontinuous.
7	Change from brown-khaki sediments to grey-black silts and fine sands, minor anhydrite nodules, coarsening upward upper portion, low angle cross beds in sandstone. Higher dolomite component.	Major regression – tectonically induced?	Hangingwall Argillite and Sandstone – across NKM.
SOB Shaft COM Facies			
1	Interbedded siliceous dolomite and micaceous argillite – dolomite bands up to 1 cm thick.	Transgression	Contact Ore Shale
2	Well laminated to finely bedded, higher carbon contect at basal portion, increasing carbonate towards upper portion, lighter grey bands increased dolomite proportion.	Transgression, change is marked by Unit 7 which is seem across the NKM area.	Ore Shale

lacustrine?)-evaporitic to carbonate environment in the upper portion of the Kitwe Formation. No significant coarse-grained alluvial input.

Observations and questions: Cu-Co mineralisation relationship to basin architecture

Several observations and questions to date include:

- All barren gaps in the area have a close geographic relationship to thinning of MCF, basement highs (basin margins?) and in two places also reflect significant facies changes in the lower portion of the COM.
- Mineralisation trends observed on plans and profiles are sometimes oblique to major fold axis. What is controlling this — early basinal structures vs post main Lufilian fold structures?
- At a larger scale, the general grade distribution is away from interpreted 'basin margins' in the mineralised COM at Mindola North Shaft. Can the basin edges and orientation be accurately defined and can a clear relationship between basin margins and mineralisation in the COM be presented?
- The overall same sedimentary sequence of the Lower Roan is recognised on the West Limb. Why is there no economic Cu mineralisation hosted within the COM on the western limb of the Nkana Syncline?
- All drilling within the NKM targets the Ore Shale and rarely drills deeper into the lower portion of the MCF. Work by Selley and Bull (2001) and observations from the Basal Quartzite Orebody at SOB Shaft demonstrate the lower sequence of the MCF does host Cu orebodies within the Chambishi Basin. Could footwall orebodies exist at Mindola and on the West Limb? If no mineralisation can be identified, what is the reason for the lack of mineralisation?

Follow-up sedimentology and basin architecture work

To date I have been able to make some critical observations regarding the depositional environment of the Lower Roan and relationship to a basinal setting. Further work is required to:

- Obtain, if possible, more archived drill information for the West Limb area. Because of the very good existing geological maps and the clear changes in facies distribution within the Mindola Clastic Formation it is envisaged this area may provide further information to help define 3D architecture of the footwall basins.
- Complete the structural and basin analysis of Nkana Synclinorium Project area, allowing for possible linkage between basin forming and basin inversion structures.
- Ascertain, if possible, a 3D geometry and the spacing of main structures controlling the footwall sequence at NKM.
- Collect palaeocurrent data to assist in understanding subtle changes in the Kitwe Formation facies.

- Does a systematic relationship exist between the mineralisation distribution in the COM (Ore Shale) and structures controlling the deposition of the footwall sequence?
- Can facies variations in the hangingwall sequence be identified between Mindola and SOB Shaft, considering significant lateral facies variations have been observed in the lower portion of the COM? This work will very much depend on availability of old drill core.

References

Clemmey, H. 1974. Sedimentary geology of a late Precambrian copper deposit at Kitwe, Zambia. In Bartholome (eds), Gisements stratforms et provinces cupriferes. Society of Geologie Belgium. pp 255-265.

Clemmey, H. 1976. Aspects of stratigraphy, sedimentology and ore genesis on the Zambian Copperbelt. PhD dissertation, University of Leeds, United Kingdom. 356p.

Clemmey, H. 1978. A Proterozoic lacustrine interlude from the Zambian Copperbelt. In Matter, A. and Tucker, M.E. (eds) Modern and ancient lake sediments: proceedings of a symposium. Special Publication of the International Association of Sedimentologists, 2. pp259-278.

Selley, D. and Bull, S. 2001. Stratigraphy and basin geometry at the Chibuluma West copper-cobalt deposit, Zambia. In AMIRA Progress Report, P544 Proterozoic Sediment Hosted Copper Deposit, December 2001.

Selley, D., Scott, R. Bull, S. and Croaker, M. 2002. Chambishi Basin progress report (includes work from east of Kafue Anticline). In AMIRA P544 volume – Proterozoic Sediment Hosted Copper Deposits, November 2002.

Sweeney, M.A. 1985. Diagenetic processes in Ore Formation with special references to Zambian Copperbelt and Permian Marl Slate. PhD dissertation, University of Aston, United Kingdom, 269p.

C and O isotopes from Nkana Mindola area – Preliminary results

Mawson Croaker
Centre for Ore Deposit Research, University of Tasmania.

Mineralisation at Nkana-Mindola (NKM) is predominantly hosted within the Copperbelt Orebody Member (COM, commonly referred to as the 'Ore Shale'). Work as part of this study and by company geologists has identified a strong correlation between Cu and Co mineralisation and carbonate rich lithotypes. This preliminary study was aimed at identifying isotopic differences between mineralised carbonate rich lithotypes, alteration and veins and unmineralised carbonate rich rocks in the COM at NKM.

Twenty-five samples from various lithotypes of the COM and veins hosted within the COM were selected as an initial set (Table 1, Fig. 1). Samples include black carbonaceous shale, carbonate rich shale-siltstone beds, different generation of carbonate bearing veins and rocks from Kitwe Barren Gap and the talc-dolomite SOB Barren Zone. All powders analysed were collected by individually hand drilling specific sites in a sample.

Several significant trends can be observed from the small dataset, particularly when compared to the more regional dataset compiled from drillholes NN42, RCB 1 and RCB 2 as discussed in the preceding section.

Points of interest from the NKM sample set are:

- All samples from the mineralised COM plot in close proximity to each other (Fig. 2a). This suggests geographic position and facies variations have little influence on the isotopic signature of the mineralised samples. Several generations of vein sets were analysed, all with similar compositions to mineralised COM samples.
- Depleted $\delta^{13}C$ characterise all mineralised samples including host rocks and vein sets (Fig. 2a).
- Samples from the 'barren zones' plot as distinctly separate group with heavier $\delta^{13}C$ and $\delta^{18}O$ values, however differences between the geographically separate barren gaps are noted. No further work has been undertaken to date to address this result. Possible explanations for the difference include metamorphic mineralogy and original sedimentary facies. These samples plot close to the 'sedimentary carbonate' field (Fig. 1), similar to samples from higher stratigraphic levels in RCB 1A and RCB 2 (Large and McGoldrick, this volume).
- One sample, obtained close to the mined out Basal Quartzite Orebody at SOB, has a heavier $\delta^{13}C$ value than 'Ore Shale' samples.
- A variation on the scale of individual beds within a sample is interpreted to be a factor of relative amount of carbonaceous content in particular beds and metamorphic processes.
- Samples from mineralised 'carbonate alteration' at SOB Shaft have the same $\delta^{13}C$ and $\delta^{18}O$ values as the mineralised ore shale samples. More work is required to understand the 'carbonate alteration' relationship compared to the original rock composition (Fig. 2a).
- Isotope values of mineralised Ore Shale from NKM area have a very similar $\delta^{13}C$ and $\delta^{18}O$ values to Ore Shale samples from Konkola reported by Sweeney (1987) (Fig. 2b).

To further expand upon the C and O isotopes results to date, future work will explore several avenues including:

- Detailed petrographic descriptions and mineral chemistry of carbonates from each sample and relationship to sulfide assemblage.
- Further carbon and oxygen isotopes of mineralised Ore Shale, and from the uneconomic areas such as the West Limb, with particular detail to 'alteration'.
- Total carbon analysis of a suite of samples will assist in interpreting any metamorphic reactions affecting the carbon and oxygen isotopic signature.
- Carbon and oxygen isotope trend modelling to ascertain possible fluid mixing and fluid/rock interaction.

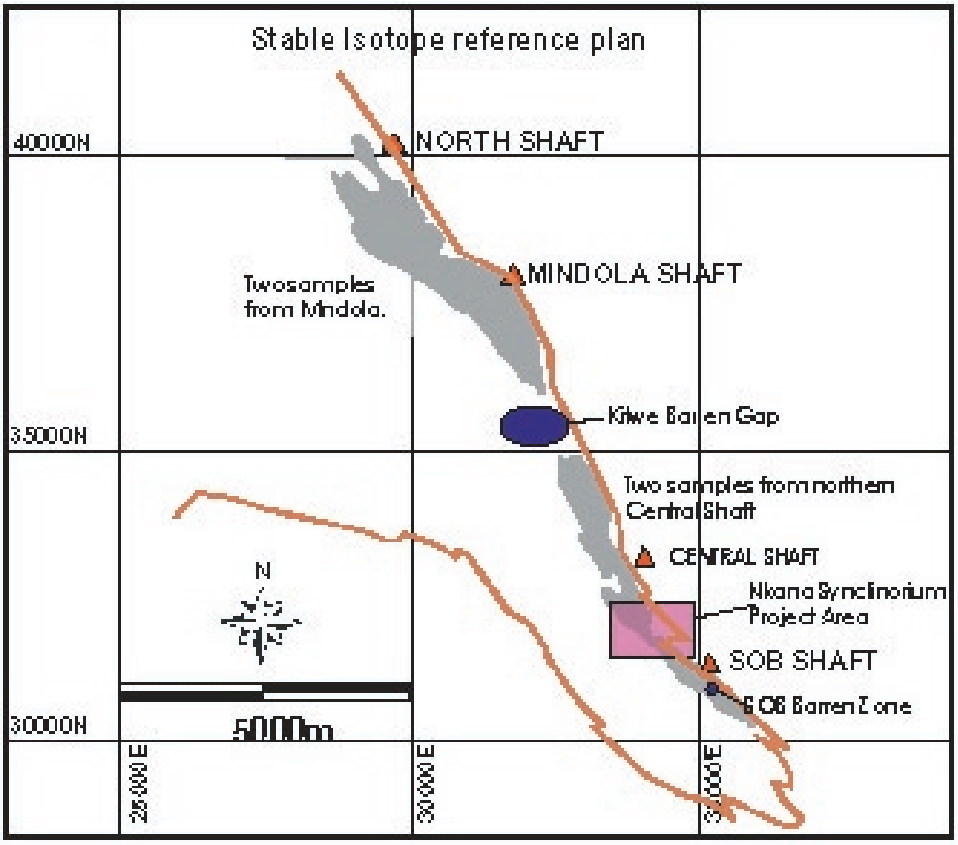

Figure 1. Carbon and oxygen isotope data for samples from the eastern limb of the Nkana-Mindola area. All samples from the mineralised Ore Shale, veins and alteration have similar values. However samples of the same stratigraphic level from the uneconomic Kitwe Barren Gap and SOB Barren Zone, have distinctly heavier carbon and oxygen isotopes, very similar to the generalised 'sedimentary carbonate' field (see Fig. 2). The samples from the barren zones are talc-dolomite schists.

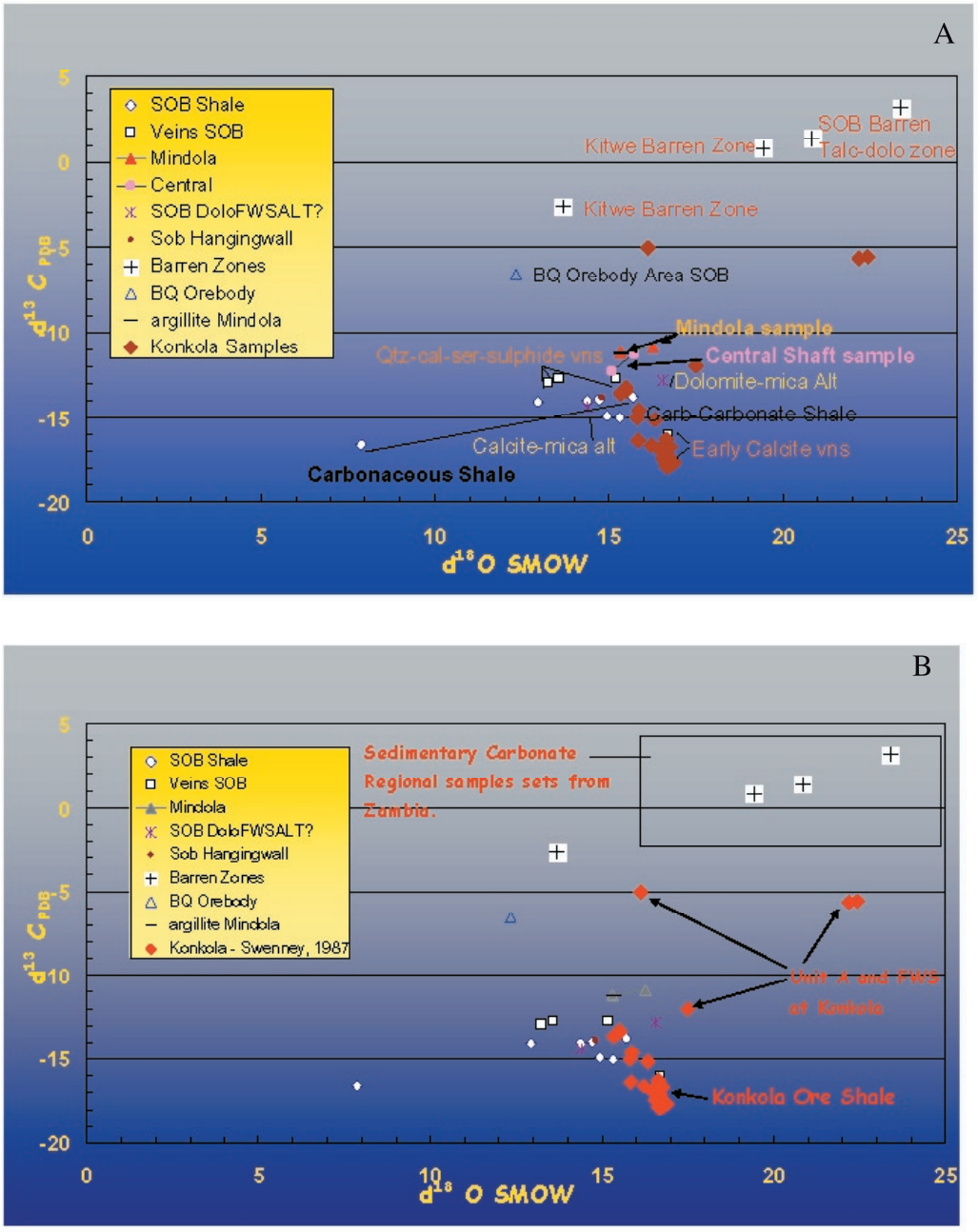

Figure 2. (A). Carbon and oxygen isotope data for all samples from the NKM area. Two distinct fields define samples from mineralised Ore Shale included veins and alteration and samples from the Kitwe Barren Gap and SOB barren zone (see Fig. 1). (B). Carbon and oxygen isotope data from NKM and the mineralised ore shale at Konkola (Sweeney, 1987). Both deposit have similar carbon and oxygen isotopic signatures for the mineralised Ore Shale and veins hosted within the Ore Shale horizon.

Table 1. Carbon and Oxygen isotopic data from the Nkana-Mindola deposit.

Sample Name	Delta 45	Delta 46	Delta 13C wrt PDB	Precision Delta 13C	Delta 18O wrt PDB	Precision Delta 18O	Delta 18O wrt SMOW	Brief sample description	Location
MCI-001-1/10134	-8.294	-2.226	**-15.018**	0.014	**-15.072**	0.029	**15.323**	Ore Shale from Nkana	SOB
MCI-001-2/10135	-8.206	-2.607	**-14.912**	0.034	**-15.447**	0.008	**14.936**	Ore Shale from Nkana – carbonate rich horizon, not vein.	SOB
MCI-002-1/10136	-6.390	-4.275	**-12.929**	0.032	**-17.099**	0.043	**13.234**	Vein	SOB
MCI-002-2/10137	-6.170	-3.944	**-12.706**	0.008	**-16.772**	0.003	**13.571**	Early folded fibre vein	SOB
MCI-003-1/10138	-10.007	-9.557	**-16.589**	0.014	**-22.305**	0.013	**7.867**	Ore Shale bed	SOB
MCI-003-2/10139	-7.101	-1.859	**-13.764**	0.012	**-14.712**	0.015	**15.694**	Carbonate rich shale bed.	SOB
MCI-004-1/10140	-4.733	-2.208	**-11.240**	0.022	**-15.062**	0.029	**15.334**	Argillite bed	SOB
MCI-004-2/10141	-4.694	-2.237	**-11.197**	0.003	**-15.090**	0.014	**15.304**	Carbonate rich bed – bedding parallel vein?	SOB
MCI-004-3/10142	-4.398	-1.288	**-10.915**	0.013	**-14.154**	0.031	**16.269**	Carbonate rich bed – bedding parallel vein?	SOB
MCI-005/10143	6.794	1.850	**0.857**	0.031	**-11.081**	0.059	**19.437**	Barren Zone	SOB
MCI-006/10144	3.331	-3.816	**-2.627**	0.012	**-16.666**	0.028	**13.680**	Barren Zone	SOB
MCI-007/10145	-0.448	-5.151	**-6.593**	0.025	**-17.976**	0.043	**12.329**	BQ Orebody from SOB	SOB
MCI-008/10146	-6.113	-2.349	**-12.700**	0.008	**-15.197**	0.030	**15.194**	Cal-qtz-ser vein	SOB
MCI-009-1/10147	-7.458	-4.560	**-14.052**	0.002	**-17.377**	0.008	**12.947**	Ore Shale	SOB
MCI-009-2/10148	-10.563	-0.880	**-17.472**	0.015	**-13.738**	0.024	**16.698**	Calcite vein	SOB
MCI-010/10149	9.107	5.750	**3.181**	0.005	**-7.236**	0.015	**23.401**	Talc carbonate schist – barren zone	Kitwe Barren Gap
MCI-011/10150	7.357	3.229	**1.408**	0.004	**-9.721**	0.009	**20.839**	Talc carbonate schist – barren zone	Kitwe Barren Gap
MCI-012-1/10151	-4.778	-1.823	**-11.301**	0.005	**-14.682**	0.016	**15.725**	Carbonate rich bed – Central shaft Ore Shale	SOB
MCI-012-2/10152	-5.773	-2.459	**-12.334**	0.007	**-15.307**	0.013	**15.081**	Carbonate rich bed – Central shaft Ore Shale	SOB
MCI-020/10153	-7.738	-3.124	**-14.398**	0.010	**-15.959**	0.015	**14.409**	Calcite mica alt.	SOB
MCI-021/10154	-6.189	-1.004	**-12.825**	0.008	**-13.869**	0.005	**16.563**	Dolomite-calcite mica alt.	SOB
MCI-022-1/10155	-7.402	-3.163	**-14.040**	0.014	**-15.998**	0.019	**14.368**	Carbonate rich bed	SOB
MCI-022-2/10156	-7.311	-2.818	**-13.955**	0.006	**-15.658**	0.020	**14.719**	Carbonaceous Shale	SOB
MCI-023/10157	-7.217	-2.736	**-13.858**	0.010	**-15.577**	0.017	**14.802**	Ore Shale – hangingwall argillte	SOB
MCI-024/10158	-9.199	-0.873	**-16.024**	0.009	**-13.734**	0.017	**16.702**	Early calcite vein	SOB

Sedimentology of Konkola North copper deposit, Zambia

Nicky Pollington and Stuart Bull
Centre for Ore Deposit Research, University of Tasmania

Summary

The Konkola North deposit in the far northern end of the Zambian Copperbelt is unaffected by penetrative deformation and appears to lack obvious hydrothermal alteration. This allowed observation of primary sedimentary textures, which provides the opportunity to study the environment of deposition. Detailed sedimentological logging of the ore horizon from the most recent drilling carried out by AVMIN has been completed and a number of units have been identified. The Kafufya, Ore Shale, Upper Ore Shale and Konkola Conglomerate which are recognized units in the area, and Interbedded Siltstone and Sandstone, Arkosic Sandstone and Conglomerate, and Mixed Zone are newly defined. The Kafufya is interpreted to be a subaerial debris flow with a proximal clastic sediment source. A rapid transgression is indicated by the onset of the subwave base Ore Shale sedimentation. The Interbedded Siltstone and Sandstone facies and the Arkosic Sandstone to Conglomerate facies together comprise an upward thickening and coarsening apron of clastic debris sourced from distal faults infilling accommodation space which was generated at the Ore Shale time. As the effect of these faults died off the Mixed Sequence was deposited as a combination of deltaic and shoreline sediments. The Upper Ore Shale could represent either another transgression event or the top of a fining upward sequence marking the end of the clastic influx. The Konkola Conglomerates are more debris flows which could indicate new growth faulting and relief.

Introduction and rationale

The Konkola North deposit in the far northern end of the Zambian Copperbelt (Figs 1, 2) was chosen as a PhD research site because it is unaffected by penetrative deformation and appears to lack obvious hydrothermal alteration. This allowed observation of primary sedimentary textures, which provides the opportunity to study the environment of deposition and the burial history of the sediments and the relationship between sedimentary textures and the copper mineralisation.

This study was carried out on the most recent diamond drilling programme completed by AVMIN in 1998. This campaign of drilling was designed to explore the deeper sulphide resource indicated from drilling between 1970 and 1980. In all cases drill holes terminated immediately below the ore shale thus there is limited information available about the footwall sediments.

Two field seasons of detailed sedimentological logging of these holes has been completed and the majority of this report is based on field observations and drafting and analysis of these logs. The second phase of this work, detailed petrographic description and analysis is now underway and will be reported later.

Figure 3 shows the generalized stratigraphy for the Konkola region highlighting the ore horizon which is the focus of this study. The ore horizon was subdivided into a number of units by AVMIN when they were exploring the deposit (Fig. 3). For the purpose of the current study the ore horizon is broken into seven units – Kafufya, Ore Shale, Upper Ore Shale and Konkola Conglomerate are recognized units in the

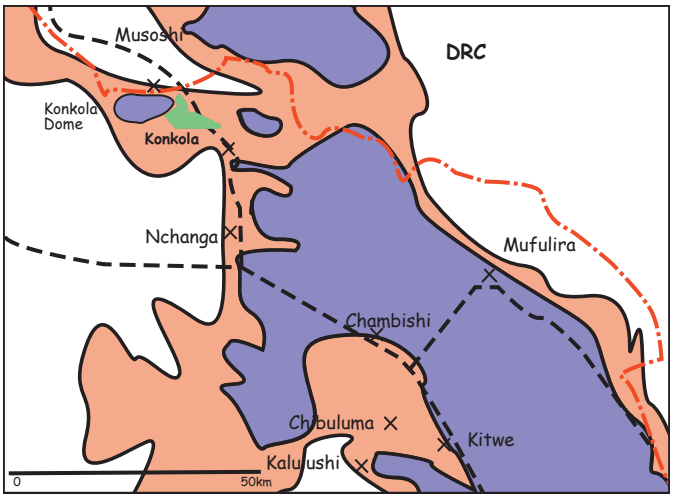

Figure 1. Generalised geology of the northern end of the Zambian Copper Belt.

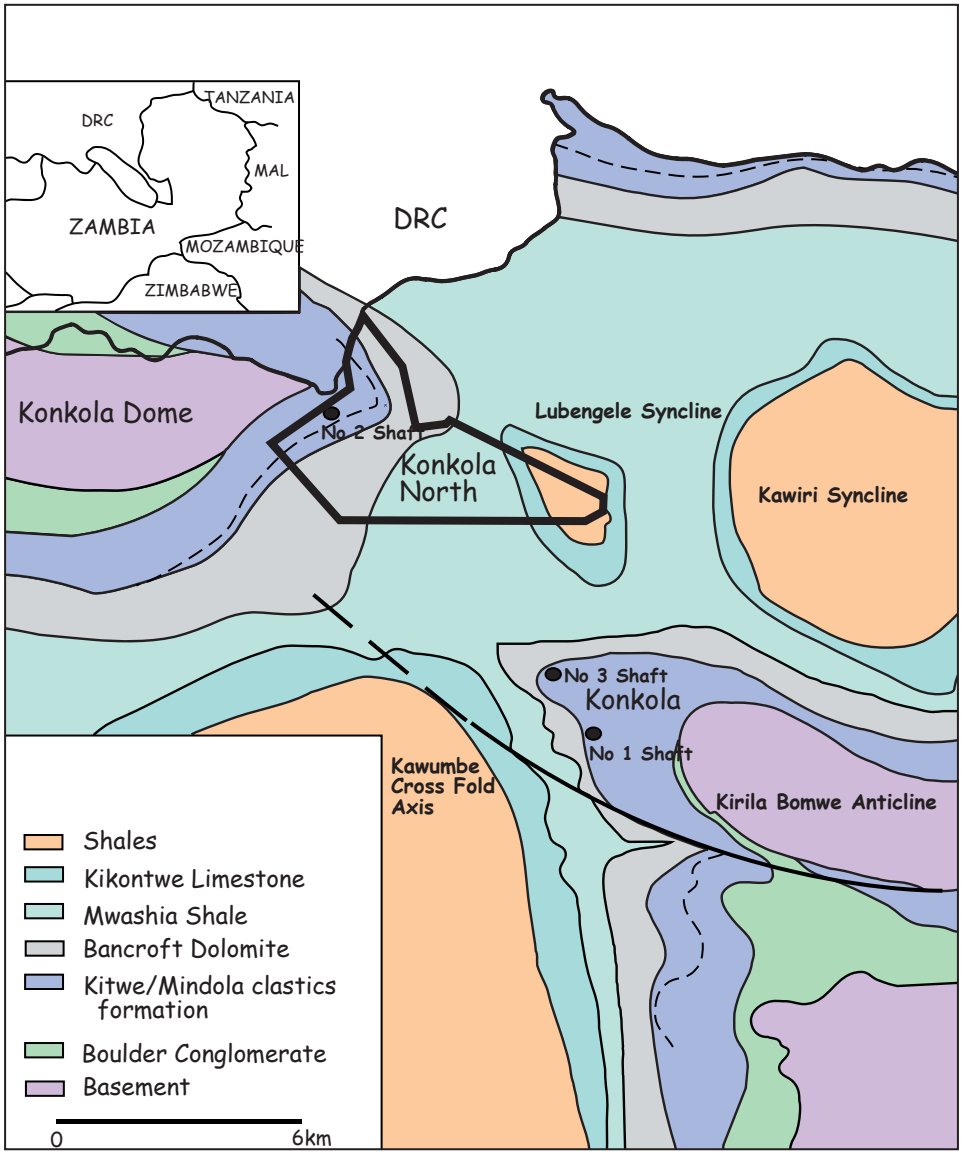

Figure 2. Geology of the Konkola area (after Sweeney and Binda, 1989)

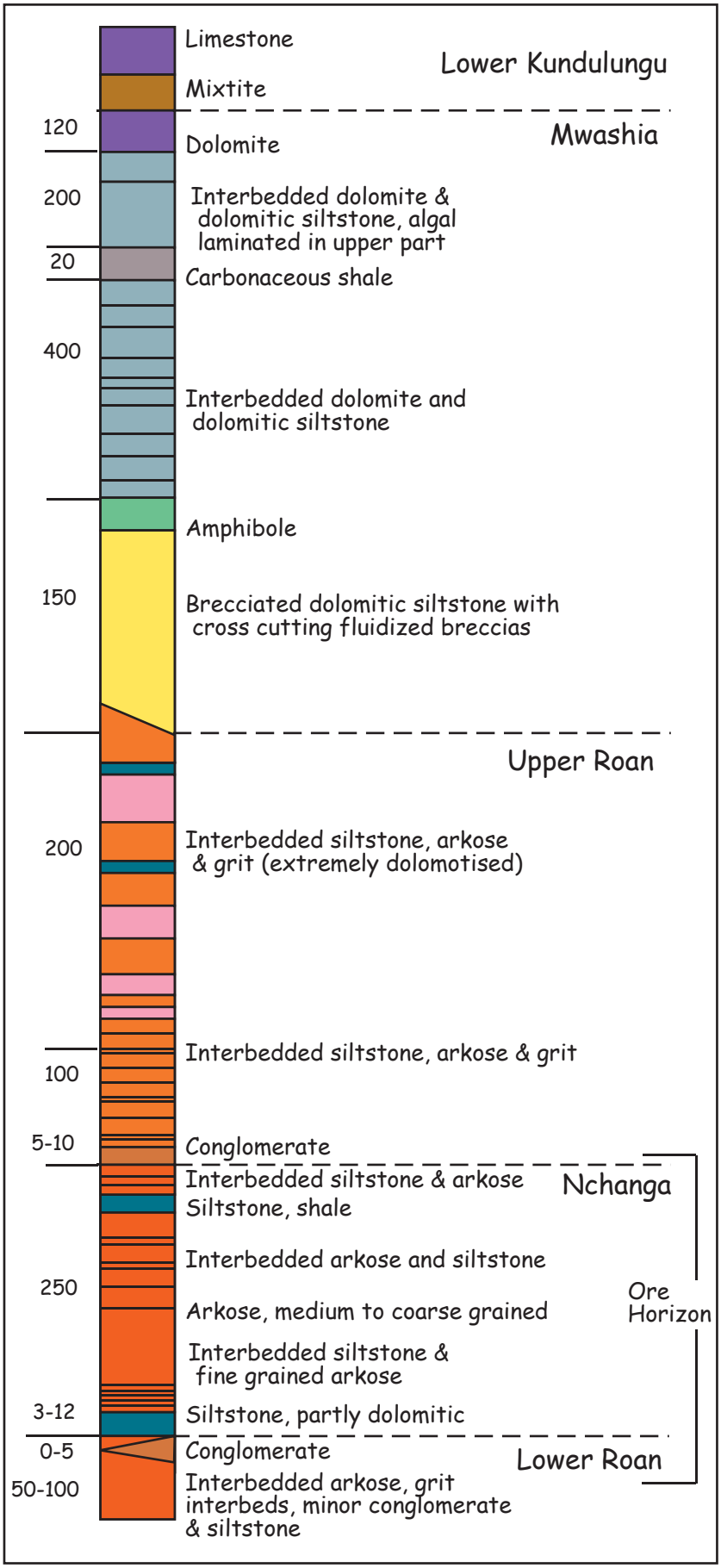

Figure 3. Generalised stratigraphy of the Konkola area – highlighting the ore horizon (after AVMIN internal report)

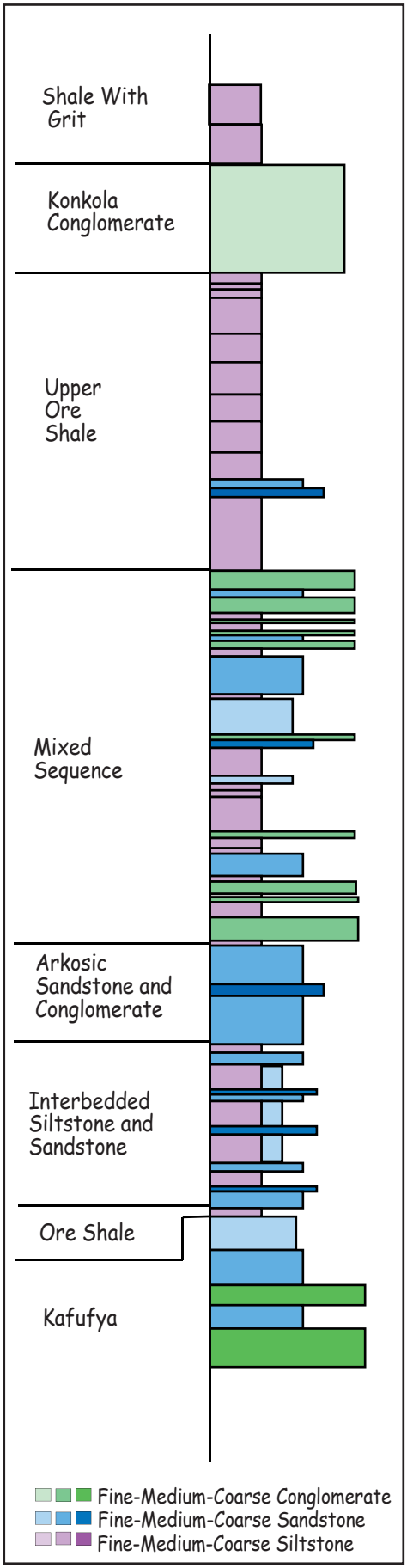

Figure 4. Typical stratigraphy of the ore horizon at Konkola North

area, and Interbedded Siltstone and Sandstone, Arkosic Sandstone and Conglomerate, and Mixed Zone are newly defined (Fig. 4). The ore horizon succession is overlain by the Shale with Grit, a regionally extensive unit of the lower roan. Each of the ore horizon units will be described and their significance to the depositional history will be discussed.

Stratigraphy

Kafufya

The Kafufya unit is the immediate footwall to the mineralization and consists of immature polymict conglomerates through to sandstones and rare interbeds of finer argillaceous material (Figs 6, 7). Average thickness was not determined from this study as the majority of the drilling terminates 10–30 m into this unit. However previous work on older drill holes indicates it has a thickness of 50–100 m (AVMIN internal report, 1999) and this is underlain by 1000-1500m of upward fining arkosic conglomerates to sandstones.

The Kafufya is more uniform and finer grained in the south of the study area, where it is generally a grey to pink arkose (Plate 1a) ranging in grain size from fine to coarse sand with rare oversize clasts up to 2 cm (Fig. 7). In the north east it is coarser grained and commonly conglomeratic consisting of subangular to rounded, matrix supported clasts ranging from common quartz and feldspar through to lesser granite and siltstone, with a maximum grainsize of 30 cm (Plate 1b).

The Kafufya is the major present day aquifer for the Konkola area. As a result the unit is very leached and oxidized, with abundant dissolution casts after possible carbonate or evaporates and iron oxide coatings of detrital grains common throughout.

The poor sorting, lack of stratification and polymict nature of the Kafufya in the north east suggests that it represents a subaerial debris flow. The presence of sub rounded clasts indicates that these have undergone some abrasion in a subaqueous environment prior to deposition in a debris flow. The variation within this facies to the more sorted, finer grained and more monomict deposits in the south could indicate greater

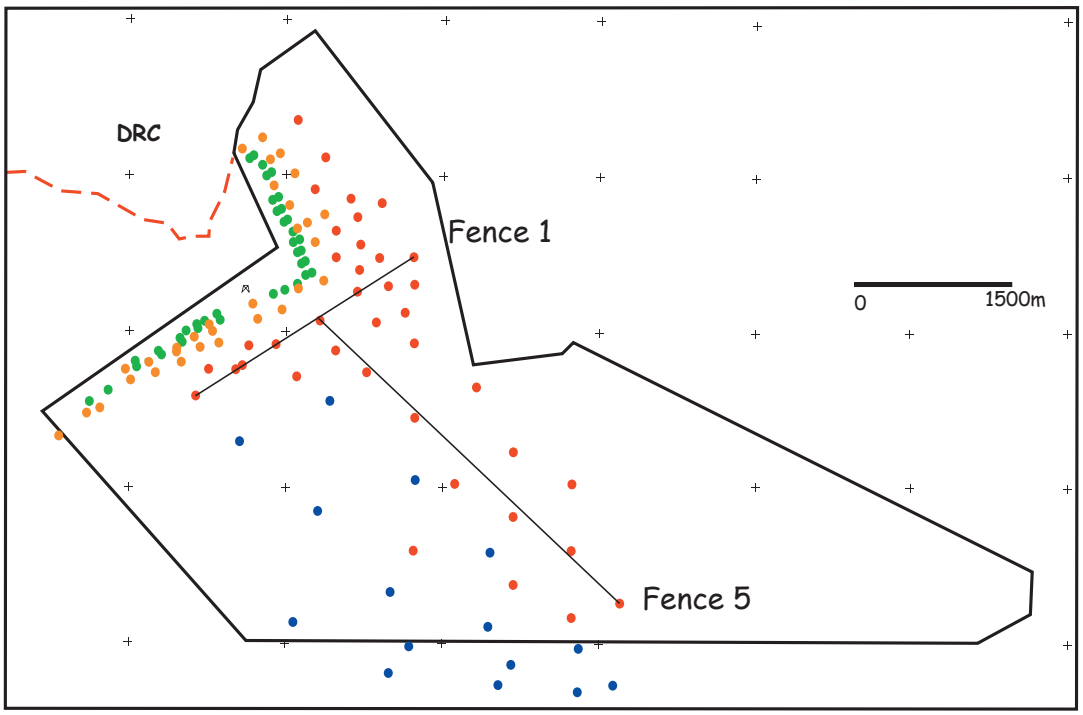

Figure 5. Konkola North tenement with traces of fences shown in Figures 6 and 7. Red, blue and green dots indicate drill holes.

abrasion and rounding during further transportation of this material to a position more distal to the source of the sediments.

"Ore Shale"

The Ore Shale is a fine dark grey siltstone (Plate 1c) which abruptly overlies the Kafufya (Figs 6, 7). It ranges from 3–12 m in thickness and includes a number of discrete beds ranging in thickness from 1–2 cm to 5–8 cm. These beds have sharp bases and are normally graded from fine sandy bases up to very fine silt and rarely mud tops.

Thin section analysis indicates potassium feldspar and quartz are the most common clastic components, with the remainder being microcline and minor subordinate minerals. More than half of the grains are less than 75 microns.

Mineralisation is variable throughout the Ore Shale in the Konkola deposit, and can include chalcopyrite, pyrite, bornite, covellite and chalcocite. These occur as fine disseminations in pore spaces and therefore are the same grainsize as the host. Mineralisation is typically confined, with very sharp boundaries, to the Ore Shale. However copper does occur locally in the immediate footwall and hanging wall, generally as supergene remobilized malachite or chalcocite.

Most of the Ore Shale exhibits some degree of late supergene effects, with iron oxide staining around fractures common and malachite and chalcocite present at the top and/or bottom contact of the Ore Shale. Rare interbeds of fine sandstones exhibit stronger oxidation features.

The fine-grained, reduced, normally graded siltstones with a lack of tractional characteristics are indicative of a subwavebase environment. These features are consistent with the Ore Shale being deposited as a series of turbidity currents with intervening fine-grained suspension deposition.

This sudden change from coarse-grained subaerial to fine-grained sub wave base sediments indicates a rapid transgression at the time of deposition of the Ore Shale. The sudden shutoff of coarse clastic debris at this time indicates the transgression resulted from a dramatic change in basin configuration.

Interbedded Siltstone and Sandstone Facies

The interbedded siltstone and sandstone facies which gradationally overlies the Ore Shale consists of fine to medium-grained dark grey siltstone interbedded and intermixed (Plate 1d) with medium-grained salmon pink sandstones. Generally the proportion of sandstone to siltstone increases up stratigraphy. The unit averages 12 m thick but can range from 5–30 m (Figs 6, 7).

The most common feature of this unit is an abundance of ball and pillow structures at sandstone bed bases (Plate 1e). Also abundant are load and flame structures. The siltstone beds of this unit are generally massive and structureless, however where undisturbed some do exhibit normal grading. The sandstones are massive and no heavy mineral bands or stratification are evident.

The abundance of load structures and the intermixed nature of the sandstones and siltstones suggests that a large volume of sands were deposited relatively quickly on water-saturated silts, leading to mixing of the two before lithification. The massive nature of the sandstones suggest deposition as gravity flows that represent the resumption of coarse sediment supply to the starved subwave base environment established at Ore Shale time.

Arkosic Sandstone – Conglomerate Facies

The arkose facies consists of medium to coarse-grained sandstone and more rarely conglomerate in the east (Figs 6, 7). Grains/clasts are almost exclusively quartz and feldspar with minor microcline. This facies ranges from 3 to 200 m thick and is generally massive and structureless.

In detail, this facies consists of a number of beds which vary in thickness from 1 to 20 m, and have a number of distinctive characteristics. The lower beds tend to be massive medium-grained sandstone with no heavy mineral bands and common siltstone rafts up to 10 cm (Plate 1f). The central part of the facies has more abundant heavy mineral bands and patches which are commonly obscured by feldspar alteration. The upper beds in this facies exhibit some clear cross stratification.

The thickly-bedded massive character of this facies and the range of sedimentary structures from dispersed intraclasts to tractional bedforms are characteristic of aggradation from one, or more likely a series of continuously fed gravity flows (Kneller and Branney, 1995). These require an abundant source of clastic sediment and forms in response to sustained, near steady current flow, which is very common in delta environments (Kneller and Branney, 1995). Sustained events such as floods and extended storms may also provide a steady enough flow if maintained for a number of hours (Smith and Lowe, 1991).

In combination with the underlying Interbedded Siltstone and Sandstone facies, these deposits represent progressively increasing influx of course sediment infilling the accommodation space generated by the abrupt transgression that formed the Ore Shale.

Mixed facies

This facies can be from 50–250 m thick and may contain any or all of the previously described rock types, from medium-grained conglomerates to coarse-grained to medium-grained sandstone through to medium-grained to fine-grained sandstone (Plate 2a, b). In addition, beds of micritic carbonate are also present that are up to 5 cm thick in the north of the deposit and more abundant and up to 1.5 m thick in the south. Scapolite is commonly associated with these carbonate beds.

This unit can be divided into two subfacies. One is a series of upward fining sedimentary cycles starting with conglomerate or coarse sandstone bases about 80 cm thick up through med to fine sandstone, siltstone and rarely a carbonate top. These cycles are generally about 5–6 m thick and 5–10 cm cross stratification is common within the coarser gravel beds (Plate 2c; Figs 6, 7). The other subfacies is composed of the same sediments where there is no regularity in the grainsize distribution. There are also a number of massive sandstone beds ranging from 20–80 cm thick with small rafts of siltstone at the base (Fig. 7). Massive siltstones range from 2 cm to 1.5 m. Open framework grit beds are also common generally ranging from 2 to 10 cm thick. The grit clasts are very well rounded and there is little or no matrix. Clastic dykes and liquefaction textures are abundant throughout this facies.

The cyclic parts of this facies may represent infilling of some kind of channel, possibly within a braided fluvial or deltaic system, which can produce upward fining sequences which range from 2 to10 m (Bhattacharya and Walker, 1992). The other subfacies could represent overbank deposits of the material being transported in the channels.

The open framework grit beds are indicative of high energy environment where the continued fluid flow or current action has winnowed out the original sandy matrix and left only the well rounded grit clasts. In the context of a deltaic setting they may represent strandline facies.

The thick massive sandstone beds with silt rafts at the base indicate that irregular mass flows inundated the area, possibly in response to flood events. These would have contributed to the development of the abundant liquefaction textures

Upper Ore Shale

The upper ore shale is not always present but can be up to 50 m thick. It is a dark, sometimes laminated siltstone and commonly contains sulphides. Pyrite is the most abundant but chalcopyrite is present in a number of places, although copper grades rarely exceed 1%.

In some areas the top and bottom contact of this facies is characterized by soft sediment folding. Rare medium-grained massive sandstone bands are also present but are generally only 20–30 cm.

Dolomite is also common in this facies as massive interbeds which range from 2 cm to 3 m thick, and as nodules within the fine siltstone (Plate 2d). Commonly the units which are finely interbedded (2–3 cm beds) exhibit abundant soft sediment deformation.

The upper ore shale facies indicates another period of low energy, subwave base fine-grained siltstone and dolomite deposition with very low clastic input.

Konkola Conglomerate

The Konkola conglomerate is a local marker bed which ranges from 1 to 25 m thick and is only found in this area (AVMIN internal report, 1999). It is a medium-grained pebble conglomerate (Plate 2e) comprising framework supported clasts of predominantly quartz

W

E

Konkola Conglomerate

Upper Ore Shale

Mixed Sequence

Arkosic Sandstone and Conglomerate

Interbedded Siltstone and Sandstone

Ore Shale

Kafufya

100m

Ore Shale
Carbonate
Siltstone
Sandstone
Conglomerate
Interbedded Siltstone and Sandstone
Cross Stratification
Silt Clast
Sampled
Thin Section prepared

Figure 6. Fence 1 – west to east across the Konkola North tenement. Horizontal scale bar shown. Vertical not to scale, distance from first to last drillhole is approximately 2km.

N

S

Konkola Conglomerate

Upper Ore Shale

Mixed Sequence

Arkosic Sandstone and Conglomerate

Interbedded Siltstone and Sandstone

Ore Shale

Kafufya

100m

Ore Shale
Carbonate
Siltstone
Sandstone
Conglomerate
Interbedded Siltstone and Sandstone
Cross Stratification
Silt Clast
Sampled
Thin Section prepared

Figure 7. Fence 5 – north west to south east across the Konkola North tenement. Horizontal scale bar shown. Vertical not to scale, distance from first to last drillhole is approximately 4km.

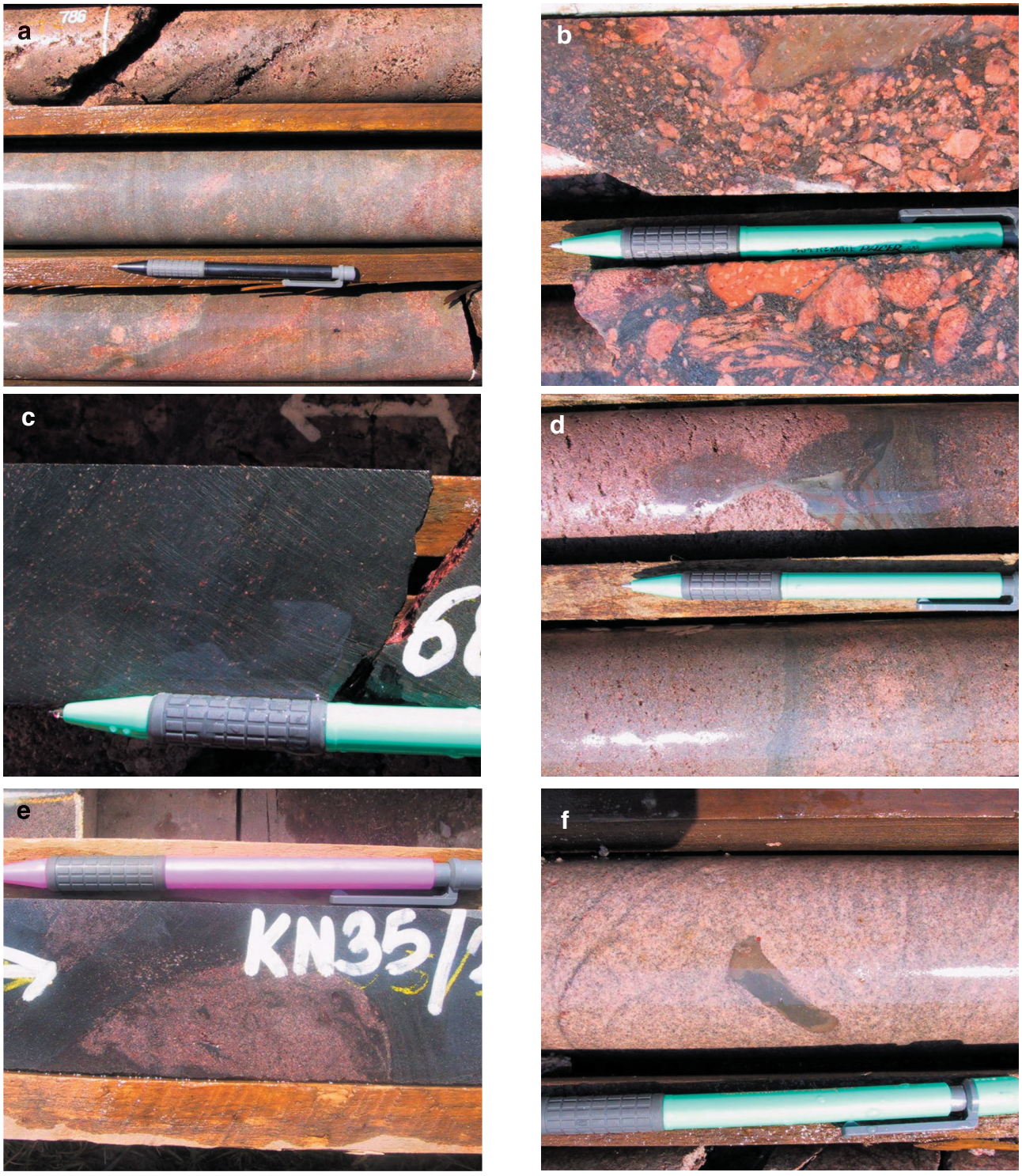

Plate 1
(a) Kafufya: Grey – Pink medium-grained arkose from the south of the deposit, dissolution casts after possible carbonate or evaporates in top piece of core.
(b) Kafufya: Polymict conglomerate with subangular clasts from the north east.
(c) Ore Shale: Fine-grained dark grey siltstone.
(d) Interbedded Siltstone and Sandstone: Pale pink sandstone and medium grey siltstone.
(e) Interbedded Siltstone and Sandstone: Ball of pink sandstone within the grey siltstone – ball and pillow structures.
(f) Arkosic Sandstone – Conglomerate Facies: Raft of altered silt within medium-grained pink arkosic sandstone.

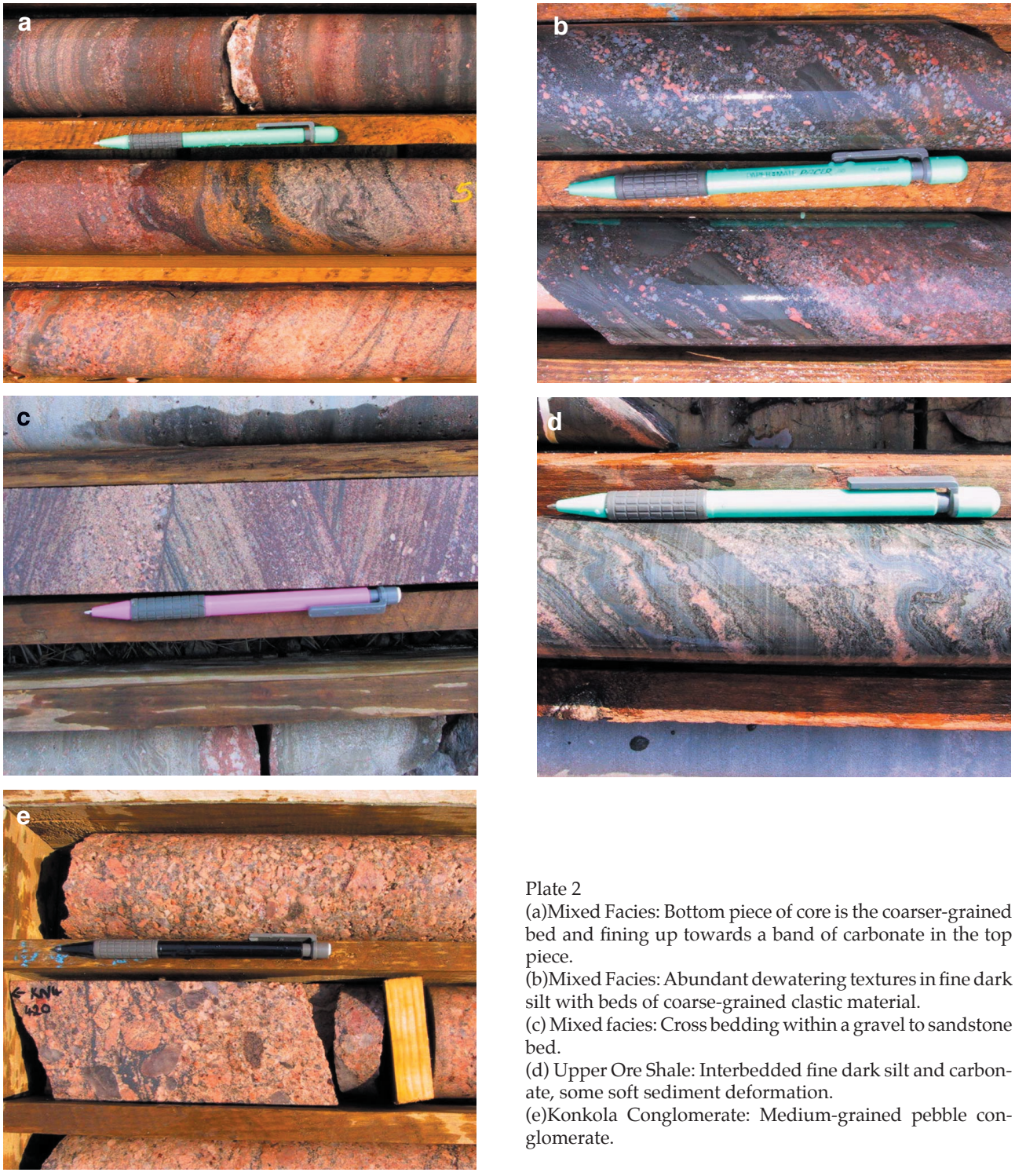

Plate 2
(a)Mixed Facies: Bottom piece of core is the coarser-grained bed and fining up towards a band of carbonate in the top piece.
(b)Mixed Facies: Abundant dewatering textures in fine dark silt with beds of coarse-grained clastic material.
(c) Mixed facies: Cross bedding within a gravel to sandstone bed.
(d) Upper Ore Shale: Interbedded fine dark silt and carbonate, some soft sediment deformation.
(e)Konkola Conglomerate: Medium-grained pebble conglomerate.

and feldspar in a medium-grained sandy matrix.

In the ore horizon the Konkola conglomerate represents the last coarse immature clastic sedimentation and thus heralds the cessation of the faulting which was providing the source for these deposits.

Summary and Conclusions

In summary, the Kafufya conglomerates and sandstones are interpreted to be a subaerial debris flow/braidplain with a proximal clastic sediment source. The onset of the subwave base Ore Shale sedimentation indicates a rapid transgression and isolation from the coarse clastic source. This suggests a major structural rejigging to control via more distal faults (D. Selley, this volume).

The Interbedded Siltstone and Sandstone facies and the Arkosic Sandstone to Conglomerate facies together comprise an upward thickening and coarsening apron of clastic debris infilling accommodation space which was generated at the Ore Shale time. This material was sourced from distal growth faults resulting in more texturally mature sediments.

The Mixed Sequence is a combination of deltaic and shoreline deposits developed as the influence of the faults die off.

The Upper Ore Shale could represent either another subsidence/transgression event like the main lower Ore Shale or the top of a fining upward sequence marking the end of the clastic influx that marks the three underlying facies as the relief from the growth faults is eroded away and therefore is the top of a fining upward sequence.

The Konkola Conglomerates are more debris flows which could indicate new growth faulting and relief.

References

Bhattacharya J. and Walker R., 1992, Deltas in Walker G. and James N., Facies Models: Response to Sea Level Change, Geological Association of Canada, 157-177.

Einsele G., 2000, Sedimentary Basins: Evolution, Facies and Sediment Budget, Springer, New York, 779pp.

Fleischer V.D., Garlick W.G. and Haldane R., 1976, Geology of the Zambian Copperbelt – Konkola and Musoshi, in Wolf K.H. ed., Handbook of Strata-bound and Stratiform Deposits: II. Regional Studies and Specific Deposits; v6, Cu, Zn, Pb and Ag Deposits, p 244-249.

Guart C., 1998, Lateral and vertical variation of lithology and mineralisation of the "Ore Shale"(OS1) in the Konkola North area, Zambian Copperbelt and constraints on the controlling factors, AVMIN internal report.

Kneller B. and Branney M., 1995, Sustained high-Density turbidity currents and the deposition of thick massive sands, Sedimentology, 42, 607-616.

Smith G. and Lowe D., 1991, Lahars: Volcano-hydrologic events and deposition in the debris flow-hyperconcentrated flow continuum. In: Sedimentation in Volcanic Settings (Ed R. Fisher and G. Smith) Special Publication from the Society of Economic Paleontologists and Mineralogists, 45, 59 – 70.

Stratigraphy, structure and copper mineralisation, Ndola West, Zambia

Robert Scott
Centre for Ore Deposit Research, University of Tasmania

Summary

1. Detailed structural and sedimentological logging of 10 diamond drill holes from Anglo-American's Ndola West prospect (Zambian Copperbelt) was conducted to characterise and determine the origin of sandstone-hosted copper mineralisation, and to facilitate correlation with the Katangan succession west of the Kafue anticline. At Ndola West, Katangan series rocks intersected by the Anglo drill holes are interpreted lie dominantly or entirely within the Lower Roan. The succession is divided into (i) Footwall, (ii) Ore and (iii) Hanging wall formations. The "Ore formation" represents an abrupt transgression-regression cycle that heralded a significant change in the character of Lower Roan sedimentation. Whole rock geochemical data (partial digestion) provided by Anglo American supports the interpretation that the Ore formation marks a transition from the deposition of relatively clean to argillaceous clastic sediments. There is also an apparent systematic change in mica composition from Footwall to Hanging wall. An apparent increase in MgO/Al_2O_3 and decrease in K_2O/Al_2O_3 ratio of mica may indicate the Hanging wall sediments were originally more dolomitic. Excellent correlation of units between drill holes along the (north)eastern limb of the Ndola West syncline demonstrates the stratabound nature of the disseminated copper mineralisation and provides a basis for interpreting drill holes on the more structurally complex (south western) limb of the syncline.

2. Copper mineralisation (disseminated fine grained bornite + chalcocite ± chalcopyrite) at Ndola west is largely restricted to an interval of intensely silicified ± carbonate-altered, diffusely stratified to massive, medium- to coarse-grained feldspathic arenite in the upper part of the "Ore formation". Minor to locally abundant coarser grained Cu-sulfides also occur in the lower few metres of the immediately overlying <5–10m thick dolomite. The sedimentary hosts to the copper are interpreted to have been deposited during the latter stages of relatively short-lived transgression–regression event (NB. the entire cycle is represented by no more than several tens of metres of stratigraphy in this area). Thinly bedded turbidites that form the immediate footwall to the copper mineralised horizon represent the deepest water sedimentation (i.e. maximum flooding surface) during deposition of the Lower Roan in the Ndola West area, and are the closest facies equivalent to the Ore Shale in the Chambishi Basin. Facies comprising the "Ore formation" at Ndola West are similar to those within the Ore Formation at Mufulira.

3. Based on current drilling, the mineralized interval attains a maximum width of ~10 m in the vicinity of KIT01DD005. The width of the *primary* mineralisation on the (north)eastern limb of the Ndola West syncline decreases along strike towards the northwest (e.g. <5 m thick in KIT01DD006) in accordance with a decrease in the thickness of the sedimentary host(s). However, poorly developed copper mineralisation in the northwestern-most of these drill holes (KIT01 DD004) is largely due to

the effects of later faulting, which oxidized and remobilised primary sulfides, and excised up to a third of the "normally mineralized" stratigraphy. Where not affected by subsequent oxidation or remobilisation the grade of arenite-hosted copper mineralisation is reasonably consistent over the width of the mineralised interval for over a kilometre along strike.

4. Two drill holes (KIT01DD001 and DD002) sited on the (south)western limb of the Ndola West syncline did not intersect the target horizon. Unforeseen structural complexities (large-scale parasitic folds, faults and shears) resulted in DD001 being essentially drilled over the top of the mineralized horizon (cut out across a large shear), while DD002 was drilled beneath it. Re-logging of these holes has substantially resolved the stratigraphy and structure of the western limb of the syncline, helping to refine predictions of the subsurface location of the target horizon in the vicinity of these drill holes. DD001 intersected a talc schist within a large shear on the eastern limb of a parasitic antiform. The schist contains small slivers of malachite-stained dolomite, similar to the dolomite capping, and in part hosting, copper mineralisation on the eastern limb of the main syncline. An overturned sequence of predom inantly argillaceous sandstones structurally below (stratigraphically above) the talc schist correlates well with the lowermost Upper Roan immediately above the mineralized horizon on the eastern limb of the syncline. Thus the talc schist (including dolomite slivers) and argillaceous sandstones are interpreted to represent the stratigraphic hanging wall to the target horizon, intersected within and below a large shear (reverse fault). The presence of minor malachite staining within the dolomite slivers, suggests that target horizon is at least locally mineralised on the western limb of the synform.

5. While the carbonate unit (<10 m thick) capping the copper mineralisation at Ndola West is interpreted to be sedimentary in origin, there is an extensive zone of carbonate alteration, best developed in the immediate footwall (i.e. the lower part of the Ore formation) and extending upward into the mineralised horizon. A genetic link between the carbonate alteration and copper mineralisation is yet to be established, however both are overprinted by the regional cleavage and may therefore be of similar age. In several drill holes bornite occurs in small quartz-feldspar fibre veins at a high angle to bedding, with prominent albite + tremolite bearing alteration haloes. The veins appear similar to quartz + albite + haematite bearing fibre veins that are locally developed in the Footwall formation, and copper sulfides are only developed in the veins where they cut the ore horizon. Like the carbonate alteration and disseminated copper sulfides, the veins are also overprinted by the regional cleavage. However the disseminated sulfides are markedly depleted in the bleached haloes surrounding the veins, indicating bornite in the veins was remobilised from the immediately adjacent wallrocks. Accord ingly formation of the veins (and associated albite + tremolite alteration) post-dates primary introduction of copper into the rocks.

6. Further SHRIMP dating by Dawson (2002, this volume) indicates a Lufilian (560–510 Ma) age for arenite-hosted copper mineralisation at Mufulira, and a similar age for mineralisation at Ndola West is inferred. Textural relations and the distribution of copper at Mufulira and Ndola West suggest it was introduced prior to significant folding and tectonic and fabric development. The absence of an obvious fracture control on the ingress of the mineralising fluids indicates grain-scale permea bility was relatively high at this stage, suggesting either that the sequence was not deeply buried at the onset of Lufilian deformation, or that reaction-enhanced permeability was important. Several lines of circumstantial evidence implicate prior hydrocarbon impregnation of the sediments as a means of extracting copper from the mineralising fluids. Migration of Cu-bearing fluids is interpreted to have been initiated and driven by compressional orogenesis during the early stages of the Lufilian Orogeny.

Introduction

Detailed structural, sedimentological and petrological examination of drill core from Anglo-American's Ndola West Prospect (Zambian Copperbelt) was conducted as part of the Centre for Ore Deposit Research/Colorado School of Mines/Collaborative Research Project (AMIRA P544) "Proterozoic Sediment-hosted Copper Deposits". The purpose of the Ndola West study was to: (1) examine the nature of the basal contact of the Katangan sedimentary sequence, (2) construct a detailed stratigraphy and chemostratigraphy for Katangan succession in this area, facilitating correlations with sequences to the west of the Kafue Anticline and (3) determine the nature, origin and geochemical signature of the copper mineralisation.

During 2000 and 2001, Anglo-American drilled a total of 13 diamond holes (including two deflections) at Ndola West (Fig. 1) to test for stratabound copper mineralisation developed near the Lower Roan – Upper Roan boundary. Initial drilling in 2000 was restricted to the (north) eastern limb of a major synform (herein termed the Ndola West synform) which dominates the structure of the area (Fig. 2). However, only KIT00DD004 and two deflections drilled from this hole successfully intersected the mineralised horizon (Fig. 3). KIT00DD004 intersected 5.0 m (true width) sandstone-hosted finely dissem inated chalcocite + bornite (±chalcopyrite). The overlying 1.53 m of dolomite and talc schist also contained minor disseminated copper yielding. Drill holes KIT00DD001, DD004 (including deflections 1 and 2) were logged and sampled as part of the P544 study in July 2001.

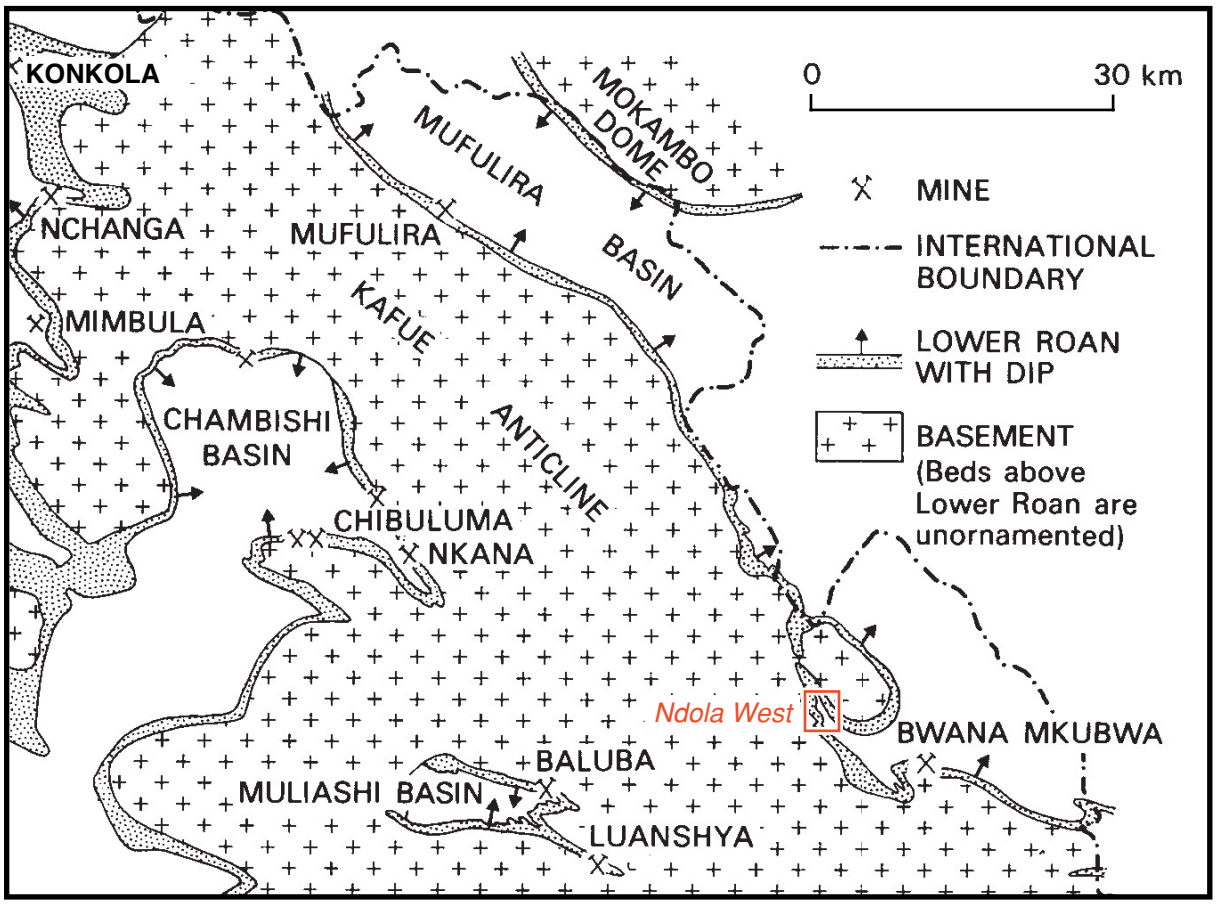

Figure 1. Location of Ndola West prospect on the northeastern limb of the Kafue Anticline (modified from Fleischer et al., 1976).

Results were integrated with down-hole geochemical data provided by Anglo-American to help delineate a chemostratigraphy for the Katangan sequence in this area (Scott, 2002b).

A further six holes (KIT01DD001 to DD006) testing for extensions of the mineralisation intersected in KIT00DD004 were drilled in 2001. Four of these holes (KIT01DD003–DD006) were drilled along strike to the northwest of the original intersection in KIT00DD004, on the eastern limb of the Ndola west syncline. The other two holes (KIT01DD001 and DD002) were designed to test for a continuation of the mineralized horizon at shallow depth on the western limb of the syncline. All six holes were re-logged by the author in July 2002.

New drilling from the eastern limb of the syncline (all holes successfully intersected the mineralised horizon) has enabled construction of a detailed stratigraphy for the Lower Roan. Excellent correlation of units between drill holes along the (north)eastern limb of the Ndola West syncline demonstrates the stratabound nature of the disseminated copper mineralisation and provides a basis for interpreting drill holes on the more structurally complex (south western) limb of the syncline.

Stratigraphy

The locations and trajectories (in plan) of the drill holes logged in this study are shown in Figure 2. Stratigraphic subdivisions and structural inter pretations of all drill holes logged by the author are presented as a series of drill sections projected to the nearest grid line section (Figs 3–9). Figure 10 illustrates larger scale structural geometry and stratigraphic relations for Line 12600 (based on KIT01DD001 and DD004 and the Anglo summary log for KIT00DD003). Figures 11 and 12 summarize stratigraphic correlations across the Lower Roan – Upper Roan boundary, on the eastern limb of the Ndola West synform. Figure 11 shows the proposed correlation of units intersected drill holes KIT00 DD004 and KIT01DD003–006, with copper distri bution superimposed. Drill holes are aligned using the base of the dolomite as an arbitrary datum. Vertical scales correspond to down-hole metres for individual drill holes. Figure 12 is similar but shows calculated true widths of the units rather than the widths of the drill intersections. The vertical scale in Figure 12 therefore indicates the true thickness of the units, with drill holes again aligned relative to the arbitrary datum (base of dolomite). Down hole depth scales for individual drill holes in Figure 12 are non-linear and have been omitted for simplicity.

This report concentrates on the stratigraphy of the upper part of the Lower Roan (e.g. pink heavy mineral stratified arkose and stratigraphically higher units). Herein this sequence is informally divided into three main units, termed the Footwall, Ore and Hanging wall formations. Where intersected by drill holes on the eastern limb of the Ndola West synform (Fig. 2) this stratigraphic sequence is remarkably consistent with only minor differences between drill holes (e.g. Figs 3, 6–12.). Detailed stratigraphic correlations between drill holes demonstrate the stratabound nature of the copper mineralisation and the generally excellent lateral continuity of units in the upper part of the Lower Roan and at least the lowermost Upper Roan (Figs 11, 12).

The upper part of the Footwall formation is dominated by a succession of generally medium- to coarse-grained pale pink arkosic sandstone and lesser conglomeratic sandstone and conglomerate (Figs 2, 9). The sequence is characterised by prominent heavy mineral stratification and cross stratification, recognised in core by concentrations of fine grained specular haematite (Fig. 13a). As no drill hole was drilled completely through this sequence, its total thickness is unknown, but estimated to be at least 80 m (e.g. Figs 3, 10). It is generally a fairly uniform sequence of medium- to coarse-grained sandstone, but contains minor intervals of pebbly sandstone and conglomerate (Fig. 13b) as well as thinly interbedded generally grey, fine-grained sandstone, siltstone and shale.

The pink arkosic sandstone of the Footwall formation is transitionally to abruptly overlain by pinky-grey to grey, generally more poorly sorted and argillaceous arkosic sandstone and conglomeratic sandstone (basal unit of the Ore formation sequence). On the NE limb of the syncline the Ore

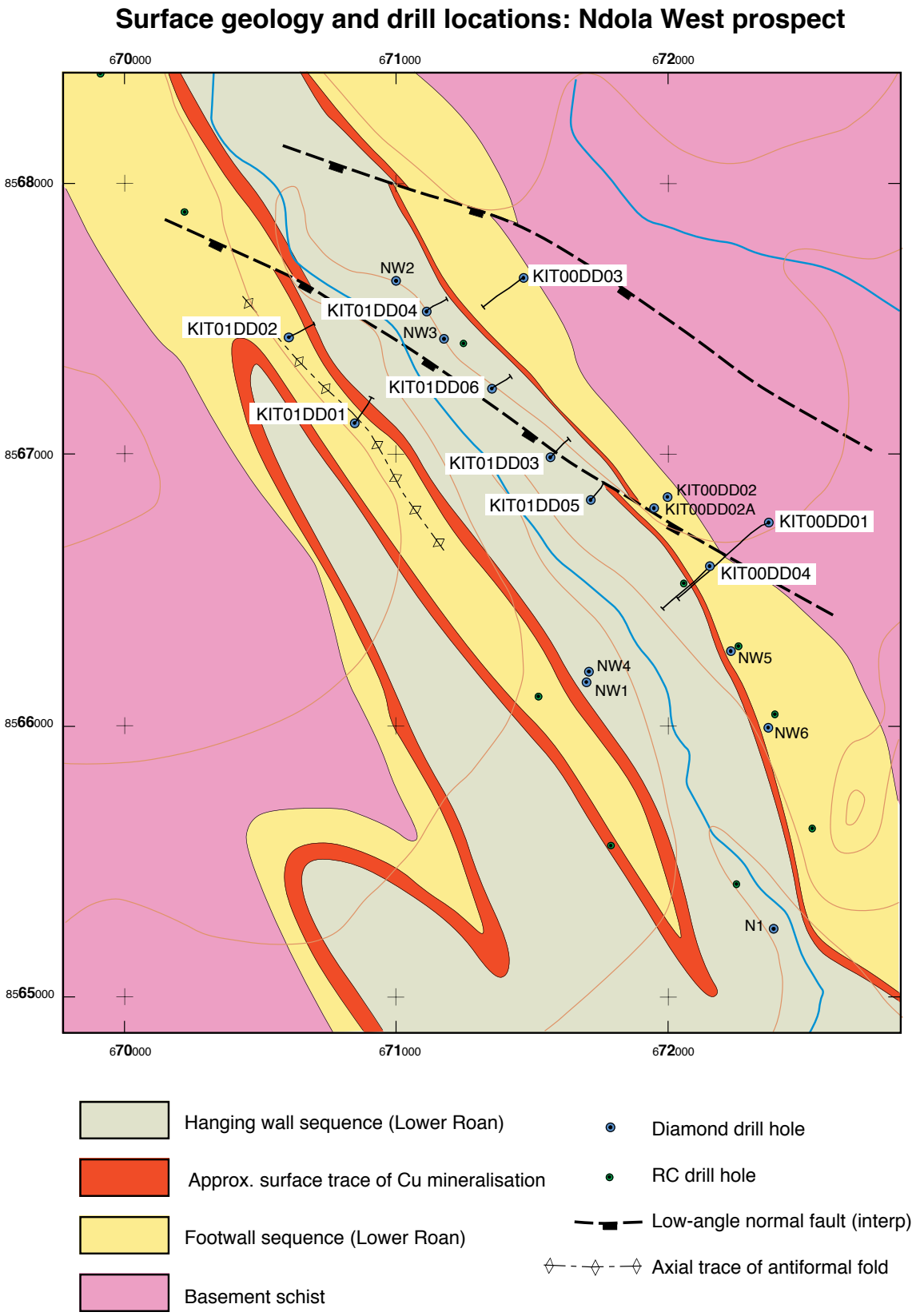

Figure 2. Surface geology and drill hole locations for the Ndola West prospect. Map provided by AngloAmerican, with minor modification by the author. Drill holes used in this study are shown in plan projection.

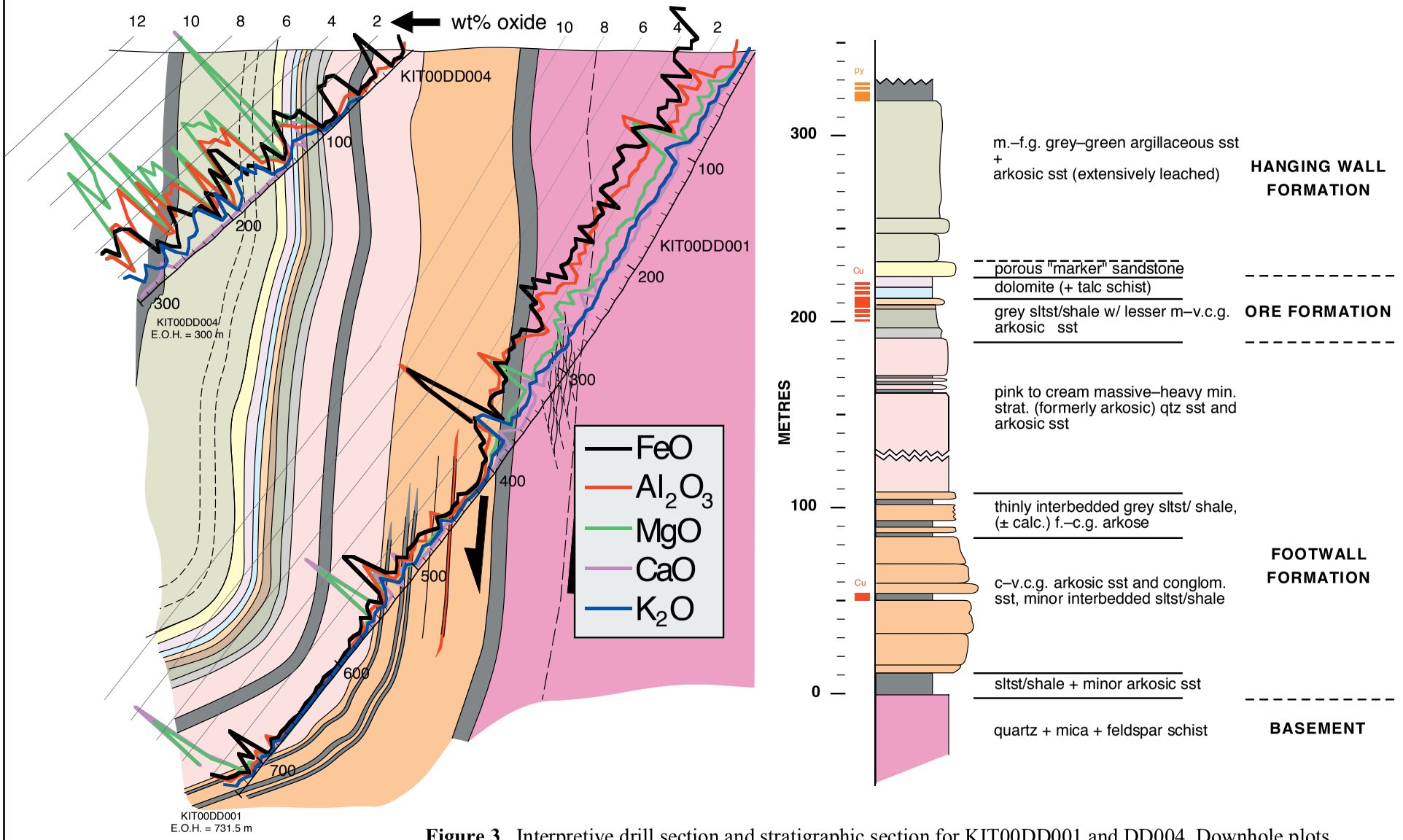

Figure 3. Interpretive drill section and stratigraphic section for KIT00DD001 and DD004. Downhole plots of major element abundances (Anglo America partial digestion geochemical data) are superimposed.

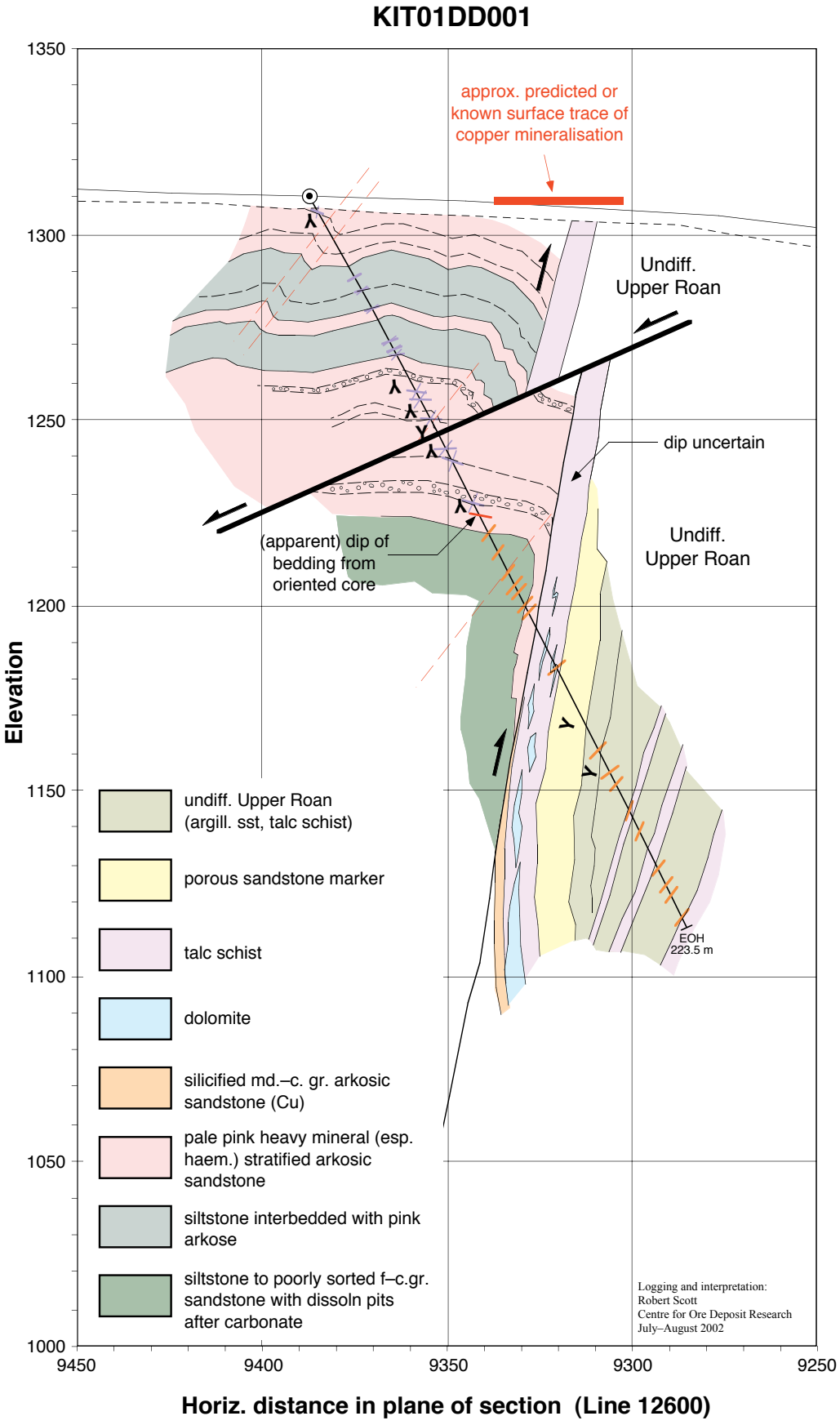

Figure 4. Interpretative section for KIT01DD001, Line 12600W (9450–9250S)

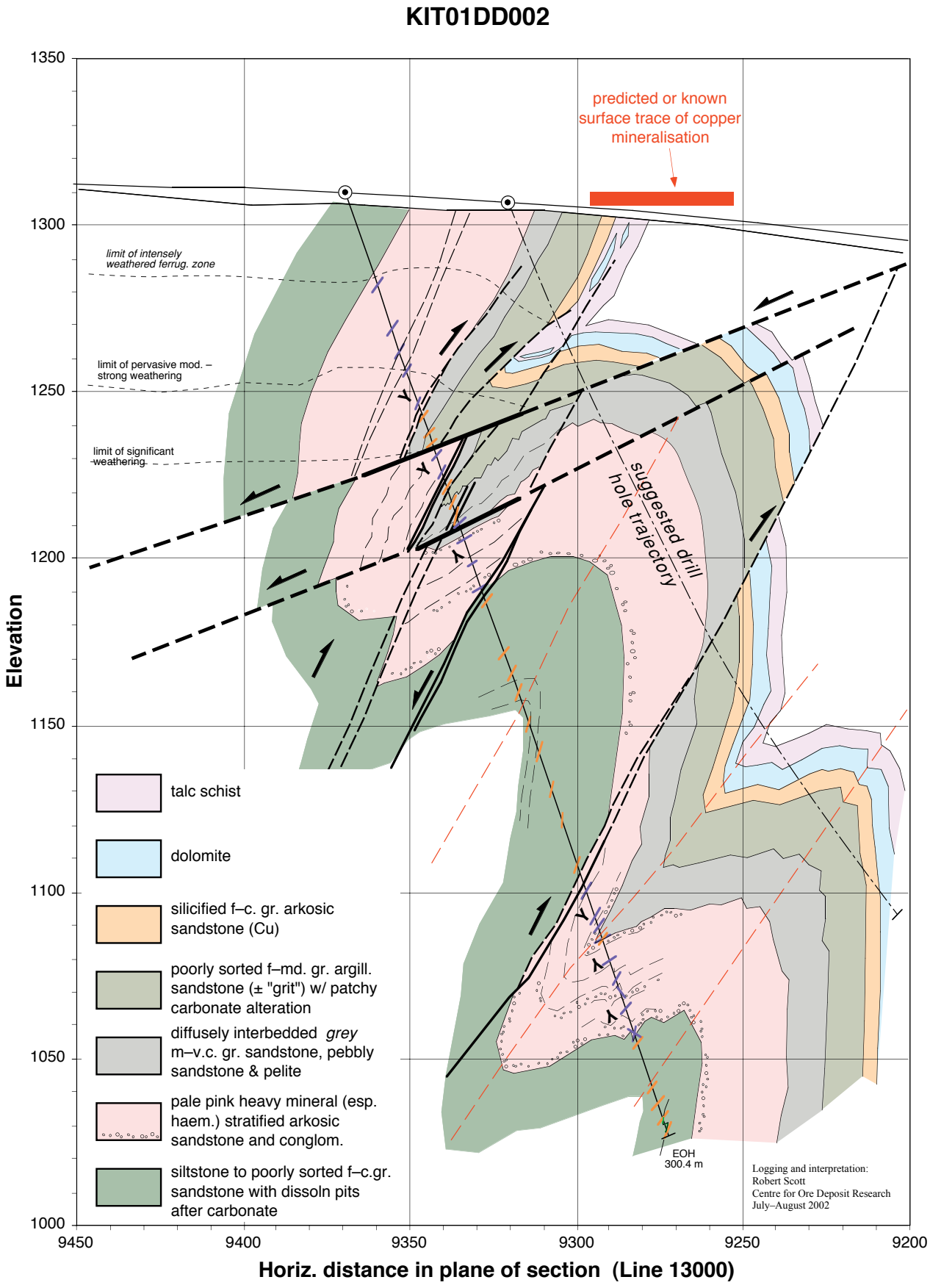

Figure 5. Interpretative section for KIT01DD002, Line 13000W (9450–9200S)

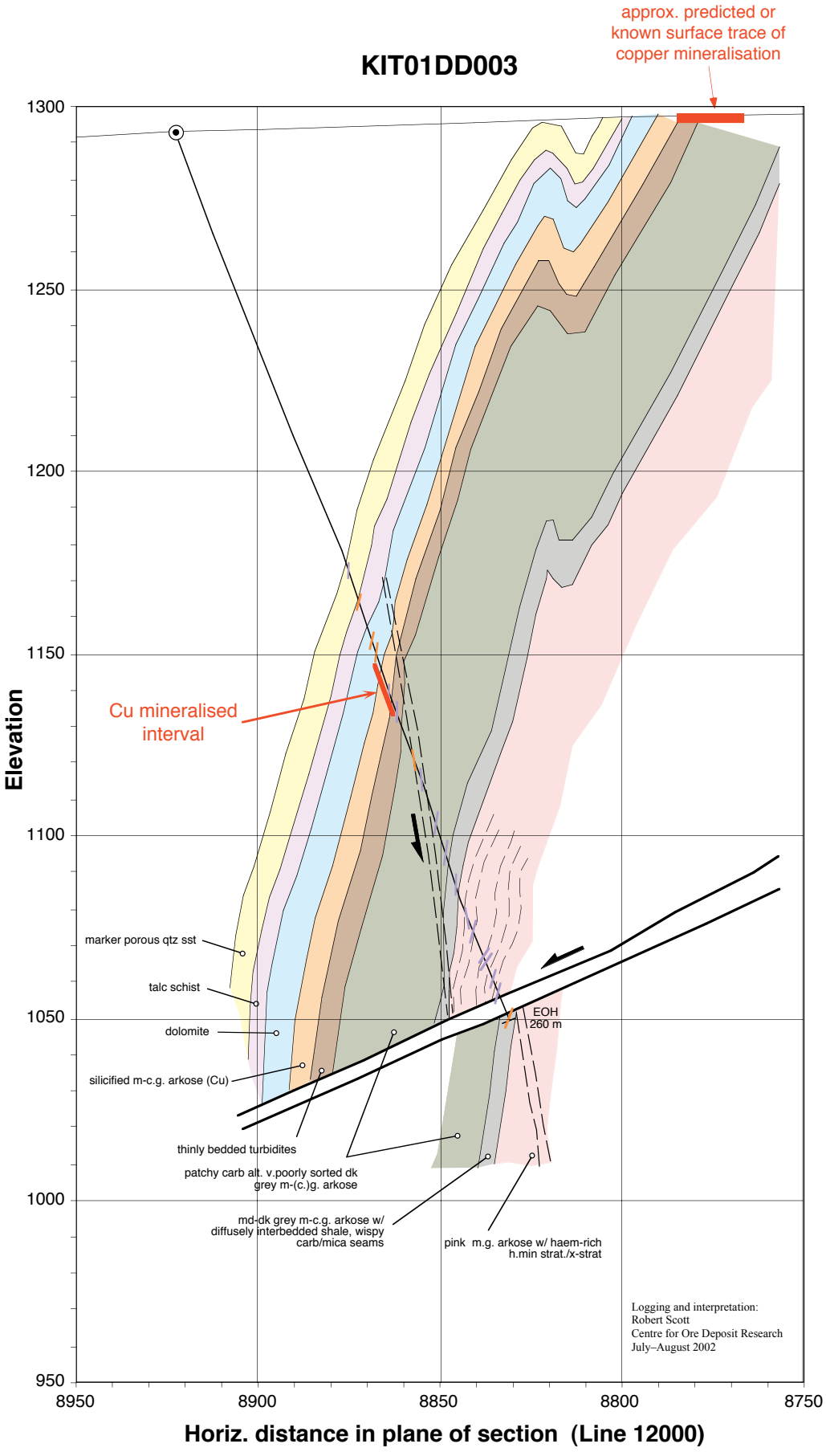

Figure 6. Interpretative section for KIT01DD003, Line 12000W (8950–8750S)

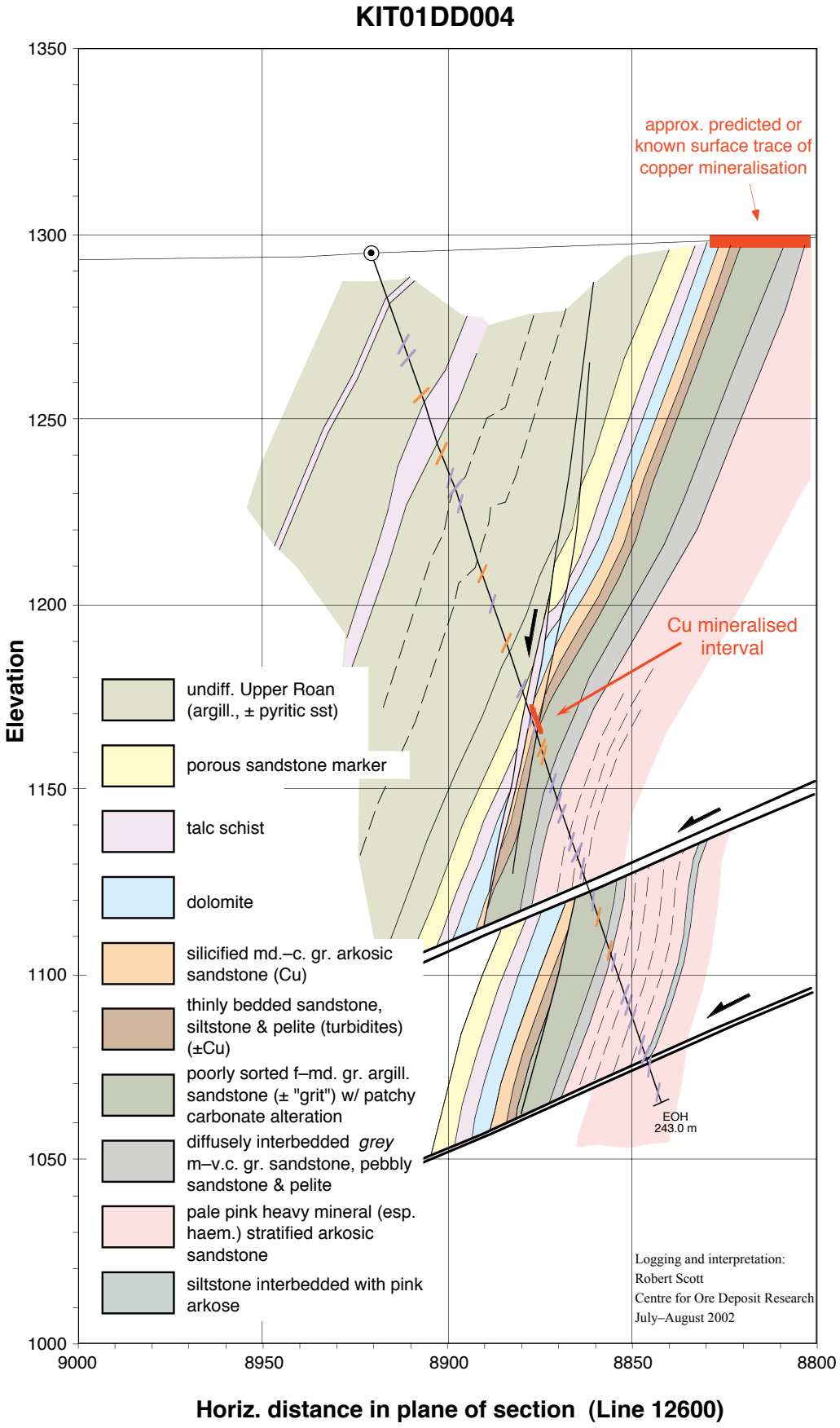

Figure 7. Interpretative section for KIT01DD004, Line 12600W (9000–8800S)

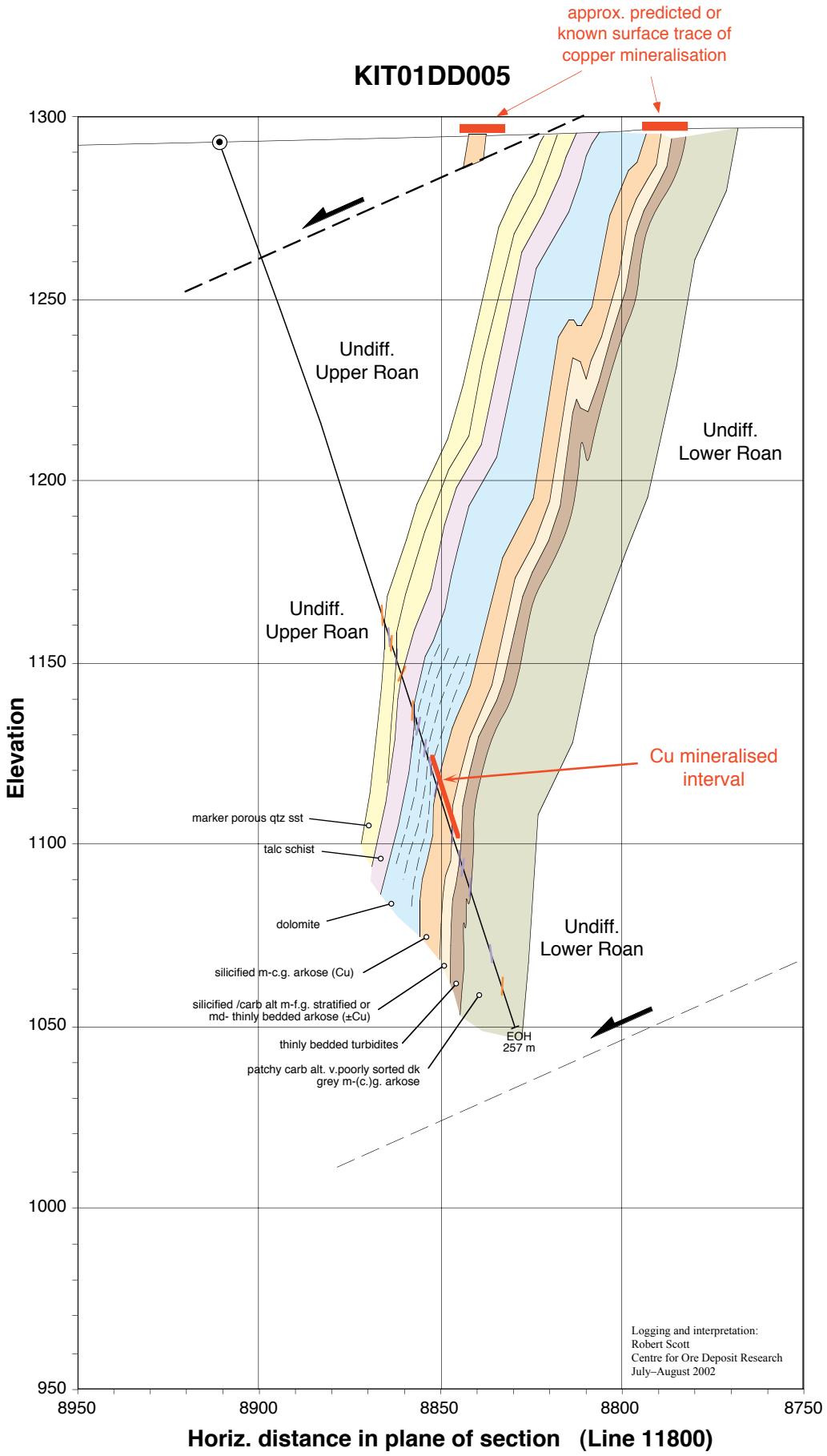

Figure 8. Interpretative section for KIT01DD005, Line 11800W (8950–8750S)

Formation is subdivided into five primary units (Figs 11, 12), although as contacts between several of the units are transitional, individual units may not have not discriminated in the logging where they were not well developed.

The basal unit of the Ore formation often contains diffusely interbedded thin shale bands, and/or thicker shale interbeds. The interval marks a transition from predominantly mica-poor, moderately- to well-sorted pink arkosic sandstones to more poorly-sorted, commonly more argillaceous, medium to dark grey sandstones (siltstones, shale) that comprise much of the overlying succession.

The basal unit of the Ore formation is overlain by medium to dark grey, relatively massive, poorly-sorted fine- to medium-grained argillaceous (biotite-rich) sandstone (and minor true siltstone and shale). This is characteristically strongly foliated with patchy white carbonate alteration (Fig. 13c), and contains minor to abundant carbonate veins with thin biotite selvedges. Locally portions of this unit are so poorly sorted as to approach a "shale with grit" texture. Coarse to very coarse quartz and lesser feldspar grains are most obvious within the narrow carbonate altered domains, where the normally dark matrix is bleached white. While this gives the appearance that carbonate alteration is concentrated in (more porous) coarser grained material, overall, coarse detritus is probably equally abundant in the adjacent non-carbonate altered material. This package is generally barren, but contains minor copper within its uppermost part in KIT01DD006 (Fig. 11).

The massive argillaceous package is overlain by a distinctive very well stratified thinly bedded fine grained turbidite package, with common beds grading from medium to dark blue grey sandstone to thin light tan coloured shale. Some of the sandstones exhibit stratabound, patchy to pervasive white dolomite alteration, such that the unit has distinctive cyclic white to blue-grey to tan colour banding (Fig. 13c, d). This unit is also generally barren, however the upper part (transitional to the overlying arkose) is mineralised in several holes (KIT00DD004, KIT01DD003 and DD004). Coarser grained sandstone layers lower in the turbidite package may also contain minor stratabound disseminated sulfides (e.g. KIT01DD003 and DD006, Fig. 11).

In some drill holes the thinly bedded turbidites are (transitionally) overlain by moderately to strongly altered massive to stratified, (?medium to thinly bedded), medium to pale grey, medium to fine grained arkosic sandstone (Fig. 13e). This unit appears to represent a gradational transition between the underlying relatively fine-grained, well stratified turbidites and the overlying poorly stratified to massive to medium- to coarse-grained arkose. Although the entire well stratified interval may be mineralised (e.g. KIT01DD004), where the unit is best developed in successions unaffected by faulting (e.g. KIT01DD005 and DD006) significant copper sulfides are restricted to the upper part of the unit (Fig. 11).

The massive to poorly stratified medium to coarse grained sub-arkosic to arkosic sandstone that overlies the moderately to well stratified succession is the main host to the disseminated copper sulfides (Fig. 11). It is usually medium to dark grey, intensely silicified ±carbonate-altered (Fig. 13d). The arkose is directly overlain by dolomite (Fig. 13f) in all holes except KIT01DD004, where the latter (and a portion of the former?) were apparently excised by later faulting. Sparse, finely disseminated and minor <0.5–5 cm wide segregations of coarser grained Cu-sulfides occur in the lower 1–3 m (true thickness) of the dolomite. The dolomite is invariably overlain by (± interleaved with) talc schist. The talc schist is interpreted to have formed as a result of shearing and metamorphism of the dolomite (and adjacent quartzite and arkose) during deformation. The dolomite ± talc schist caps the Ore formation.

In all drill holes, the talc schist is overlain by a distinctive cream-coloured coarse grained porous sandstone. The unit is massive to normally graded, and in some drill holes, consists of at least two thick beds. Compared to the pink arkose in the Lower Roan, the porous sandstone is (white-)mica-rich and lacks feldspar. However given its porous character and the presence of abundant interstitial kaolinite, the unit was probably sub-arkosic to arkosic originally, similar to the Lower Roan sandstones. Another distinctive feature of the porous sandstone is the presence of sparse

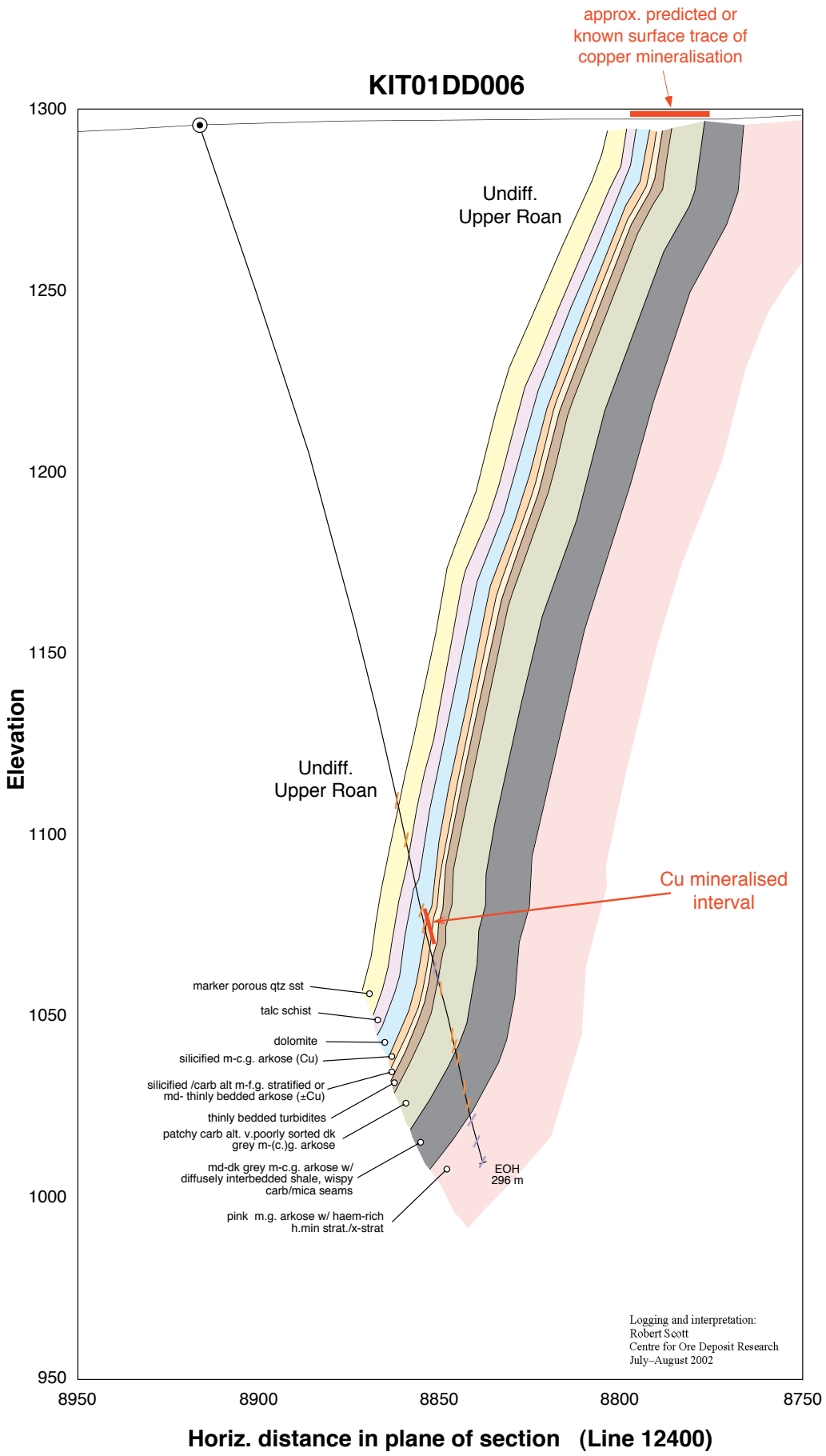

Figure 9. Interpretative section for KIT01DD006, Line 12400W (8950–8750S)

cubes to 3 mm of diagenetic(?) pyrite (now variably oxidized and in some holes may only be recognised as large rusty spots scattered through the sandstone, Fig. 13g). Abrupt variations, between drill holes, in the thickness of both the porous sandstone, above the talc schist, and the dolomite below, suggest the schist, at least partly, occupies a fault that cuts across stratigraphy at a low angle.

Detailed subdivision of the sequence above the porous sandstone marker has not been attempted at this stage, as it is generally much more weathered and poorly preserved compared to the Lower Roan. It is dominated by fine to medium grained green-grey argillaceous sandstones, often with a diffuse white to green-grey colour banding (Fig. 13h). The Upper Roan also contains a number of thin talc schist zones, absent in the Lower Roan. Whole rock geochemical data for KIT01DD004, suggests phlogopite (i.e. Mg-biotite) is the dominant mica phase throughout much of the Upper Roan in this area, suggesting that prior to (syn-deformational) metamorphism, dolomitic cement or alteration was widespread through this part of the succession (Fig. 14).

Deposition of the Ore formation is interpreted to have occurred during a relatively short-lived marine transgression–regression event (Fig. 15). The cycle commenced with the change from relatively clean, fluvial–(?)aeolian *pink* arkosic sandstone to *grey* sandstones with interbedded shale, and increased interstitial clay (now mica). The overlying poorly-stratified, poorly-sorted argillaceous sandstones (and siltstones) continue the trend towards deeper water sedimentation. The thinly bedded turbidites at the base of the well mineralised package reflect maximum flooding, and the most significant marine trans gression evident during deposition of the Lower Roan in this area. Despite the lack of significant copper mineralisation, the thin turbidite package appears the closest *facies equivalent* to the Ore Shale at Konkola within the Lower Roan in this area. Locally, however, thin sandstone beds within the turbidite succession (e.g. KIT01DD003) do host minor "Konkola Ore Shale-style" disseminated copper sulfides.

Sandstones overlying the turbidites show a trend from medium to thinly bedded to massive, probably reflecting a gradual marine regression and change to shallower water higher energy conditions. The trans-gression–regression cycle ends with deposition of the carbonate (now dolomite) capping the Ore formation and possibly the porous sandstone at the base of the Hanging wall formation. the poorly stratified argil-laceous sandstone and siltstone comprising most of the hanging wall formation, probably reflect deeper water sedimentation (perhaps deltaic) than for the Footwall formation, consistent with an overall change in subsidence rates and/or basin configuration fol-lowing deposition of the Ore Formation.

The sequence rocks that host the majority of the copper mineralisation at Mufulira also appear to have been deposited during the regression stages of short-lived(?) transgression–regression cycles. Deposition of the Ore Formation at Mufulira apparently involved three discrete transgression–regression cycles. Units hosting the A-, B- and C-Orebodies are all fairly mas-sive medium to coarse grained arkosic sandstones (similar to the principal sulfide host at Ndola West), and all are capped by either carbonate, and more argillaceous sediments (Fig. 16). All units comprising the "mineralised package" at Ndola West have direct facies equivalents within the Mufulira Ore Forma-tion. However, their (stratigraphic) disposition is a little different, possibly reflecting the more complex transgression–regression cycles at the latter. Whether the Ore Formation at Mufulira and the mineralised package at Ndola West are stratigraphic equivalents (as suggested by Scott, 2002a) as well as broad facies equivalents, is the subject of ongoing work by Dave Broughton and Robert Scott as part of AMIRA Project P544.

Distribution of copper mineralisation

Copper mineralisation occurs at two stratigraphic levels in the Lower Roan at Ndola West (e.g Fig. 3). The main horizon, at the top of the Ore formation, was intersected in five drill holes (i.e. KIT00DD004, KIT01DD003–006), while the lower, and much less significant mineralised horizon was only intersected in KIT00DD001 (Fig. 3). KIT00DD003 appears to

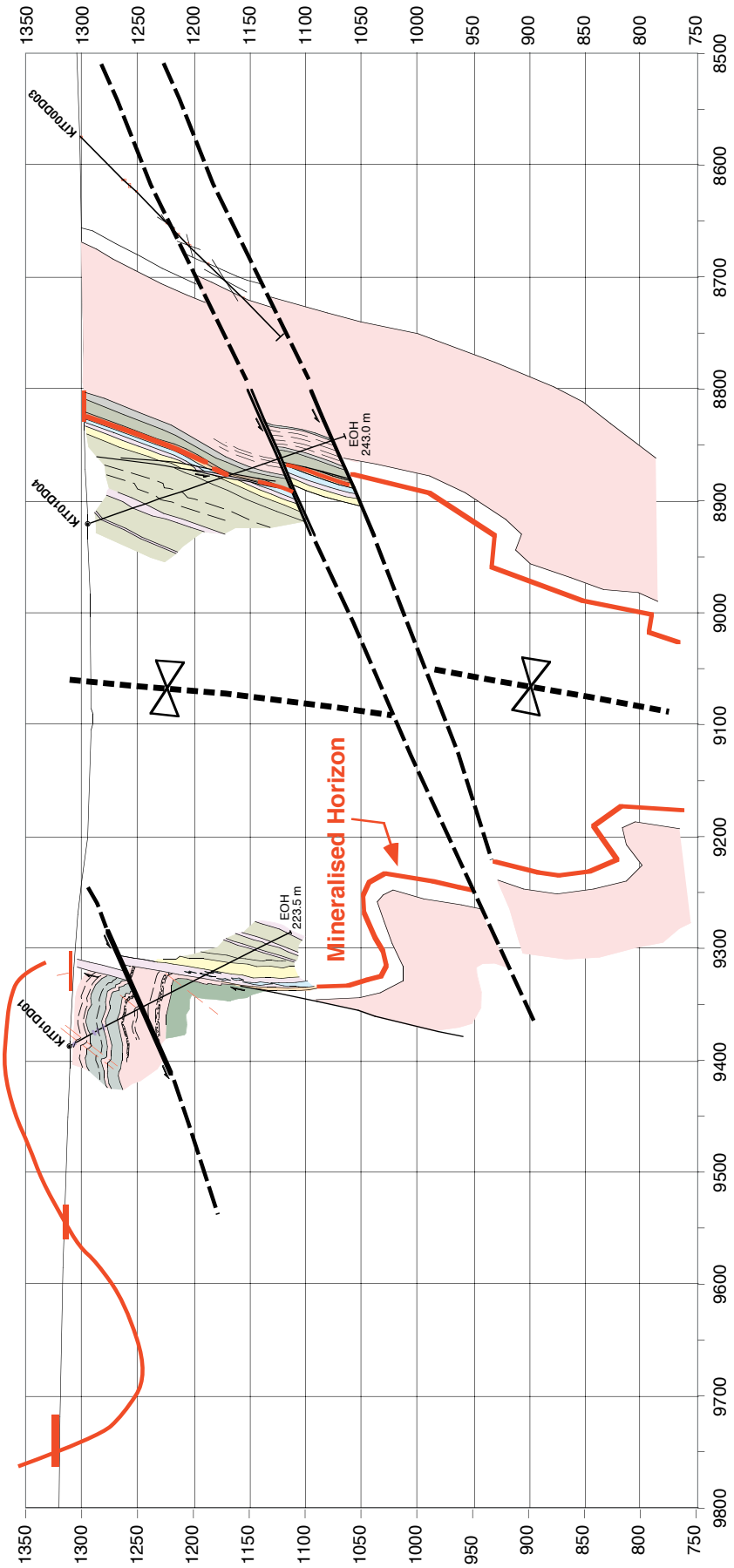

Figure 10. Simplified geological interpretation of Line 12600 (9800–8500S).

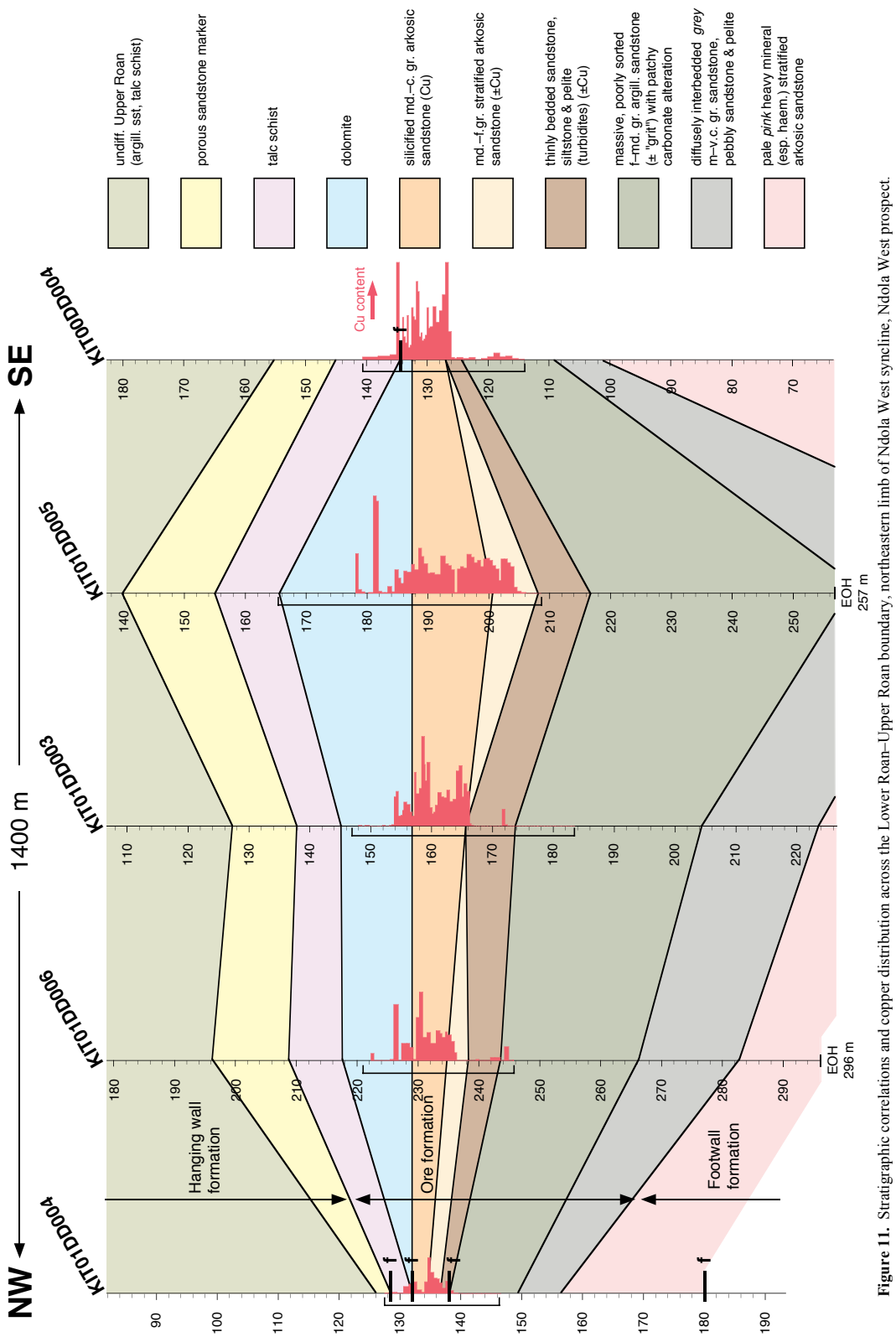

Figure 11. Stratigraphic correlations and copper distribution across the Lower Roan–Upper Roan boundary, northeastern limb of Ndola West syncline, Ndola West prospect.

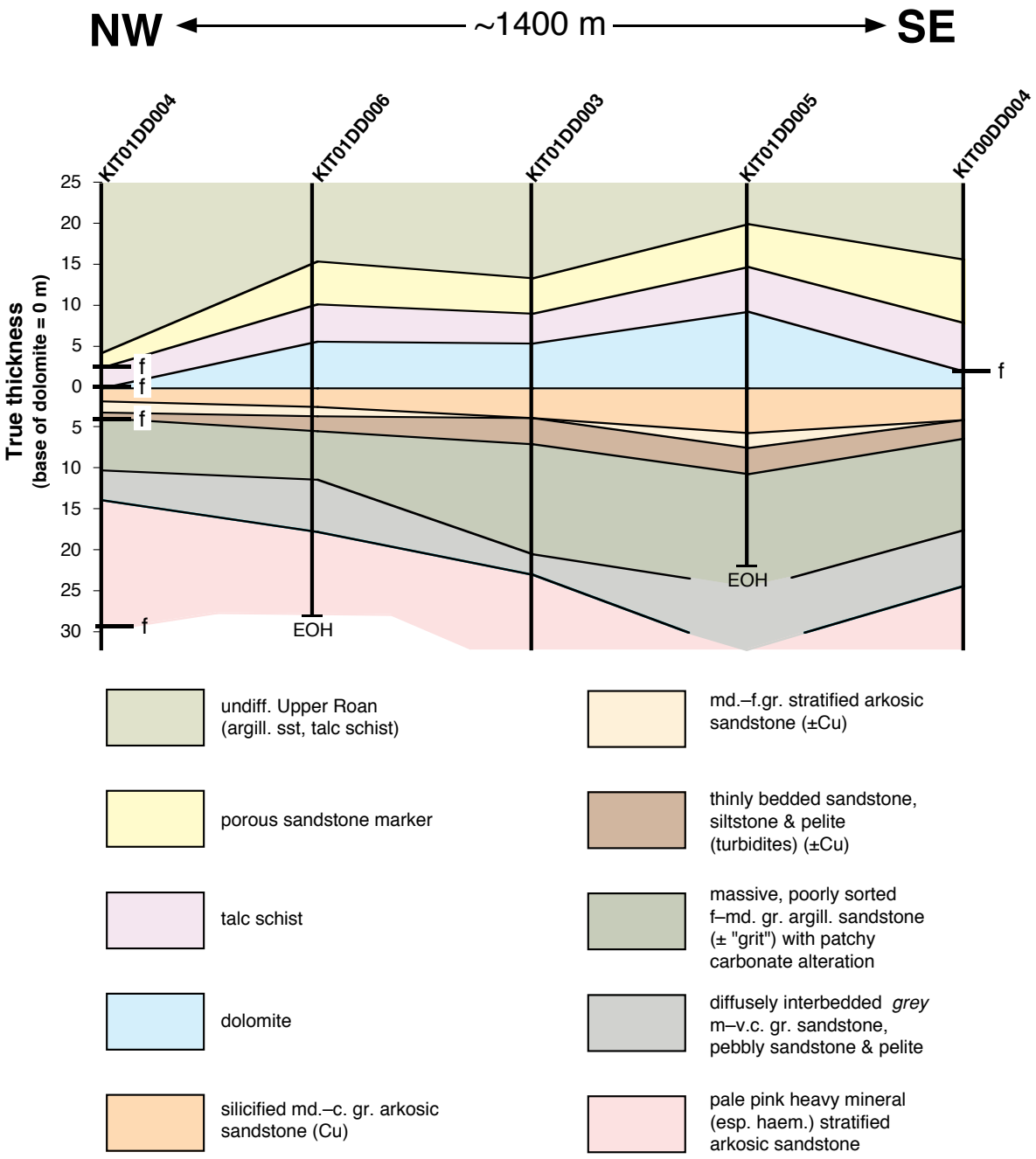

Figure 12. Stratigraphic correlations and variation in the *estimated true thickness* of units on the eastern limb of the syncline at Ndola West. Thickness estimates determined using average core-to-bedding angle over the width of the unit intersection in each drill hole.

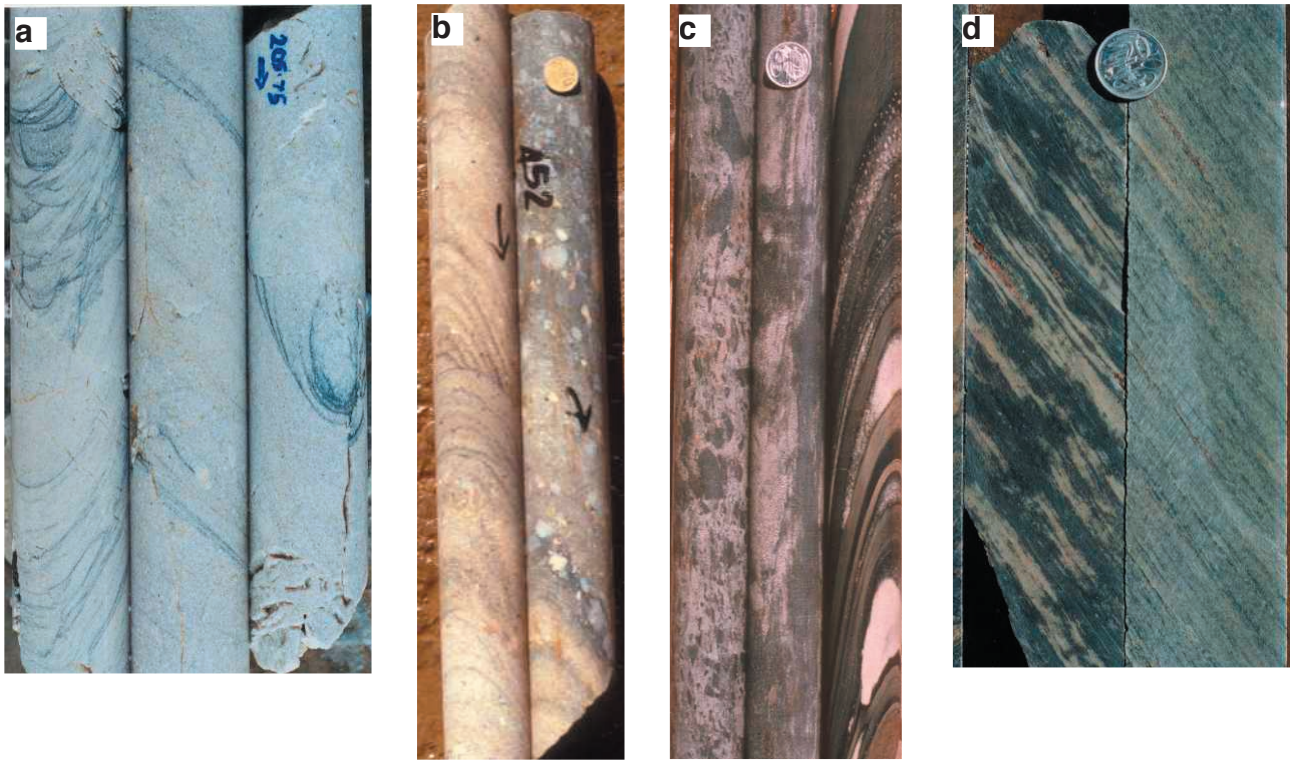

Figure 13.
(a) Heavy mineral stratified and cross stratified pale pink arkosic sandstone (upper Footwall formation). Dark colour of heavy mineral bands due to abundant fine grained specular haematite (after primary Fe(Ti) oxides). Drill hole KIT01DD004, samples from interval 205.75–226.4 m (see Fig. 7), core diameter ~4.5 cm.
(b) Heavy mineral stratified and cross-stratified sandstone and conglomeratic sandstone (lower footwall formation). Drill hole KIT00DD001, samples from interval 452–453 m (see Fig. 3), core diameter ~4.5 cm.
(c) Carbonate alteration in lower part of Ore formation. Drill hole KIT01DD005, core diameter ~4.5 cm (see Fig. 8). From left to right: ~253 m, carbonate-fill breccia or pseudo breccia within poorly sorted argillaceous sandstone, ~233.5 m, patchy carbonate alteration within poorly sorted argillaceous sandstone overprinted by main cleavage, S_1, and ~214 m, patchy (spotty) to pervasive stratabound carbonate alteration within thinly bedded turbidite facies immediately below the copper mineralised horizon.
(d) Patchy to pervasive carbonate alteration within the Ore formation. Drill hole KIT01DD004, samples from ~146 m (left) and 144.5 m (right) (see Fig. 7), core diameter 6 cm.
(e) Samples from Cu mineralised interval in drill hole KIT01DD004, samples from within interval 137.5 m (left) and 134.5 m (right) (see Fig. 7), core diameter ~6 cm.
(f) Dolomite horizon capping the main Cu mineralised interval in Lower Roan. Drill hole KIT01DD005. Samples from interval 175.8–176.5 m, core diameter ~4.5 cm (see Fig. 8).
(g) Porous marker sandstone in drill hole KIT01DD005 (interval 142.3–144.5 m, see Fig. 8). Diameter of core 6 cm.
(h) Examples of argillaceous ±carbonate altered(?), locally pyritic sand- and siltstone of the Hanging wall formation. Drill hole KIT01DD004, from left to right: ~94 m, ~93.5 and ~74 m. Diameter of core 6 cm.

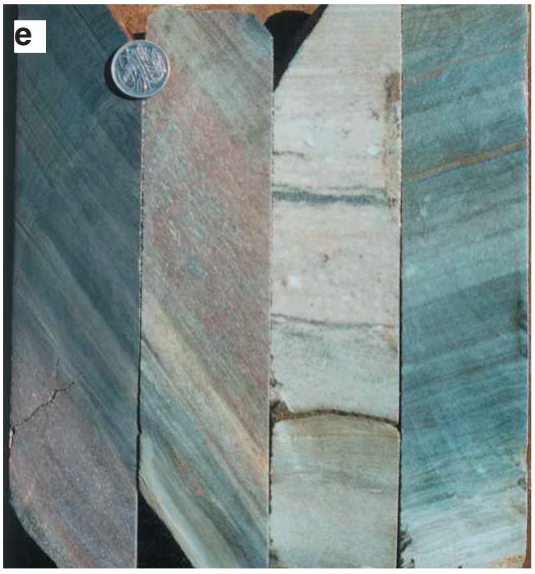
e


f


g


h

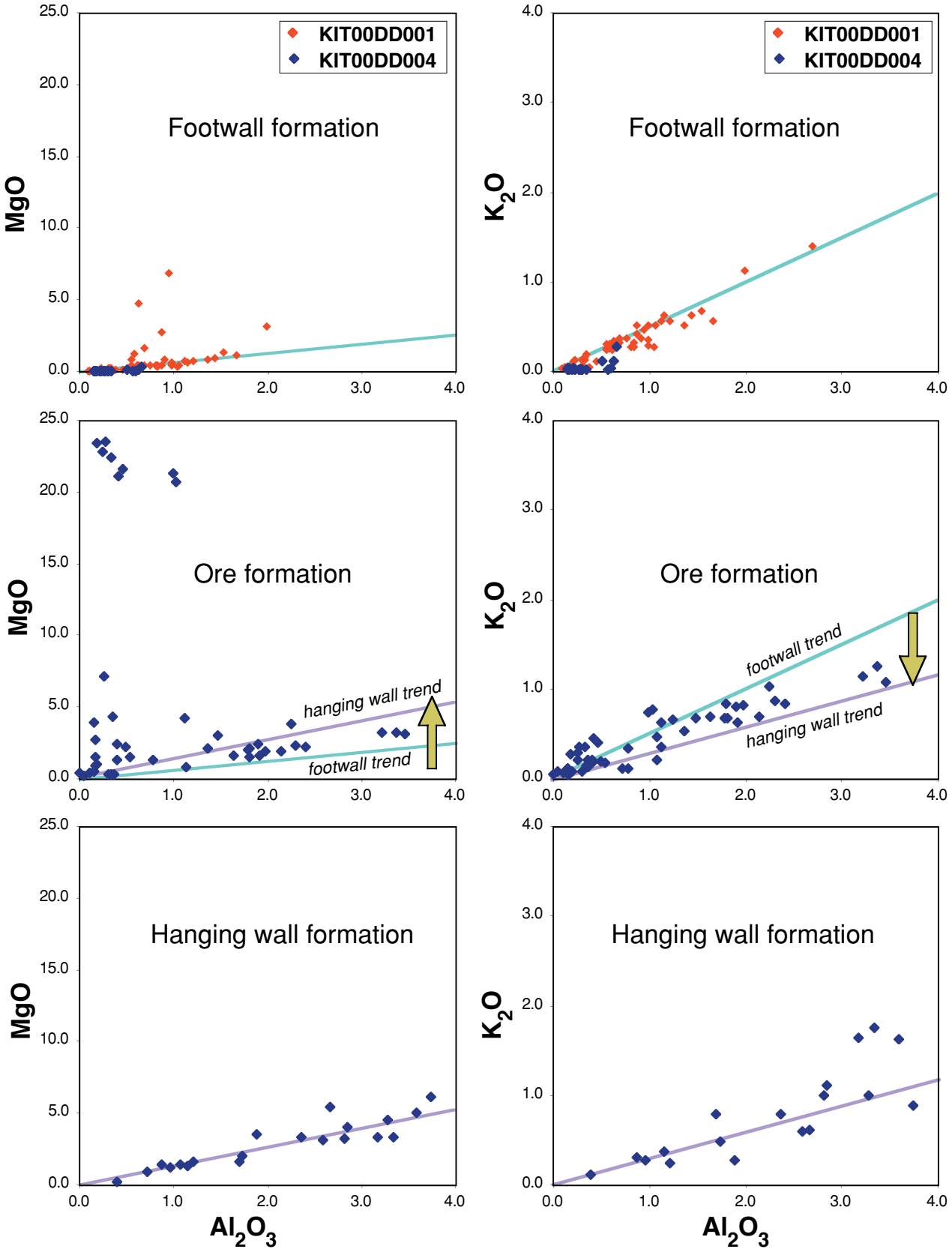

Figure 14. Selected Anglo America partial digestion whole rock geochemical data for KIT00DD001 and DD004. Although major element abundances do not reflect complete dissolution of all phases present, strong linear correlations between Al, K and Mg suggest these elements were largely source from mica (and or clay) phases in the rock. If so, in addition to the overall increase in mica abundance from Footwall to Hanging wall, a progressive shift to higher MgO/Al_2O_3 and lower K_2O/Al_2O_3 mica compositions is apparent. The changes are consistent with hanging wall sediments being more argillaceous, possibly with initially higher dolomite content s.

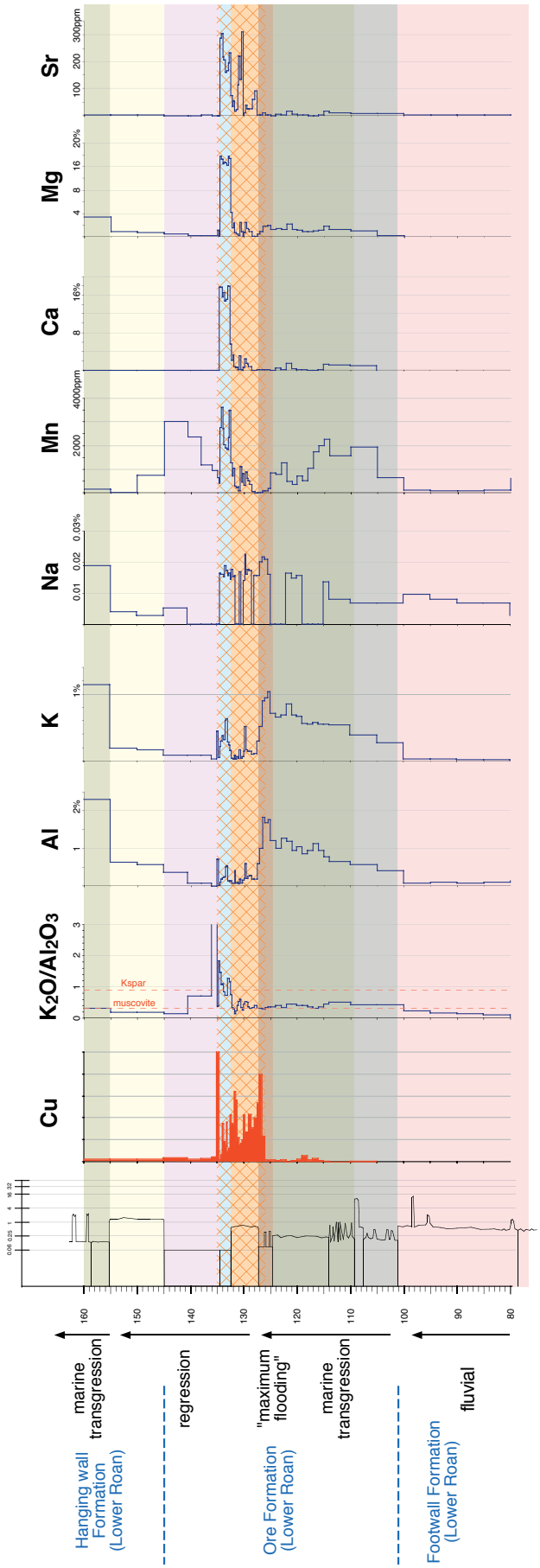

Figure 15. Selected Anglo America partial digestion whole rock geochemical data for KIT00DD004. Major element abundances interpreted to principally reflect carbonate and mica phases present in rock. Anomalously low Mg for the talc schist (talc confirmed by PIMA) suggests additional sampling or sample preparation problems. Apparent increase in mica content (increasing Al, K) across the lower part of the Ore formation is interpreted to reflect a marrine transgression. The most micaceous unit is the package of thinly bedded shale-rich turbidites in the immediate footwall of the copper mineralised horizon. the turbidite package represents maximum flooding (greatest water depth) in the basin and is the closest facies equivalent , within the Ndola West area, to the Chambishi Basin "Ore Shale".

Figure 16. Provisional comparison of Lower Roan stratigraphy between Ndola West and Mufulira (east of Kafue Anticline).

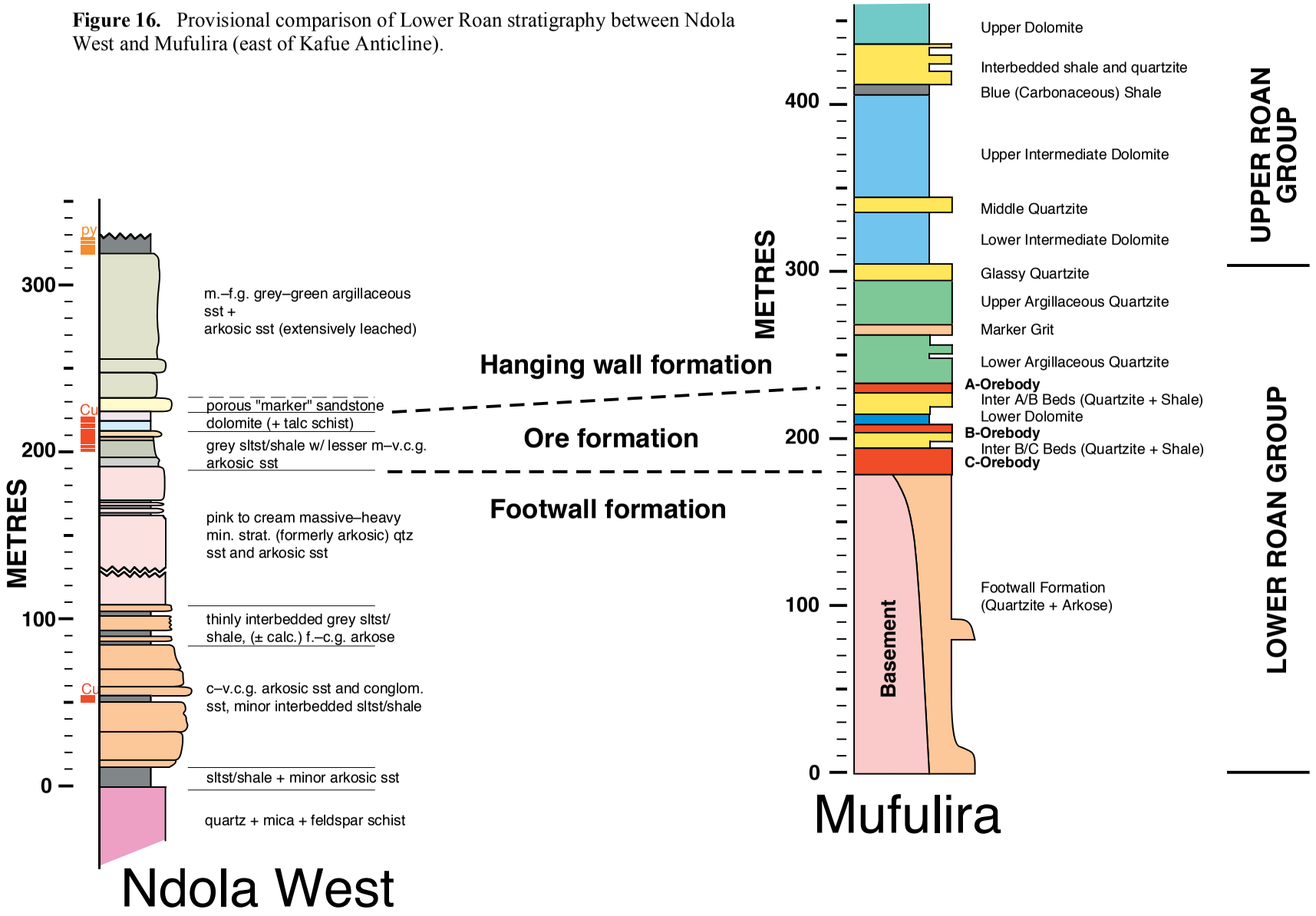

have intersected the equivalent stratigraphic position that hosts the lower mineralised horizon, but Anglo-American's continuous core-grind assay data reveals no anomalous copper in this hole.

Detailed description of the copper sulfides, and their textural and timing relations is ongoing. Sulfide mineralisation in KIT00DD004 (reported in Scott, 2002b) is predominantly very fine grained chalcocite and bornite with minor chalcopyrite. Some sulfide grains have complex (?)intergrowths of bornite and chalcocite, suggesting these phases were either co-precipitates or recrystallised (together) from a precursor phase during metamorphism. The disseminated mineralisation in the "2001 series" drilling suggests bornite is the major primary sulfide phase, and most (but not necessarily all) of the chalcocite is supergene in origin (after bornite ± chalcopyrite).

For the main mineralised horizon on the NE-limb of the Ndola West syncline the thickness of the sandstone-hosted Cu mineralisation decreases towards the northwest, from a maximum of 5–5.6 m (true thickness) in the vicinity of KIT00DD004 and KIT01DD005 to 2.83 m in KIT01DD006. Although the width of the sandstone-hosted mineralisation in the northwestern-most hole (KIT01DD004) appears somewhat greater (4.31 m), this is interpreted to be due to "bleeding" of secondary copper oxides (malachite, chrysocolla) into the normally ~barren (i.e. <1000 ppm) stratigraphically lower units. This interpretation is supported by the generally less silicified "leached" character of the usual host rocks, the predominance of copper carbonates/oxides over the original disseminated sulfides (Fig. 13e). Although stratigraphic correlations with drill holes to the southeast indicate a portion of the "host stratigraphy" in KIT01DD004 has been excised by faulting (most notably the dolomite is absent), stratigraphic trends (Fig. 11) suggest the main sandstone host was probably thinner in this area anyway.

In contrast, to variations in the width of the mineralised interval, the average grade of the primary ± secondary, (i.e. chalcocite) *sulfide* mineralisation on the eastern limb of the synform appears to be relatively uniform (Fig. 11).

Thickness and grade variations for the dolomite-hosted mineralisation are more difficult to interpret, as preserved thickness of the dolomite probably largely reflects the geometry of subsequent faulting and the extent of talc schist development. For example the greatest variation in thickness of the dolomite is between adjacent drill holes (~9 m in KIT01DD005 and <2.5 m in KIT00DD004). Copper grades in the dolomite are also much more variable than in the underlying sandstones. Carbonate-hosted dissem inated sulfides are typically coarser grained than those in the underlying sandstones. Sulfides vary from finely disseminated to semi-massive within coarse-grained veins and/or segregations up to a few centimetres wide. The thickest (most complete?) intersections through the dolomite (KIT01DD003, DD005, and DD006) suggests that only the lower 1–3 m of the dolomite contains significant copper, and exhibits zonation from Cu-sulfides at the base, upwards through Cu-sulfides + pyrite, pyrite ± minor Cu-sulfides, and finally to sulfide-free dolomite.

Malachite and copper oxide mineralisation is generally minor in the Ndola West drill holes, however drill hole KIT00DD004 (and deflection #2 from this hole) intersected a narrow "high grade" zone (true thickness <0.5 m) containing malachite nodules within talc-schist (after dolomite).

Copper sulfide textural relations

Copper sulfides in the main medium to coarse grained arkosic host rock are sub-millimetre-sized irregular grains with interstitial to replacive habit (Fig. 17a and b).The sulfide grain morphology and distribution indicate copper was present in the rock prior to at least the last stages of grain-scale recrystallisation and fabric development accompanying regional deformation (Scott, 2002b). Sulfide grains and aggregates within the lower part of the overlying dolomite unit are clearly cut by and thus predate thin talc-rich shear zones (Fig. 17c and d).

In one sample from the stratigraphically lower copper horizon intersected in KIT00DD001, chalco pyrite is apparently intergrown with syn-D_1 scapolite

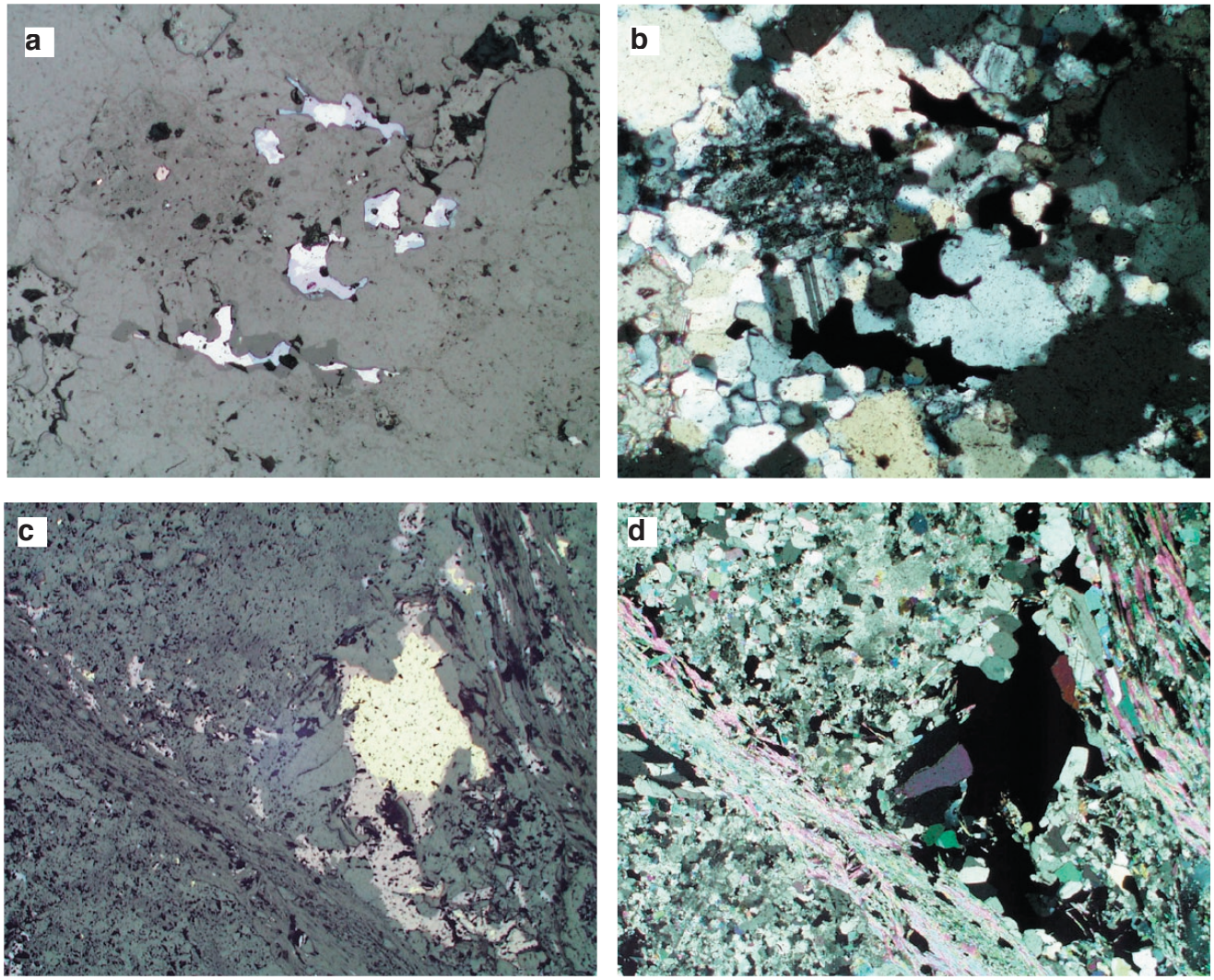

Figure 17
(a) Irregular fine grained bornite ± chalcocite ± chalcopyrite in arkosic sandstone. Drill hole KIT00DD004 (sample RJS-41, 131 m). Width of view 1.1 mm, reflected light.
(b) Same area as (a) viewed with crossed polars, illustrating advanced recrystallisation of the detrital grains. Textural relations between the silicates and the sulfides indicate copper was introduced into the rock prior to metamorphic recrystallisation.
(c) Bornite+chalcopyrite aggregate in dolomite overprinted by talc schist bands. Drill hole KIT00DD004 (sample RJS-43, 134 m). Width of view 9 mm, reflected light.
(d) Same area as (c) viewed with crossed polars to highlight the narrow talc-rich shears.

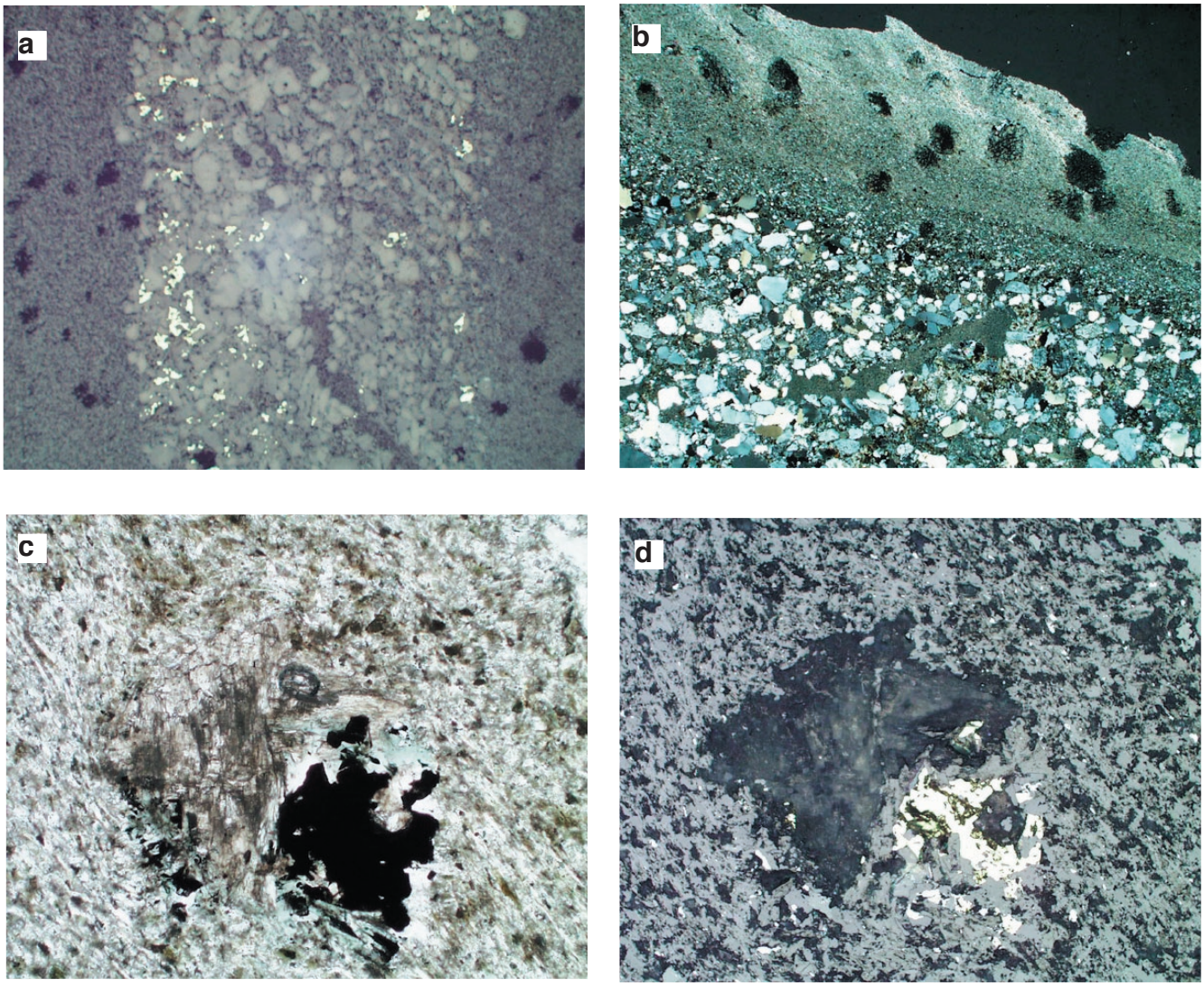

Figure 18
(a) Fine grained chalcopyrite concentrated within thin sandstone bed, near contacts with adjacent pelite. Black blebs in pelite are ~0.5 mm scapolite porphyroblasts. Drill hole KIT00DD001 (sample RJS-19, 458 m). Width of view 11.3 mm, reflected light.
(b) Same bed as illustrated in (a). Scapolite porphyroblasts all go to extinction in the same orientation suggesting a probable stress control on blast orientation. As the weak S_2 crenulation cleavage nucleates from scapolite porphyroblasts (note light domains in pelite sloping from left to right) a pre-S_2, syn-S_1 age for scapolite is indicated. Drill hole KIT00DD001 (sample RJS-19, 458 m). Width of view 9 mm, cross-polars.
(c) Detail from (b) showing intergrowth between scapolite and chalcopyrite Drill hole KIT00DD001 (sample RJS-19, 458 m). Width of view 1.125 mm, plane polarised light.
(d) Same area as (c) viewed with reflected light.

Figure 19
(a) Bleached alteration halo adjacent to quartz + feldspar + copper sulfide fibre vein in Cu-mineralised arkose. Banding at low-angle to core axis is relict bedding. Uniformly disseminated fine grained bornite in the arkose is depleted within the albite- (white spots and blebs) + tremolite- (small irregular green-grey blebs towards margin of bleached halo) halo adjacent to the vein, indicating copper sulfide in the fibre vein was leached from the adjacent wallrocks. Drill hole KIT01DD005, 203.2 m, diameter of core 4.5 cm.
(b) Quartz + feldspar + haematite (±fibre) veins in the lowermost Ore formation. The core stick on the left (KIT01DD003, ~202.4 m) shows the weakly carbonate altered host rock (grey ±argillaceous, arkosic sandstone) away from the quartz + feldspar veins. Around the veins the rock is stained orange-red (e.g. core stick on the right, 216.8 m) which is interpreted to reflect haematite dusting of albite in the alteration halo.

porphyroblasts indicating copper was either remobilised or introduced into the rock at this time (Fig. 18; Scott, 2002b)

Alteration

While the carbonate unit (<10 m thick) capping the copper mineralisation at Ndola West is interpreted to be sedimentary in origin, there is an extensive zone of carbonate alteration, best developed in the immediate footwall (i.e. the lower part of the Ore formation) but also extending upward into the mineralised horizon. A genetic relation between the carbonate alteration and copper mineralisation is yet to be established, however both are overprinted by the regional cleavage and may therefore have similar timings.

In several drill holes bornite occurs in small quartz-feldspar fibre veins, with prominent albite + tremolite bearing alteration haloes (Fig. 19a). The veins appear similar to quartz + albite + haematite bearing fibre veins that are locally developed in the Footwall formation (Fig. 19b), and copper sulfides are only developed in the veins where they cut the ore horizon. The veins are also overprinted by the regional cleavage. However as disseminated sulfides are markedly depleted in the bleached haloes surrounding the veins (Fig. 19a), it appears the bornite in the veins was remobilised from the immediately adjacent wallrocks. Accordingly formation of the veins (and associated albite + tremolite alteration) post-dates primary introduction of copper into the rocks.

Structure

Recent drilling (2000 and 2001 series) is centred on a large gently (SE) plunging syncline. Most of the drill holes were planned to test subsurface continuation of stratabound copper mineralisation on the steeply-dipping NE limb of the structure, while drill holes KIT01DD001 and DD002, were designed to test this position on the SW limb. Drilling reveals the subsurface geometry of the fold is more complex (e.g. Figs 4 , 5) than suggested by the relatively simple and continuous surface trace of the mineralised horizon (Fig. 2).

Folds and cleavage development

The overall geometry of the major syncline at Ndola West appears to change along strike to the northwest, with the structure becoming more overturned (axial plane dipping moderately to steeply towards the southwest, and the eastward younging limb overturned; cf. Figs 3 and 5). A general corres pondence between the orientation of the mineralised horizon at depth (from core to bedding angles) and the surface trace of mineralisation suggests the *eastern limb* of the synform is generally relatively planar (e.g. Figs 3, 7–9). KIT01DD003 is an exception suggesting parasitic folding may affect the sequence in this area (Fig. 6). Cleavage is moderately to well developed in the more argillaceous units and generally parallel or at a low-angle to bedding. Rocks comprising the mineralised horizon and its immed iate footwall, appear moderately to strongly attenuated, suggesting there may be some structural thinning of units along this limb of the fold.

Logging of KIT01DD001 and DD002 indicates that unlike the relatively planar eastern limb of the Ndola West syncline, strata on the western limb are folded about a series of large parasitic folds, as well as being offset across a number of shears and faults. Cleavage is generally well developed at a moderate to small angle to bedding, and locally is even developed within the usually weakly strained (internally) pink arkosic sandstone. The style of deformation suggests there may be some potential for structural thickening and/or upgrading of the mineralisation in the hinges of these folds.

Faults/shear zones

Numerous brittle-ductile to ductile faults and shear zones were intersected in the Ndola West drilling. Although the orientation, magnitude and sense of displacement for these structures is for the most part poorly constrained, most are interpreted to be relatively steep and generally at low-angles to layering and/or cleavage.

One of the most important (sets of) structures in

the overall interpretation of the subsurface distri bution (and continuity) of the mineralised horizon are the talc schist zones, principally developed within the uppermost Ore formation and overlying Hanging wall formation. The main talc schist occurs immediately above (stratigraphically) the mineralised horizon (presumably largely derived from the underlying dolomite). On the NE limb of the syncline, the talc schist varies from about 2.5 to 5 m thick, and generally separates the coarse grained porous quartz sandstone marker (lowermost Hanging wall formation) from the underlying dolomite (both units may also be cut by narrower bands or "foliation seams" of talc-rich schist that may be splays from the main structure). The consistent juxtaposition of stratigraphy across the talc schist in six of the seven drill holes intersecting this position on the NE limb of the syncline (KIT00DD004, DD004 Defl. 1, DD004 Defl. 2, KIT01DD003, DD005, DD006: representing an along strike distance of one kilometre), suggests the talc schist may simply reflect *layer-parallel* shearing concentrated within the upper part of the dolomite. However in KIT01DD004, the equivalent talc schist separates a thin porous quartz sandstone marker in the hanging wall from Cu-mineralised (arkosic) sandstones, and the dolomite is absent. Both the hanging wall and footwall units in DD004 are appreciably thinner than correlative units intersected in the other drill holes, suggesting as much as 5 m of (*normally mineralised*) stratigraphy has been excised as a result of (normal sense) slip across the talc schist (Fig. 7). Collectively these relations suggest (1) the talc schist cuts stratigraphy at a low-angle but the drill holes happen intersect the unit at about the same structural position along strike, (2) the schist was originally more-or-less layer parallel but has been partly reactivated by more steeply dipping faults where it is intersected in KIT01DD004 (interpretation shown in Fig. 6), or (3) a combination of both.

Regardless of interpretations concerning its overall geometry, the talc schist zone postdates copper mineralisation on textural grounds (Scott, 2002b), and in detail the sulfide distribution in the underlying strata shows no obvious spatial relationship to the schist.

A talc schist interpreted to correlate with the main talc schist on the NE limb of the syncline was also intersected in KIT01DD001, on the SW limb of the syncline. KIT01DD001 is collared in Lower Roan and drilled *down sequence* (i.e. younging up-hole) through a succession dominated by the heavy-mineral stratified pale pink arkose, and underlying massive grey siltstone to poorly sorted sandstone, before intersecting the talc schist (~8 m true width) at 134.5–144.5 m depth (Fig. 4). The talc schist includes several small blocks of malachite stained dolomite, super ficially similar to that capping the mineralised horizon on the NE limb of the syncline. The succession (structurally) below the talc schist appears typical of the Upper Roan in drill holes on the NE limb of the syncline, consisting predominantly of banded green-grey argillaceous locally pyritic sandstone and siltstone (colour banding reflecting patchy carbonate alteration), with several narrow zones of talc schist. Grading in porous quartz sandstone units immed iately below the talc schist suggest the sequence youngs down-hole. Although the sandstone in KIT01DD001 lacks the distinctive sparse <3 mm pyrite cubes present in most other intersections of the porous sandstone marker, it is interpreted to be the same unit. If this correlation is correct, it places an important constraint on the overall geometry of the main talc schist zone. While the "upper" contact of the talc schist in KIT01DD001 is clearly a major fault transecting stratigraphy (Fig. 3), the fact that the units "stratigraphically" overlying the talc schist are the same on both the NE- and SW-limbs of the syncline indicates it is either stratabound reflecting pre-folding layer-parallel shearing of the dolomite (as interpreted by Scott, 2002a), or perhaps more likely, localised ~ layer-parallel shear on the steeply dipping limbs of the syncline (syn-folding). However locally subsequent (or continued) strain-localisation within the talc schist, may have resulted in it developing or being incorporated into larger faults oblique to bedding.

Brittle faults

The most significant brittle faults developed at Ndola West are apparently late (interpreted to cut all other structures), gently SW-dipping faults. The faults are typically marked by the development of massive to weakly foliated, moderately indurated (poorly lithi-

fied) ochre-coloured clay gouge and/or intervals of very poor core recovery (voids). Where best constrained (e.g. KIT01DD003 (Fig. 6) and DD004 (Fig. 7)) offset of the steeply dipping stratigraphy across these faults suggests normal displacements (hanging wall down to the SW) of <10 to perhaps 50 m. The approximate orientation of these faults can be inferred from the fact that, where intersected in KIT01DD002, DD003 and DD004, the faults are at very high angles (approximately perpendicular) to the core axis (all drill holes inclined at ~70˚). This information coupled with correlation of faults at 253–258.4 m in KIT01DD003 and 180–183m in DD004 suggests a possible (i.e. viable) average fault orientation dipping 25˚ towards the SW (i.e. 25˚/217˚). If similarly oriented, the projected surface trace of a structurally-higher, ochre clay gouge fault at 81.2–82.2 m (and (?)splay at 107.3 m) in KIT01DD002 (Fig. 5) separates offset sections of the mineralised horizon on Line 11800W (Fig. 1). Both the sense and combined displacement of the low-angle normal faults intersected in DD002 are broadly consistent with the observed offset of the mineralised horizon on Line 11800W. However this correlation implies a down-dip decrease in minimum displacement on the fault, from ~50 m at surface on Line 11800, to 20–30 m (minimum combined displacement on low-angle faults) in DD002. KIT01DD005 is interpreted to intersect this fault at ~30–35 m depth (Fig. 8), KIT01DD004 and DD006 are both likely collared in the footwall and thus do not intersect the fault. However its position relative to KIT01DD003 is less certain, and this hole may also intersect the fault at shallow depth.

Structural/stratigraphic interpretations of KIT01DD001 and DD002

A critical issue in regard to the interpretation and exploration potential of the southwestern limb of the Ndola West syncline is how the stratigraphy intersected in holes KIT01DD001 and DD002 relates to that on the other side of the syncline. Specifically, has the stratigraphic position that hosts mineral isation on the eastern limb of the syncline been intersected in these drill holes, and if not why not? Geological interpretations for these drill holes (Figs. 4 and 5) indicate the target horizon was not intersected.

KIT01DD001

KIT01DD001 is collared in heavy mineral stratified pink arkose. Cross-laminations at ~5 m depth indicate the sequence is right way up at surface. Although as the core is badly broken at this point there is some doubt as to the original (true) orientation of the piece of core. The first reliable younging indicators occur below ~50 m depth and except for some minor younging reversals associated with small folds at 69–72.5 m, the entire sequence to ~95 m youngs up hole (right-way up). Bedding-to-core angles over this interval are typically in the range 55–90˚. High bedding-to-core angles (>80˚) above 50 m, indicate layering dips moderately to gently SW in the upper part of the hole (Fig. 4). Below 50 m extremes in the possible orientation of bedding are moderate dips toward the southwest or gentle dips to the southwest and northeast. (i.e. roughly subhorizontal). The latter possibility is supported by oriented core at 97.5 m, which yields a bedding orientation of 13˚/006˚. This constraint was used in the construction of the interpretive drill section shown in Figure 4. However the overall structural interpretation is not greatly affected by uncertainty in bedding orientation in this part of the drill hole.

The pink arkose overlies a fairly massive sequence of strongly cleaved grey siltstone to fine grained argillaceous sandstone, with prominent irregular dissolution pits (after carbonate, anhydrite?). This unit is interpreted to occupy the hinge of an antiformal closure, as heavy mineral stratified arkose is (?)repeated below 125 m before being truncated against talc schist at ~132 m. Although no younging criteria from the lower sandstone were observed in support of this interpretation, there are a couple of reasons why it is favoured. Firstly, the fine-grained unit underlying the pink arkose in KIT01DD002, appears much thicker than the stratigraphically-equivalent interval between 103 and 126 m in KIT01DD001, suggesting that in DD001 was just clipped in the hinge of a fold (Fig. 4). Secondly, the sequence further down-hole, below the talc schist, is overturned, indicating there

must be a fold (largely sheared out) within or immediately above the talc schist. Accordingly, neither the structural inter pretation or overall geometry of units is greatly affected by the exact position of the closure.

The talc schist between 132–147 m contains fragments of dolomite (some with minor malachite staining) suggesting it is the main talc schist that directly overlies the mineralised sequence on the eastern limb of the syncline. This indicates the upper contact of the talc schist in KIT01DD001 is a reverse fault with substantial displacement (Figs 4, 10).

The sequence below the talc schist commences with a graded porous quartz sandstone, interpreted to be the porous sandstone marker of the lowermost Upper Roan, the sequence of locally slightly pyritic green–grey argillaceous sandstones and minor talc schist is broadly similar to the Upper Roan succession intersected in drill holes on the eastern limb of the syncline. Accordingly, units intersected between the (structural) top of the talc schist and the end of the drill hole, are interpreted as a more-or-less stratigraphically continuous sequence.

KIT01DD002

The structural interpretation of KIT01DD002 is illustrated in Figure 5. The basic fold geometry depicted in the section is well constrained by bedding orientations and younging reversals, and the depicted geometry is probably the simplest possible alternative consistent with stratigraphic and structural informa tion in the drill hole. One of the most significant poorly constrained aspects of the interpretation concerns the geometry and amount of displacement on the various faults intersected in the drill hole. Accordingly, it is important to discuss some of the evidence and assumptions used in the construction of the section, particularly where these affect on the overall structural geometry, and thus the likely subsurface position of the mineralised horizon.

Faults intersected at 81.2–82.2 m and 102.2 m are shown as structures dipping gently to the left of the section. Both faults have a distinctive poorly indurated ochre clay gouge interpreted to be characteristic of a set on small to moderate displacement normal faults (e.g. see sections for KIT01DD003 and DD004) with an average orientation 25˚/217˚. The interpreted surface trace of the upper fault in DD002 is shown Figure 2. It is interpreted to be the fault responsible for the offset of the mineralised horizon on the eastern limb of the Ndola West syncline (Line 11800).

The existence and locations of the folds shown on the section is well constrained by younging criteria (numerous foreset truncations and graded beds in the pink arkose), cleavage-bedding relations and asymmetry of minor folds (i.e. vergence changes), and fairly consistent changes in bedding core angles (bedding on right-way-up, moderately–gently dipping limbs is generally at 70–90˚ to the core axis, while it is at <60˚ to the core axis on the overturned limbs).

Dissolution pitted (after carbonate ± anhydrite?) argillaceous green-grey siltstones and poorly sorted sandstones similar to those in KIT01DD001 occur in at least two places down hole in Ddoo2. At each of the three contacts between the pink arkose and argillaceous siltstones and sandstones in the lower half of the hole, the pink arkose youngs away from the contact, indicating it overlies the siltstone dominated succession. The identical stratigraphic relationship is observed between these units in the upper part of KIT01DD001 (Fig. 4).

Only the lowermost contact between the pink arkose and siltstone dominated succession (268.7 m) is a relatively undisturbed sedimentary contact; the upper two are both faulted. The lowermost (right-way-up) intersection of the pink arkose has three main bands of conglomerate or conglomeratic sandstone. Only the uppermost of these bands is repeated around the synform, on the overturned limb of the fold. This observation coupled with the decreased thickness of the pink arkose on the overturned limb of the lower synform suggests about half the thickness of the unit is excised by slip on the overlying fault (intersected at 216.5–219.4 m). The sense of stratigraphic juxtaposition across this fault indicates reverse displacement. Its dip is unknown, but shown as steep, at a low angle to the axial plane of the folds in Figure 5. A similar argument holds for the faulted upper contact of the siltstone-dominated sequence at ~128–129 m, although in this case the sense of stratigraphic juxtaposition

implies normal displacement. The net effect of these two faults is to "pop out" the hinge of the antiformal fold, cored (in DD002) by the siltstone sequence.

The mineralised horizon (or its stratigraphic equivalent) is not intersected in DD002. Its approximate position (NE of the drill hole) shown on the drill section is based on the thickness of the equivalent succession above the pink arkose in the nearest well constrained holes (namely KIT01DD004 and KIT01DD006, on the northeastern limb of the Ndola West synform) and roughly conforms to the position of the surface trace of anomalous copper (Figs 2, 5).

The interpreted thickness of pink arkose *above* the massive, poorly sorted green-grey argillaceous siltstones and sandstones in KIT01DD002 is much less than in KIT01DD001, although the holes are only 400 m apart along strike. However, the interpreted thickness difference may not be correct, as it results from the tentative correlation between the fine-grained package at the top of DD002 (4.6–26.2 m) and the unit intersected at 129.2–156.5 m and 268.7–300.4 m. This correlation is imposed by the correlation of strongly leached and pitted arkose in the core of the lower synform in the pink arkose (235.8–237.6 m) with the grey arkose and lesser diffusely interbedded pelite intersected around the upper synform between 70.5 and 103.3 m. The package in the upper part of the drill hole definitely correlates with the transitional basal unit of the Ore Formation in drill holes on the eastern limb of the Ndola West syncline. However, if these correlations are incorrect, the upper fine grained package in DD002, may correlate with the fine grained intervals in the upper part of DD001 (e.g. 22–33.7 m and 38.5–49 m (these packages certainly look similar in core, although the rocks are strongly weathered) then the total thickness of the pink arkose in DD002 is much thicker than shown in the interpretation. This interpretation implies the pink arkose is exposed in the top half of the hole (above 129 m) represents the top of the unit, while the pink arkose is intersected in the lower half of the hole (219.5–268.7 m) forms the base. This alternative interpretation necessitates larger displacements on either or both of the steeply west dipping faults at ~70 m (and its offset continuation at ~91–92 m) and ~128–129 m. Furthermore, in at least the lower half of the section., the interpreted position of the mineralised horizon in Figure 5 would shift to the right (NE) by an amount equal to the additional thickness of the pink arkose.

Although DD001 and DD002 are only 400 m apart and are nominally along strike, the structural interpretations of the two drill holes appear markedly different. Both drill holes are collared essentially within the pink arkosic succession. However in DD001 the sequence is interpreted to be gently dipping and youngs up-hole, while in DD002, it is steeply west dipping and youngs down-hole, indicating the collars of the two drill holes must be separated by a fold closure. Two alternatives exist: either a synform whose trace is located to the west of DD001 and to the east of DD002, or an antiform whose trace is located east of DD001 and west of DD002. Consideration of the gross structure of this area (i.e. surface trace of copper zone) suggests the latter interpretation is more likely, and that this structure is the in fact the major antiformal closure, immediately west of the Ndola West synform (Fig. 2).

An important question relating to the correlation of structures between DD001 and DD002 is how does the steeply-dipping shear zone occupied by the talc schist in DD001 (Fig. 4) project to the north? One possibility is that the shear zone strikes at a low-angle to the stratigraphy and correlates with the zone of (interpreted) steeply dipping (reverse) faults intersected at about 70 m down-hole depth in DD002 (Fig. 5). If this interpretation is correct displacement on the shear zone must die out abruptly towards the north. Alternately, the shear zone may have a more northerly strike and project east of the DD002 drill section depicted in Figure 5. The first option is considered more likely, because the talc schist occurs in the same stratigraphic position (relative to the Hanging wall formation) in DD001 as it does on the eastern limb of the Ndola West synform. This relationship is seemingly more consistent with shear localisation initiating along a favourably oriented "weak" position in the stratigraphy (i.e. the dolomite), rather than being entirely discordant to stratigraphy (the latter implies the occurrence of the shear at the base of the Hanging wall formation in DD001 is merely a coincidence).

Genetic model for copper mineralisation

Age of copper mineralisation

The gross geometry and textural relations of stratabound copper ores at Ndola West indicate mineralisation occurred after early diagenesis but prior to significant folding and regional cleavage development (i.e. main stage Lufilian Orogeny). Scott (2002b) suggested a late-stage diagenetic origin for the ores because (i) there is no evidence for either macro- or micro-scale structural control on ore fluid introduction (metal distribution), implying rocks were relatively porous at the time, and (ii) the Lufilian deformation in the Copperbelt occurred under greenschist facies conditions (implying low rock porosity), and tectonic fabrics generally appear to post-date the copper sulfides. However, textural relations do not preclude a younger age for copper introduction, only that it must pre-date greenschist facies metamorphism significant tectonic fabric development during the Lufilian Orogeny. Newly established temporal constraints for the Mufulira deposit to the north (Fig. 1), suggest copper introduction may have indeed occurred during the earliest stages of Lufilian deformation.

Preliminary results of xenotime dating at Mufulira reveal three broad populations with average ages of 560, 535 and 510 Ma (Dawson, 2002). Analysis of CODES sample MUF-4 yielded a 517±17 Ma SHRIMP age (Dawson, pers. comm. 2002) for a xenotime overgrowth (apparently intergrown with chalco pyrite) on a detrital zircon grain from and a Cu-mineralised heavy mineral band in the footwall to the A-Orebody at Mufulira. This age is consistent with, but refines, previously reported 534±92 Ma, 529±68 Ma microprobe ages for other xenotime overgrowths from same sample (Scott, 2002c). The *formation* of xenotime in sandstones is thought to only occur during episodes significant fluid flux (McNaughton, 2002). The presence of "Lufilian ageÓ xenotime overgrowths within rocks lacking obvious evidence for fracture-enhanced permeability, implies at least locally grain-scale permeability was still relatively high during the early stages of the Lufilian deformation.

Both the metamorphic grade and microstructural character of the Lower Roan at Mufulira and Ndola West were buried to depths with ambient rock temperatures in excess of 300–350°C, i.e. 8–10 km or more. The depth of burial of these rocks at the onset of Lufilian deformation is unknown. During the Lufilian orogeny structural thickening within the eastern part of the Zambian Copperbelt appears to have been largely accomplished by folding as there is little evidence for stratigraphic duplication through thrust stacking (e.g. Fig. 1). Whatever the mechanism, if substantial crustal thickening resulted in the progressive burial of rocks at Mufulira and Ndola West during Lufilian deformation, they were not necessarily deeply buried at the onset of the event. Alternately, development of reaction-enhanced permeability through the partial dissolution of soluble phases in the rock (e.g. diagenetic carbonate cements) at the onset of compressional deformation may have also facilitated fluid migration through parts of the sequence at that time.

Hydrocarbons and copper – a connection?

Preferential copper development along heavy mineral bands at Mufulira and elsewhere, and specifically the nucleation of Cu-sulfides on zircon and monazite grains within these bands requires the presence of a local reductant.

Away from mineralised areas, heavy mineral bands are typically haematite-rich (after original Fe(Ti)-oxides) and thus should have formed an oxidising micro-environment. Thermochemical fixing of hydrocarbons around radioactive heavy minerals (e.g. Rasmussen et al., 1989; Parnell et al., 1990; Buick et al., 1998) could trap/concentrate a suitable reductant within these bands. Hydrocarbon coatings on detrital zircons have been widely described (Stach and Depireux, 1964), although Parnell et al. (1990) note that abundant zircon grains from the Silurian Folley Sandstone (Welsh border) were less commonly associated with hydrocarbon nodules than thorium-bearing heavy minerals thorite and thorianite. Such hydrocarbon nodules may ultimately become sites of sulfide precipitation (including chalcopyrite) at the redox boundary between hydrocarbons (low Eh) and the surrounding (higher Eh) host sediment (Parnell, 1988; Parnell et al., 1990). Local thermo chemical fixing of hydrocarbons along heavy mineral bands is consistent

with previous studies implicating prior hydrocarbon impregnation in the formation of sandstone-hosted deposits (e.g. Mufulira: Annels, 1979).

Model for sandstone-hosted deposits

Gross similarities in character and stratigraphic position of copper ores at Mufulira and Ndola West suggests the following features were important in the formation of these deposits:

1. Relatively clean sandstone host-rocks capped by or sandwiched between less permeable units providing favourable aquifers for lateral ± vertical migration of both hydrocarbons and Cu-bearing fluids
2. Preferential fluid flow and copper precipitation within the Ore formations may have been promoted by (i) proximity to a major regional seal (overlying argillaceous sandstones) and their greater (basin-scale) lateral continuity compared to sandstone units in the footwall (deposited in fault-compartmentalised sub-basins) or (ii) differences in the evolution of grain-scale porosity and permeability across the Lower Roan. For instance, rapid development of diagenetic cements in the relatively clean footwall sandstones, may have inhibited subsequent fluid flow in this part of the stratigraphy.
3. Prior impregnation of sandstone aquifers by hydrocarbons is favoured as a mechanism for sulfate reduction and development of chemical traps to precipitate the copper ores
4. Particularly at Ndola West, the reduced siltstone/shale-dominated package (i.e. Ore Shale facies equivalent) immediately below the mineralised horizon may have originally contained organic matter and provided a local hydrocarbon source.

New age constraints from Mufulira (Scott, 2001c; Dawson, 2002) suggests mineralisation occurred in response to migration of Cu-bearing fluids initiated and driven by compressional orogenesis during the early stages of the Lufilian Orogeny.

Acknowledgments

Peter Mann, Fortson Chisenga (Anglo America, Zambia) are thanked for their support of this research. Dave Selley and Peter McGoldrick for numerous helpful discussions. Galvin Dawson for providing a SHRIMP age for xenotime from one of my Mufulira deposit samples.

References

Annels, A. E., 1979, Mufulira greywackes and their associated sulphides, IMM Transactions / Section B, v. 88, p. B15–B23.

Buick, R., Rasmussen, B., Krapez, B., 1998, Archean Oil: evidenc for extensive hydrocarbon generation and migration 2.5–3.5 Ga: American Association of Petroleum Geologists, v. 82, p. 50–69.

Dawson, G., 2002, Initial SHRIMP geochronology of xenotime and monazite from Mufulira, Konkola North, Ndola East and Chambishi: AMIRA Project P544 – Proterozoic Sediment Hosted Copper Deposits, November 2002 Sponsors Meeting Presentations.

McNaughton, N., 2002, AMIRA P544 status report: *In situ* xenotime and monazite U-Th-Pb geochronology: AMIRA Project P544 – Proterozoic Sediment Hosted Copper Deposits, May 2002 Sponsors Meeting Presentations, P20a.1–P20a.17.

Parnell, J., Metal enrichments in solid bitumens: A review: Mineralium Deposita, v. 23, p. 191–199.

Parnell, J., Monson, B. and Tosswill, R. J., 1990, Petrography of thoriferous hydrocarbon nodules in sandstones, and their significance for petroleum exploration: Journal of the Geological Society, London, v. 147, p. 837–842.

Rasmussen, B., Glover, J. E., and Alexander, R., 1989, Hydrocarbon rims on monazite in Permian–triassic arenites, northern Perth Basin, Western Australia: pointers to the former presence of oil: geology, v. 17, p. 115–118.

Scott, R. J., 2002a, Basement–Roan relations: Ndola West: AMIRA Project P544 – Proterozoic Sediment Hosted Copper Deposits, May 2002 Sponsors Meeting Presentations, P9.1–P9.8.

Scott, R. J., 2002b, Style and stratigraphic context of copper mineralisation: Ndola West: AMIRA Project P544 – Proterozoic Sediment Hosted Copper Deposits, May 2002 Sponsors Meeting Presentations, P18.1–P18.13.

Scott, R. J., 2002c, Character, distribution, timing and origin of copper mineralisation at Mufulira: AMIRA Project P544 – Proterozoic Sediment Hosted Copper Deposits, May 2002 Sponsors Meeting Presentations, P17.1–P17.13.

Stach, E. and Depireux, J., 1964, Kunstliche radioactive Inkohlung: Brennstoff Chemie, v. 46, p. 7–13.

Stratigraphy, regional alteration and mineralization patterns in the Zambian Copperbelt

David Broughton
Colorado School of Mines

Introduction

This report summarizes investigations to date on the stratigraphy and stratigraphic correlation of the Lower Katangan section in the Zambian Copperbelt, presented as a series of slides at the November 2002 meeting. Comments are also made on the regional distribution of alteration and mineralization. A comprehensive tabular summary of regional correlations and previous stratigraphic nomenclatures is underway and will be made available in the near future. The area under discussion is shown in Slide 5, and subdivided for convenience into the western and eastern parts of the Copperbelt.

Western Copperbelt

Lower Roan

Drill hole locations for the sections along the western side of the ZCB are shown in Slide 6, and include holes from Konkola North, Konkola, Kakosa, Nchanga, Chambishi, and Nkana West Limb. The Lower Kundelungu stratigraphy is presented in two sections, hung on the base of the Ore Shale (Lower Roan, Slide 7) and the top of the Shale-With-Grit (Upper Roan and Mwashia, Slide 10).

The Ore Shale footwall is characterized by arkosic sandstones and conglomerates, arenaceous sandstones, and minor siltstones, which show major local thickness changes related to basement topography and early fault-controlled basin compartmentalization. Two kilometres west of the Chingola Open Pit, hole NE112 was collared on a basement high where the Ore Shale was deposited directly on quartz-muscovite-biotite schist (Lufubu Schist). Depth to basement in the Konkola area ranges up to 1000 m. The footwall sequence comprises largely first-cycle siliciclastics, derived from the granitic, gneissic and metasedimentary basement, deposited in fluvial and alluvial fan environments.

The Ore Shale marks a significant change in basin configuration, to a hangingwall sequence characterized by mixed clastic and carbonate (including possible algal laminites) beds, more regionally continuous lithostratigraphic units, and predominance of tidal to shallow-marine conditions. This transgression is recorded by carbonaceous mudstones in the Nkana, western Chambishi and Nchanga areas, versus siltstones and minor mudstones in the Kakosa-Konkola area. In many places it immediately and sharply overlies a conglomerate or conglomeratic sandstone, such as the thin bed of well-rounded quartz pebble conglomerate exposed in the Mindola Pit. In other areas the Ore Shale caps a fining upward cycle initiated with a similar basal conglomerate, and containing dolomitic beds (e.g. hole WL73, Nkana West Limb; Kakosa and Konkola holes).

The Ore Shale hangingwall (Lower Roan) stratigraphy can be regionally subdivided into three major sequences, each of which contains numerous smaller, and commonly correlatable cycles. The lowermost sequence contains mixed clastic and carbonate beds in the south (Nchanga-Chambishi area) and more dominant and coarser-grained clastics in the north (Konkola), and is capped by a regionally extensive sandstone, the TFQ (Upper Quartzite at

Nkana and Chambishi). The sandstone is interpreted to represent a regional base level fall.

The second sequence, the Chingola Dolomite, comprises mixed clastic and carbonate cycles that become increasing carbonate-dominant up section, and usually culminates in a several metre-thick, massive dolomite. The sequence is more dolomitic in the south, and more clastic in the Konkola area, similar to the change in clastic/carbonate ratio in the lower sequence. This reflects proximity to a regional basement high in the Konkola area.

The third and uppermost sequence is the Shale-with-Grit (SWG), which consists of interbedded siltstones and sandstones or conglomeratic sandstones. The SWG commonly begins with a thin basal conglomerate with basement clasts, again indicating a regional base level fall, and shows a general fining upwards trend. Up-section, it becomes interbedded with dolomite, and its top (and the top of Lower Roan) is placed at the base of the first significant (~0.5 m) dolomite bed. The SWG is characterized by abundant millimetre to centimetre scale sandstone dykes, which typically form bridging structures between sandstone and across siltstone ("shale") beds. They are taken as evidence for abrupt release of fluid pressure due to compaction and overpressuring. These features, along with the stratigraphic position and lack of carbonate beds, suggest the SWG formed under conditions of rapid sedimentation in a relatively proximal environment.

At the south end of the Chambishi basin, the Lower Roan sequence is truncated against an albitized polylithic breccia enclosing a thick, locally albitized gabbro (hole WL73). The breccia lacks any recognizable basement clasts, and instead contains generally rounded, intrabasinal clasts of dolomite and sandstone-siltstone. Further to the west at Chibuluma, and along a NW trending structure to just south of the Mwambashi "B" deposit, the breccia is responsible for the Ore Shale "pinch-out". The NW strike extension of this structure coincides with a basement lineament in the Chiryongoli Dome, adjacent to which the basement-hosted Samba Cu deposit occurs. The breccia is similar to others within the Upper Roan and Mwashia on both the eastern and western parts of the Copperbelt, and in the DRC, as described below.

Evidence of evaporitic diagenesis is present from within the Ore Shale (syneresis cracks, halite casts, dolomite nodules after gypsum-anhydrite) through the hangingwall (interpreted polygonal salt teepees on tops of dolomite beds) sequences. Subaerial exposure formed some of these features, others (ie the nodules) formed below the sediment surface. They all indicate evaporitic conditions that would have provided a source of sulfur for later mineralization, and promoted development of a brine capable of metal mobilization.

The Lower Roan sandstones exhibit four main types of cement and/or alteration: quartz, feldspar, carbonate and anhydrite. These can alternate and intermingle on a centimetre scale within a given bed. In some cases the mineralogy is controlled by cross-stratification, in others it is more irregular, with one type forming patches within another. The cements are much more evident in the arenaceous sandstones, which appear to have had primary porosity, versus the arkosic and argillaceous sandstones (greywackes) which probably had little. This is particularly true for the regionally extensive sandstones in the Ore Shale hangingwall (eg the TFQ), which are almost invariably marked by quartz ± feldspar alteration. In some places, two stages of alteration can be discerned, the younger related to discordant quartz-carbonate veinlets. Horizontal fluid flow appears to have been repeatedly focused within these units.

The distribution of visible copper sulfide, pyrite and specular hematite mineralization in the Lower Roan is indicated on the section (Slide 7). On a deposit scale, the distribution of sulfide versus hematite mineralization is broadly stratigraphic. Regionally, copper mineralization in the Ore Shale is discordant, along both N–S (Kakosa to Konkola) and E–W (Chambishi basin) trends. Significant copper mineralization occurs in the Ore Shale footwall in RCB2 (equivalent to the Chibuluma orebody) and NE112 (thin mineralized zone at the top of the basement high), in the Ore Shale and its immediate hangingwall and footwall (Konkola area) and locally in the TFQ at Nchanga (the "Upper

Orebody", not shown). The TFQ elsewhere contains sparse chalcopyrite-pyrite mineralization at its upper contact. Copper mineralization in the Samba deposit is structurally controlled within zones of deformed basement metasediments, probably of the Muva Group.

Specular hematite predominates in the subaerial sandstones and conglomerates of the Ore Shale footwall, and at least locally the basement, and also characterizes the SWG. Hematite also forms vertically continuous, discordant zones in at least two places: the northern part of the Konkola North area (KN8) and the Konkola Barren Gap (KLB67, between KLB94 and KLB145, not shown). There is typically an antithetic relationship between sulfides and hematite, and evidence from textural and cathodoluminence studies of hematite- versus copper sulfide-bearing veins suggests that the specular hematite and sulfide formed synchronously. The hematite may represent a lateral zoning of the sulfide mineralization, or a metamorphic overprint of a "Rote Fäule" type alteration (denoting regional zones of oxidized, metal-leaching fluid flow in the Kupferschiefer).

Upper Roan and Mwashia

The Upper Roan and Mwashia stratigraphy in the western Copperbelt is presented in Slide 10, using the base of the first carbonate bed in the SWG as a datum. The base of the Grand Conglomerat (diamictite) marks the Mwashia Group – Kundelungu Group contact.

In the Konkola area, logging of more than 20 drill holes (not shown) indicates that the Upper Roan consists of individual cycles that are laterally continuous over distances of at least 5 km. The lower part comprises ±metre-thick dolomite beds separating thicker units of SWG (sandstone-siltstone). This grades up to an upper section with ± metre-thick, shallowing-upwards cycles of sandstone/siltstone–dolomitic sandstone/siltstone–dolomite, commonly with white dolomite or talcose nodules and "chicken-wire" evaporite textures at the top. These are interpreted to have formed in subtidal to tidal conditions similar to modern sabkha environments. Within this package are two regionally extensive and quartz-feldspar-cemented/altered sandstones with locally preserved trough cross-bedding, similar to the sheet sandstones in the Lower Roan. These are indicated as marker units on the drill section, and tentatively correlated with similar units in the Nchanga-Chambishi area. They are interpreted to indicate a significant fall in base level.

The stratigraphic division between the Upper Roan and Mwashia Groups coincides with a lithological change from mixed carbonate and argillaceous sandstone deposits to carbonate and siltstone-mudstone, with the mudstones increasingly dominant up-section. In the NW trending "saddle" between the Konkola and Konkola North deposits the transition is abrupt, across a polylithic breccia (KLB145), which has traditionally been interpreted as a basal conglomerate at the base of the Mwashia. However, the breccias are present at a variety of stratigraphic levels on the eastern and western sides of the Copperbelt, and are therefore poorly suited for regional stratigraphic correlation. South and north of the NW trending "saddle" between the Konkola and Konkola North deposits, the breccias are overlain by a sequence of thick dolomites normally interpreted as a lower, dolomitic formation within the Mwashia, which passes upwards into an upper, clastic-dominated formation of siltstones, dolomitic siltstones, fine-grained sandstones, and locally carbonaceous mudstones (KLB94, KN18). These lower and upper formations are comparable to the Mwashia Inferieur and Superieur recognized in the DRC (Cailteux et al., 1995). The lower, dolomitic formation of the Mwashia commonly contains scattered to crudely stratiform grey-white, 1–10 cm-sized cherty nodules and patches, interpreted as silicified evaporitic nodules. They can be distinguished from the nodules in the underlying Upper Roan beds by their larger size and silicification, but are not unique to the lower Mwashia: similar cherty patches occur in the Kakontwe Dolomite above the Grand Conglomerat in KLB94.

The Konkola saddle area may mark the location of a NW trending structural high, which isolated platformal environments to the north and south. An alternative explanation was presented at the P544 field meeting in Zambia, and suggested that the absence of the lower dolomite sequence in the saddle area was

due to fault removal associated with the polylithic breccias, interpreted to represent a highly fluidized fault plane. This interpretation of the breccias parallels arguments put forth in the DRC to explain the origin of similar breccias there (Cailteux and Kampunzu, 1995), and will be discussed later in this report. In this context it is relevant that the breccias commonly mark a significant increase in the amount of deformation recorded in the Mwashia hangingwall, versus the Upper Roan footwall, but are themselves relatively undeformed. Transposition, layer-parallel folds and foliation boudinage are common in the Mwashia siltstones-sandstones, and raise the possibility of large-scale fold repetition of units.

The thin shallowing-upwards cycles characteristic of the Upper Roan stratigraphy are absent in KLB94, such that the SWG is directly overlain by polylithic breccia, followed by a sequence of thick-bedded dolomites and interbedded dolomite-siltstone. KLB94 is the southernmost deep hole in the Konkola area, and there are no drill holes collared in or above the Mwashia between KLB94 and the Chambishi Basin, save NE112 at Nchanga. In NE112, the Kundelungu Grand Conglomerat directly overlies mixed dolomites and clastics placed in the Upper Roan Group, indicating erosion or non-deposition of at least the upper, siltstone-mudstone dominated formation of the Mwashia Group. The Mwashia Group is also absent or unrecognized from the area southwest of the Copperbelt.

Sill-like gabbro bodies are present in the Mwashia (Konkola area, KN18), Upper Roan (northern and central Chambishi basin, e.g. RCB2), and Lower Roan (southern Chambishi basin, Chibuluma South) and therefore show a regional, north–south, "step-down" geometry. Although they most commonly occur within dolomites and polylithic breccias, drill cores at south and west of the Chambishi Basin (Chibuluma South, Kabula) demonstrate that they have intrusive, non-brecciated, footwall contacts with Lower Roan rocks. The latter examples, at least, are unlikely to represent allochthonous bodies transported along fault breccias, an explanation favoured by many authors for the emplacement origin of the gabbros (see summary in Binda and Porada, 1995). Similar gabbroic bodies, mafic flows and tuffs are known in the central and western parts of the Zambian Copperbelt, within the Mwashia Group and Grand Conglomerat, and have been dated at ~740 to 760Ma (Key et al., 2001; J. Barron, pers. comm.. 2002). They record extension associated with continental breakup, roughly temporal with the Sturtian glaciation and deposition of the Grand Conglomerat. Lufilian-aged (503 Ma) gabbro intrusions are known in the vicinity of the Hook Granite, and have tentatively been linked to Fe skarn mineralization (Meinert et al., 2001).

Eastern Copperbelt

Drill hole locations for the sections along the eastern side of the ZCB are shown in Slide 11, and include holes from Konkola, Kawiri, Lubembe, Luansobe, Mufulira, Ndola and Ndola West. The Lubembe stratigraphic section is compiled from Lefebvre (1989) and Lefebvre and Tshiauka (1986). The Ndola West drill hole was logged by Rob Scott, CODES. The Lower Kundelungu stratigraphy is presented in two sections, hung on the base of the Mudseam (Lower Roan, Slide 17) and the top of the Glassy Quartzite (Upper Roan and Mwashia, Slide 19).

Lower Roan

In the Mufulira-Luansobe area, the Mudseam is a ~1-2 m thick sequence of interbedded dolomite and siltstone/mudstone that overlies the C Orebody sandstone. Below the Mudseam, the Lower Roan Group consists of thickly bedded fluvial-alluvial arkosic sandstones and conglomerates, and lesser large-scale cross-bedded, possibly aeolian, quartz sandstones, and is characterized by significant lateral facies and thickness changes. Above the Mudseam, the Lower Roan Group comprises a series of laterally persistent sandstone-siltstone-dolomite cycles, which gradually become finer-grained and show an increasing abundance of evaporitic textures up-section.

The Mudseam therefore appears to mark a flooding surface that signals a significant change in basin tectonics and architecture, and is correlated with

the base of the Ore Shale in the western Copperbelt. In the Lubembe area (Lefebvre, 1989), the equivalent unit and surface is here interpreted to be the "F.Q". horizon, a 30–180 cm unit of greenish siltstone that separates arkosic and quartz sandstones of the Lubembe and Simbi Members from argillaceous and dolomitic sandstones with local evaporitic textures of the Kabemba and Kitotwe Members. Lefebvre (1989) recognized that the F.Q. horizon separated a lower compartmentalized from an upper amalgamated basin phase, and even commented on its lithologic similarity to the Ore Shale, but correlated the Ore Shale with a siltstone near the top of the Lower Roan Group, at the base of the Glassy Quartzite. His interpretation has been followed by researchers in IGCP Project 302 in discussing stratigraphic correlation in the Musoshi-Kinsenda district, and between the DRC and Zambian Copperbelts (Cailteux et al., 1995; Tshiauka et al., 1995). This new interpretation will be tested by incorporation of detailed historical drill data from the Kawiri area, and logging of drill core in the Lubembe area in March, 2003.

The gradual fining upwards trend in the Lower Roan above the Mudseam is punctuated by the deposition of two regionally traceable sandstone or pebbly sandstone units, the Marker Grit and the Glassy Quartzite. Both locally contain trough cross-bedding and are interpreted as fluvial deposits marking a relative fall in base level. The sandstones are characterized by patchy to intense development of white alteration, consisting of quartz-muscovite-(albite), and minor chalcopyrite-pyrite mineralization along their upper contacts, similar to that in the TFQ throughout most of the western Copperbelt. The Marker Grit is tentatively interpreted as equivalent to the TFQ, and the Glassy Quartzite as the lower of the two sheet sandstones in the Upper Roan in the western Copperbelt. The Glassy Quartzite at Mufulira-Luansobe is taken as the top of the Lower Roan, and correlated with the base of Lefebvre's (1989) Musoshi Formation at Lubembe.

In the Itawa/Ndola area, the Itawa drill holes IT25 and IT28 intersected a similar and reasonably correlative stratigraphic sequence to that at Mufulira, including sandstone cycles tentatively correlated with the C Orebody, Marker Grit and Glassy Quartzite. At Ndola West, the stratigraphy above the interpreted equivalent of the C Orebody sandstone is less well defined.

The Lower Roan stratigraphy is difficult to correlate in detail through the Kawiri area between Konkola and Lubembe. The thickness of the Lower Roan changes dramatically between western Kawiri (hole KW24), where the Ore Shale apparently pinches out against a basement high, and Konkola (KLB145), where the sub-Ore Shale depth to basement is up to a kilometre. This supports the interpretation of a NW-SE, basin-controlling structural high separating an eastern (Lubembe-Mufulira-Ndola) from a western (Konkola-Nchanga etc) sub-basin.

The NW structural high also influences the sedimentary environment above the Ore Shale, most obviously by the difficulty in correlating the Shale-with-Grit east of hole KW24. Correlation is made here on the basis of the Chingola Dolomite, the sheet sandstones, and the base of the sabkha-type cycles of the Upper Roan. Although "gritty" sandstones and siltstones are common in the Lower (and Upper) Roan both east and west of the Kafue Anticline, the thin bedding and sandstone dykes characteristic of the SWG are only found in the west.

The NW structural high coincides with a west-to-east change in the Upper Roan stratigraphy, including the development of extensive polylithic and tectonic breccias and the recognition of DRC-type Mines Group and Dipeta Group lithologies in the eastern Copperbelt (see below). In the DRC, the breccias occur along NW trending breached anticlines that dominate the regional structural grain (Slide 5). Two similarly oriented structures marked by development of breccias, gabbro intrusions, and truncation of the Ore Shale occur in the southern Chambishi basin, and at Chibuluma South. Stratigraphic cut-outs related to breccias and gabbros are also known in the Luanshya basin, and on the western side of the Konkola dome (ie west of the Konkola North/Musoshi deposit).

Lower Roan Group mineralization in the eastern Copperbelt occurs in at least three settings. Northeast faults localize copper mineralization in the basement and the basal arkosic sandstones and conglomerates

just across the international border at Lubembe and Kinsenda (9Mt @ 5.85% Cu), and have associated quartz-sericite-calcite-(chlorite-epidote-albite) alteration (Lefebvre, 1989). The Musoshi deposit is characterized by NE trending corridors of intense quartz-sericite alteration and veins (Richards et al., 1988). The Kasumbalesa Fe (hematite) deposit just north of Musoshi-Konkola is also localized along a NE fault within basal Lower Roan arkosic sandstones and conglomerates, again with associated quartz-sericite alteration (Lefebvre, 1989). In the Kinsenda and Lubembe areas these faults host gabbroic dykes that are aeromagnetic targets; the horst and graben geometry they produce would also constitute a gravity target. Evaluation of widely spaced drill holes at Luansobe suggests the presence of similar controls there, based on recognition of localized basement alteration and variations in basal Lower Roan thickness and facies distribution.

The A, B and C sandstones of the Mufulira orebodies are relatively "clean", with good potential for porosity and permeability, in comparison to the underlying arkosic and overlying argillaceous units, and represent a second type of mineralization setting. These orebodies are much more laterally continuous than those directly related to faults, and may have formed through ore fluid reduction via hydrocarbons (Annels, 1979). The two settings appear mutually exclusive: there are no known Lubembe-type "footwall" orebodies at Mufulira, nor any Mufulira-type "hangingwall" orebodies at Lubembe-Kinsenda.

The Ore Shale-type setting of mineralization typical of the western Copperbelt is also worth comment. Ore Shale-equivalent lithologies occur at Lubembe and also Itawa, but are thin and poorly mineralized. Better mineralization may occur against basement highs, or where the siltstones/mudstones were more pyritic (availability of reductant for later cupriferous fluids). The Marker Grit and Glassy Quartzite are typically altered and host weak chalcopyrite-pyrite mineralization along their upper contacts. They are therefore similar to the TFQ, which is regionally altered but only hosts economic mineralization at Nchanga.

Regional metal zoning between proximal copper and distal zinc mineralization is hinted at by the presence of sphalerite mineralization in two deep holes at Luansobe, L80 and L83, and by four holes downdip from a small Cu deposit approximately midway between Luansobe and Mufulira. Values occur in the C sandstone, and range from 1 to 2% Zn over true thicknesses of 5–16 m. The mineralization was examined in L80, within a dark grey, slightly carbonaceous, feldspathic sandstone (greywacke). The sphalerite occurs as replacements and mantles on earlier-formed pyrite, disseminated anhedral grains (completely replaced pyrite?), and in dolomite veinlets — in other words, in an identical setting to that of chalcopyrite in the copper zones. Further work is required to determine whether this mineralization represents a regional zoning, or a local feature.

Upper Roan and Mwashia

The base of the Upper Roan is marked by a metre-thick, grey dolomitic siltstone that lies between the Glassy Quartzite and the overlying shallowing-upwards sabkha cycles of sandstone-siltstone-dolomite. These cycles are comparable to those overlying the SWG in the western Copperbelt. They tend to thicken up-section, and are overlain by a locally trough-cross-bedded, white, quartz-feldspar altered sandstone, termed the Middle Quartzite at Mufulira. It is overlain by more cycles of sandstone-dolomite, followed by another grey dolomitic siltstone, which becomes carbonaceous in the central Mufulira area and is termed the Blue Shale. In the Mufulira area, a second, up to 100 metre thick sequence of argillaceous to feldspathic and in places cross-bedded sandstone is present higher in the section, and locally termed the Barrier Quartzite. It is thin or absent at Luansobe. There is no correlative thick sandstone in the western Copperbelt, but similar rocks are described at this approximate stratigraphic level in the Tenke area of the DRC. Texturally, clasts of these sandstones would be difficult to distinguish from some of the Lower Roan sandstones, particularly in the (typically altered) polylithic breccias.

The upper part of the Upper Roan in the eastern Copperbelt is characterized by extensive

and repetitious accumulations of polylithic breccia, lithologically similar to breccias in the western Copperbelt. They contain intrabasinal clasts and lack recognizable basement clasts, have a matrix that may include chlorite, quartz, dolomite, anhydrite and albite, and are typically accompanied by the development of tectonic crackle and mosaic breccias, particularly in their footwall (Slide 19). The tectonic breccias comprise mm-sized stockworks of quartz-dolomite-anhydrite-talc that range from less than five to more than 50% of the rock volume, and grade into mosaic breccias. All of these features are comparable to those described for tectonic and polylithic breccias in the DRC. The polylithic breccias are developed at numerous stratigraphic levels, but are less laterally continuous than the regionally extensive sheet sandstone and dolomitic siltstone markers.

Importantly, the Middle Quartzite and Blue Shale can be traced from areas where the tectonic and polylithic breccias occur only much higher in the section (MW107), to areas where they are enveloped by breccias (DH218, 219). Despite the clearly tectonic (brittle fracture) origin of the crackle and mosaic breccias, this precludes the interpretation of the breccias, at least at this stratigraphic level, as representing zones of significant horizontal dislocation. This conclusion is in contrast to that of Cailteux et al. (1994), who interpreted the Blue Shale and adjacent dolomites in hole DH218 as a tectonically emplaced block of stratigraphy equivalent to the Mines Group, in the DRC. The stratigraphy may well be equivalent, but it does not appear to be structurally emplaced. If their identification of these units as belonging to the Mines Group is correct, a stratigraphic correlation is implied between the DRC ore-hosting Mines Group and the Zambian Upper Roan. Higher in the Upper Roan stratigraphy, there is at present insufficient stratigraphic data to similarly constrain the origin of the breccias.

The regional distribution of the breccias appears to bear a spatial relationship to the Mufulira deposit, as they are far more extensive there, and are present much lower in the stratigraphic section, than at Itawa and Luansobe. This is similar to their regional distribution with respect to copper-cobalt and polymetallic deposits in the DRC, where the association is almost ubiquitous, as well as in certain other parts of the Zambian Copperbelt (Samba, Mwambashi B, and Nkana along a major NW lineament with breccias; Chibuluma South along a parallel lineament).

The matrix and clast rims of the polylithic breccias are commonly altered to an assemblage that includes albite, dolomite, anhydrite, scapolite, and talc, that texturally appears to overprint an earlier, unaltered chloritic matrix. This assemblage is similar to that of the tectonic crackle and mosaic breccias, which can locally be seen to overprint the polylithic breccia. However, the polylithic breccias also contain clasts of brecciated material, suggesting a link between the two types of breccia, or multiple stages of polylithic breccia generation. These complexities aside, the mineral assemblage indicates that the breccias were preferred sites for saline fluid flow, and evaporite dissolution is thought to have been critical to their formation. It is unclear whether evaporites were originally present at the current stratigraphic position of the breccias, or elsewhere in the stratigraphic section. The general lack of such breccias and much diminished abundance of evaporitic textures in the Mwashia and Kundelungu Groups indicates that the evaporites originated in the Upper Roan.

The transition between the Upper Roan and Mwashia is similar to that in the western Copperbelt, with a lower, thick-bedded, silicified nodular-bearing, dolomitic sequence locally present at the base of the Mwashia. In the Luansobe area, and possibly at Mufulira, a middle sequence of interbedded dolomite and siltstone/mudstone can be distinguished from an upper sequence of carbonaceous mudstones, mudstones and siltstones. As in the western Copperbelt, there is commonly a shear/fault zone up to 10 metres thick at or near the base of the Mwashia. This zone can provisionally be traced over much of the northern part of the Copperbelt, and typically overlies the uppermost polylithic breccia horizon. It may be responsible for removal of the basal Mwashia stratigraphy in some areas.

Alteration is widespread in the Upper Roan, as albite-dolomite-anhydrite associated with the breccias, and as K-feldspar and/or albite-quartz

in the sheet sandstones. Silicification of evaporitic nodules is prevalent at the base of the Mwashia. The entire Roan package appears to have undergone extensive alteration, which would have provided a much larger source volume for leaching metals. Fine-grained disseminated pyrite is more common than in the Lower Roan, and characteristic of the dolomitic sequences and altered sheet sandstones. Hematite is more typical of the argillaceous sandstones, both in the Lower and Upper Roan.

Preliminary geochemical results on drill holes MW107, L80 and DH219 indicate that the basement and the first-cycle clastics of the Lower Roan and Upper Roan are relatively low in Cu and associated metals, outside of the mineralized zones (MW107), typically with values ranging from 1 to 10 ppm Cu. This is up to an order of magnitude lower than the average background values for first-cycle sandstones and conglomerates, and supports a model whereby metals were locally derived.

Summary

Regional correlation suggests that the base of the Ore Shale and the Mudseam are stratigraphically equivalent, and represent a fundamental change in basin tectonics and sedimentation. Correlation of the overlying Lower and Upper Roan sequences is possible using siltstone/mudstone deposits representing base level rise, and laterally extensive sheet sandstones representing base level fall. Polylithic and tectonic breccias characteristic of the Upper Roan do not define major zones of horizontal detachment, at least where sufficient data exists for constraint. However, similar breccias in the DRC clearly form important dislocations, along NW trending breached anticlines, and are associated with mineralization. In the Zambian Copperbelt, breccias are also prevalent along NW and E-W oriented structures, at least some of which have associated mineralization. Their mineralogical and stratigraphic characteristics can be explained by derivation from evaporites, through dissolution. The Lower and Upper Roan sequences contain abundant evidence for the presence of evaporitic conditions, and passage of saline fluids, likely a significant factors in the genesis of the deposits.

Mineralization occurs at multiple stratigraphic levels and in a variety of lithologies on both a local and regional scale. Early extensional faults associated with the accumulation of the immature Lower Roan footwall clastics were rooted in the basement, and localized mineralization. Many of the large orebodies are spatially associated with the Ore Shale – Mudseam interval, representing an important tectonic, stratigraphic and sedimentological change in the basin. One major orebody (TFQ) occurs in one of the sheet sandstones higher in the section, and minor mineralization occurs locally in dolomitic siltstones and dolomites of the Upper Roan, possibly equivalent to the orebodies in the DRC.

References

Annels, A.E., 1979. Mufulira greywackes and their associated sulphides. Trans. Inst. Mining Metall., v. 88, B15-B23.

Binda, P.L. and Porada, H., 1995. Observations on the Katangan Breccias of Zambia. Musee Royal de L'Afrique Centrale, Telveuren, Belgique, Annales Sciences Geologiques V. 101, p. 49-62

Cailteux, J., Binda, P.L., Katekesha, W.M., Kampunzu, A.B., Intiomale, M.M., Kapenda, D., Kaunda, C., Ngongo, K., Tshiauka, T., and Wendorff, M., 1994. Lithostratigraphical correlation of the Neoproterozoic Roan Supergroup from Shaba (Zaire) and Zambia, in the Central African copper-cobalt metallogenic province. J. African Earth Sci., v.19, p. 265-278.

Cailteux, J.L.H., and Kampunzu, H.A.B., 1995. The Katangan Tectonic Breccias in the Shaba Province (Zaire) and their genetic significance. Musee Royal de L'Afrique Centrale, Telveuren, Belgique, Annales Sciences Geologiques, V. 101, p. 63-76.

Cailteux, J., Binda, P.L., Kampunzu, A.B., Katekesha, W.M., Kaunda, C., and Wendorff, M., 1995. Results of lithostratigraphic correlation of the Late Proterozoic Roan Supergroup between Zambia and Zaire, Central African Copperbelt. Musee Royal de L'Afrique Centrale, Telveuren, Belgique, Annales Sciences Geologiques, V. 101, p. 21-27.

Key, R.M., Liyungu, A.K., Njamu, F.M., Somwe, V., Banda, J. Mosley, P.N., and Armstrong, R.A., 2001. The western arm of the Lufilian Arc in NW Zambia and its potential for copper mineralization. J. African Earth Sci, v. 33, pp 503-528.

Lefebvre, J.J., 1989. Depositional Environment of Cu-Co Mineralization in the Katangan Sediments of Southeast Shaba (Zaire). In: Boyle, R.W., Brown, A.C., Jefferson, C.W., Jowett, E.C., and Kirkham, R.V. (eds.), Sediment-hosted Stratiform Copper Deposits, Geol. Assoc. Canada Sp. Paper 36, p. 401-426.

Lefebvre, J.J. and Tshiauka, T., 1986. Le Groupe de Mines a Lubembe, Shaba, Zaire. Annales de la Societe geologique de Belgique, T. 109, pp. 557-571.

Meinert, L.D., Nicolescu, S., Mortensen, J.L., and Cornell, D.H., 2001. U-Pb dating of hydrothermal garnet from skarn deposits – Implications for petrogenesis and ore deposits. Geological Society of America Annual Meeting Program with Abstracts, paper 53-0 (web address: http://gsa.confex.com/gsa/2001AM/final program/abstract_23197.htm).

Richards, J.P., Krough, T.E., and Spooner, E.T.C., 1988b, Fluid inclusion characteristics and U-Pb rutile age of late hydrothermal alteration and veining at the Musoshi stratiform copper deposit, Central African copperbelt, Zaire. Economic Geology, v. 83, p. 118-139.

Tshiauka, T., Katekesha, W.M., Cailteux, J., Intiomale, M.M., Kampunzu, A.B., Kapenda, D., Chabu, M., Ngongo, K., Mutombo, K., and Nkanika, W.R., 1995. Lithostratigraphy of the Neoproterozoic Katangan sedimentary sequences in the Musoshi Copper District (SE Shaba, Zaire) and incidences on copper and cobalt economic geology in Central Africa. Musee Royal de L'Afrique Centrale, Telveuren, Belgique, Annales Sciences Geologiques,V. 101, p. 29-48.

Towards a unified geologic and exploration model for the Zambian Copperbelt

Murray W. Hitzman
Colorado School of Mines

The attached PowerPoint® presentation from the November 2002 meeting summarises the important results to date for P544. The project has made great strides in understanding the stratigraphic and structural controls to mineralisation and is beginning to produce results on the regional alteration architecture. Significant work remains to be done in all areas, however. The stratigraphic architecture of the Lower Roan is fairly well understood. Selley's detailed work relating stratigraphy to structure answers many questions concerning the location of mineralised centres. However, the stratigraphy of the upper portions of the sedimentary sequence – Upper Roan, Mwashia, and Lower Kundelungu – require additional work. This work is actively underway (Broughton/Hitzman). The dataset may not allow us to develop a well integrated stratigraphic/structural model for the upper portion of the sequence, but the results will be a quantum leap beyond what is available in the existing literature. Research in the next several months focused on the regional alteration architecture of the sequence should provide critical data to evaluate the models presented in the attached PowerPoint presentation. Work by both CODES and CSM personnel on the geochemistry (major element, particularly K, Na; trace element; and isotope) of the Lower Roan should allow us to determine whether geochemical vectors to ore are present. This work may also allow a better determination of the actual mechanisms of sulfide precipitation which are thought to be largely an oxidation/reduction control. We will more closely evaluate possible reductants (and palaeo-reductants). Looking more broadly at the geochemistry of the entire sedimentary sequence below the Grand Conglomerate should allow evaluation of broad-scale fluid-flow mechanisms. This work is in progress (Broughton/McGoldrick).

Important Results to Date - Towards a Unified Geologic and Exploration Model

Murray W. Hitzman
Colorado School of Mines

Outline

- Sedimentary architecture / structure
- Alteration and lithogeochemistry
- Mineralization
- A Genetic Model for the Zambia Copperbelt
- Implications of the Model
- Remaining problems and future work to solve them.

Sedimentary Architecture and Structure

Sedimentary Architecture / Structure

- **Sedimentary architecture of the Lower Roan indicates it was deposited in an extensional (rift) environment.**
- **Basal sediments are arkosic conglomerates and sandstones derived from granitic basement in a fan-delta environment.**
- **"Ore shale" represents a starved basin and occurs at a major change in basin configuration.**

Sedimentary Architecture / Structure

- First-order, NW-trending faults (Konkola, Nchanga sycline, east side Chambishi basin) and third-order faults (Chambishi, Lusombe) are recognized.
- These faults controlled Lower Roan sedimentation; the first order faults appear to have continued to have controlled some aspects of sedimentation up into the lower Kundelungu.

Sedimentary Architecture / Structure

- The Upper Roan is a mixed carbonate-siliciclastic sequence with punctuated extensional tectonic phases recognized by coarse siliciclastic layers.

Sedimentary Architecture / Structure (cont.)

- The Upper Roan contains abundant breccias making tracing of stratigraphy throughout the Upper Roan extremely difficult.
- Origins of the breccias are diverse and probably include:
  - Sedimentary
  - Dissolution / collapse
  - Intrusive-related
  - Tectonic
  - Combinations of events
- Upper Roan breccias (combined with alteration of Upper and Lower Roan sediments) probably indicate significant thicknesses of halite-bearing evaporites were once present in the Upper Roan.

Sedimentary Architecture / Structure (cont.)

- The Roan - Mwashia sequence is relatively thin (1-2 km) in the Copperbelt; evaporites could have increased section to 3km.
- The Mwashia grades upward from a carbonate-rich base to dominantly siltstones. It apparently served as a regional "seal."
- The Grand Conglomerate serves as a regional marker unit. It appears to consist of both glacial diamictites and turbidites (indicating tectonically active basin conditions?).

Sedimentary Architecture / Structure (cont.)

- Gabbro intrusions are concentrated in the Upper Roan section but are recognized from the basement to the Grand Conglomerate. Dating elsewhere in northern Zambia suggests ages of 765-740 Ma.
- Gabbro intrusions appear to cluster adjacent to first-order faults; therefore magnetics may aid in locating these faults (e.g. Chambishi basin).

Sedimentary Architecture / Structure (cont.)

- Zambian Copperbelt does NOT occupy a major basin.

Alteration and Mineralization

Alteration and Lithogeochemistry

- **Alteration is recognized in the Katangan sequence from at least the basal portion of the Mwashia down into the basement.**
- **Both potassic and sodic styles of alteration are observed.**

Alteration and Lithogeochemistry (cont.)

- Potassic alteration produces fine-grained potassium feldspar (commonly confused with albite during logging) and provides the potassium for later (?) biotitization.
- Potassic alteration appears to be concentrated in siliciclastic lithologies which were probably more porous and permeable.
- Sodic alteration produces albite and scapolite. It is well developed in the Upper Roan and locally in clean sands, near the base of the section. Sodic alteration is also present adjacent to gabbro bodies and in some carbonate units (scapolitized).
- It appears that potassic alteration generally predates sodic alteration.

Mineralization

- Zambian Copperbelt mineralization is fundamentally controlled by oxidation change.

Mineralization (cont.)

- The location of footwall orebodies is controlled by the sedimentary architecture related to third order faults and the presence of sedimentary "seals."
- Ore shale orebodies are controlled by the presence of carbonaceous (relatively reducing) lithologies and adjacent (generally stratigraphically below) permeable lithologies.
- Arenaceous (and probably footwall) orebodies controlled by the former presence of hydrocarbons (natural gas and petroleum) which served as reducants. These reducants were in physical traps.

Mineralization - Footwall Orebodies

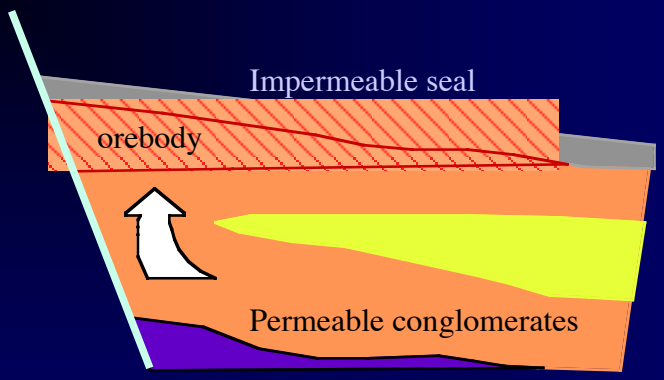

- The location of footwall orebodies is controlled by the sedimentary architecture related to third order faults and the presence of sedimentary "seals."

Mineralization - Ore Shale Orebodies

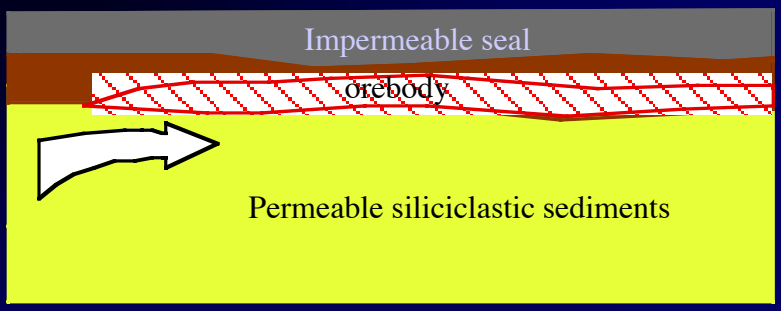

- **Ore shale orebodies are controlled by the presence of carbonaceous (relatively reducing) lithologies and adjacent (generally stratigraphically below) permeable lithologies.**

Mineralization - Arenaceous Orebodies

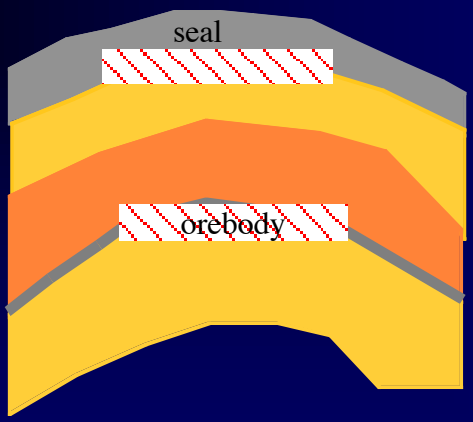

- **Arenaceous (and probably footwall) orebodies controlled by the former presence of hydrocarbons (natural gas and petroleum) which served as reducants. These reducants were in physical traps.**

Genetic Model for the Zambian Copperbelt

Key Ages

- 870 Ma — Nchanga Granite (basement)
- 765 — Volcanic rocks in Mwashia
- 765 - 740 — Gabbros
- 735 — Volcanic rocks in Grand Conglomerate (Sturtian glaciation)
- 650 — Initial metamorphism of Katangan sequence
- 670 - 620 — Shinkolobwe U deposit
- 645 — Albite-Cu veins at Musoshi
- 615 — Xenotime/monazite ages - Mufulira
- 560 — Xenotime/monazite ages - Copperbelt ; Hook Granite
- 535-470 — Xenotime/monazite ages - Copperbelt
- 510 - 490 — Vein Cu-Mo-U mineralization (Kansanshi)
- 495 — Cooling below 300°C blocking T for Ar in biotite
- 470 — Cooling below blocking T for Ar in muscovite

Lower Roan Sedimentation

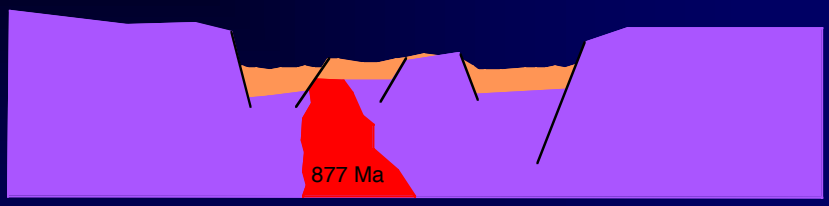

- **Extensional environment (post 870 Ma) leads to complex fluvial/alluvial basal section (lower Roan) dominated by basement derived arkose.**

Lower Roan Sedimentation

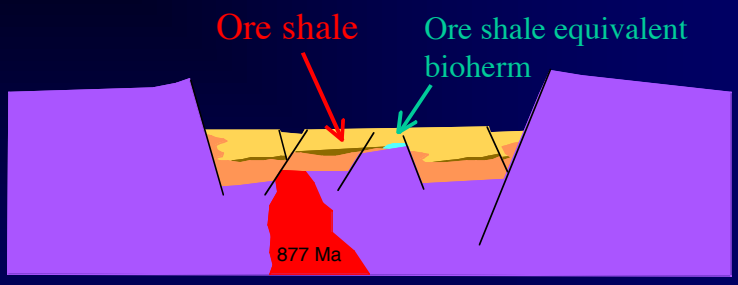

- **Coarse basal siliciclastics covered by mixed sequence of siltstones, rare shales (“Ore Shale”), and carbonates.**

Lower - Upper Roan Sedimentation

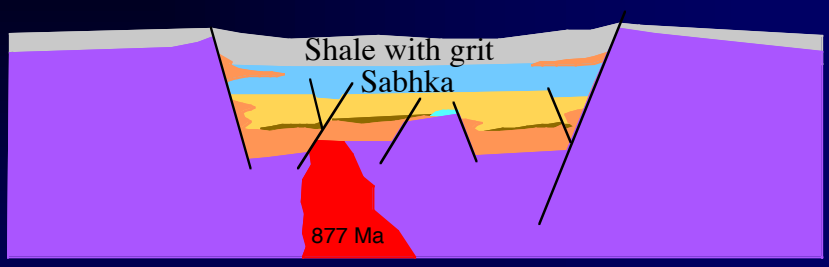

- **Covering of basement topography leads to more mature, layer-cake sedimentary geometry with mixed marine (?) siliciclastic-carbonate facies overlain by sabhka carbonate facies.**
- **Punctuated extensional events provide coarse siliciclastic input.**

Upper Roan Sedimentation

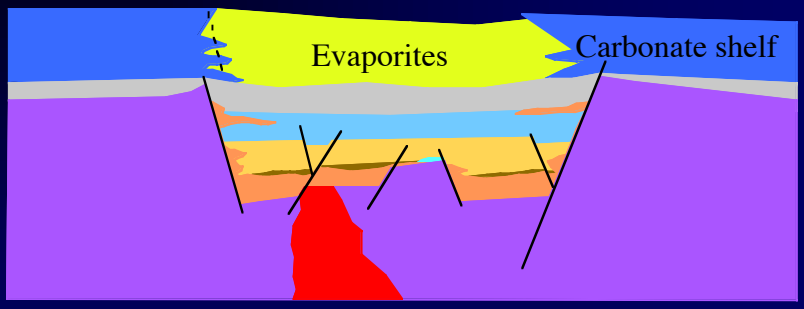

- **Probable restriction of basin leads to evaporite (gypsum + halite) precipitation.**

Mwashia Sedimentation

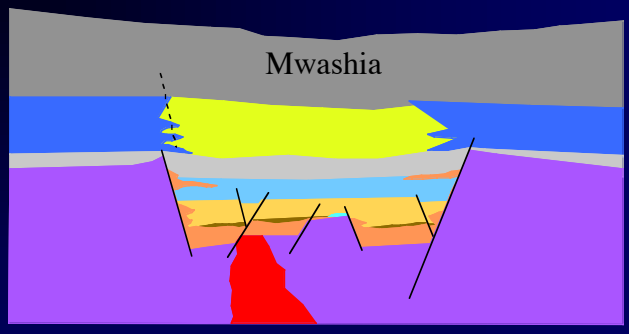

- **Mwashia consists of basal carbonate-rich sediments grading up to siltstones.**

Lowermost Kundelungu + Gabbros

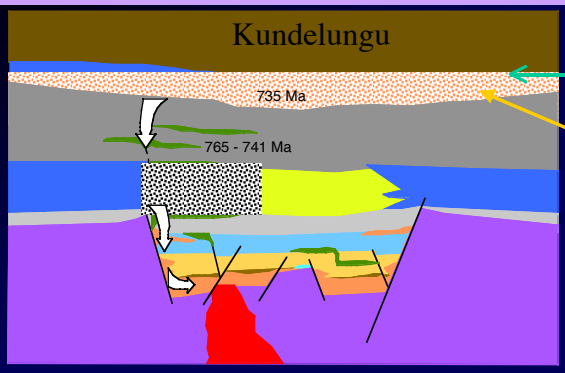

"Cap" carbonates

Grand Conglomerate diamictite

- **Extensional event (765-740 Ma) with intrusion of gabbros.**
- **Close to time of Grand Conglomerate - "Snowball Earth."**
- **Extensional event probably caused thermal maturation and migration of hydrocarbons. This event may also have allowed incursion of water (glacial, meteoric?), evaporite movement and dissolution, and brine formation.**

Initiation of Lufilian Deformation (circa 650 Ma)

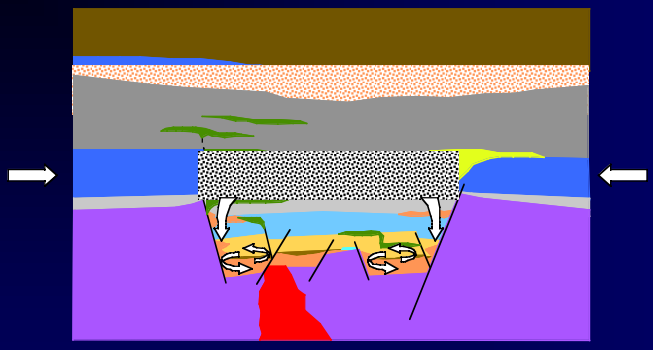

- Salt tectonics continue during earliest Lufilian deformation (probably around 650 Ma).
- Continued brine formation and movement downward.
- Breccia formation (collapse and tectonic) in Upper Roan section.

November 2002

Lufilian Deformation (650 - 500 Ma)

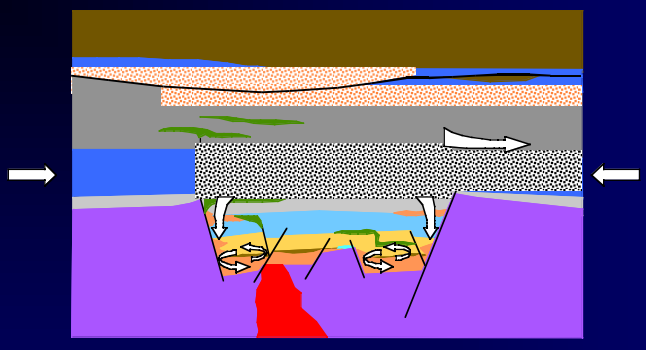

- Continued compression with salt movement and dissolution.
- Brines continue to sink into Upper and Lower Roan sequence.
- Mineralization occurring during this time - reaction of oxidized, metal- and sulfur-rich brines with local oxidation traps (carbonaceous sediments and gas/oil accumulations).

November 2002

Lufilian Deformation (~540 - 510 Ma)

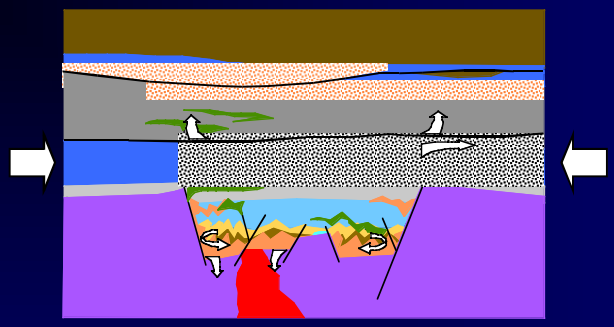

- Continued deformation results in upright tight folding in Lower Roan sequence nucleated on early faults.
- Structural decoupling near base of Mwashia.
- Deformation in upper sequence largely recumbent folds and low-angle (thrust) faults.
- Deformation provides energy for renewed brine movement and escape in basement and overlying rocks.

Basin-scale Alteration

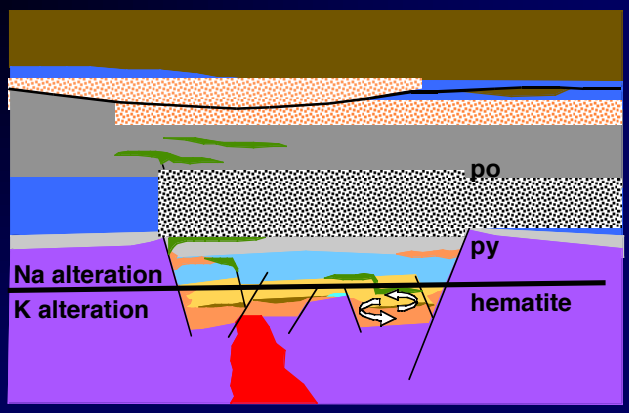

- Upper and Lower Roan sections highly altered from brines ("pickled")
- General pattern of upper sodic alteration and lower potassic alteration with hematite.

Implications of the Model

Implications of the Model

- **Whole basin hydrothermal system.**
- **Dominant fluid flow pattern is downward.**
- **Downward flow probably concentrated along first-order original basin-bounding faults; would probably alter gabbros.**
- **Flow within sedimentary sequence is lateral and controlled by porous and permeable units (coarser siliciclastics).**

Implications of the Model (cont.)

- Basin-scale alteration pattern.
- Dominant alteration zones are potassic and sodic - appears that sodic best developed at higher level and potassic in more basal position.
- May not be deposit-specific alteration patterns.

Implications of the Model (cont.)

- Delineation of reduced zones within the basin is critical.
- Any type of reduced zone may be favorable
  - Carbonaceous sediments
  - Physical gas or petroleum trap

Implications of the Model (cont.)

- **Multiple deposit types may be present at multiple stratigraphic horizons:**
  - **Zambian Copperbelt type**
  - **Congo Copperbelt type**
  - **Kipushi type**
  - **Kansanshi type**

Implications of the Model (cont.)

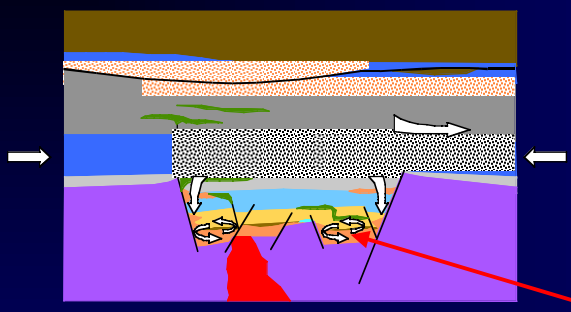

- Zambian Copperbelt —
  Ore deposits in carbonaceous sedimentary layers and physical gas/oil traps in Lower Roan.

Implications of the Model (cont.)

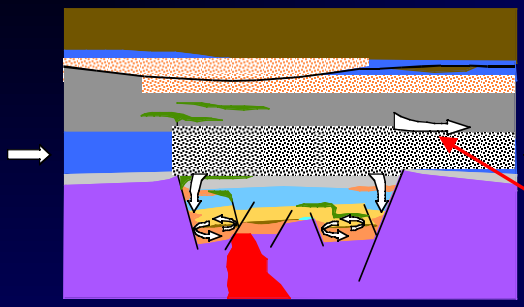

- Congo Copperbelt —
  Ore deposits in stratiform breccia zones (gas traps?) and fetid dolostones (carbonaceous) in Upper Roan equivalent sediments.

Implications of the Model (cont.)

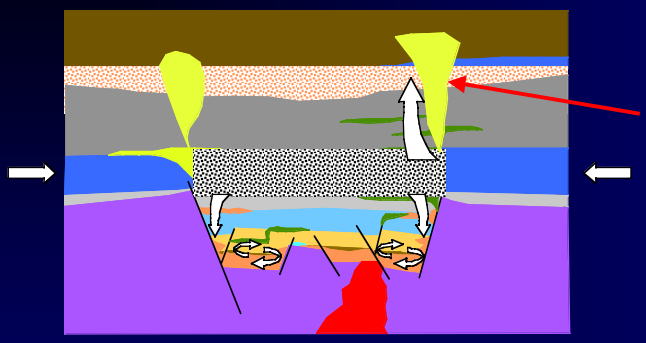

- Southern Congo / Namibia —
  Ore deposits in cross stratal breccia pipes (paleo salt domes) charged with gas/oil cutting Mwashia and Kundelungu sequence.

Implications of the Model (cont.)

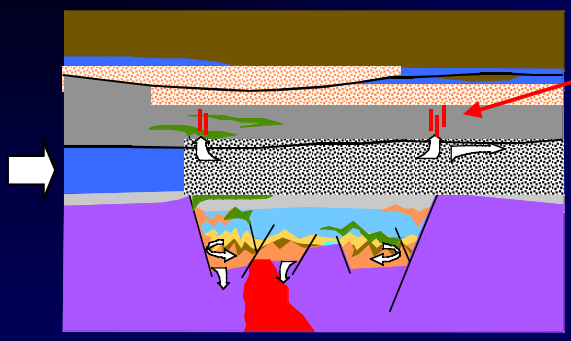

- Northern Zambia / Southern Congo —
  Tectonically-induced fluid escapeways into the reduced Mwashia. (e.g. Kansanshi, Shinkolobwe)

Implications of the Model (cont.)

- **Global exploration for Copperbelt-type systems should focus on:**
  - **Basins which contained salt.**
  - **Basins where salt underwent dissolution to form brine which caused large-scale, intense alteration.**
  - **Search for reducing zones within such basins.**

Remaining problems and future work to solve them.

Remaining Problems / Future Work

- Source of mobile reductants?
- Utilize further stratigraphic investigations and investigations of heavy minerals

Remaining Problems / Future Work

- Geometry of different basin-scale alteration zones?
- Age of different alteration zones?
- Mine existing data and additional fieldwork.
- Detailed petrographic studies.

Remaining Problems / Future Work

- Are there geochemical vectors to ore?
- Continue major and trace element analyses.
- Continue C, O, and S isotopic studies to look for changes caused by oxidation change during sulfide precipitation.

Remaining Problems / Future Work

- What is the source of cobalt (which differentiates Copperbelt from other systems)?
- Continue whole rock and trace element studies of gabbros. Preliminary work shows least altered gabbros with up to 60 ppm Co; depletion in altered gabbros?

Remaining Problems / Future Work

- Geochemistry of ore fluid?
- Utilize stable mineral assemblages and alteration assemblages to try and calculate.
- Calculate possible ore fluids at different temperatures and salinities.

Remaining Problems / Future Work

- Degree of metamorphic mineral redistribution?
- Utilize and expand geochronological database.

Geological development and mineralisation in the Yeneena Basin – Paterson Orogen, W.A.

Robert Scott
Centre for Ore Deposit Research, University of Tasmania

Summary

A preliminary review of the geological development of the Paterson Orogen of central Western Australia is presented. This work provides essential background to the ongoing study into the origin and distribution of mineral deposits hosted by Neoproterozoic rocks of the Yeneena Basin. Comparatively little previous research has been undertaken in the Paterson Orogen, due to the remoteness of the area, harsh climate, and general paucity of outcrop. This report synthesises the results of recent regional mapping in the Paterson Orogen by Geological Survey of Western Australia geologists, and the findings of recent PhD and Masters studies of mineral deposits in the region. The Paterson Orogen consists of three main elements: Palaeo- to Mesoproterozoic Rudall Complex (>2015–1765 Ma), the Neoproterozoic Yeneena Supergroup (<1132–816 Ma) and the Neoproterozoic Tarcunyah Group (<700–610 Ma). The present geometry and structure of the Paterson Orogen is largely due to deformation in the 800–700 Ma Miles Orogeny. Subsequent deposition of the Tarcunyah Group, is interpreted to reflect initial development of the Officer Basin, in a probable foreland basin setting along the southwestern margin of the Paterson Orogen.

The age, setting, structural evolution and mineral endowment of the Yeneena Basin all invite comparisons with the Zambian Copperbelt. Available evidence indicates major deposits in the Yeneena Supergroup (Telfer, Nifty and Maroochydore) formed during inversion of the Yeneena Basin succession during the Miles Orogeny, consistent with a Lufilian age for major copper mineralisation in Zambia. However, characteristics of the Nifty deposit, the major stratabound Cu deposit in the Yeneena Basin, are distinctly different to the Copperbelt deposits, and suggest much closer affinities to Mt Isa-style copper ore bodies.

Introduction

The Paterson Orogen is a 1200 km-long SE-trending belt of Palaeo- to Neoproterozoic rocks at the eastern margin of the Pilbara Craton in central Western Australia (Fig. 1). It consists of three main elements (Fig. 2):

- Rudall Complex (Palaeo- to Mesoproterozoic basement, >2015–1765 Ma)
- Yeneena Supergroup (Neoproterozoic, <1132–816 Ma)
- Tarcunyah Group (Neoproterozoic, <700–610 Ma)

As a whole, the orogen is moderately to strongly deformed, poorly exposed, and – with the exception of the larger mineral deposits – poorly studied. As a result, age constraints and relationships between many of the between major lithostratigraphic units (particularly within the Yeneena Supergroup) are not well understood.

The age, setting, structural evolution and mineral endowment of the Yeneena Basin all invite comparisons with the Zambian Copperbelt (Haines et al., 1993). Neoproterozoic sedimentary rocks of the Yeneena Basin host the giant Telfer Au-Ag deposit (~25 Moz Au, 1 Mt Cu), stratabound copper deposits Nifty (148 Mt @ 1.3% Cu) and Maroochydore (140 Mt @ 0.5% Cu), unconformity related uranium deposits (Sunday Creek) and carbonate-replacement Zn-Pb deposits (Warrabarty). Western Mining Corporation

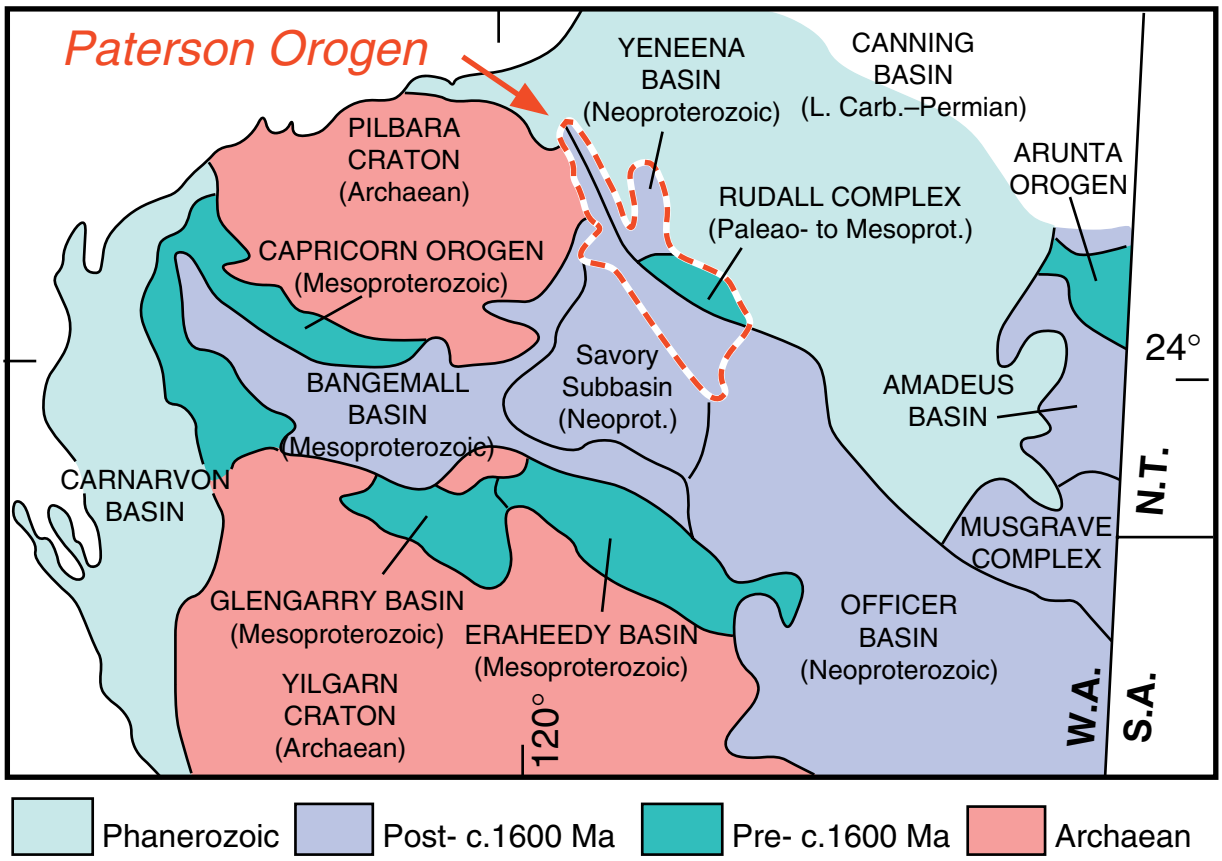

Figure 1. Regional geologic setting of the Paterson Orogen (from Hickman and Bagas, 1998)

discovered Nifty in 1982 using an exploration model based on the Zambian Copperbelt (Haines et al., 1993).

We are conducting a study into the geological development of Paterson Orogen and the origin and distribution of mineral deposits within the Yeneena Basin as part of AMIRA / ARC Project P544. The study aims to synthesise (i) previous (largely deposit-based) PhD, Masters and Honours studies within the area, (ii) recent 1:100,000 mapping by Geological Survey of Western Australia (GSWA), and (iii) potential field data (magnetics, gravity, EM) for part of the area provided by P544 sponsors Straits Resources and Rio Tinto. Key objectives of the study are to:

1. Develop models for the formation and subsequent deformation of the Yeneena Basin
2. Evaluate the origin, timing and distribution known mineralisation in terms of structural architecture and geological development of the Yeneena Basin.
3. Compare the geological development, mineral endowment (known and potential) of the Yeneena Basin with the Zambian Copperbelt.

Analysis of Paterson Orogen geophysical data is ongoing and will be presented in the final meeting and reports for P544 in mid-2003. This report provides an overview of the geological development of the Paterson Orogen based on review of existing literature, and observations by the author during a two-week field visit in October 2001. A major objective of this synthesis is to delineate key problems requiring more detailed study, particularly in regard to regional structure and stratigraphic relationships, that may be addressed during analysis of the geophysical data provided. This report also discusses constraints on the timing and origin of stratabound copper deposits in the Yeneena basin and compares them to Neoproterozoic sediment-hosted copper deposits of the Mount Isa Inlier (western Queensland) and the Zambian Copperbelt.

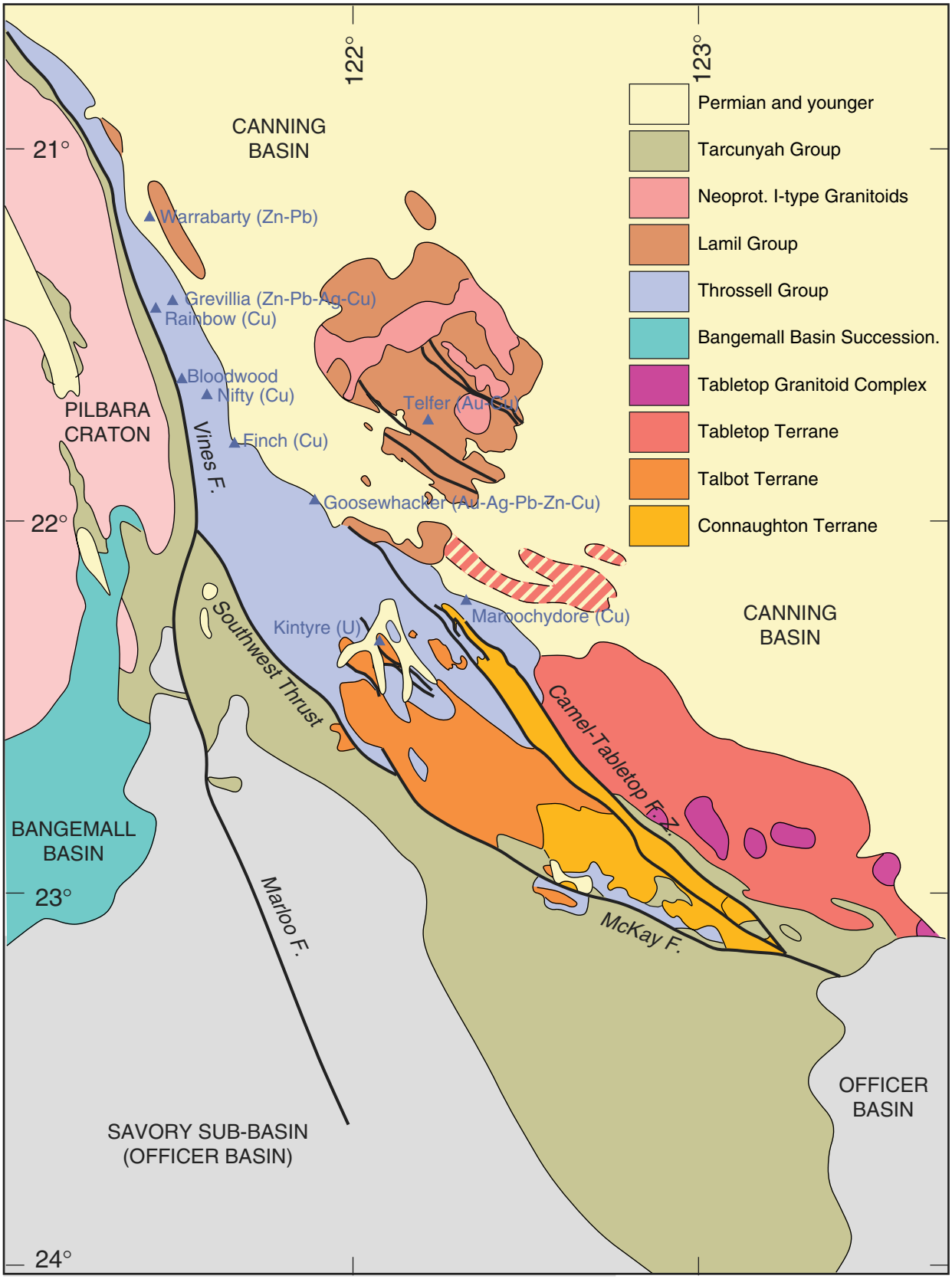

Figure 2. Simplified geological map of the Paterson Orogen showing the location of major mineral deposits and prospects. The AMIRA P544 study is focussed on the northern two thirds of the exposed portion of the orogen.

Geological setting

Figure 2 is a simplified geological map of the Paterson Orogen, based largely on recent GSWA mapping. The location of major mineral deposits, several smaller prospects, and the area delineated for detailed analysis in this study are also shown. Temporal constraints on the age of the major constituent rock packages, intrusions and deformation events are summarised in Figure 3.

Palaeo- to Mesoproterozoic rocks

Rudall Complex

The oldest exposed rocks in the Paterson Orogen are Palaeo- to Mesoproterozoic gneisses and schists of the Rudall Complex (Figs 2 and 3). The Rudall Complex is interpreted as broad zone of imbricate thrust sheets that young towards the east. Two major thrusts divide the complex into three main tectono-stratigraphic elements: the Talbot, Connaughton and Tabletop Terranes (Figs 2 and 3). The Talbot Terrane predominantly consists of metamorphosed (medium pressure, amphibolite facies) siliciclastic sedimentary rocks (paragneiss) and granitoids (orthogneiss). The Connaughton Terrane contains mafic schist and gneiss, chert, carbonates, pelite and BIF metamorphosed to high-pressure amphibolite (–granulite) facies. The poorly-exposed, potentially exotic Tabletop Terrane consists of granitoids, amphibolite, BIF, dolerite dykes and (?)felsic volcanic rocks dated at ~1300 Ma (Bagas and Smithies, 1998).

The oldest rocks of the complex underwent two episodes of folding, faulting and fabric development, prior to deposition of unconformably overlying Yeneena Supergroup, during the 2000–1760 Ma Yapungku Orogeny. Peak amphibolite(–granulite) facies metamorphism of these rocks occurred during the younger phase of the orogeny (D_2: 1790–1760 Ma). Two generations of orthogneiss comprise approximately 50% of the exposed Rudall complex. The older gneisses contain both S_1 and S_2 Yapungku Orogeny fabrics, while the younger orthogneisses, dated at 1787–1765 Ma (Hickman and Bagas, 1998) contain only S_2 (Fig. 4). With the exception of one small outlier south of the McKay Fault, the northwest-trending Southwest Thrust and McKay Fault form the southern margin of the Rudall Complex (Fig. 2)

Neoproterozoic rocks

Yeneena Supergroup

The Yeneena Supergroup was deposited in the Yeneena Basin, that is interpreted to have either been a failed rift or a pull-apart basin formed during strike-slip faulting (Williams, 1990; Hickman and Bagas, 1998; Williams and Bagas, 1999). The Yeneena Supergroup unconformably overlies the Rudall complex along its northwestern and locally along its southwestern flanks (Fig. 2). The Yeneena Supergroup is divided into two groups: the Throssell Group (exposed in the west and south) and the Lamil Group (exposed in the east) (Fig. 2). Contacts between the groups are not exposed and while the Lamil Group has generally been considered younger (Hickman and Clarke, 1994), stratigraphic relations have not been reliably established. The successions may be, at least in part, temporally equivalent (Bagas, pers. comm. 2002). The Throssell Group consists of a basal siliciclastic package (Coolbro Sandstone, Fig. 5) and a conformably overlying package of interbedded sandstone, siltstone and carbonaceous and sulfidic shale with minor carbonate (Broadhurst Formation, Fig. 6). The Lamil Group (Williams and Bagas, 1999) is predominantly composed of sandstone, shale and carbonate. Carbonate and pelitic rocks of the Isdall Formation that were originally interpreted to overlie the Broadhurst Formation across a disconformable contact or fault (Williams et al., 1976; Hickman and Clarke, 1994). The unit is lithologically similar to portions of both the Broadhurst Formation (Hickman and Clarke, 1994) and the Lamil Group (Chin et al., 1982; Bagas, 2000) and is currently interpreted to represent the basal formation of the Lamil Group (Williams and Bagas, 1999). Both the Throssell and Lamil Groups have undergone lower greenschist-facies metamorphism and are moderately to strongly folded.

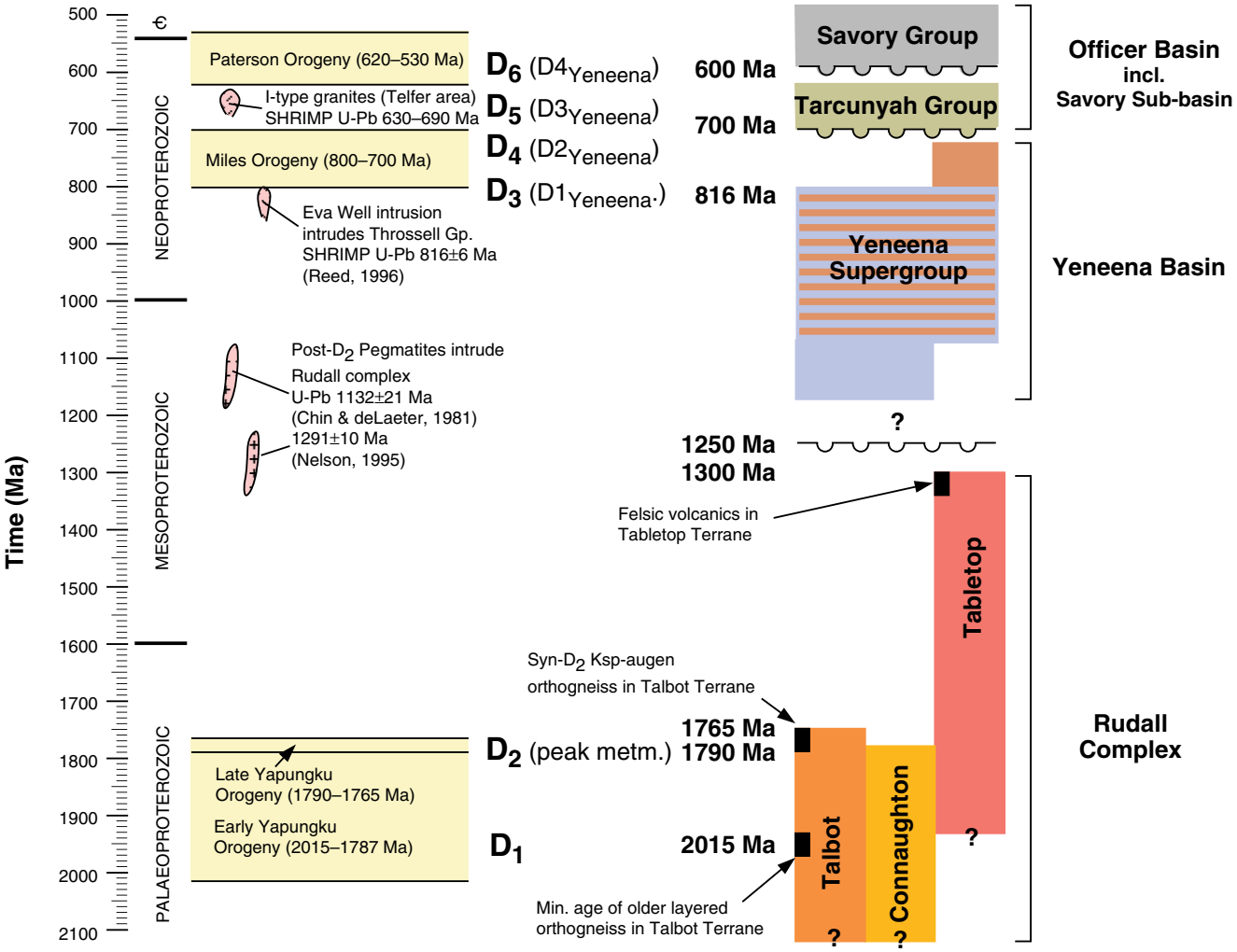

Figure 3. Temporal constraints on the geological evolution of the Paterson Orogen.

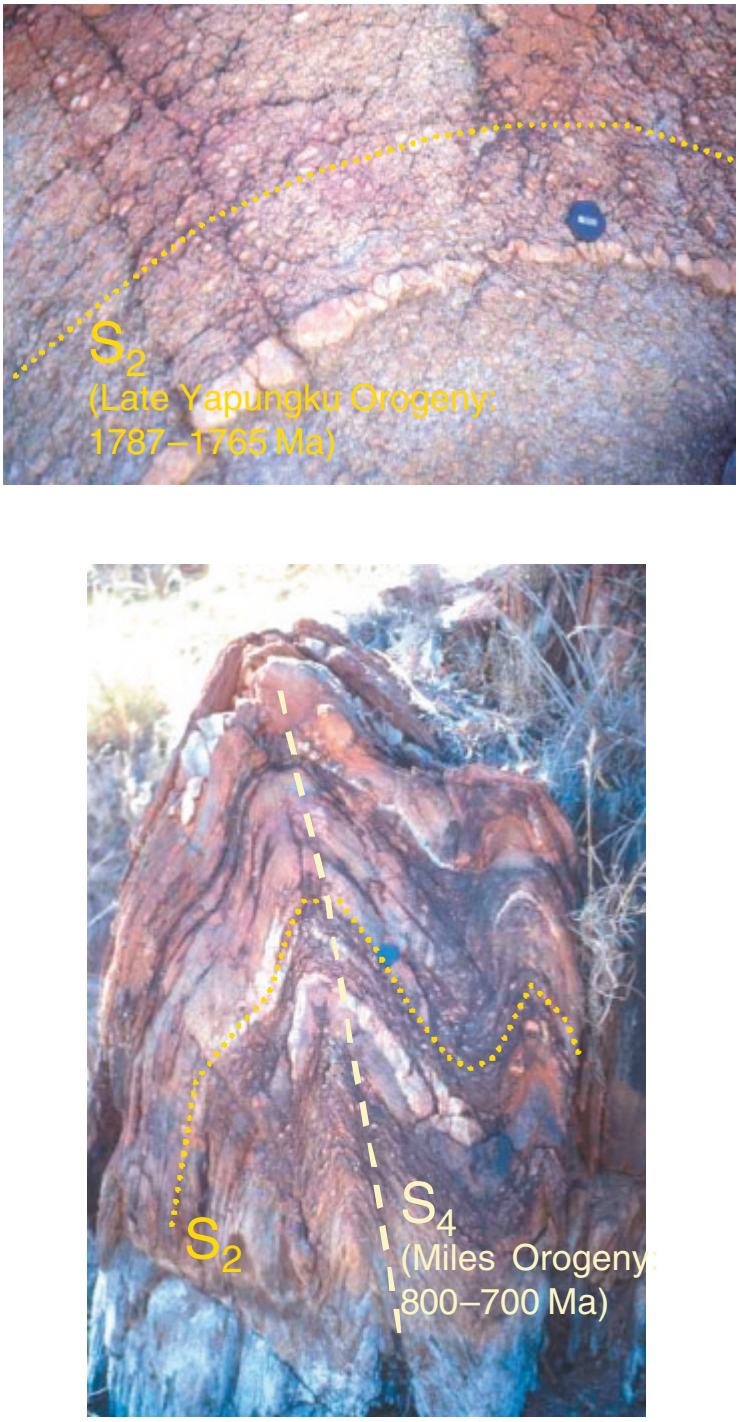

Figure 4. Folded regional S_2 fabric in folded orthogneiss of the Talbot Terrane. Folds are interpreted to have formed during the 800–700 Ma Miles Orogeny. The axial plane cleavage (regional S_4) corresponds to the major cleavage (S_2) developed in the Yeneena Supergroup rocks.

Figure 5. Basal conglomerate of the Coolbro Sandstone, exposed just to the north of the Kintyre uranium deposit.

Figure 6. Exposure of the Broadhurst Formation in the wall of the Nifty open pit.

Age constraints on the Yeneena Supergroup are poor. The Throssell Group is younger than 1290–1132 Ma pegmatites (Chin and de Laeter, 1981; Nelson, 1995) that intrude the Rudall complex and are either truncated by or not recognised within the Yeneena Supergroup (Hickman and Clarke, 1994). A minimum age for the Throssell Group is provided by an 816±6 Ma U-Pb SHRIMP age for the sill-like mafic to intermediate Eva Well intrusion, which both intrudes the Throssell Group and was affected by the main fabric forming event, D_2, of the Miles Orogeny (Reed, 1996). Dolerite dykes emplaced pre- and post-greenschist facies metamorphism occur in the Telfer district (Goellnicht, 1992) and post-D_2 dolerite dykes cut the Broadhurst Formation at Nifty (Anderson, 1999) and Warrabarty (Smith, 1996). Poor Rb-Sr isochrons of 700–750 Ma have been obtained from dolerite sills that intrude the Throssell Group (Williams, 1990). The Lamil Group is older than 1070 Ma, based on the minimum age of detrital zircons from sandstones within the group, and younger than the >630 Ma post-orogenic I-type monzogranites and syenogranites that locally intrude the group (Bagas, 2000). Three samples from the Mount Crofton Granite yielded concordant titanite SHRIMP U-Pb ages that range between 639±9 and 678±12 Ma, are considered the more reliable constraints on the age of I-type plutonism. SHRIMP U-Pb zircon ages from these samples range from c. 600 to 630 Ma, but are considered unreliable due to significant lead-loss resulting from extreme radiation damage to the crystals (Dunphy in Bagas, 2000).

Tarcunyah Group

Sandstone, conglomerate and lesser siltstone and dolomite of the Tarcunyah Group (Bagas et al., 1995; 1999; Williams and Bagas, 2000) is extensively developed along western and southwestern margins of the Paterson Orogen (Fig. 2) and it is now thought to represent initial deposition within the Savory Sub-basin of the latest Neoproterozoic Officer Basin (Bagas et al., 1995; 1999; Williams and Bagas, 2000). A thin belt of gently to moderately dipping Tarcunyah Group strata unconformably overlies the eastern margin of the Pilbara Craton mark the western margin of the Paterson Orogen (Figs 2 and 8). In this area,

the Tarcunyah group is separated from the Yeneena Supergroup by the N- to NNW-trending Vines fault. The Tarcunyah Group is more extensively exposed further south where the belt swings southeastward (Fig. 2). In this region the Tarcunyah group is either in fault contact with or unconformably overlies both the Yeneena Supergroup and Rudall complex. Where the belt first swings southeastward, the Tarcunyah group is restricted the area south (footwall) of the NW-trending Southwest Thrust. Further to the southeast, where the Southwest Thrust links with the NW-trending McKay Fault, the Tarcunyah Group is exposed both to the north and south of fault system (Fig. 2). In the south of the present study area (Fig. 2) the Tarcunyah group is unconformably overlain by younger gently-dipping to flat-lying sedimentary rocks of the Officer Basin (Williams and Bagas, 2000).

Although the Tarcunyah Group is tightly folded locally, and an axial plane cleavage is developed in fold closures, it lacks the penetrative foliation and low grade regional metamorphism of the older Coolbro Sandstone of the Throssell Group (Williams and Bagas, 2000). Absolute age constraints on the age of the Tarcunyah Group are poor. Williams and Bagas (1999) considered the maximum age <830 Ma and the minimum age 610 Ma. The minimum age for the formation is based on unconformably overlying strata of the Savoy Sub-basin of the Officer Basin (Bagas and Smithies, 1998). Stromatolites and acritarchs from the Tarcunyah Group are interpreted to indicate an age of approximately 800 Ma (Bagas et al., 1995; Grey and Stevens, 1997). However, as it is presently thought deposition of the Tarcunyah formation post-dates the Miles Orogeny (Bagas and Smithies, 1998), a maximum age younger than 700 Ma seems likely (Fig. 3; and see below). A sample collected from a (?) hydrothermally altered tuffaceous bed within one of the basal formations of the Tarcunyah Group yielded zircon populations of 544±10 Ma, 574±62 Ma and 1204±35 Ma (Nelson, 1999). This suggests a maximum depositional age of 544 Ma, which is significantly younger than expected, and may indicate the rock collected for dating was not from the Tarcunyah Group (Williams and Bagas, 2000).

Stratigraphic relations across the southern margin of the Paterson Orogen

All moderately to strongly deformed sedimentary rocks overlying the Rudall Complex were originally included in the Yeneena Group (Williams et al., 1976). GSWA geologists considered the Yeneena Group to be older than the largely undeformed (~flat-lying), but lithologically similar rocks that occur to the south. The latter were regarded as the eastern continuation of the Middle Proterozoic Bangemall Basin (Williams et al., 1976). However, stratigraphic relations between these successions were controversial. Goode and Hall (1981) cite the broad lithological similarity of the Yeneena and Bangemall Groups, the absence of any definite unconformable relationships between the groups, and the apparently gradational nature of the structural and metamorphic transition across the southern margin of the Paterson Fold Belt (now Paterson Orogen) as evidence that the sequences are correlative. Goode and Hall (1981) and Goode (1981) thus interpret the original Yeneena Group as the easternmost exposures of the Bangemall Basin.

Recent GSWA work has led to a complete revision of the stratigraphic relations and affinities of the rocks in this area. It is now thought that the original Yeneena Group consists of two distinct tectono-stratigraphic successions. The older sequence forms the present Yeneena Supergroup, and is unconformably overlain by the younger Tarcunyah Group (Bagas et al., 1995; 1999). Rocks assigned to the Tarcunyah Group are much less deformed than the Yeneena Supergroup, and interpreted to have been deposited after the 800–700 Ma Miles Orogeny. Tarcunyah Group sedimentation is now thought to record initial deposition within the Savory Sub-basin of the latest Neoproterozoic Officer Basin (Bagas et al., 1995; 1999; Williams and Bagas, 2000). Much of the predominantly flat-lying succession immediately south of the Paterson Orogen (originally interpreted as the Mesoproterozoic Bangemall Group; Williams et al., 1976; Goode, 1981; Goode and Hall, 1981) is now also interpreted as part of the younger Officer Basin and unconformably overly the eastern Bangemall Basin succession, just to the west of the present study area (Figs 1 and 2; Bagas et al., 1995; 1999). The present

interpretation substantially reconciles the opposing interpretations of the early workers. Re-assignment of both the moderately to weakly deformed succession along the southern margin of the Paterson Orogen and the largely undeformed rocks to the south into the same tectono-stratigraphic unit is consistent with the arguments by Goode (1981) and Good and Hall (1981) outlined above. Recognition that this entire package is younger than both the Bangemall Basin succession, and the Yeneena Supergroup supports the original GSWA interpretation that (most of) the deformed rocks in the Paterson Fold Belt are older than those exposed to those immediately to the south, but not necessarily older than the Bangemall Basin succession as noted by Goode and Hall (1981).

Phanerozoic Rocks

Paterson Formation

Permian fluvioglacial rocks and tillite of the Paterson Formation (Canning Basin succession) and Cainozoic sediments cover a substantial proportion of the Paterson Orogen (Fig. 2). Within the present study area, the thickest Permian sequences were deposited in north-south palaeovalleys. Glacial stria and chatter marks indicate the average direction of ice movement was towards the north (Hickman and Clarke, 1994). Company drilling indicates the Paterson Formation is at least 100 m thick in some palaeovalleys, and that valley sides are typically steep, consistent with U-shaped profiles (Hickman and Clarke, 1994).

Structure and deformation history of the Yeneena Supergroup and younger successions

Six deformation events have been recognised in the Paterson Orogen, however, only the last four affect rocks of the Yeneena Supergroup (Fig. 3; Hickman and Clarke, 1994; Smithies and Bagas, 1997). The Yeneena Supergroup rocks underwent two phases of folding and fabric development in response to NE–SW directed compression (D_1–D_2 in the Yeneena Supergroup, or D_3–D_4 regionally, see Fig. 3) during the ~800–700 Ma Miles Orogeny. D_1 produced local recumbent folds, thrusts and local development of a near bedding-parallel cleavage in the Throssell Group (Hickman and Clarke, 1994; Reed, 1996), while D_2 – the main deformation phase – produced open to tight, upright to overturned (towards the southwest) NW-trending folds and SW directed thrust faults and a pervasive slaty to crenulation cleavage (Goode, 1981; Hickman and Clarke, 1994; Reed, 1996). Greenschist facies metamorphism (prograde in the Yeneena Supergroup, retrograde in the Rudall Complex) accompanied the latter stages of deformation (D_2) during the Miles Orogeny (Hickman and Clarke, 1994; Bagas and Smithies, 1995). Age constraints on the Miles Orogeny are provided by the816±6 Ma U-Pb SHRIMP age for zircon from the deformed Eva Well intrusion and a 717±5 Ma $^{40}Ar/^{39}Ar$ age for syn-D_2 phlogopite (Reed, 1996).

D_3 (D_5 regionally) is poorly defined event or series of events (Blake Movement: Williams, 1992) responsible for local faulting and folding of variable style and orientation, principally affecting rocks of the Sunbeam Group (Tarcunyah Group correlate) along the northwestern margin of the Officer Basin (Williams and Bagas, 2000). In the area west of the Southwest Thrust (Fig. 2), the event is interpreted to be responsible for NE-trending folds, and NW-directed transport steep on reverse faults in the Tarcunyah and Sunbeam Groups (Bagas et al., 1999; Williams and Bagas, 1999; 2000). This event preceded deposition of the Boondawari Formation, a glacigenic succession thought to correlate with the ~600 Ma Marinoan glaciation event (Williams, 1992).

The variably, but generally weakly deformed, Tarcunyah Group lacks the penetrative (S_2) cleavage, well developed poly-deformation and greenschist facies metamorphism developed in lithologically similar rocks of the Yeneena Supergroup. On this basis, deposition of the Tarcunyah Group is thought to have not occurred until after the Miles Orogeny (Bagas and Smithies, 1995). Deformation of the Tarcunyah Group is interpreted to have occurred during the Paterson Orogeny (Bagas and Smithies, 1995), the last significant phase of deformation to affect the region (regional D_6, D_4 in Yeneena Supergroup). The NNE–SSW shortening during the Paterson Orogeny is younger than 610 Ma, based on the minimum depositional age of the Tarcunyah

Group (Bagas and Smithies, 1995). Many of the major faults in the area cut the Tarcunyah Formation (Vines Fault, Southwest Thrust, McKay Fault, Marloo Fault; Fig. 2) and thus were either initiated or reactivated during the Paterson Orogeny (Bagas and Smithies, 1995; Bagas and Williams, 1999; 2000). The Paterson Orogeny is thus of apparently similar age and similar style to the 560–525 Ma Petermann Orogeny in central Australia (Bagas and Smithies, 1998; Bagas and Williams, 2000). Geophysical data indicate Petermann age structures in the Musgrave block continue beneath cover northwest into the Paterson Orogen (Goode and Hall, 1981; Bagas and Smithies, 1998). These structures our now recognised as (regional) D_6 structures, in the Paterson Orogen, where they controlled deposition of the Disappointment Group (formerly Wells Foreland Basin Succession (Williams, 1992) of the upper Savory Group) in the area to the south (Williams and Bagas, 2000). The Disappointment Group post-dates the ~600 Ma Boondawari Formation and was apparently deposited in a foreland basin setting (Williams, 1992; Bagas et al., 1995).

Mineral deposits within the Paterson Orogen

Most significant mineral deposits in the Paterson Orogen are hosted by Neoproterozoic rocks of the Yeneena Supergroup. Although minor base metal mineralisation is hosted by pelitic, chloritic and carbonaceous schists of the Rudall Complex (Hickman and Clarke, 1994) the vein-hosted Kintyre uranium deposit (Jackson and Andrew, 1990) is the only (known) significant deposit hosted by the older rocks.

Kintyre (U)

The Kintyre deposit (36,000 t U_3O_8 with average grades 1.5–4.0 kg/t U_3O_8) is hosted by chlorite-quartz schist of the Yandagooge Formation within the Talbot Terrane of the Rudall Complex (Jackson and Andrew, 1990; Hickman and Clarke, 1994). Although hosted by rocks of the Rudall Complex the Kintyre deposit is situated just below the unconformable basal contact of the Coolbro Sandstone (basal Throssell Group). Other uranium occurrences in the area (e.g. Sunday Creek) are also unconformity-related located at or close to the base of the Coolbro Sandstone (Jackson and Andrew, 1990; Hickman and Clarke, 1994).

Telfer (Au-Cu)

Telfer is one of the largest gold deposits in Australia. From the commencement of mining in 1977 until 1999 Telfer produced 178 t (5.7 Moz) of gold (Howard et al., 2000)

The Fallows Field deposit, 8 km to the south produced a further 1.5 t Au (Bagas, 2000). A recent reappraisal of the deposit identified resource of 19 Moz Au (based on $A 500/oz) and 740,000 t Cu. Early syn-genetic and sedimentary replacement models for the Telfer mineralisation have been superceded more recently by models recognising the importance of structural controls (e.g. Inglis, 1995). Mineralisation is hosted by a series of vertically-stacked, laterally-extensive stratabound quartz-carbonate-sulfide reefs and intervening (linking) sheeted vein arrays and stockworks, centred on the hinge zone of the Telfer Dome (Fig. 7). The reefs are up to several metres thick and hosted by interbedded calcareous or carbonaceous siltstone and massive sandstone of the Malu Formation (Lamil Group). Narrow zones of silica–dolomite alteration are developed around the reefs. Fluid inclusion studies indicate the ore fluids were rich in H_2O–CO_2–CH_4-NaCl and reached temperatures in the range 225–450°C (Goellnicht et al., 1991; Rowins et al., 1997). Goellnicht et al. (1989; 1991) argue the mineralising fluids were largely derived from the ~630 Ma post-tectonic I-type granite. In contrast, Rowins et al. (1997), favour a model where the granites provided the heat source that drove fluid circulation, but the ore fluids were sourced from the sedimentary sequence. Involvement of post-orogenic granites in generating the Telfer mineralisation seems at odds with the clear deformation controlled geometry and distribution of the reefs and associated vein arrays (e.g. Inglis, 1995), suggesting that if granites were important, they were older than those currently known and dated.

Nifty (Cu)

The stratabound Nifty copper deposit is hosted by carbonaceous (±sulfidic) and dolomitic shales and siltstones rocks of the Broadhurst Formation (Figs 6 and 9; Anderson, 1999; Hooper, 2002). The total resource is 148 Mt @ 1.3% Cu which includes a primary chalcopyrite resource of 110 Mt @ 1.4%

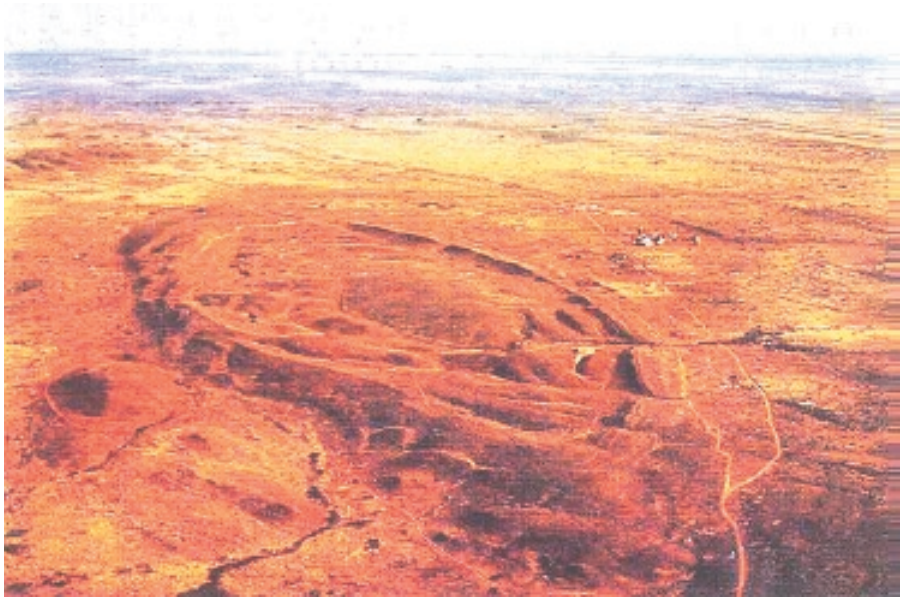

Figure 7. Telfer Dome prior to mining (photo provided by Newcrest Mining, and appears on the cover of Bagas, 2000)

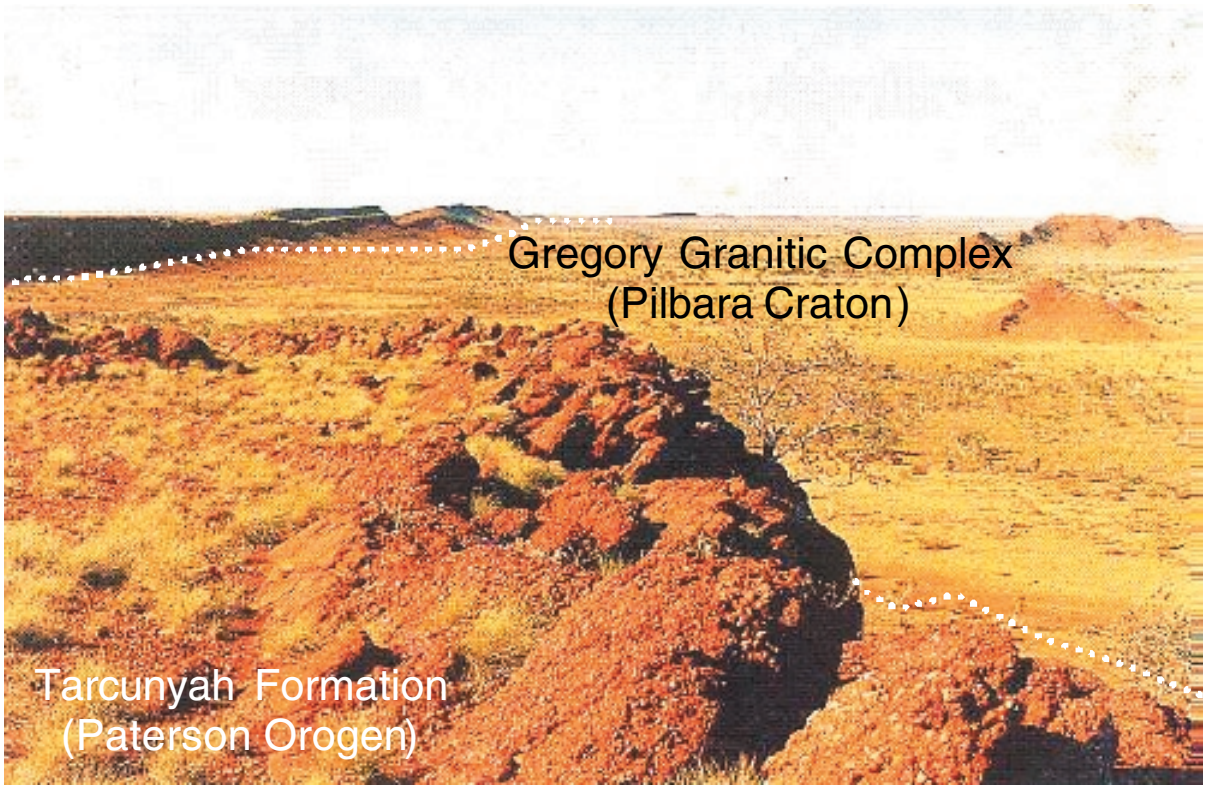

Figure 8. Tarcunyah Group unconformably overlying the Gregory Granitic Complex along the eastern margin of the Pilbara Craton (Photo: Williams and Trendall, 1998).

Cu, and a leachable (secondary copper) reserve of 27.6 Mt @ 1.1% Cu (Hooper, 2002). The orebody and host sequence is folded around a large NW-trending D_2 (Miles Orogeny) synform (Nifty Syncline) with a steeply dipping to overturned north limb, and a steeply- to moderately-dipping western limb (Fig. 9). The hinge of the syncline plunges at 10°–20° to the southeast. Currently only the secondary copper ores (chalcocite ± malachite ± cuprite ± native copper) in the upper 200–300 m on the steeply northern limb of the syncline are mined (Figs 6 and 9). Primary copper mineralisation is associated with intense quartz-dolomite alteration, and consists only of disseminated to massive medium to coarse-grained chalcopyrite and is best developed in the hinge region of the synform (Anderson, 1999; Hooper, 2002). Anderson (1999) interprets copper mineralisation at Nifty to be synchronous with D_2 the second phase of folding and cleavage development during the 800–700 Ma Miles Orogeny.

Maroochydore (Cu)

Disseminated copper mineralisation at Maroochydore (140 Mt @ 0.5% Cu, including 51.3 Mt @ 1.0% Cu, 0.04% Co) is hosted by carbonaceous and dolomitic shale of the Broadhurst Formation (Fig. 2). Primary chalcopyrite rims and replaces framboidal pyrite. Reed (1996) interpreted a syn-D_2 (Miles Orogeny, regional D_4) timing for the copper mineralisation. Copper precipitation was associated with dolomite alteration of the host rocks (Reed, 1996).

Warrabarty (Zn–Pb)

Warrabarty is a sub-economic carbonate-replacement Pb-Zn deposit within the Broadhurst Formation, in the north of the exposed Paterson Orogen. Disseminated to massive galena occurs in breccias and veins that post-date late-diagenetic dolomitisation and bedding parallel pressure solution, but predates D_2 (regional D_4) (Smith, 1996).

Origin of stratabound copper deposits within the Yeneena Basin

There are numerous minor base metal occurrences within the Yeneena Basin, but to date only two significant deposits, Nifty and Maroochydore, have been identified. Recent PhD studies of Nifty (Anderson, 1999) and Maroochydore (Reed, 1996) indicate the deposits are hosted by similar interbedded carbonaceous, pyritic and dolomitic shale and dolostone successions within the upper Broadhurst Formation (~1500 m above Coolbro Sandstone). In both cases, copper mineralisation is interpreted to be synchronous with second phase of deformation affecting the Throssell Group (i.e. D_2 of the Miles Orogeny, regional D_4).

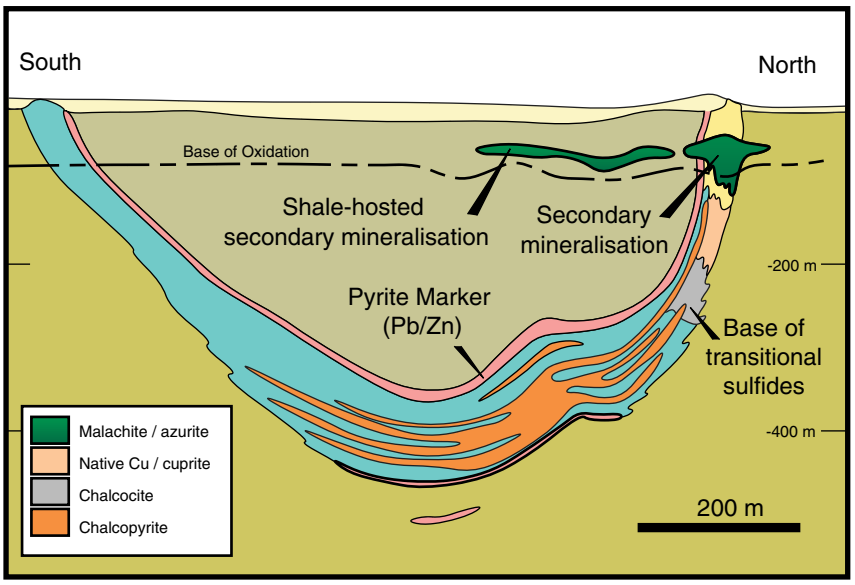

9. Schematic cross-section through the Nifty deposit (From Hooper, 2002, adapted from Haines et al., 1993)

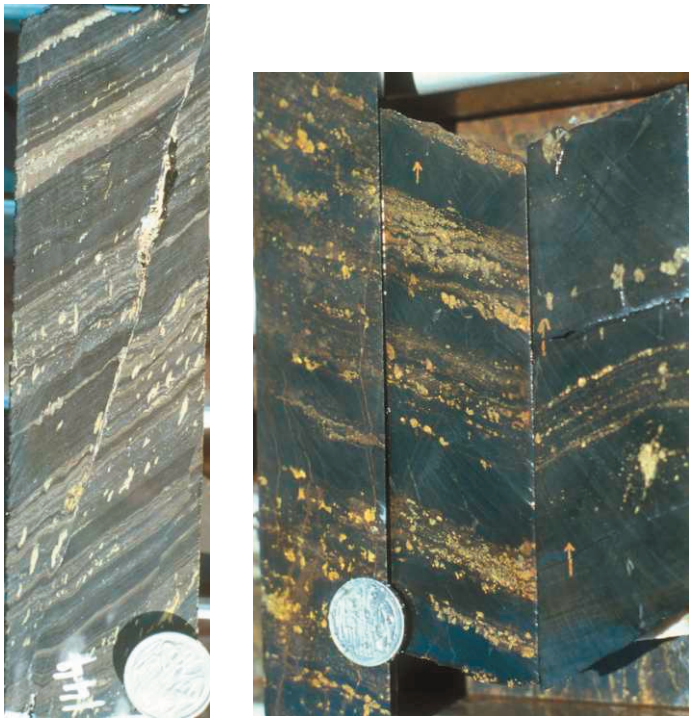

Figure 10. Similar styles of copper mineralisation at the Maroochydore and Nifty deposits.
(a) Maroochydore copper mineralisation. Chalcopyrite replaces early pyrite and D_2 fills pressure shadows to form elongate blebs aligned in the S_2 cleavage (drill hole YNC-82, 144 m)

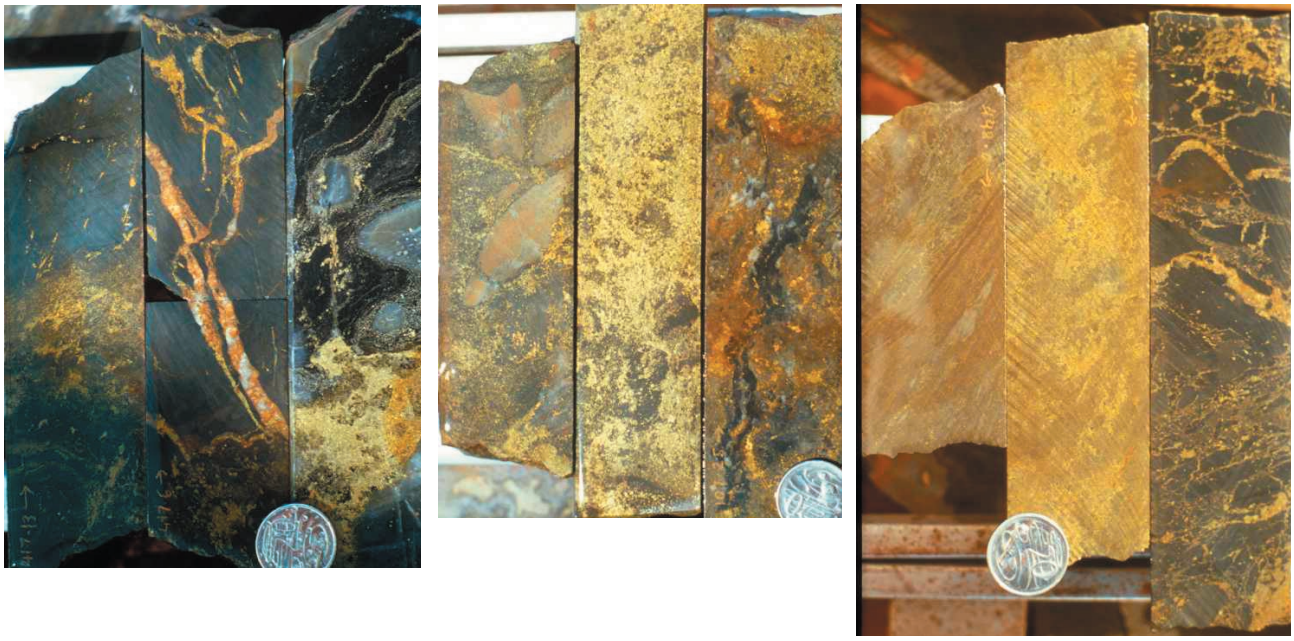

Figure 11. Nifty primary mineralisation styles in drill hole THRD 780 W1.
(a) Left (417.2 m): Semi-massive to disseminated chalcopyrite discordant to bedding in silicified shale and siltstone, not elongation of chalcopyrite blebs parallel to the S2 cleavage. Centre (417.7 m): carbonate + quartz + chalcopyrite veins. Right (421.4 m): massive chalcopyrite replacing(?) black-quartz. Both overprint clasts of earlier (pre-mineralisation) green quartz + pyrite alteration.
(b) Semi-massive chalcopyrite overprints brecciated pre-mineralisation red–green quartz altered dolomitic shale (left, 403.5 m), semi-massive to massive chalcopyrite and black quartz (centre, 405.7 m), black quartz and chalcopyrite vein and semi-massive chalcopyrite (right, 407.35 m).
(c) Brecciated and shear-laminated massive chalcopyrite ore (left, 448 m), massive chalcopyrite (centre, 444.7 m), chalcopyrite occurs as vein- and breccia-fill within brecciated silicified dolomitic siltstone and shale (right, 442.7 m).

A 717±5 Ma $^{40}Ar/^{39}Ar$ apparent age for phlogopite associated with chalcopyrite mineralisation at Maroochydore (Reed, 1996) is currently the most reliable absolute constraint on the age of copper mineralisation. Pb model ages for Nifty (galena from within the pyrite marker bed) are substantially older and range 850–900 Ma (Fletcher in Brockley and Myers, 1990). The older age is consistent with the 840 Ma Pb-Pb secondary isochron age inferred for Throssell Group mineralisation, based on the linear trend in Pb isotope ratios from a number of deposits (Smith, 1996). More recently, however, Anderson (1999) has reinterpreted the linear trend in Throssell Group Pb isotope ratios to reflect variable degrees of mixing between crustal and magmatic sources of lead, rather than the age of mineralisation.

Mineralisation styles

At Maroochydore chalcopyrite is variably disseminated through the host succession where it rims and replaces framboidal pyrite. Chalcopyrite is also preferentially developed in D_2 dilational sites (veins, fold hinges and pressure shadows adjacent to existing minerals) and within narrow bedding-parallel shears (Fig. 10a; Reed, 1996). The distribution of chalcopyrite at Maroochydore indicates precipitation during D_2 (regional D_4) (Reed, 1996). Primary copper mineralisation at Nifty is associated with intense quartz-dolomite alteration. Chalcopyrite occurs as isolated spots and blebs through to bedding-parallel to bedding-transgressive bands (Figs 10b and 11a, left), vein-fill (Fig. 11a, centre), semi-massive to massive aggregates with replacive habit (Fig. 11a, left, 11b) and as the matrix to breccias of altered wall rock (Fig. 11c) (Anderson, 1999; this study). Chalcopyrite also occurs as <100 μm ragged inclusions of replacive origin in syn-mineralisation euhedral pyrite (Anderson, 1999). Overall, textural and overprinting relations indicate chalcopyrite was relatively late in the paragenetic sequence at Nifty, and is principally of replacive habit. Although the occurrence of chalcopyrite in cleavage parallel veins, F_2 fold hinges and blebs elongate parallel to the S_2 cleavage indicate a syn-D_2 (Yeneena Supergroup) age for the Nifty mineralisation (Anderson, 1999), based on my inspection of drill hole THRD 780 W1, which passes through the thickest part of the orebody, evidence for deformation, and a syn-D2 timing is less apparent than at Maroochydore. This probably reflects the intensity of the relatively competent quartz and quartz-dolomite alteration at Nifty, which may have acted to shield the orebody from the deformation.

Fluid inclusions

Fluid inclusions from syn-mineralisation veins at Maroochydore and Nifty have similar salinities (8–27 eq. wt % NaCl), homogenisation temperatures (180°–450°C) and estimated trapping temperatures (median values: 360°–440°C). The compositions and high trapping temperatures of the inclusions are consistent with epigenetic mineralisation at greenschist facies metamorphic conditions (Reed, 1996; Anderson, 1999).

Stable isotopes

Sulfur isotopes

$\delta^{34}S$ sulfur isotopic values for diagenetic framboidal pyrite are $\delta^{34}S$ +16 to –27 ‰ at Nifty (Anderson, 1999) and $\delta^{34}S$ –22 to –31 ‰ at Maroochydore (Reed, 1996). Pre- to syn-mineralisation euhedral pyrite at Nifty has $\delta^{34}S$ +3.8 to –12 ‰ (Anderson, 1999) and $\delta^{34}S$ –4.0 to –10 ‰ at Maroochydore (Reed, 1996). $\delta^{34}S$ sulfur isotopic values for chalcopyrite at Nifty range from +6 to –6 ‰ (Anderson, 1999). At Maroochydore coarse-grained chalcopyrite has $\delta^{34}S$ –13 to –23 ‰ while for fine--grained chalcopyrite the range in $\delta^{34}S$ is –25 to –31 ‰ (Reed, 1996).

The wide range of framboidal pyrite $\delta^{34}S$ values is consistent with bacterial reduction of seawater sulfate in a system closed to SO_4^{2-} (Anderson, 1999; Anderson et al., 2001). The difference between the framboidal pyrite and chalcopyrite $\delta^{34}S$ values at Nifty suggests that sulfur in chalcopyrite was not sourced from existing sulfides or sulfates in the immediate host rocks but was derived from H_2S in the hydrothermal fluid. Furthermore, the relatively narrow range of $\delta^{34}S$ values for both chalcopyrite and euhedral pyrite suggests a homogeneous source for the sulfur (Anderson, 1999; Anderson et

al., 2001). In contrast, Reed (1996) argues for a local heterogeneous sulfur source (diagenetic framboidal pyrite and sulfate) for copper mineralisation at Maroochydore. As median $\delta^{34}S$ values for euhedral pyrite and chalcopyrite at Nifty are similar to the median $\delta^{34}S$ value for framboidal pyrite, it is possible homogenisation of footwall sulfur was the source of sulfur for the Nifty deposit. However the $\delta^{34}S$ values are also consistent with either a magmatic source or the inorganic reduction of Proterozoic seawater sulfate, such that the source of the sulfur at Nifty is not well constrained (Anderson et al., 2001)

Carbon and oxygen

Unaltered dolostone and calcareous mudstone from the host sequence at Nifty have $\delta^{13}C$ (+0.4 to +4.9 ‰) and $\delta^{18}O$ (+18.8 to +21.4‰), similar to Maroochydore ($\delta^{13}C$: +0.2 to +4.1 ‰ and $\delta^{18}O$: +19 to +23.3‰, Reed, 1996), but lighter than the majority of unaltered carbonates in the Yeneena Supergroup (Anderson et al., 2001). Syn-mineralisation quartz–dolomite hydrothermal alteration at Nifty has $\delta^{13}C$ in the range -10.3 to +2.4 ‰ and $\delta^{18}O$ in the range +14.3 to +21.5 ‰ (Anderson et al., 2001). While depletion of ^{13}C is most likely the result of decarbonation of the host rocks, it is not strongly coupled to ^{18}O depletion, which may be the result of water-rock interaction independent of decarbonation reactions (Anderson et al., 2001). ^{13}C and ^{18}O are less depleted in syn-mineralisation carbonates at Maroochydore ($\delta^{13}C$: –1.6 to +3.1 ‰ and $\delta^{18}O$: +18.3 to +27.3 ‰, Reed, 1996).

Mineralisation models

At Maroochydore Reed (1996) argues copper was transported as chloride complex, and diagenetic pyrite and sulfate provided a local heterogeneous sulfur source. Fluid infiltration during regional deformation (D_2, Yeneena Supergroup) was by a combination of distributed structurally-enhanced permeability and intergranular flow. However, there is no evidence for significant fluid focussing, either structurally-enhanced or otherwise, at the site of deposition. Copper deposition was interpreted to be due to increased H_2S activity and decreased fO_2 due to interaction between Cu-bearing fluid and sulfidic sediments.

Although copper mineralisation is also thought to be syn-D_2, Anderson (1999) and Anderson et al. (2001) propose a very different mineralisation model for the Nifty deposit. Rather than being sourced from the immediate host rocks, at Nifty, sulfur was introduced via H_2S in the ore fluid. The source of the sulfur was homogeneous but it is unclear whether it was ultimately derived from homogenisation of sulfur from diagenetic sulfates and pyrite in the footwall, magmatic fluids or seawater . Copper precipitation is interpreted to have been as a result of both cooling of the ore fluid and decarbonation of the wall rocks driving the fluid to higher pH.

Anderson (1999) and Anderson et al. (2000) argue the mineralising fluids ascended D_2 (Yeneena Supergroup) thrust faults interpreted to intersect the hinge and north limb of the Nifty Syncline. The lack of magnetite, haematite, bornite and chalcocite, and only trace amounts of pyrrhotite, present in association with the chalcopyrite + pyrite + quartz + carbonaceous material ore-stage assemblage suggests the ore fluid was at least slightly reduced. The underlying strongly oxidised Coolbro Sandstone was not considered a viable aquifer for such an ore fluid. Thus Anderson et al. (2000) postulated the D_2 thrust conduits were linked directly to a basal decollemént.

Pit exposures (October 2001) and the results of the more recent drilling at Nifty do not support existence of D2 thrust faults postulated by Anderson (1999).

Gross geometry of mineralisation and associated alteration halo (particularly Pb+Zn-enriched Pyrite Marker bed in the hanging wall of the copper ore body) suggests initial stages of deposit formation prior to, or during the earliest stages of D_2 folding. The Pyrite Marker bed is remarkably consistent in width and Pb+Zn grade around the Nifty Syncline (Fig. 9), and thus appears to reflect folding of an already mineralised layer, rather than introduction of the mineralising fluids at a later stage in the folding. Accordingly lateral rather than vertical fluid flow implied.

Comparison between the Yeneena Basin deposits and stratabound copper deposits of the Zambian Copperbelt and Mount Isa

Although stratabound Cu mineralisation in the Zambian Copperbelt and the Yeneena Basin (Nifty, Maroochydore) both appear epigenetic (formed during the early(?) stages of inversion in their respective basins), the Yeneena Basin deposits appear to have only the most superficial similarities to those in the Zambian Copperbelt. In both cases the host sedimentary basins have a lower siliciclastic succession, probably deposited during active rifting, overlain by a sag-phase dominated by dolomitic sediments, argillaceous sandstones, siltstones and shale. Host rocks to the Yeneena deposits (medium to thinly bedded dolomitic siltstones and shale) are lithologically similar to the Ore Shale that hosts a number of the major Zambian deposits. However, deposits in the Zambian Copperbelt (including those hosted by the Ore Shale) predominantly occur within or towards the top of the siliciclastic succession (main rift phase). In contrast, the Yeneena Basin deposits are hosted well into the sag phase (~1500 m above the Coolbro sandstone), and are underlain by substantial thicknesses of rocks similar to those hosting the copper mineralisation.

The strong silica–dolomite alteration and abundance of coarse grained chalcopyrite as breccia-fill replacive habit at Nifty is also atypical of the majority of the Zambian Copperbelt deposits. In the majority of the Zambian Copperbelt deposit, primary copper minerals are very fine grained, occupy intergranular pore-space or preferentially replace existing grains in the rock. Coarser grained vein-hosted copper sulfides are abundant locally within the Copperbelt, but are generally minor. Quartz-dolomite, and particularly cherty black quartz alteration associated with the Nifty mineralisation is absent or minor at most of the Copperbelt deposits. Chalcopyrite, bornite, chalcocite were all deposited as primary sulfides in the Zambian deposits, although their relative proportions vary considerably both between and within the individual deposits. In addition, haematite is widespread around the peripheries of many of the Zambian deposits, suggesting that both the ore fluids and host successions were more oxidised, than appears to have been the case at Nifty.

Although there are important differences between the deposits, collectively the similar host-rocks, alteration and ore mineral assemblages, textures and zonation patterns suggest Nifty has much closer affinities to the Mount Isa Cu ore bodies, than those of the Zambian Copperbelt (Waring et al., 1998; Anderson, 1999; Anderson et al., 2001). Nifty has a higher concentration of quartz alteration at its centre than the Mt Isa copper ore bodies. Although the relationship between the copper and lead–zinc ore bodies at Mt Isa is contentious, the spatial association (if not the scale) of copper and lead–zinc mineralised horizons at both Mt Isa and Nifty, may be significant. Significant Pb–Zn accumulations (peripheral or otherwise) are not features of the Zambian deposits.

Critical issues

There are a number of outstanding issues that need to be addressed in order to improve constraints on the geological development of the Yeneena Basin. Clarifying stratigraphic relationships across the orogen is critical. The relationship between the Tarcunyah Group and both the Yeneena Supergroup to north and east, and Officer Basin succession to the south is contentious (e.g. Goode and Hall, 1981) and has a direct bearing on models for the southern and western margin of the Yeneena Basin. Is the Tarcunyah Group a less deformed and metamorphosed age equivalent of the Yeneena Supergroup (Goode and Hall, 1981) or an unconformably overlying sequence as suggested by Williams et al. (1976) and the recent work of the GSWA? Despite significant refinements to stratigraphic relations across the western margin of the Paterson Orogen as a result of recent GSWA regional mapping, some apparent contradictions remain. For example the estimated 800 Ma age for the Tarcunyah Group (Bagas et al., 1995; 1999) is seemingly inconsistent with the proposed post-Miles Orogeny deposition of the group, if Reed's (1996) 717 Ma (and post-816 Ma)

age constraints on the deformation are correct.

The stratigraphic relationship between the Lamil and Throssell Groups of the Yeneena Supergroup is also currently unresolved. Does the Lamil overlie Throssell Group as suggested by early workers (e.g. Chin et al., 1982; Hickman and Clarke, 1994) or are these correlative sequences deposited in different parts of Yeneena Basin? Is it possible that the Yeneena and Throssell groups were deposited in separate terranes juxtaposed across the northern continuation of Camel–Tabletop fault zone during the Miles (±Paterson) Orogeny? The Camel–Tabletop fault zone separates the easternmost and potentially exotic Connaughton terrane from the rest of the Rudall complex (Fig. 2, Bagas & Smithies, 1998).

What was, and what controlled, the original geometry of the Yeneena Basin? What defined the basin margins? What was the original internal architecture of the Yeneena Basin and how did this influence the structural geometry during subsequent basin inversion (Miles and Paterson orogenies)? Can available geophysical data for the Paterson Orogen and existing constraints on facies distribution and palaeocurrent directions from the basin and surrounding areas provide the answers to these questions?

Recent PhD studies of stratabound copper deposits at Nifty and Maroochydore both propose copper mineralisation occurred during the main deformation phase (D_2) of the Miles Orogeny. Yet the nature and architecture of the fluid pathways, and compositions of the ore fluids, proposed for these deposits are very different (Anderson, 1999; Anderson et al., 2000). Do these differences account for differences in the style and grade of the deposits, or were other important factors also at play? To what extent do local syn-depositional structure and facies architecture control patterns of fluid flow in the basin?

Conclusions

The Paterson Orogen consists of three main elements: Palaeo- to Mesoproterozoic Rudall Complex (>2015–1765 Ma), the Neoproterozoic Yeneena Supergroup (<1132–816 Ma) and the Neoproterozoic Tarcunyah Group (<700–610 Ma). The present geometry and structure of the Paterson Orogen is largely due to deformation in the 800–700 Ma Miles Orogeny. Subsequent deposition of the Tarcunyah Group, is interpreted to reflect initial development of the Officer Basin, in a probable foreland basin setting along the southwestern margin of the Paterson Orogen. The Tarcunyah Group was deformed by NNE–SSW shortening during the Paterson Orogeny after ~610 Ma). Many of the major faults in the Paterson Orogen cut the Tarcunyah Formation (e.g. Vines Fault, Southwest Thrust, McKay Fault, Camel–Tabletop Fault Zone, Marloo Fault) were reactivated at this time.

The age, setting, structural evolution and mineral endowment of the Yeneena Basin all invite comparisons with the Zambian Copperbelt. Available evidence indicates major deposits in the Yeneena Supergroup (Telfer, Nifty and Maroochydore) formed during inversion of the Yeneena Basin succession during the Miles Orogeny, consistent with a Lufilian age for major copper mineralisation in Zambia. Anderson (1999) and Anderson et al. (2001) argue for ore fluid introduction at Nifty along D_2 thrust faults that intersect the Nifty Syncline at depth. Presently available data provides little evidence to support the existence of such structures. The model favoured here, is for development of the Nifty ore body earlier in the inversion history, prior to significant folding of the host succession. Characteristics of the Nifty deposit are distinctly different to the Copperbelt deposits, and suggest much closer affinities to Mt Isa-style copper ore bodies.

Acknowledgments

I am indebted to Bruce Hooper for discussions, encouragement and provision of considerable amounts of data for this project. Rio Tinto are also thanked for providing a compilation of aeromagnetic data covering much of the central-western portion of the Paterson Orogen. Ivan Jerkovic and Phil Shields (Straits Resources) provided considerable assistance while in the field. Leon Bagas (Geological Survey of

Western Australia) provided copies of recent GSWA maps and explanatory notes for portions of the study area, and his willingness to share his detailed and extensive knowledge of the region is greatly appreciated. Discussions with Alistair Reed (Mineral Resources Tasmania) have also been valuable.

References

Anderson, B., 1999, Structure, alteration and mineralisation of the Nifty Copper Deposit, Western Australia: Unpublished PhD Thesis, University of Tasmania, 225p.

Anderson, B. R., Gemmell, J B. and Berry, R. F., 2001, The geology of the Nifty copper deposit, Throssell Group, Western Australia: implications for ore genesis: Economic Geology, v. 96, p. 1535-1565.

Bagas, L., 1999, Geology of the Paterson 1:100,000 Sheet: Western Australia Geological Survey, 1:100,000 Geological Series Explanatory Notes, 20p.

Bagas, L., Grey, K., Hocking, R. M. and Williams, I. R., 1999, Neoproterozoic successions of the northwestern Officer Basin: A reappraisal: Western Australia Geological Survey, Annual Review 1998–99, p. 39–44.

Bagas, L., Grey, K. and Williams, I. R., 1995, Reappraisal of the Paterson Orogen and Savory Basin: Western Australia Geological Survey, Annual Review 1994–95, p. 55–63.

Bagas, L. and Smithies, R. H., 1995, Geology of the Connaughton 1:100,000 Sheet: Western Australia Geological Survey, 1: 100,000 Geological Series Explanatory Notes, 38p.

Blockley, J. G. and Myers, J. S., 1990, Proterozoic rocks of the Western Australian Shield – geology and mineralization t, *in* Hughes, F. E. (ed), Geology and Mineral Resources of Australia and Papua New Guinea: Australian Institute of Mining and Metallurgy Monograph 14, p. 607–615.

Chin, R. J. and de Laeter, J. R., 1981, The relationship of new Rb-Sr isotopic dates from the Rudall Metamorphic Complex to the geology of the Paterson Province, Western Australia: Western Australia Geological Survey, Annual Report 1980, p. 80–87.

Chin, R. J., Hickman, A. H. and Towner, R. R., 1982; Paterson Range, W. A. (2nd Edition): Western Australia Geological Survey, 1:250,000 Geological Series Explanatory Notes, 29p.

Goellnicht, N. M., 1992, Late Proterozoic fractionated granitoids and their role in the genesis of Gold and base-metal mineralisation in the Telfer district, Western Australia: Unpublished PhD Thesis, University of Western Australia.

Goellnicht, N. M., Groves, D. I., McNaughton, N. J. and Dimo, G., 1991, Late Proterozoic fractionated granitoids of the mineralized Telfer area, Paterson Province, Western Australia: Precambrian Research, V. 51, p. 375–391.

Goellnicht, N. M., Groves, D. I., McNaughton, N. J. and Dimo, G., 1989, An epigenetic model for the Telfer gold deposit, *in* Keays, R. R., Ramsay, W. R. H., and Groves, D. I., The geology of gold deposits: the perspective in 1988: Economic Geology Monograph 6, p. 151–167.

Goode, A. D. T., 1981, Proterozoic geology of Western Australia, *in* Hunter, D. R. (ed.) Precambrian of the southern hemisphere: Developments in Precambrian Geology 2, Elsevier, Amsterdam, p. 105–203.

Goode, A. D. T. and Hall, W. D. M., 1981, The Middle Proterozoic eastern Bangemall Basin, Western Australia: Precambrian Research, v. 16, p. 11–29.

Grey, K and Stevens, M. K., 1997, Neoproterozoic palynomorphs of the Savory Sub-basin, Western Australia and their relevance to petroleum exploration: Western Australia Geological Survey, Annual Review 1996–97, p. 49–54.

Haines, D. W., Brooke, W. J. L., and Mazzoni, P.P., 1993, Application of conceptual models of sediment –hosted ore deposits in the discovery of the Nifty Copper and adjacent zinc–lead deposits, Yeneena Basin, Western Australia, *in* Kirkham, R.V., Sinclair, W. D., Thorpe, R. I. and Duke, J. M., (Eds.), Mineral deposit modelling: Geological association of Canada, Special Paper 40, p. 75–88.

Hooper, B. G. D., 2002, The Nifty copper deposit, structural and alteration setting: Applied Structural Geology for Mineral Exploration and Mining, Kalgoorlie 2002, Abstract Volume, Australian Institute of Geoscientists, Bulletin 36, p. 87–88.

Howard, G. R., Hansen, T., Moore, C., Moffitt, P. J., Inglis, R. J., Carlson, R. D., Kirchner, I., Coupland, D., Leary, S. and Tomsett, A., 2000, Current geological understanding of the Telfer Gold Mine, 4th International Mining Geology Conference, Coolum Queensland, p. 135–142.

Inglis, R. J., 1995, The paragenesis and structural evolution of the M10 Reef, Telfer, Western Australia, Unpublished BSc. (Hons) thesis, University of Tasmania.

Jackson, D. G. and Andrews, R. L., 19890, Kintyre uranium deposit, *in* Hughes, F. E. (ed), Geology and Mineral Resources of Australia and Papua New Guinea: Australian Institute of Mining and Metallurgy Monograph 14, p. 653–658.

Nelson, D. R., 1995, Compilation of SHRIMP U-Pb zircon geochronology data, 1994: Western Australia Geological Survey Record 1995/3, 244p.

Hickman, A. H. and Clarke, G. L., 1994, Geology of the Broadhurst 1:100,000 Sheet: Western Australia Geological Survey, 1:100,000 Geological Series Explanatory Notes, 40p.

Reed, A., 1996, Structural, stratigraphic, and temporal setting of Neoproterozoic stratabound copper mineralisation at Maroochydore, Paterson Province, Western Australia: Unpublished PhD thesis, University of Western Australia, 289p.

Rowins, S. M., Groves, D. I., McNaughton, N. J., Palmer, M. R. and Eldridge, C. S., 1997, A reinterpretation of the role of granitoids in the genesis of Neoproterozoic gold mineraliszation in the Telfer Dome, Western Australia: Economic Geology, v. 92, p. 133–160.

Smith, S. G., 1996, Geology and geochemistry of the Warrabarty carbonate-hosted Zn-Pb prospect, Paterson Orogen, Western Australia: Unpublished PhD Thesis, University of Tasmania, 162 p.

Smithies, R. H. and Bagas, L., 1997, High-pressure amphibolite–granulite facies metamorphism in the Palaeoproterozoic Rudall Complex, central Western Australia: Precambrian Research, v. 83, p. 243–265.

Waring, C. L., Heinrich, C. A., and Wall, V. J., 1998, Proterozoic metamorphic copper deposits: AGSO Journal of Australian Geology and Geophysics, v. 17, p. 239–246.

Williams, I. R., 1990, Yeneena Basin, *in* Geology and mineral resources of Western Australia: Western Australia Geological Survey Memoir 3, p. 276–279.

Williams, I. R., 1992, Geology of the Savory Basin, Western Australia: Western Australia Geological Survey Bulletin, 141, 115 p.

Williams, I. R. and Bagas, L., 1999, Geology of the Throssell 1:100,000 Sheet: Western Australia Geological Survey, 1: 100,000 Geological Series Explanatory Notes, 24p.

Williams, I. R. and Bagas, L., 2000, Geology of the Poisonbush 1:100,000 Sheet: Western Australia Geological Survey, 1:100,000 Geological Series Explanatory Notes, 21p.

Slide 1

Geological development and mineralisation Yeneena Basin – Paterson Orogen, W.A.

Robert Scott
Centre for Ore Deposit Research

CODES / CSM AMIRA PROJECT P544 – NOVEMBER MEETING, 2002

Slide 2

Paterson Orogen

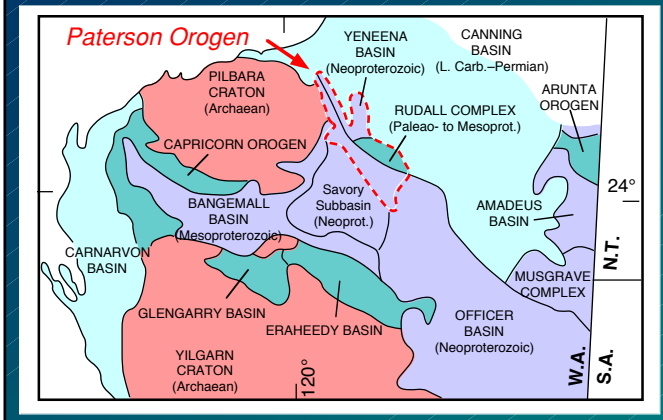

- Paterson Orogen: 1200 km long SE-trending belt of Palaeo- to Neoproterozoic rocks at the eastern margin of the Plibara Craton,central Western Australia

Phanerozoic
Post- c.1600 Ma
Pre- c.1600 Ma
Archaean

Slide 3

Paterson Orogen

- Paterson Orogen consists of three main elements:
  - Rudall Complex (Palaeo- to Mesoproterozoic, >2015–1765 Ma)
  - Yeneena Supergroup (Neoproterozoic, <1250–816 Ma)
  - Tarcunyah Group (Neoproterozoic, <700 Ma)
- As a whole, orogen is moderately to strongly deformed, poorly exposed, and – with the exception of several mineral deposits – poorly studied
  - as a result, age constraints and relationships between many of the between major lithostratigraphic units (particularly within the Yeneena Supergroup) are poor.

Slide 4

Background to Study

- Neoproterozoic sedimentary rocks of the Yeneena Basin, within the Paterson Orogen, host the giant Telfer Au-Ag deposit, stratabound copper deposits (e.g. Nifty) and carbonate-replacement Zn-Pb deposits (Warrabarty)
- The age, setting, structural evolution and mineral endowment of the Yeneena Basin all invite comparisons with the Zambian Copperbelt
- Apart from Geological Survey of Western Australia 1:100,000 mapping and reports and PhD, MSc and Honours studies of major mineral deposits, the region has received little study, and many aspects of the geological development are not well understood.

Slide 5

Aims

- Provide synthesis of geological development of Paterson Orogen based on:
  - review of previous (largely deposit-based) studies
  - recent 1:100,000 mapping by Geological Survey of Western Australia
  - interpretation of available potential field data (magnetics, gravity, EM)
- Develop model(s) for the formation and subsequent inversion of the Yeneena Basin
- Evaluate origin, timing and distribution known mineralisation in terms of geological development of the Yeneena Basin
- Compare with Zambian Copperbelt

Slide 6

This Presentation

- Synthesis and analysis of Paterson Orogen geophysical data is ongoing
- This report presents
  - overview of the geological development of the Paterson Orogen based on review of existing literature, and observations by the author during a 2 week field visit in October 2001
  - review of models for stratabound copper deposits in the Yeneena basin and comparisons with the Zambian Copperbelt
  - delineation of critical problems to be addressed by this study

Slide 7

Regional Geology

- Simplified geology of the Paterson Orogen showing location of major mineral deposits

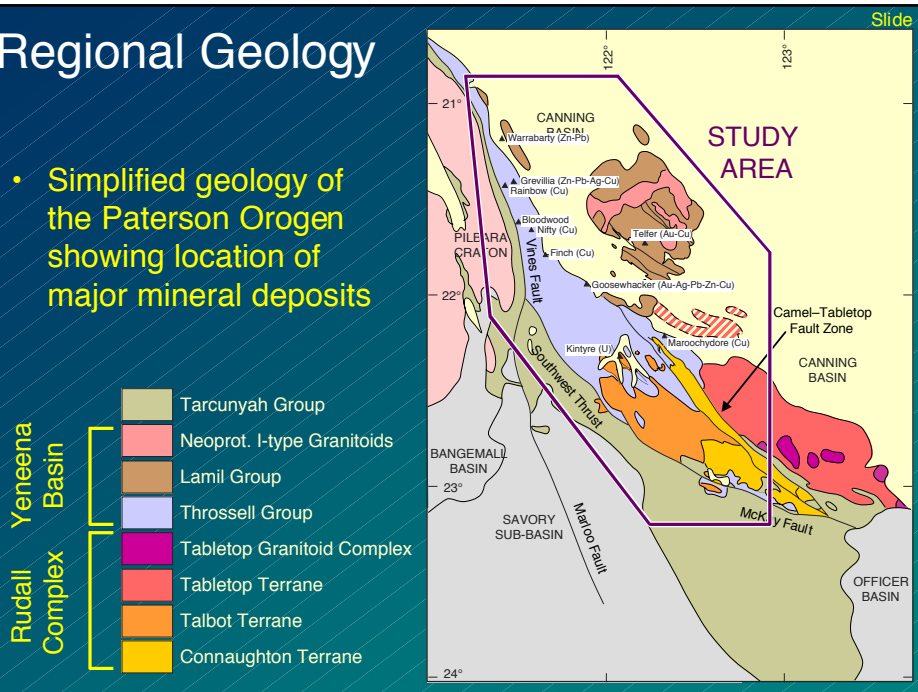

Slide 8

Temporal Evolution of Paterson Orogen

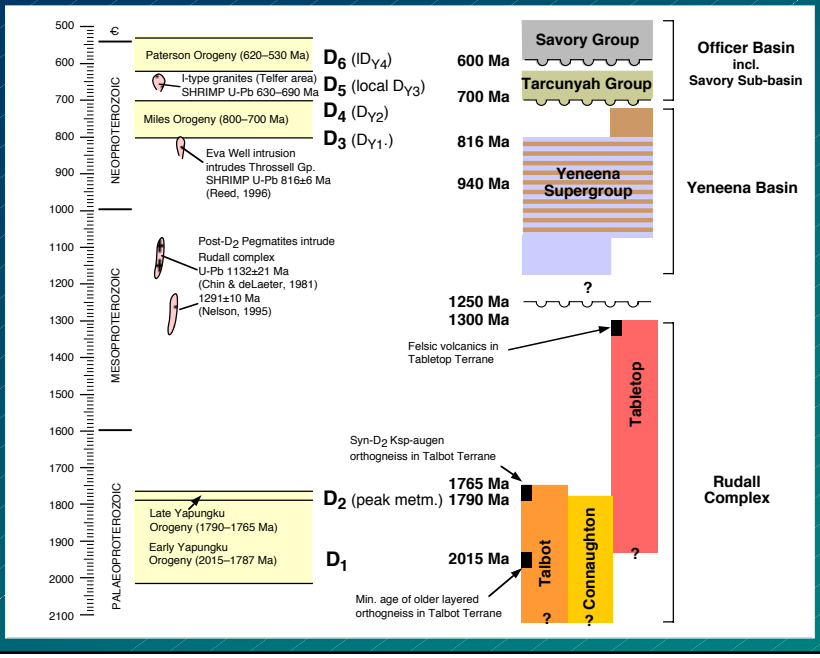

Metal Endowment

Slide 9

- Telfer (Au-Cu) *Malu Formation, Lamil Group*
  - >175 t (5.6 Moz) Au prior to closure in 2000
  - Recent reappraisal identified resource of 19 Moz Au (based on $A 500/oz) and 740,000 t Cu
- Nifty (Cu) *Broadhurst Formation, Throssell Group*
  - Total resource 148 Mt @ 1.3% Cu
  - includes chalcopyrite resource 110 Mt @ 1.4% Cu, leachable reserve 27.6 Mt @ 1.1% Cu
- Maroochydore *Broadhurst Formation, Throssell Group*
  - 140 Mt @ 0.5% Cu, including 51.3 Mt @ 1.0% Cu, 0.04% Co
- Warrabarty (Zn–Pb) *Broadhurst Formation, Throssell Group*
  - sub-economic
- Kintyre (U) *Yandagooge Formation, Rudall Complex*
  - 36,000 t U_3O_8 @ 1.5–4.0 kg U_3O_8 per tonne

Rudall Complex

Slide 10

- The Palaeo- to Mesoproterozoic Rudall complex broad zone of imbricate thrust sheets (younger to east)
- Major thrusts separate three main tectono-stratigraphic elements:
  - Talbot, Connaughton and Tabletop Terranes
- Oldest rocks of the complex underwent two episodes of folding, faulting and fabric development (2000–1760 Ma Yapungku Orogeny), prior to deposition of unconformably overlying Yeneena Supergroup
- Peak amphibolite(–granulite) facies metamorphic conditions during D_2 (1790–1760 Ma)

Slide 11

Tectono-stratigraphic elements of the Rudall Complex

- Talbot Terrane
  - siliciclastic sedimentary rocks (paragneiss) and granitoids (orthogneiss) metamorphosed to intermediate-pressure amphibolite facies
- Connaughton Terrane
  - mafic schist and gneiss, chert, carbonates, pelite and BIF metamorphosed to high-pressure amphibolite(–granulite) facies
- Tabletop Terrane (potentially exotic)
  - granitoids, dolerite dykes and (?)felsic volcanic rocks dated at ~1300 Ma

Slide 12

Constraints on deformation and metamorphism in Rudall Complex

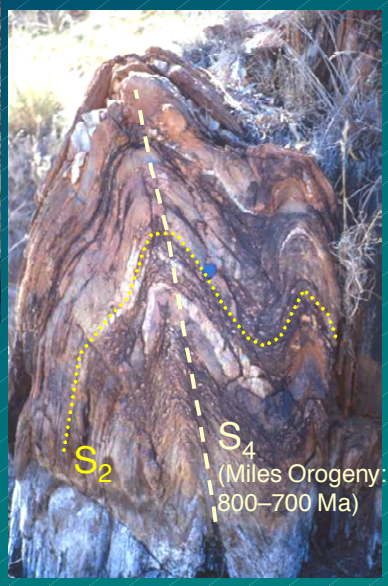

- Two generations of orthogneiss form ~50% of Rudall complex. Younger series 1787–1765 Ma (illustrated) contain S2 fabric but not S1. The gneisses were refolded and locally retrogressed during the post-Yeneena Supergroup Miles Orogeny.

Slide 13

Yeneena Supergroup

- Yeneena Basin interpreted as either pull-apart basin formed during strike-slip faulting or a failed rift
- The Yeneena Basin succession unconformably overlies the Rudall complex and is divided into two groups:
  - Throssell Group (exposed in the west and south) and
  - Lamil Group (exposed in the east)
- Contacts between the groups are not exposed and while the Lamil Group is considered younger, stratigraphic relations have not been reliably established. The successions may be, at least in part, temporally equivalent (Bagas, pers. comm. 2002).

Slide 14

Yeneena Supergroup (Throssell Group)

- Coolbro Sandstone
  - Basal unit of Throssell Group
  - Unconformably overlies Rudall Complex
  - Qtz-rich sandstone with lesser siltstone and shale, locally developed basal polymict conglomerate
  - Thins against basin edge in S and SE, N- to NE-directed palaeocurrents

Hickman & Clarke, 1994
Hickman & Bagas, 1998

Slide 15

Yeneena Supergroup (Throssell Group)

- Broadhurst Formation
  - conformably overlies Coolbro Sst.
  - main host to mineral deposits
  - carbonaceous, graphitic and sulfidic shale, minor sandstone and dolomite
  - records rapid subsidence of Yeneena Basin

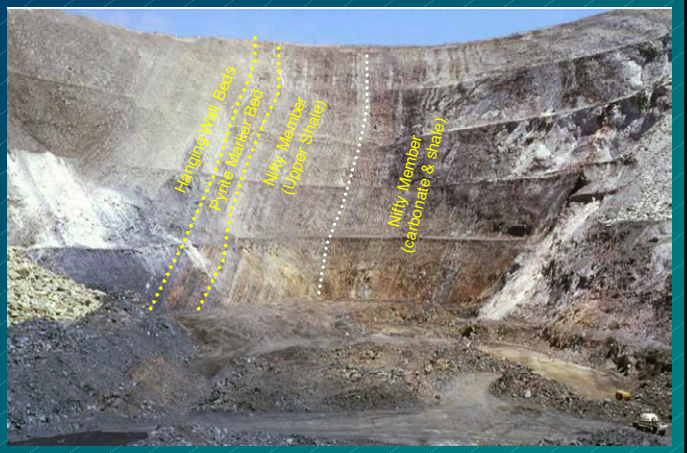

View west along Nifty Pit. Steeply S-dipping dolomitic and graphitic shales of the Broadhurst Formation

Slide 16

Yeneena Supergroup (Lamil Group)

- Contact with Throssell Group not exposed
  - stratigraphic relationship unresolved, potentially exotic
- Age constraints:
  - younger than 1070 Ma detrital zircons
  - older than post orogenic 678±12 Ma Mt Crofton Granite
- Sandstone–shale–carbonate succession

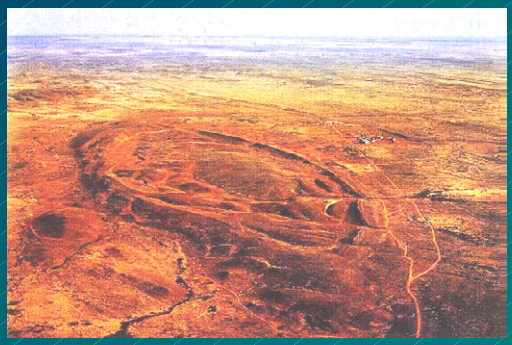

Main Dome at Telfer, prior to commencement of mining in the mid 1970s. Photo Newcrest Mining.

Slide 17

Tarcunyah Group

- Initial deposition within the Savory Sub-basin of the Officer Basin
- Extensive development along western margin of the Paterson Orogen

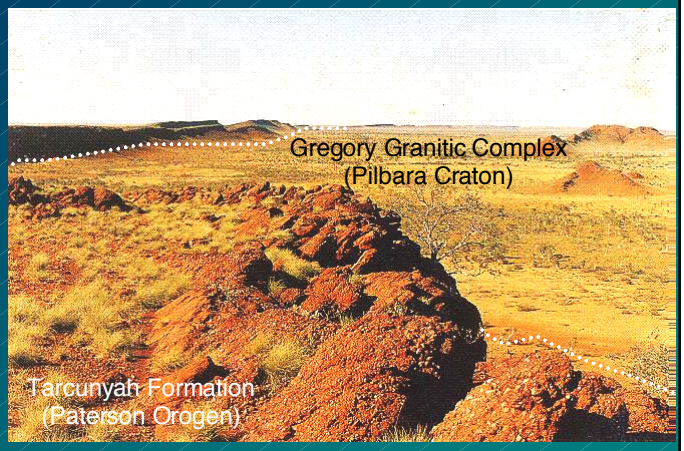

Photo (looking south): Williams and Trendall (1998)

Slide 18

Canning Basin (Permian)

- Permian fluvioglacial strata (Paterson Formation) of the Canning Basin succession cover much of the Paterson Orogen
- Thickest sequences deposited in N-directed palaeovalleys
  - deep palaeovalley between regions of outcropping Throssell and Lamil Groups, consistent with possible underlying crustal weakness (i.e. northern continuation of Camel–Tabletop fault zone)

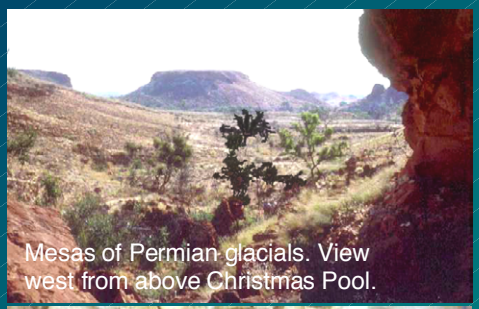

Mesas of Permian glacials. View west from above Christmas Pool.

Aboriginal rock art on Permian glacials

Slide 19

Stratabound copper deposits within the Yeneena Basin

- Two major deposits known
  - Nifty (operating mine)
  - Maroochydore (140 Mt low grade resource)
- Recent PhD studies of Nifty (Anderson,1999) and Maroochydore (Reed,1996) indicate
  - deposits hosted by similar successions of interbedded carbonaceous, pyritic and dolomitic shale and dolostone within the upper Broadhurst Formation (~1500 m above Coolbro Sandstone)
  - copper mineralisation synchronous with second phase of deformation (D_{Y2}) affecting the Throssell Group (i.e. main phase of basin inversion during Miles Orogeny, regional D_4)
  - 717±5 Ma $^{40}Ar/^{39}Ar$ apparent age for phlogopite associated with chalcopyrite mineralisation at Maroochydore

Slide 20

Syn-deformational mineralisation

- chalcopyrite
  - partial replacement of individual beds, particularly those having undergone bedding-parallel shear
  - rims and replaces diagenetic framboidal pyrite
  - occurs within the hinges of D_{Y2} folds, along the associated cleavage and faults and within syn-D_{Y2} pressure shadows and cleavage parallel veins

Maroochydore
YNC-82, 144 m

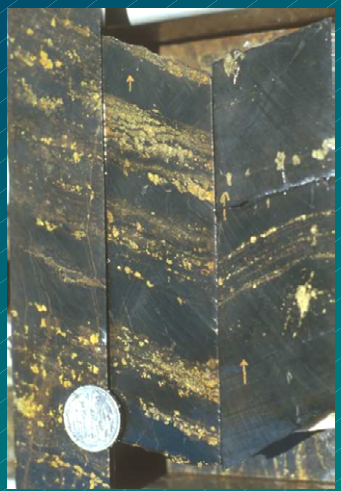

Nifty
THRD 780 W1
386–396 m

Slide 21

Mineralisation styles

- Maroochydore
  - chalcopyrite predominantly disseminated or precipitated in dilational sites
- Nifty
  - massive chalcopyrite replacive, associated with intense quartz-dolomite alteration
  - lesser disseminated and vein-hosted mineralisation

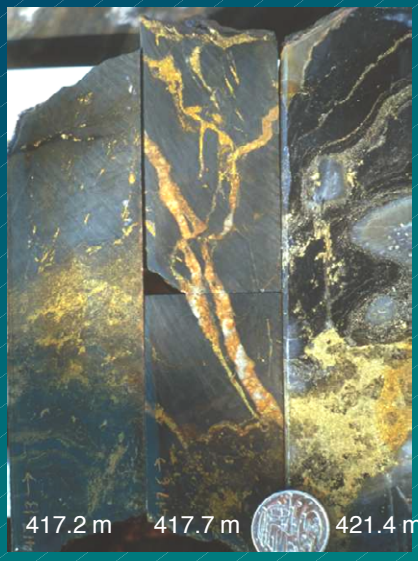

Nifty
THRD 780 W1

Slide 22

Mineralisation styles

- late-stage massive and breccia matrix chalcopyrite mineralisation at Nifty

Nifty
THRD 780 W1

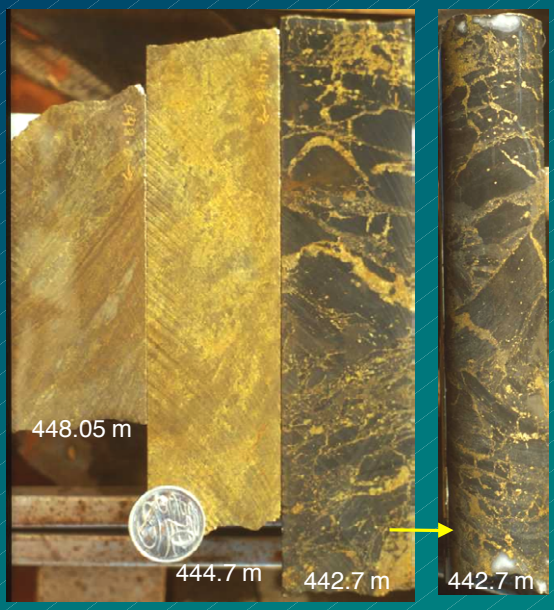

Slide 23

Deposit comparisons

- Fluid inclusions
  - inclusions from syn-mineralisation veins at Maroochydore and Nifty have similar salinities (8–27 eq. wt % NaCl), homogenisation temperatures (180°–450°C) and estimated trapping temperatures (median values: 360°–440°C), consistent with epigenetic mineralisation at greenschist facies metamorphic conditions
- Sulfur isotopes
  - (i) diagenetic framboidal and (ii) pre- to syn-mineral euhedral pyrite:
    - (i) $\delta^{34}S$ +16 to –27 ‰ (ii) $\delta^{34}S$ +3.8 to –12 ‰ (Nifty)
    - (i) $\delta^{34}S$ –22 to –31 ‰ (ii) $\delta^{34}S$ –4.0 to –10 ‰ (Marooch.)
  - chalcopyrite:
    - $\delta^{34}S$ +6 to –6 ‰ (Nifty)
    - $\delta^{34}S$ –13 to –23 ‰ (c.g., Maroochydore)
    - $\delta^{34}S$ –25 to –31 ‰ (f.g., Maroochydore)

Slide 24

Mineralisation models

- At Maroochydore Reed (1996) argues
  - Cu transported as chloride complex
  - local heterogeneous sulfur source (diagenetic pyrite and sulfate) for syn-D_{Y2} epigenetic copper mineralisation
  - syn-mineralising fluid infiltration by a combination of distributed structurally-enhanced permeability and intergranular flow, with no evidence for significant fluid focussing at the site of deposition
  - Cu deposition due to increased H_2S activity and decreased fO2 due to interaction between Cu-bearing fluid and sulfidic sediments
- At Nifty, Anderson (1999) argues
  - homogeneous sulfur source for chalcopyrite and coeval (euhedral) pyrite
  - H_2S dominant in the fluid phase not sourced from host rocks
  - syn-D_{Y2} mineralisation with fluids ascending thrusts interpreted to intersect the hinge and north limb of the Nifty Syncline

Slide 25

Mineralisation models - Nifty

- Subsequent drilling at Nifty, does not support existence of thrust faults postulated by Anderson (1996).
- Gross geometry of mineralisation and associated alteration halo (particularly Pb+Zn-enriched Pyrite Marker bed) suggests initial stages of deposit formation prior to, or during the earliest stages of D_{Y2} folding
- Lateral rather than vertical fluid flow implied.

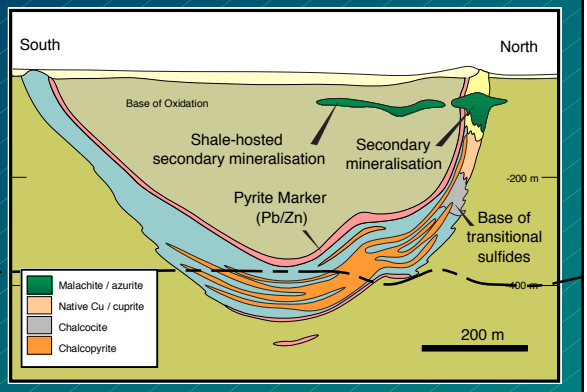

Idealised cross-section of the Nifty ore body showing mineralogical zonations (Hooper, 2002)

Slide 26

Yeneena Basin vs. Copperbelt

- Although stratabound Cu mineralisation in both areas may be largely epigenetic (formed during the early(?) stages of inversion in their respective basins), the Yeneena Basin deposits appear to have only the most superficial similarities to those in the Zambian Copperbelt
- strong silica–dolomite alteration and predominance breccia-fill, vein and replacement style mineralisation at Nifty suggests greater affinities with Mount Isa Cu ore bodies

Slide 27

Critical Questions to be addressed

- Ongoing studies of the Yeneena Basin / Paterson Orogen will focus on a number of key issues:
  - Determining the original architecture of the Yeneena Basin and how this influenced structural geometry during subsequent basin inversion (Miles Orogeny)
  - Evaluate distribution, timing and character of deposits in terms of their regional stratigraphic and structural context. Implications for patterns of fluid flow during basin inversion

Slide 28

Critical Questions

- A critical aspect to be addressed in reconstructing the Yeneena Basin is the relationship between the Lamil and Throssell groups
  - Does Lamil overlie Throssell?
  - Correlative sequences deposited in different parts of Yeneena Basin?
  - Were these groups deposited in separate terranes juxtaposed in the Miles Orogeny across the northern continuation of Camel–Tabletop fault zone, i.e. the fault system separating the easternmost and potentially exotic Connaughton terrane from the rest of the Rudall complex (Bagas & Smithies, 1998)

Acknowledgments

- Bruce Hooper, Ivan Jerkovic, Phil Shields (Straits Resources)
- Rio Tinto Exploration
- Leon Bagas (Geological Survey of Western Australia)
- Alistair Reed (Mineral Resources Tasmania)

Structure of the Curdimurka Subgroup, Willouran Range, South Australia

Wallace Mackay
Centre for Ore Deposit Research, University of Tasmania

Summary

Mapping of key outcrops in the northern Willouran Range area during 2002 has shown that the Curdimurka Subgroup has been affected by three folding events. The first, F_1 was bedding-parallel and confined to specific levels of the stratigraphy. It comprised both folding, with a fanning axial plane cleavage S_1, and low-angle (relative to bedding) faulting, with a transport direction to the southeast. F_1 was of regional significance and can be seen along the Norwest Fault, where it can be seen to have deformed the Burra Group, although not with the intensity seen within the Curdimurka Subgroup.

F_2 folds are upright and close to tight non-cylindrical folds, trending northwest–southeast, with an axial planar cleavage, S_2. In profile, the folds have rounded anticlinal hinges and sharp synclines, with thinning on the limbs and thickening within fold hinges. Within the Willouran Range area, many of the dominant structures are related to F_2 and the timing is considered to be the first phase of Delamerian folding.

The final phase of folding is F_3. F_3 folds are open with moderate plunges to the southwest. They have a cleavage, S_3, which is typically at a high angle to both bedding and S_2.

Mapping at Dunns Mine was also undertaken during 2002 to determine the origins of the mineralisation. Copper mineralisation (now mainly malachite with minor chalcocite) is restricted to a black siltstone and shale facies of the Dunns Mine Limestone. The highest grade mineralisation occurs within a fault zone along the limb of a small F_2 fold but there is also lower grade mineralisation within the siltstone and shale out-with the fault zone. Mineralisation is thought to have resulted from the remobilisation of copper from the siltstone and shale into the fault zone during F_2.

Background

Compared with the Katangan Supergroup, which hosts the copper mineralisation of the central African Copperbelt, the Adelaide Fold Belt appears to be considerably under-endowed with copper. Based on depositional age, lithology and perceived tectonic setting during deposition, the comparison appears valid but it is the aim of this project to look beyond these superficial similarities. The validity will be tested by looking in detail at the structure and sedimentology of the Curdimurka Subgroup, the upper-most package of the Callanna Group, the basal group of the Adelaide Fold Belt (Fig. 1 shows a stratigraphic column for the northern Flinders Ranges).

The Callanna Group comprises two subgroups, the basal Arkaroola Subgroup and the Curdimurka Subgroup but the relationship between these two subgroups remains nebulous. The Arkaroola Subgroup crops out only around the Palaeoproterozoic to Mesoproterozoic Mt Painter Block, at the far northeastern corner of the Adelaide Fold Belt, whereas the Curdimurka Subgroup crops out in series of fault slices in the Willouran Range at the northwestern edge of the Adelaide Fold Belt. Supposed correlates of both are found in megabreccias attributed to salt diapirism in the northern and central Adelaide Fold

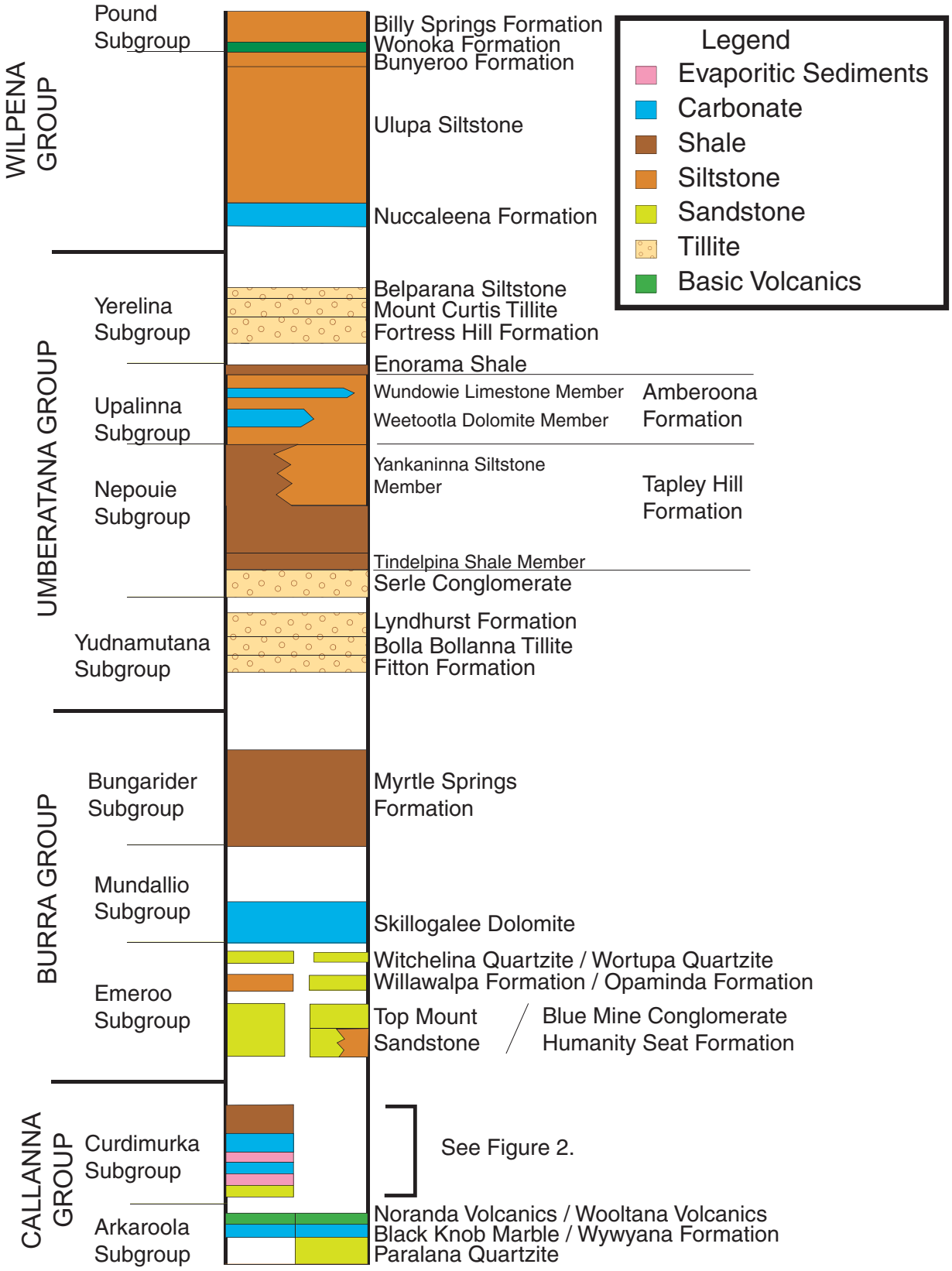

Figure 1. A stratigraphic column for the northern Flinders Ranges and the Willouran Range (Based on Preiss, 1993 with modifications from Preiss et al., 1998 and Preiss and Cowley, 1999). Note; from the level of the Emeroo Subgroup down, the left column refers to the Willouran Range and the right to the Arkaroola area.

Belt (Preiss, 1987). There has been an assumption that the Curdimurka Subgroup in the Willouran Range is underlain by the Arkaroola Subgroup, based on the presence of mega-clasts of mafic volcanics (the Noranda Volcanics) within breccias above, within and below the Curdimurka Subgroup. That assumption is probably correct but because of differing theories on the origins of the breccias, and because the basal contacts of the Curdimurka Subgroup are structural and not lithological, it remains unproven (e.g, Murrell, 1977; Rowlands et al., 1981; Preiss, 1987). Finally, both the Arkaroola Subgroup and the Curdimurka Subgroup host copper mineralisation but in all known cases, that mineralisation is small or low grade or both.

It is the Curdimurka Subgroup which bears the closest similarity to the sediments hosting copper mineralisation in the Copperbelt, being at the base of the sedimentary basin, being of a similar (Cryogenian) age and having a lithological stacking of initial siliciclastic deposition followed by carbonates and evaporites, overlain by siltstones and shales. The Arkaroola Subgroup also has a siliciclastic unit at its base, the Paralana Quartzite, overlain by a carbonate unit, the Wywyana Formation but these are overlain by the Wooltana Volcanics, which by their presumed correlation with the Gairdner Dyke Swarm, have been dated at 827 ± 6 Ma (Wingateet al., 1998).

Introduction

Mapping in the northern Willouran Range during 2002 has shown that the Curdimurka Subgroup has been affected by a complex combination of folding and faulting (Fig. 2). Normal faulting has removed much of the stratigraphy at the northern and southern ends of the area under consideration and the contact with the Burra Group in the southern half of the area and the Umberatana Group in the northern half are faulted. In addition, there are a number of reverse faults and thrusts which are locally important. It is not the intention to consider the faulting in detail in this report; interpretation of the faulting is continuing and it will be reported at a later date.

In this report, the focus will be on the folding events which have affected the Curdimurka Subgroup. At the macroscopic scale there are several northwest–southeast trending folds which have affected the stratigraphy below the Hogan Dolomite. In addition, the Boorloo Siltstone has been affected by northwest–southeast trending folds adjacent to the contact with the Burra Group west of Breaden Hill and have been folded into an open syncline and anticline from about Breaden Hill, north and west to about 4 km east of Callanna Homestead. At the outcrop scale, there are a range of fold-styles ranging from broad folds to rootless isoclinal folds, with orientations varying from recumbent to upright and shallow to steep plunges.

To make sense of these general observations, two areas were identified where more detailed structural mapping would provide the key to the understanding of folding within the Curdimurka Subgroup. The first (here informally termed Boorloo Anticline) is around the core of an anticline within the Boorloo Siltstone, about two kilometres south of the old Noranda exploration camp and the second is at the top of the Dunns Mine Limestone at Dunns Mine. The locations of these areas are shown in Figure 2.

At the Boorloo Anticline locality, a series of outcrops around an anticline show steeply plunging folds with axial planes sub-parallel to bedding. The vergence of these folds does not change around the hinge of the anticline showing that they pre-date the upright folding. In addition, the trend of the hinge line of the anticline changes from southeast–northwest to east–west, indicating a third deformation.

The Dunns Mine outcrop was grid-mapped at a scale of 1:200, with one area mapped at a scale of 1:40. It demonstrates two deformations; the first having upright folds with variable plunges and trends changing from southeast to west, with a normal trend of northwest–southeast, and the second having broad folds with a moderate plunge to the southwest.

Having developed an understanding of the structure of the Curdimurka Subgroup, the relationship between structure and copper mineralisation was investigated by mapping Dunns Mine at a scale of 1:1000. At Dunns Mine there are a series of workings (trenches, shafts and pits) which follow a unit of shale,

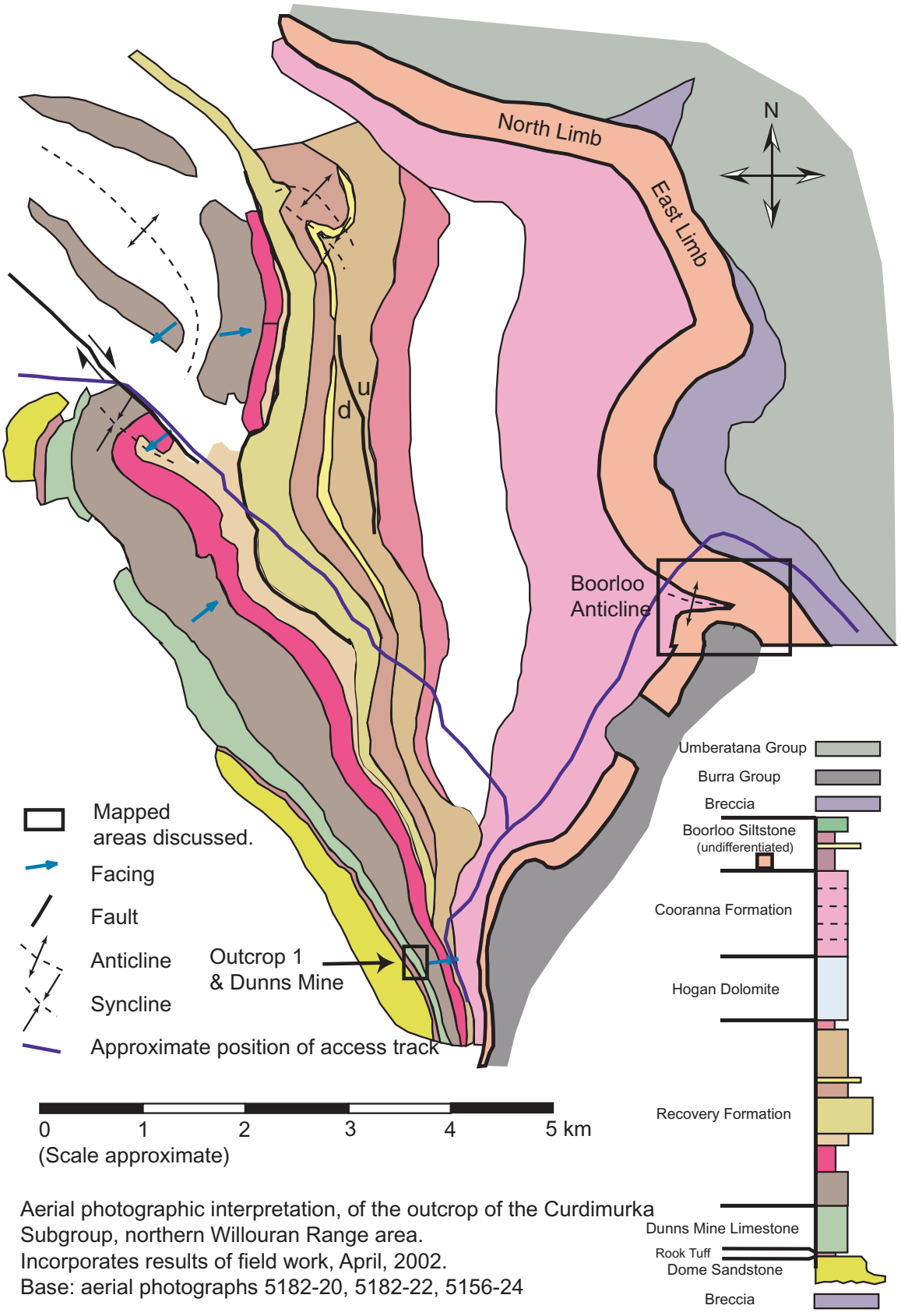

Aerial photographic interpretation, of the outcrop of the Curdimurka Subgroup, northern Willouran Range area.
Incorporates results of field work, April, 2002.
Base: aerial photographs 5182-20, 5182-22, 5156-24

Figure 2. Draft geological map of the Curdimurka Subgroup, northern Willouran Range, South Australia, showing areas discussed in report.

siltstone and carbonate over a strike length of about 400 m. Malachite and chalcocite occur in fault breccia, in veins and in weathered, kaolinitic shale along the unit and mapping showed that the mineralisation is associated with one of the folding events identified.

Boorloo Anticline

Within the Boorloo Siltstone, about 20 m above the base, is a unit of six dolomite beds, with a total thickness of six to ten metres. In the northern half of the area, a distinguishing feature of the unit is the presence of bedding-parallel folding. The intensity of deformation is variable, from being restricted to a metre or so at the top of the unit, to the almost complete destruction of bedding across the entire unit and cleavage being the dominant fabric. At one locality, it is estimated that folding has resulted in roughly a 300% thickening of the unit. East of Dunns Mine, the same unit is present but it is undeformed.

The Boorloo Anticline area shows that the bedding-parallel folding has been folded around the limb of a macroscopic upright anticline, the anticline being double plunging, with a syncline to the south, forming a dome and basin style structure. A faulted contact between the Curdimurka Subgroup and the Burra Group terminates the structure south of the syncline. The fold axis and bedding around the limbs of this macroscopic fold have been folded into an open fold about a northerly trending axis. Taken together, this area provides evidence for three generations of folding; the bedding parallel folding being F_1, the Boorloo Anticline structure representing F_2 and the open folding being F_3.

The orientation of the F_1 structures was examined on each of the four limbs and in the eastern hinge of the anticline. Outcrop on the southeastern limb is poor and little information was gained there. More information was gathered on the northeastern and southwestern limbs but most of the information on the style of the F_1 structures was gained from the northwestern (and longest) limb. Within the hinge of the anticline, data was gathered around several F_1 fold closures. Most of this data was cleavage-bedding intersections. Figure 3 shows the geology of this area, with stereoplots of structural data collected.

Northwestern Limb

The northwestern limb was mapped along a strike length of about 1 kilometre. Along much of this strike length the form of outcrop is a series of mounds, raised about 50 cm above the general level of outcrop, with an irregular spacing along the dolomitic unit (Fig. 4). Each mound represents an F_1 fold closure. Along the limb, the intensity of deformation is variable with in some places, cleavage being the dominant fabric although this is unusual.

The folds have a steep plunge to the northwest. There is a divergent axial planar cleavage, steeply dipping to the north. As the general strike of the limb changes from northwest–southeast to east–west, the strike of the cleavage and axial plane change to east–west, dipping northward. At the scale of tens of centimetres, both 'Z' and 'S' folds (in plan view) are present, but these reflect metre-scale folds with vergence to the east ('Z' fold). Figure 5 shows an example of a metre-scale F_1 fold. Also along this limb is a small outcrop which displays a mushroom fold-interference pattern, indicating the re-folding of a recumbent fold by a non-coaxial upright fold (Fig. 6).

Removing the affect of F_2 on the F_1 fold plunges and axial planes (two rotations were used, the first to account for the F_2 plunge, the second rotated average bedding to horizontal) resulted in shallow fold plunges to the northeast and southwest, with axial planes dipping to the northwest and southeast. Transport direction is to the southeast.

Northeastern Limb

The northeastern limb has a strike length of about 500 m, before it becomes covered by scree and is eventually terminated by a faulted contact with the Burra Group. Its general strike is southeast–northwest with steep dips to the southwest and northeast. F_1 folds along this limb are on the tens of centimetre scale. Fold axial surfaces strike southeast–northwest with steep dips to the northeast and southwest. Plunges are moderate to steep to the southeast and northwest.

Removing the effect of F_2 on these folds results in the fold plunges becoming shallow to the east and northwest. Axial planes dip to the north at shallow to moderate angles. Transport is to the south.

Southwestern Limb

The southwestern limb has a strike length of about 700 m before reaching the synclinal closure. Beyond the syncline, the Boorloo Siltstone is terminated by a faulted contact with the Burra Group. F_1 folds within the dolomitic unit have axial planes with a moderate to steep dip to the south-southeast and steep plunges to the southeast and southwest. The metre-scale folds form 'Z' folds, verging to the southeast.

Outcrop along the southeastern limb is poor and did not provide reliable structural data on folds along this hinge. It will not be discussed further at this stage.

Hinge

In the eastern hinge of the anticline, six outcrops were examined for structural data. Each outcrop shows complex structural relationships and interference patterns. There are upright F_2 folds and inclined to recumbent folds which are F_1 folds, re-folded by F_2. The complexity is seen at all scales from centimetre to tens of metres. Figures 7 and 8 show examples of these folds in the hinge.

Three cleavage-bedding intersections lineations are present; two are subparallel and shallow whereas the third is typically steep. At any one outcrop, any one of these lineations may be dominant. Between the shallow lineations, timing relationships are difficult to determine but one of the sub-parallel lineations can be seen to wrap around the other in some outcrops. The steep lineation is not affected by the sub-parallel lineations and is identified as L^3_0.

F_1 at other Locations within the Boorloo Siltstone

F_1 folds were noted at two other locations within the Boorloo Siltstone. Bedding trends east–west at the first of these localities and at the second, it trends north–south. At the first locality, folding occurs not only within the dolomite unit but also in a thin sandy unit about 50 m stratigraphically above the dolomite unit and within the dolomitic unit at the top of the Boorloo Siltstone. A strong cleavage locally developed within the black shale above the dolomitic unit likely reflects F_1 structures. The vergence of the folds here is to the east. At the second locality, deformation occurs in the dolomitic unit and along the contact with the Cooranna Formation. Fold plunges are steep to the east, and while most folds verge to south, there are some northerly verging structures. Figure 9 shows stereoplots for these areas.

F_1 at other stratigraphic levels

F_2 is the dominant regional structure but F_1 is seen throughout the Curdimurka Subgroup in this area. It is most commonly observed in carbonate beds, where it may occur as isoclinal or recumbent folds, typically verging to the south or east, or as dextral strike-slip faults at a low angle to bedding, indicating transport to the southeast quadrant. Rare sinistral strike-slip faults are also attributed to F_1 and may represent back-thrusts. Nowhere is F_1 or related structures seen to cross-cut stratigraphy to any significant degree; it always appears to be restricted to specific stratigraphic levels.

At the regional scale, many of the structures along the Norwest Fault (mainly dextral strike-slip faulting, recumbent folding on the hundreds of metres scale) are here attributed to F_1 (Fig. 10). The main transport direction of these structures is to the southeast, although some back-thrusting is also present (Mackay, 2001).

F_1 Summary

F_1 can be summarised as being southeasterly verging recumbent folds which have been re-folded by F_2. The associated cleavage is sub-parallel to bedding, except within the hinges of F_1 folds. It is largely confined to specific layers. Associated with F_1 is what is seen today as mainly dextral strike-slip faulting, although relative to bedding, they would be described as thrusts. From structures along the Norwest Fault, F_1 is of regional significance.

Boorloo Anticline: Lithology and Structure

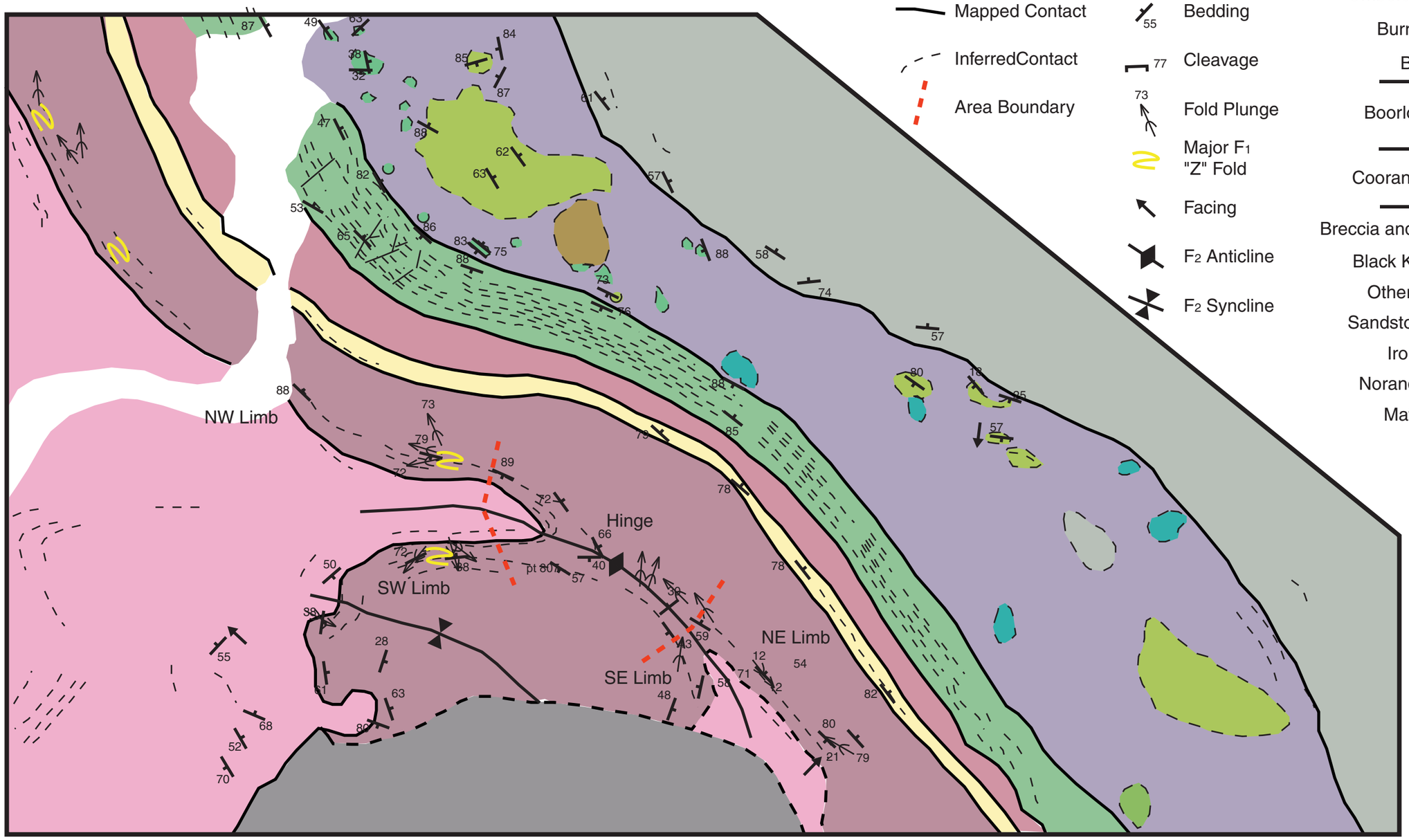

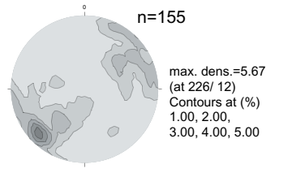

Contoured poles to bedding; all data

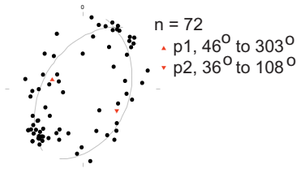

poles to bedding, excluding around F_1 folds in F_2 fold hinge

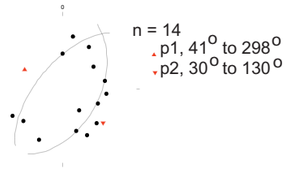

poles to bedding, hinge only

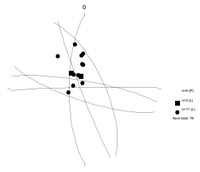

NW Limb, fold plunge and axial planes

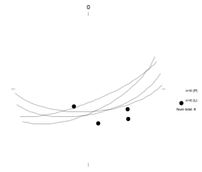

SW Limb, fold plunge and axial planes

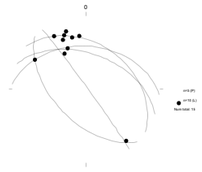

NE Limb, fold plunge and axial planes

Figure 3. Boorloo Anticline, showing lithologies and structures.

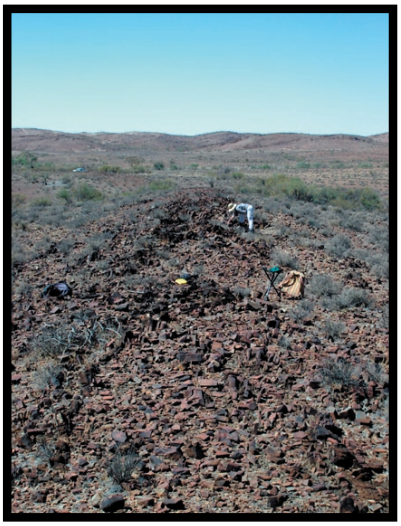

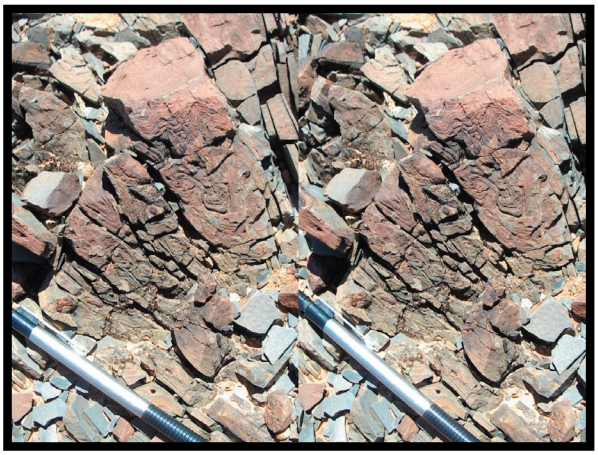

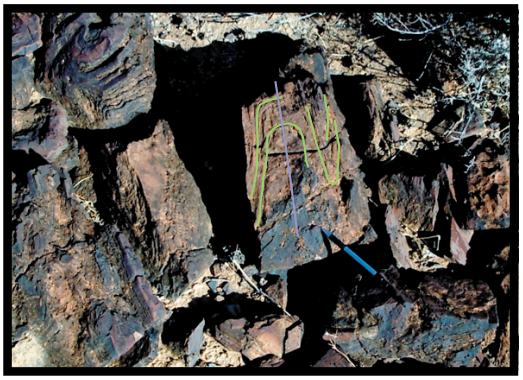

Figure 4 *(top left)*. Outcrop of basal dolomitic unit of the Boorloo Siltstone.
Figure 5 *(top right)* A recumbent F_1 fold. Bedding trace is green and S_1 trace is yellow. Photograph looking to the west.
Figure 6 *(middle)*. Stereoscopic photograph showing fold interference patterns for F_2 on F_1. Line drawing on the right is a trace of bedding (green), F_1 (yellow) and F_2 (blue). Black is shears between fold hinges.
Figure 7 *(bottom left)*. F_2 fold in the core of the Boorloo Antcline
Figure 8 *(bottom right)*. F_1 fold in the core of the Boorloo Anticline.

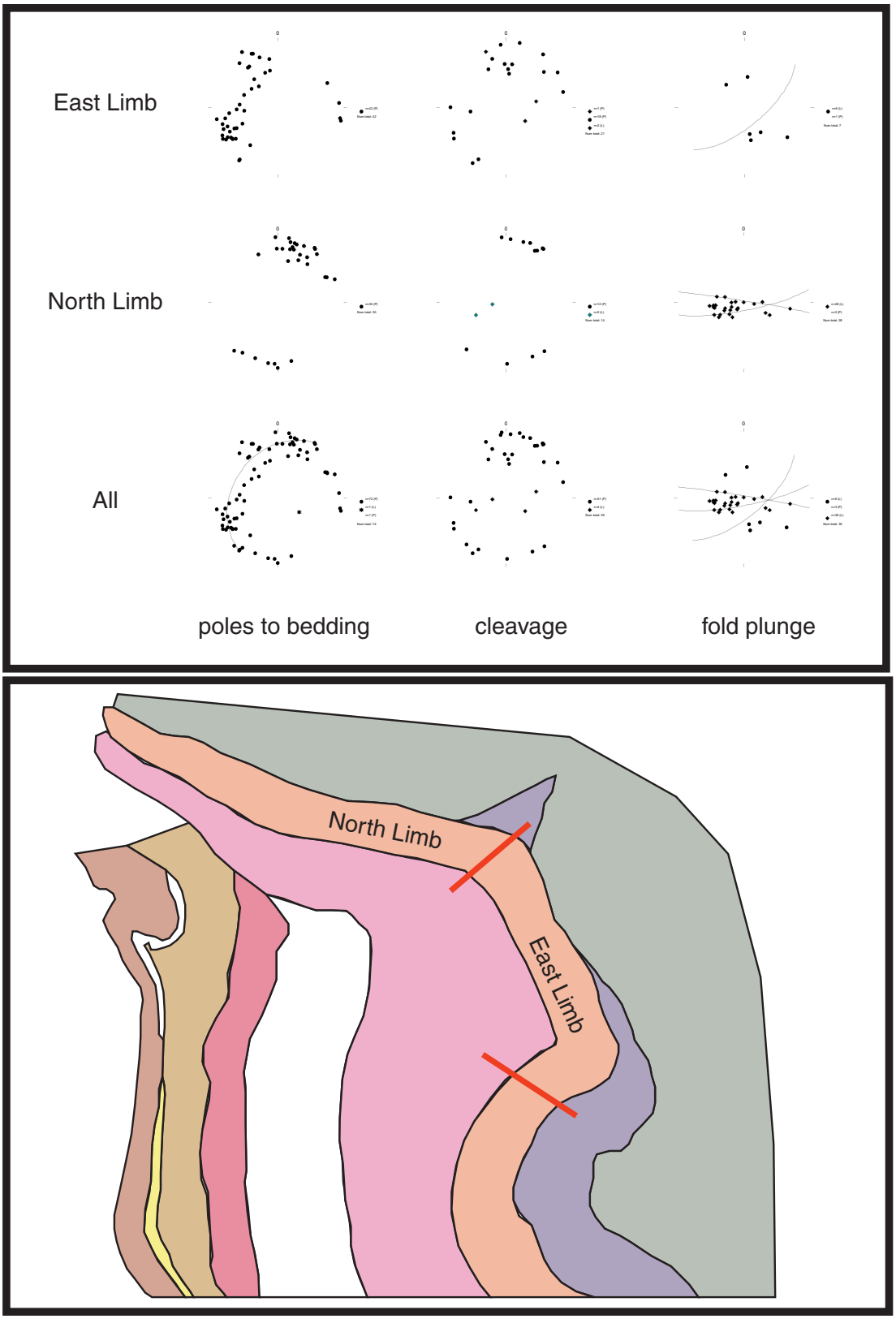

Figure 9. Stereoplots for structural data from within the Boorloo Siltstone, north of Boorloo Anticline. Diagramatic map shows the position of the limbs. See Figure 2 for locality and legend.

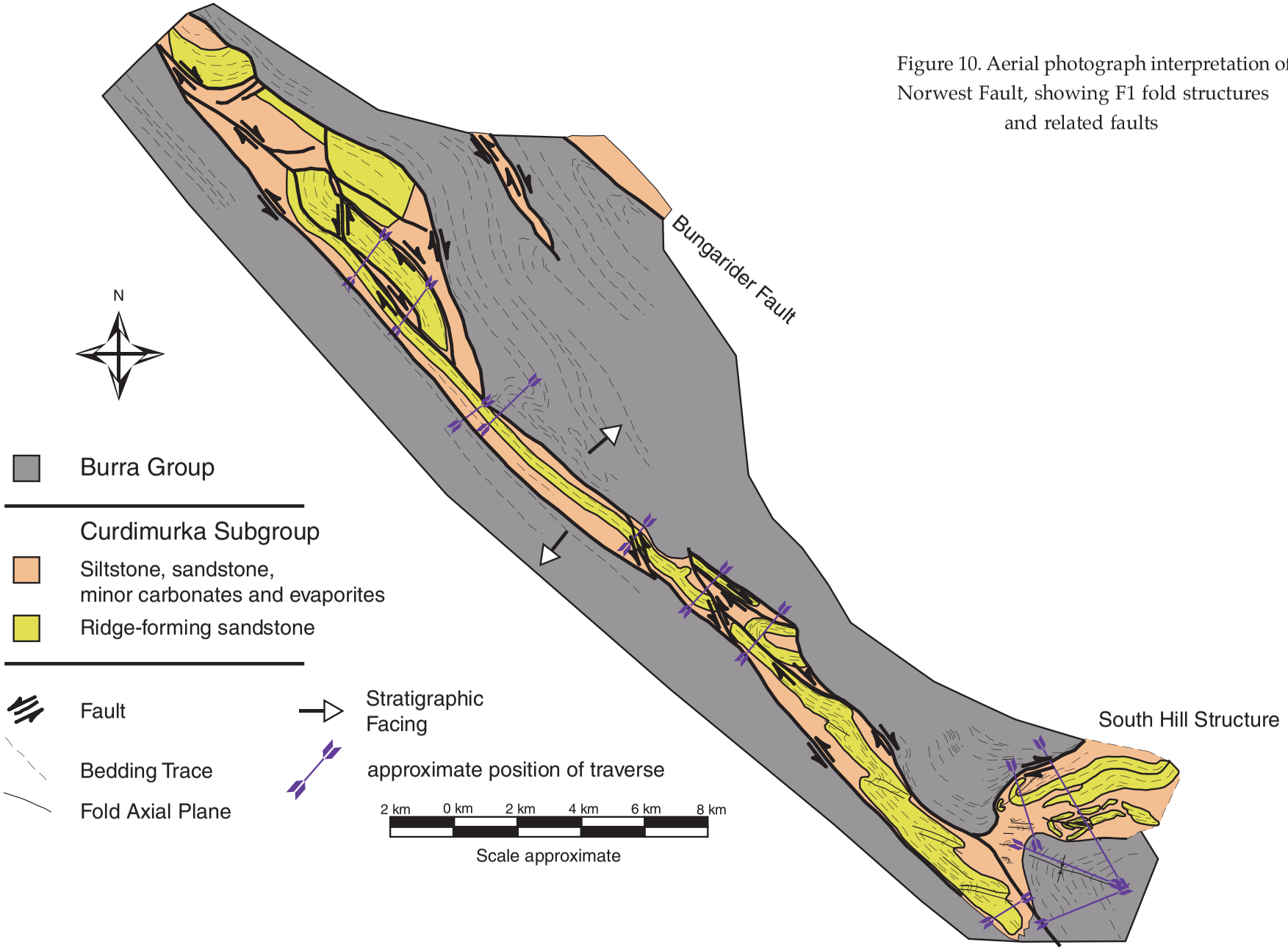

Figure 10. Aerial photograph interpretation of the Norwest Fault, showing F1 fold structures and related faults

Dunns Mine, Outcrop 1

Introduction

The Boorloo Anticline outcrop demonstrates three fold phases, providing especially good evidence for F_1 but the presence of F_1 in the hinge of the F_2 anticline obscures much of the detail of F_2 and F_3. A second outcrop, within the Dunns Mine Limestone, adjacent to Dunns Mine provides more detailed information on F_2 and F_3, without the complications of F_1 being present.

Over an area of about 50 m by 40 m, the Dunns Mine Limestone, comprising calcitic sandstone, siltstone and limestone, is folded into a series of tight to isoclinal folds, with variable plunges. The area was mapped at a scale of 1:200, noting where possible fold plunges, cleavages and cleavage–bedding intersection lineations. One area of particular complexity was mapped at a scale of 1:40. No facing was found at this outcrop but overall facing of the sediments in this region is to the northeast. The mapping showed that the area could be divided into eight domains based on the mapped structure. In four of these domains (Domains1, 2, 3 and 8) there is significant folding, in two (Domains 4 and 5) there is little visible structure and these were defined on the basis of strike. Another two domains (Domains 6 and 7) are not considered because of poor outcrop. A map of the outcrop with interpreted form surfaces is shown in Figure 11. Stereoplots of structural data collected at Outcrop 1 are shown in Figure 12.

Domain 1

Within domain 1, there are a series of tight anticlines plunging at a shallow angle to the southeast. This generation of folds is termed F_2. From bedding, the calculated plunge of the folds is 21° to 163°, and from measured fold plunges, the average plunge is 26° to 175° (having removed several outliers). Anticlines have rounded hinges, whereas synclines have angular profiles and are overturned by a few degrees. The axial plane dips steeply to the southwest and a divergent axial plane cleavage, S_2 is present and can be seen in Figure 13. Axial plane traces are folded slightly within Domain 1, from trending southeast to east-southeast. Within carbonate units, there is considerable thinning of the limbs and thickening of the hinges (Figure 14).

A second weaker cleavage cuts across bedding and S_2 at a high angle and is termed S_3. On the flanks of the anticlines, two cleavage bedding intersections are present. The first has a shallow plunge to the southeast and is termed L^2_0 whereas the second has a steep plunge to the south west and is termed L^3_0.

Domain 2

Domain 2 is centred on a prominent anticline with a gently curving axial trace. The outer surface of the anticline is sandstone, with carbonate beds in the core. The trend of the anticline changes from northwest to west, with shallow plunges to those directions. From bedding, the plunge of F_2 is calculated to be 30° to 312°, with an axial plane dipping at 85° to 040°. At the tip of the fold, the plunge, calculated from bedding is 40° to 282°. A syncline is inferred to the west of the anticline but no synclinal closure was observed. On the limbs, bedding is steep to overturned, with gentle undulations of the bedding surface about vertical. S_2 is present in the anticline hinge but it is weakly developed. S_3 was not observed within this domain. Figure 15 shows this fold.

Two prominent lineations are present; L^2_0 has a shallow plunge matching the plunge of the anticline, whereas L^3_0 has a steep plunge at a high angle to the axial trace of the fold.

Domain 3

The overall structure of Domain 3 is of an F_2 anticline with a steep plunge to the west. Within the anticline hinge, a series of three parasitic anticlines are present and so the western two thirds of Domain 3 was mapped at a scale of 1:40 to show the greater detail. Calculated from bedding, the plunge is 71° to 243° and from measured fold plunges, the average plunge is 66° to 248°. As with Domain 1, the anticlines have rounded profiles and the synclines are angular. A carbonate bed within the core of the anticline shows interlimb angles of less than 0°, with thinning along the limbs and thickening in the core (Figure 16).

Geology of Outcrop 1 - Dunns Mine

- Limestone - siltstone
- Calcitic Sandstone
- Bedding trace
- Bed contact
- 79 Bedding dip and strike
- 77 Cleavage dip and strike
- 57 Cleavage-Bedding Intersection
- Anticline, Syncline
- 79 Fold plunge
- Domain Boundary

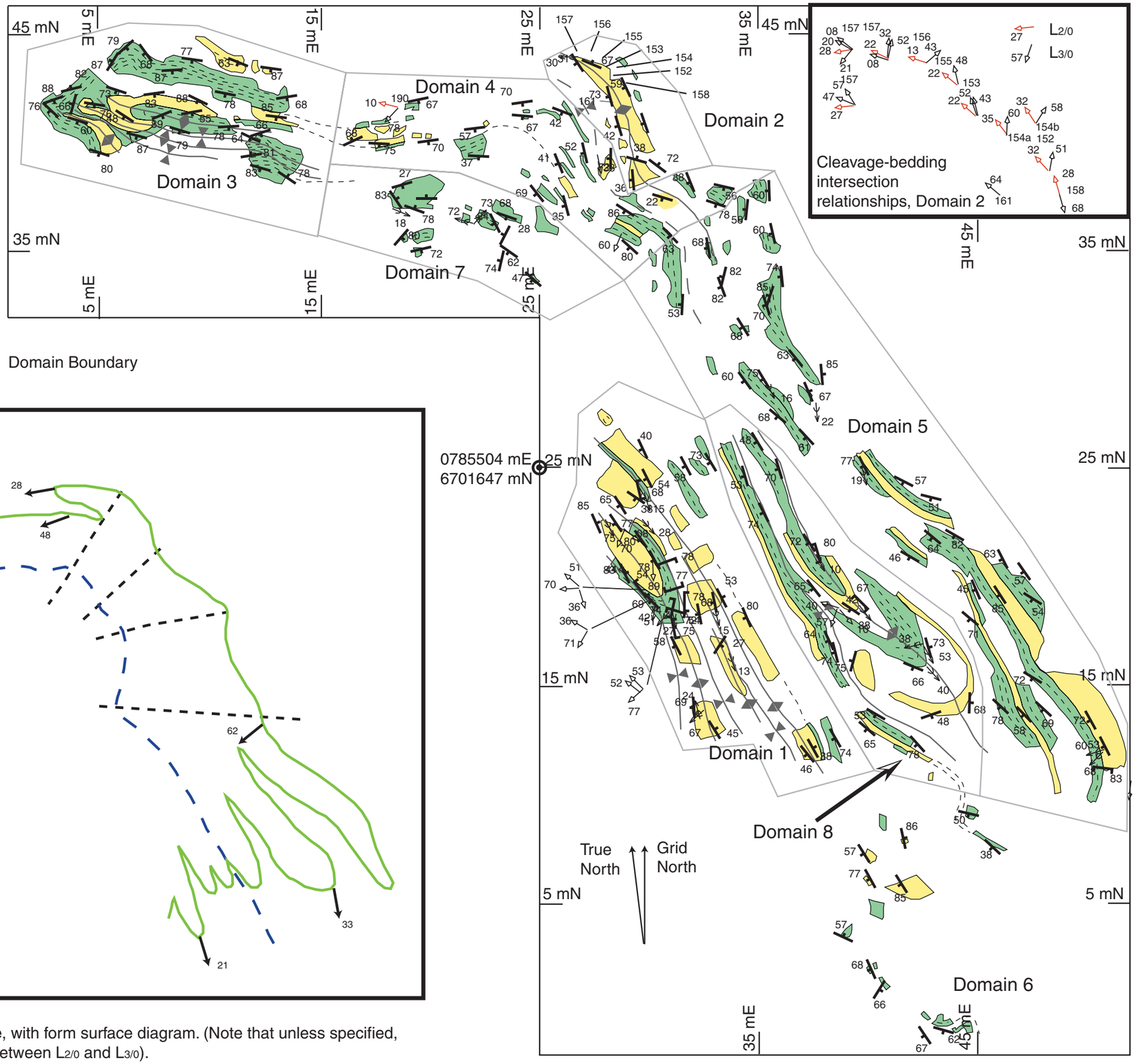

Figure 11. Geology of Outcrop 1, Dunns Mine, with form surface diagram. (Note that unless specified, no differentiation has been made between $L_{2/0}$ and $L_{3/0}$).

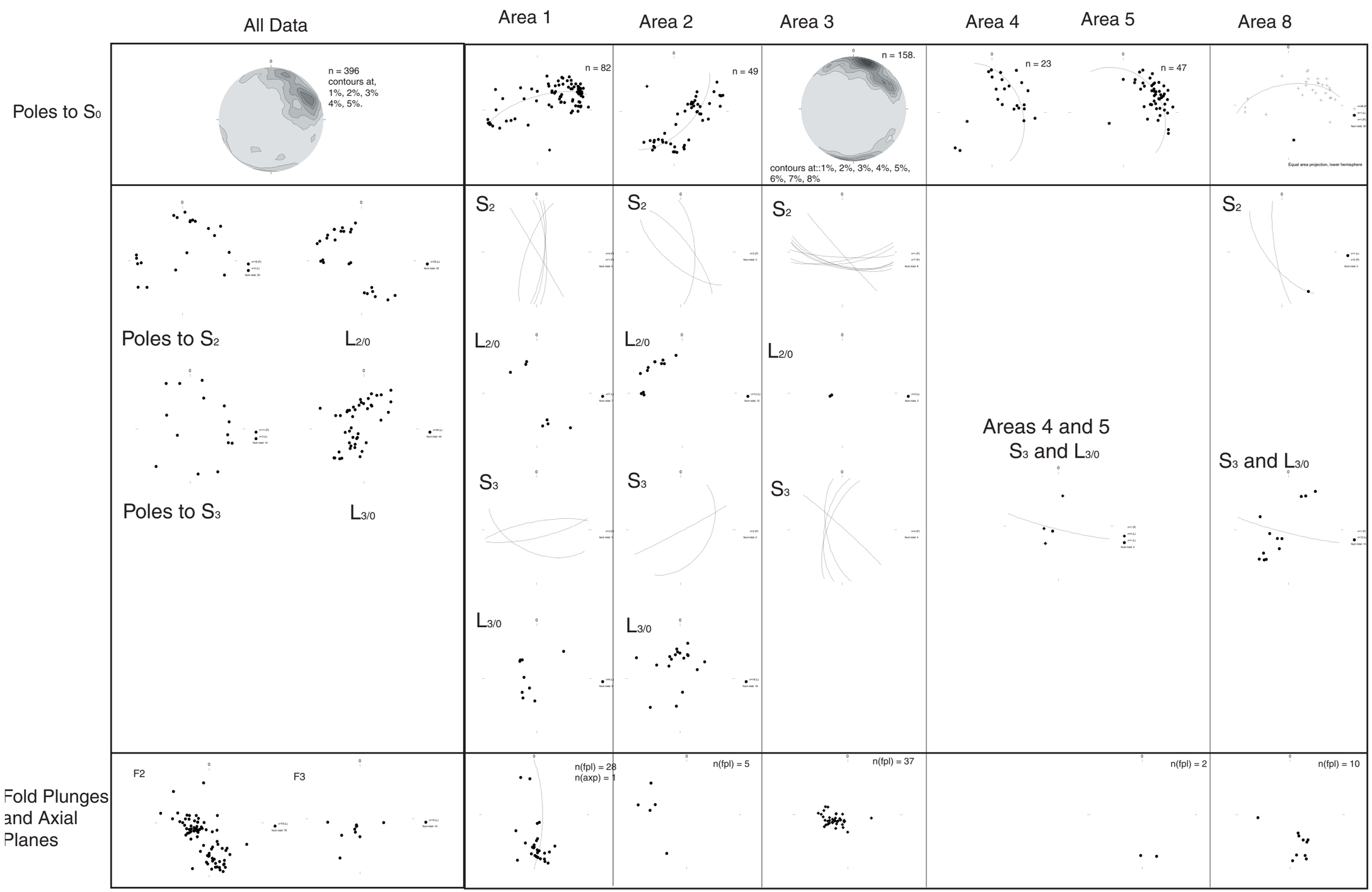

Figure 12. Stereonets of structural data collected at Outcrop 1, Dunns Mine. All stereonets are equal area projection, lower hemisphere.

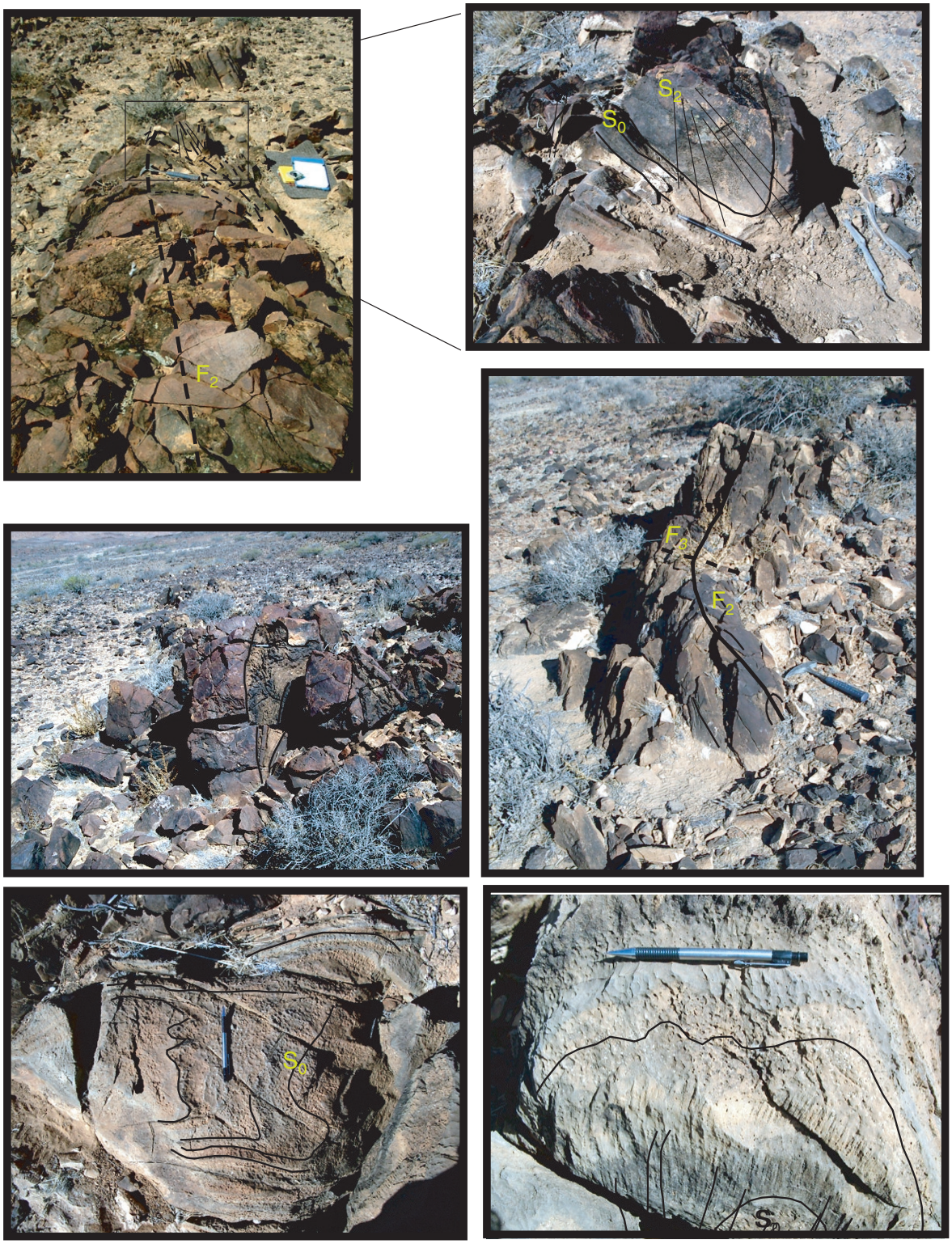

Figure 13a *(top left)*. Domain 1. Looking down the fold axis of F_2.
Figure 13b *(top right)*. Domain 1. Hinge of F_2 fold showing over-turning of syncline and S_2.
Figure 14 *(middle left)*. Domain 1. F_2 anticline showing thickening of a carbonate bed within the hinge and thinning along limbs.
Figure 15 *(middle right)*. Domain 2. Looking along a F_2 anticline. Note the folding of F_2 by F_3.
Figure 16 *(bottom left)*. Domain 3. F_2 fold plunging steeply to the west.
Figure 17. *(bottom right)*. Domain 3. Axial plane cleavage, S_2 in an evaporitic limestone.

S_2 is a fanning cleavage with an average dip to the south (Figure 17). The axial traces of the F_2 have been folded by F_3. S_3 is weakly developed and fans around the broad F_3 fold, roughly perpendicular to bedding and cutting S_2 at a high angle. In the carbonate beds around the larger scale anticline, there are a series of F_2 folds which have been rotated by F_3 folds so that they plunge now to the southwest. Cleavage-bedding intersections are poorly developed in Domain 3, with only two L^2_0 lineations having been measured. Figure 18 shows the map of Domain 3.

Domains 4 and 5

Domain 4 is between Domains 2 and 3. Within Domain 4, the strike of bedding varies from east–west to northwest–southeast. Dips are steep to the south and southwest. No F_2 folds were noted and the folding within Domain 4 is ascribed to F_3. From bedding, the plunge of these folds is 48º to 250º.

Domain 5 is along the eastern edge of the outcrop. Bedding in Domain 5 trends south-southeast–north-northwest, with a steep dip to the west-southwest. No F_2 fold closures were noted in Domain 5, although an anticline and syncline are inferred. There is some minor folding of bedding attributed to F_3. Calculated from bedding, the plunge of F_3 is 62º to 232º. Combining the bedding data from domains 4 and 5, the calculated dip for F_3 is also 62º to 232º.

S_3 was mapped in Domain 5 and L^3_0 is prominent on one surface in Domain 5. L^3_0 has a steep plunge, reflecting the high angle between S_3 and bedding.

Domain 8

Domain 8 is centred on an anticline and syncline pair between Domains 1 and 5. The folds, particularly the anticline, have divergent trends from Domain 1. A sandstone bed which defines the outer bed of the anticline is interpreted to boudinage on the southern limb of the anticline.

As calculated from bedding, F_2 in Domain 8 plunges at 33º to 171º. Calculated from fold plunges, the average plunge is 33º to 160º. There appears to be some rotation of minor folds around a central fold axis and these may represent an early phase of F_2. The axial plane of F_2 in Domain 8 dips steeply to the east-southeast. One measurement of S_3 was collected, with 12 L^3_0 plunges. Again, S_3 cuts across bedding and S_2 at a high angle.

Interpretation

Figure 11b shows the form surfaces for S_0, S_2 and S_3. The overall interpretation of the outcrop is that it is a 'Z' fold on the limb of a macroscopic fold, the hinge of which is not seen. From the trace of the S_0 and the F_2 fold plunges, F_2 folds are interpreted to be non-cylindrical. Although folding of F_2 by F_3 would generate double plunging structures, the large difference in the F_2 plunges between Domain 3 and Domains 1 and 2, reflects an initial variation in plunge. Non-cylindrical folds have been noted in folded limestone beds within the Recovery Formation also.

It is possible to infer a fold closure that has been folded by F_2 in Domain 6; that is an isoclinal anticline, refolded by F_2, giving a domal appearance. Although this interpretation would not violate the interpretation of F_2 fold traces, it is not favoured because there is no direct evidence for an earlier deformation at this outcrop.

The thickening in the hinges and the thinning in the limbs has important regional implications. There is evidence of extension within the Dunns Mine Limestone along its entire strike length in this area. The strike of the Dunns Mine Limestone is an F_2 trend and so likely to lie on the limb of a regional F_2 fold. Boudins mapped in the Dunns Mine Limestone and the Rook Tuff in the vicinity of Dunns Mine are tablet-shaped with necks plunging at 32º to 316º and 27º to 135º (average plunges calculated from 10 measurements for each direction), roughly the same plunges as F_2 folds. By contrast, the Dome Sandstone has behaved in a brittle fashion along this limb, undergoing brecciation in extension.

Discussion

F_2 is the dominant regional structure across the Willouran Range. The northwest–southeast trend of F_2 folds follows the trend of the major regional faults; the Norwest Fault and the Bungarider Fault and the associated drag folds. Dome and basin

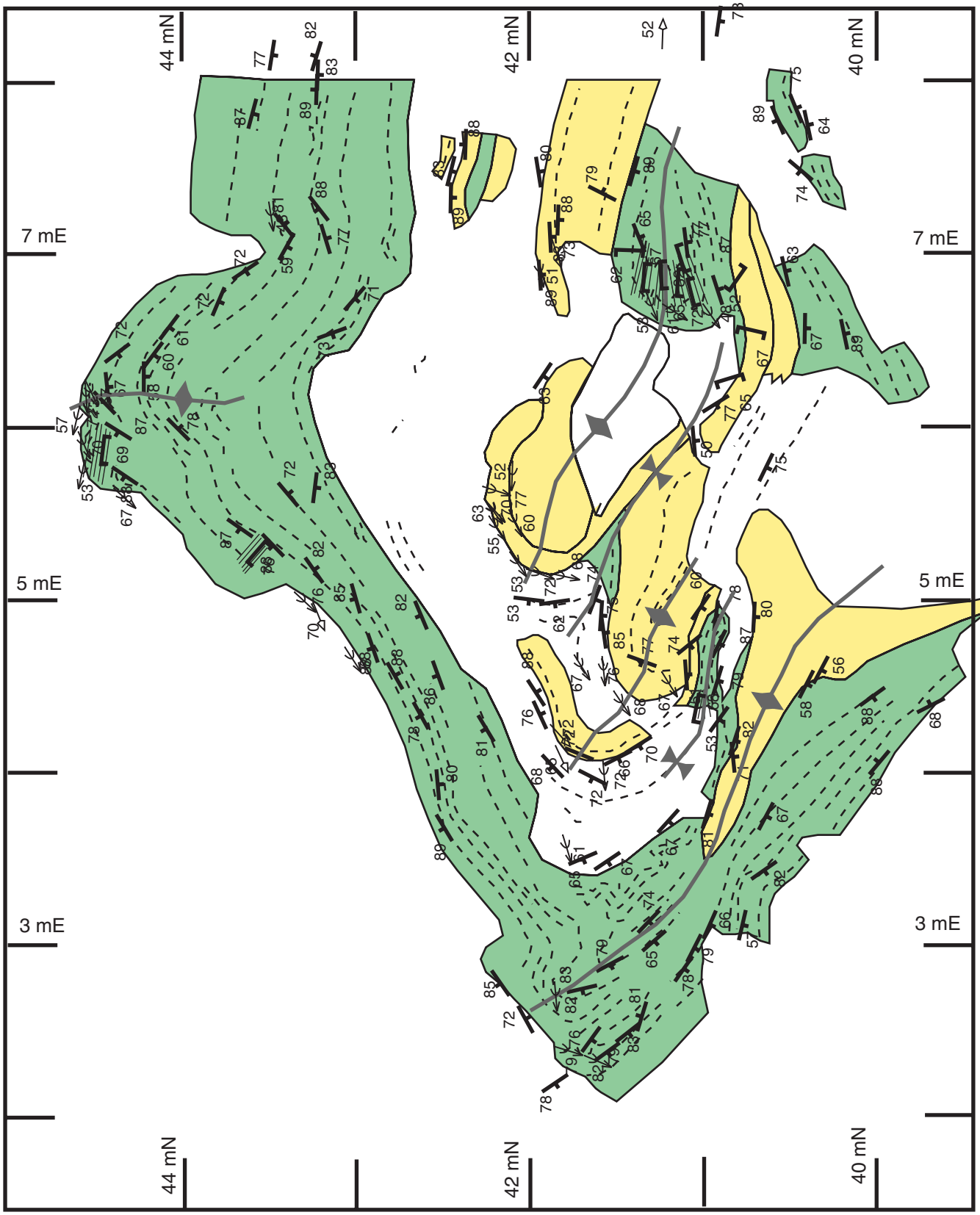

Figure 18 . Detailed map of Domain 3, Outcrop 1, Dunns Mine. See Figure 11 for Legend.

structures within the Burra Group to the southwest of the mapping area, have their major axis trending northwest–southeast. Likewise, the broad folding affecting the Umberatana and Wilpena Groups west of the Norwest Fault on the Torrens Hinge Zone have a similar trend. In the central Flinders Ranges, the dome and basin structures have major axes trending northwest–southeast. Preiss (1987) concluded that northwest–southeast trending structures elsewhere in the Adelaide Fold Belt were formed in the first phase of the Delamerian Orogeny.

F_3 is of regional significance but it is usually secondary to F_2. The dome and basin structures within the Burra Group mentioned above have a southwesterly trend for their minor axis and so the significance of F_3 extends beyond the immediate mapping area of the northern Willouran Range. Figure 19 shows the major regional structures in the Willouran Range area. In the central Flinders Ranges, the minor axes of the dome and basin structure also trend southwest–northeast and so F_3 would appear to have regional importance also. The one area where a northeast–southwest trend dominates is in the northern Flinders Ranges, however the trend changes to east–west and then northwest–southeast, coming towards the Willouran Range so that it is likely that these folds are F_2, modified by a different bounding structure, the northeast–southwest trending Paralana Fault. Paul et al (1999) attributes the structure of the Northern Flinders Ranges to south directed, thick-skinned thrusting, the thrusts being reactivated normal faults.

As F_1 pre-dates F_2, the timing of F_1 is likely pre-Delamerian. Parker (1983) concluded that the Curdimurka Subgroup in the Rischbieth Structure had been deformed prior to the deposition of the Burra Group, however to the east of the Norwest Fault, it can be seen that the Emeroo Subgroup of the Burra Group has been affected by structures associated with F_1 within the Curdimurka Subgroup. Selley and Bull (2001) identified localised folding affecting the Burra Group prior to or during deposition of the Umberatana Group in the Bungarider Depocentre. Along the Norwest Fault, the Curdimurka Subgroup is thinnest, with the least development of evaporites and siltstones, which in the northern Willouran Range have absorbed the bulk of the strain. The conclusion is that along the Norwest Fault, the Burra Group rode above a deforming Curdimurka Subgroup, the Curdimurka Subgroup absorbing most but not all of the strain, during the F_1 fold event. The Norwest Fault was then reactivated as a high-angle reverse fault during the F_2 fold event.

In the eastern Willouran Range, the Burra Group appears to be largely undeformed but it sits upon the Curdimurka Subgroup which has undergone extreme deformation. There is also evidence (which will be reported on in detail at a later date) that the carbonate beds in which F_1 structures have been found have taken extensional strain, which in the less elastic sandstone and siltstone units has been accommodated by normal faulting. On this basis, a working hypothesis is that the timing of F_1 is related to the extension which resulted in the deposition of the Umberatana Group. The most likely scenario is that the listric faults forming the half-grabens into which the Umberatana Group was deposited, sole-out into the bedding-parallel structures seen within the Curdimurka Subgroup.

Structure and Mineralisation at Dunns Mine

Dunns Mine is at the southern end of a series of scattered workings occurring at the same stratigraphic level of the Dunns Mine Limestone over a strike-length of about 4500 m. It is the most extensive of these workings, providing the best exposures of the mineralisation. Having developed an understanding of the structural history of the Curdimurka Subgroup, mapping was undertaken at Dunns Mine to determine the relationship between copper mineralisation and structure. Figure 20 is a map of the Dunns Mine workings.

Workings at Dunns Mine are restricted to a black shale unit, with minor siltstone and carbonate between two sandstone-carbonate units. The mineralised unit is about eight metres thick. At the southern end of Dunns Mine, the stratigraphy is folded into a ‘Z’ fold,

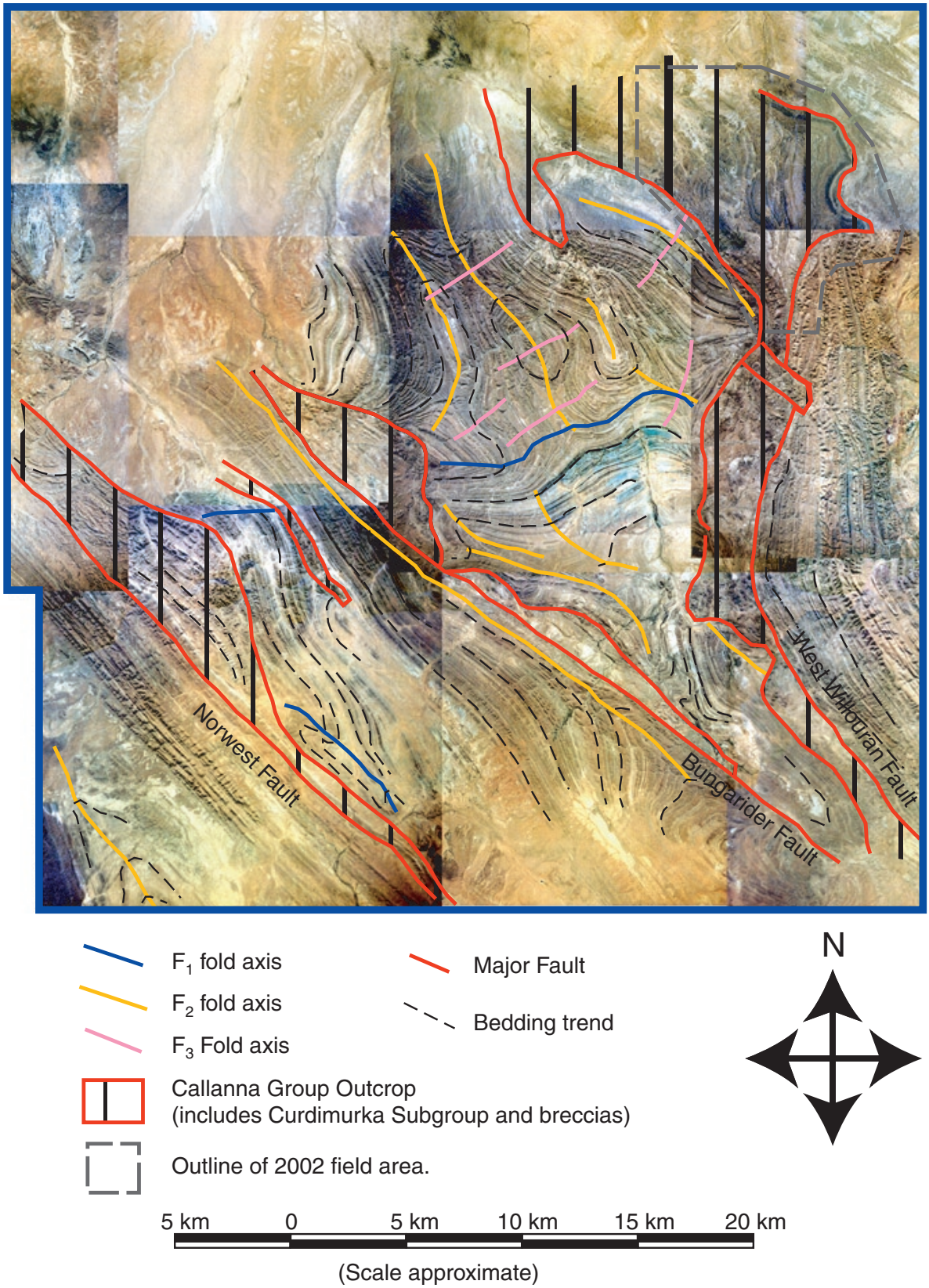

Figure 19. Aerial photograph composite showing the Willouran Range area, with major structures with annotations showing an interpretation of major fault positions and fold axes. F_2 folds tend NW - SE, F_3 folds trend NE - SW. Note that smaller outcrops of Callanna Group along the Bungarider Fault are not shown, and the Burra Group and Umberatana Group are not differentiated here.

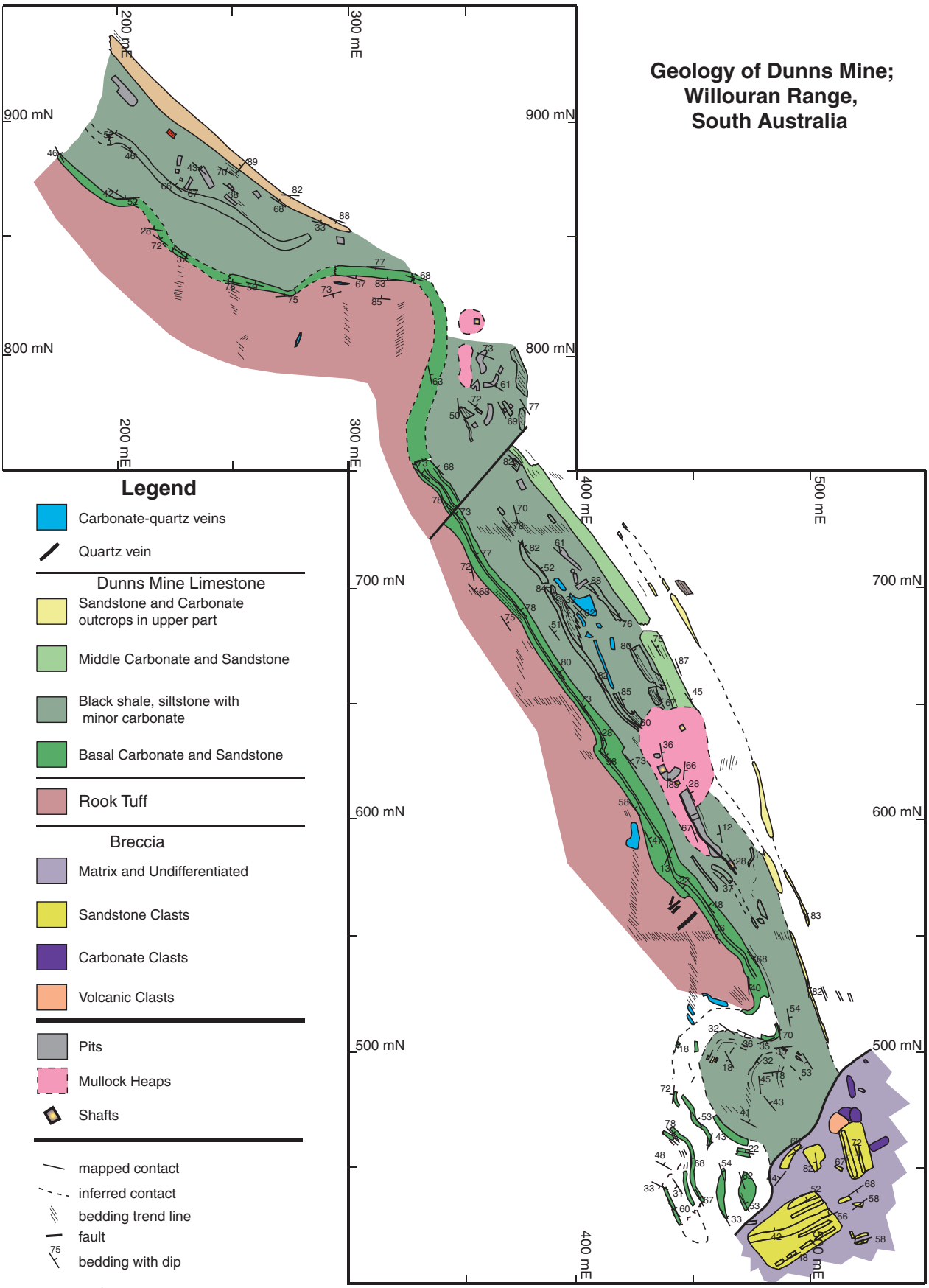

Figure 20. Geology of Dunns Mine, Willouran Range.

with a shallow plunge to the south, leading to its interpretation as an F_2 fold. A cleavage sub-parallel to bedding is rotated around the hinge of the fold, confirming the interpretation. South of this fold, the Dunns Mine Limestone is truncated by a breccia with clasts of Rook Tuff and Dome Sandstone. West of the area mapped, the Dome Sandstone has been brecciated and to the northwest, the brecciation extends into the Rook Tuff.

The workings follow a sub-vertical fault zone which cuts bedding at differing angles. Along the fault zone is abundant quartz, carbonate and quartz–carbonate veins. The carbonate weathers to red-brown but is a red-grey colour on cut surfaces and is siderite and a ferruginous calcite. There has also been some silicification and carbonatization of the host-rock. Figure 21 shows the fault zone in the walls of a shallow open pit.

Copper mineralisation is seen in a number of sites. Most spectacular, chalcocite was found in the matrix of fault breccia, along with malachite (Figure 22). Malachite was seen in microveins, possibly with Mn oxides and in areas of silicification and carbonatisation of the wall Green staining and malachite was observed forming parallel laminations within white, kaolinised shale. From these styles of mineralisation it then appears that there are several possible sources of mineralisation.

In the first instance, the malachite and copper staining in the kaolinised shale supports the possibility that there is primary stratiform mineralisation. Utah Development Company reported that this level of stratigraphy is regionally anomalous in copper and drilling at Dunns Mine identified chalcopyrite (Rowlands et al., 1979). The presence of high-grade mineralisation in the fault zone and the association of mineralisation with veins infers that the mineralisation was introduced by hydrothermal fluids along the fault. Organic matter in the shale served as a reductant, reacting with oxidised copper-bearing fluids, causing the deposition of copper. Although they are largely absent at the Dunns Mine locality, pseudomorphs of anhydrite and scapolite (?) are common within the Dunns Mine Limestone, indicating an ample supply of sulphate and chloride at about the same stratigraphic level as the mineralisation. Evidence against the veins being the source of mineralisation is the absence of mineralisation in or around the same generation of veins, not only in the black shale of the Rook Tuff but along strike from known mineralisation within the same unit. Hence, the veins can be ruled out as the source of mineralisation.

An alternative hypothesis is that the veins and the mineralisation are two products of the same process. The presence of mineralisation within the kaolinised shale of the mineralised unit reflects an earlier, low-grade mineralisation, noted by Utah Development Company. Faulting along the limb of the F_2 fold has created dilational zones into which fluids from the surrounding rock mass have moved, including quartz, carbonates and sulphides. Where the earlier mineralisation was not present, there is no mineralisation associated with the veins. Essentially then, the mineralisation process is an upgrading of early low-grade copper mineralisation at the local scale. More work is required to confirm and refine these conclusions.

Conclusions

The Curdimurka Subgroup has been affected by three fold events. These may be summarised as follows.

F_1

- confined to specific layers of the stratigraphy
- recumbent folds with a layer-parallel cleavage S_1 (where developed)
- thrusting now seen as mainly dextral strike-slip faulting
- southeast directed transport
- have regional significance but are not the dominant regional structure.

F_2

- upright southeast–northwest trending folds
- noncylindrical
- rounded anticlinal hinges with sharp synclinal hinges
- produce an axial plane cleavage S_2

Figure 21. The fault zone at Dunns Mine Workings.
Figure 21a *(top left)*. Looking south, Cu mineralisation along the edges of the fault.
Figure 21b *(top right)*. Looking north. Pit in the middle of the area. Here the fault zone has massive siderite - quartz veining. Copper mineralisation sites are shown.
Figure 21c *(middle)*. Stereoscopic picture looking north from between Figures 21a and 21b.
Figure 22a *(bottom left)*. Malachite (mal) in fault breccia
Figure 22b *(bottom right)*. Chalcocite (cc) and malachite (mal) in fault breccia.

- have thinning on limbs and thickening in the hinges.
- the dominant regional structure

F_3

- open folds
- moderate plunge to the southwest
- produce a cleavage S_3 at a high angle to bedding and S_2

Mineralisation at Dunns Mine is associated with F_2. It has formed by the remobilisation of earlier low-grade mineralisation into dilational zones created by faulting along the limb of an F_2 fold.

References

Mackay, W.G., 2001. PhD project: Sedimentology and structure of the Curdimurka Subgroup, Willouran Range, South Australia. *In* P544–Proterozoic sediment-hosted copper deposits. AMIRA / ARC Progress Report December 2001, 47–68.

Murrell, B., 1977. Stratigraphy and tectonics across the Torrens Hinge Zone between Andamooka and Marree, South Australia. University of Adelaide, PhD Thesis (unpublished).

Parker, A.J., 1983. Tectonic development of the Adelaide Fold Belt. Geological Society of Australia, Abstracts 10., 23-28.

Paul, E., Flottmann, T. and Sandiford, M., 1999. Structural geometry and controls on basement-involved deformation in the northern Flinders Ranges, Adelaide Fold Belt, South Australia. Australian Journal of Earth Sciences 46, 343–354.

Preiss, W.V., 1987. The Adelaide Geosyncline: Late Proterozoic stratigraphy, sedimentation, palaeontology and tectonics. Geological Survey of South Australia Bulletin 53, 438p.

Preiss, W.V. (Compiler), 1993. Neoproterozoic. In Drexel, J.F., Preiss, W.V. and Parker, A.J. (Eds) The geology of South Australia. Vol.1, The Precambrian. South Australian Geological Survey Bulletin 54, 170-203.

Preiss, W.V. and Cowley, W.M., 1999. Genetic stratigraphy and revised lithostratigraphic classification of the Burra Group in the Adelaide Geosyncline. Mesa Journal 14, 30-40.

Preiss, W.V., Dyson, I.A., Reid, P.W. and Cowley, W.M., 1998. Revision of lithostratigraphic classification of the Umberatana Group. Mesa Journal 9, 36-42.

Rowlands, N.J., Jarvis, D.M., Rayner, R.A. and Blight, P. 1979. S.A. stratiform copper project, EL. 461 Willouran Ranges. Third annual report on exploration activities (period 21.12.78–21.12.79). Utah Development Company Report No. 317 (unpublished).

Rowlands, N.J., Jarvis, D.M., Benade, D.R., Circosta, G. and Blight, P.G., 1981. S.A. stratiform copper project, EL. 461 Willouran Ranges. Fourth annual report on exploration activities (period 24.12.79–3.4.81). Utah Development Company Report No. 338 (unpublished).

Selley, D. and Bull, S., 2001. Basin architecture during deposition of the lower to middle Umberatana Group, Adelaide Fold Belt, South Australia; implications for Cu mineralisation. *In* P544–Proterozoic sediment-hosted copper deposits. AMIRA / ARC Progress Report December 2001, 1–45.

Wingate, M.T.D., Campbell, I.H., Compston, W. and Gibson, G.M., 1998. Ion microprobe U-Pb ages for Neoproterozoic basaltic magmatism in south-central Australia and its implications for the break-up of Rodinia. Precambrian Research 87, 135–159.